Dissertation

submitted to the

Combined Faculties for the Natural Sciences and for Mathematics

of the Ruperto-Carola University of Heidelberg, Germany

for the degree of

Doctor of Natural Sciences

Presented by

Kalliopi Pervolaraki, M.Sc.

Born in Heraklion, Greece

Oral-examination: 18th of September 2018

Functional differences in type I versus type III interferon mediated immunity

Referees:

Prof. Dr. Ralf Bartenschlager

Dr. Steeve Boulant

Once you set out for Ithaka
hope your road to be long,
full of adventures, full of knowledge.

Don't be afraid of the Laistrygonians and the Cyclops,
the angry Poseidon
you'll never find them on your way
if you keep your thoughts high,
if rare excitement touches your spirit and your body.

You won't meet the Laistrygonians and the Cyclops,
the wild Poseidon
unless you bring them along inside your soul,
unless your soul puts them in front of you.

Hope your road to be long
may there be many summer mornings
when you'll enter with pleasure, with joy,
the harbours you've seen for the first time

Stop in Phoenician trading stations
and get the good wares
pearls and corals, ambers and ebony,
and sensual herbs of every kind
as many sensual herbs as you can

Go to many Egyptian cities
to study and learn from the educated ones
keep Ithaka always in your mind
your arrival there is your destiny

But don't rush the journey at all
it better lasts for many years,
and then when you're old to stay on the island,
wealthy with all you've gained on the way
without expecting Ithaka to make you rich.

Ithaka gave you the beautiful journey.
without her you wouldn't have set out
there's nothing else to give you anymore

And if you find her poor, Ithaka hasn't fooled you.
now that you became wise with so much experience
you should have already understood what Ithakas mean

Kostantinos Kavafis

Table of contents

To my parents, *Maria and Marko,*

Acknowledgements

This project is the outcome of a collaborative work and for this first of all I want to thank all the people who contributed with their work and ideas.

First of all, I would like to thank my supervisor and mentor Dr. Steeve Boulant for giving me the opportunity to perform my PhD in his lab and for introducing me to the world of interferons. He was inspiring me by being always enthusiastic and passionate about science and fully supportive to my ideas and initiatives. Through our endless but very fruitful discussions, I have learned how to turn from a student into a scientist. Many special thanks go to my co-supervisor Dr. Megan Stanifer for her scientific, but also personal, support and advice. I am grateful to her for supporting me with all her knowledge on the project, the lab and the research world and for helping me developing my skills in all the aspects of my scientific life. Her guidance and scientific passion were vital for the fulfillment of this work.

I want to thank Prof. Ralf Bartenschlager for being my first referee for this thesis and for giving me the opportunity to present my data at his department and all his fruitful feedback. I am thankful also to Prof. Alexander Dalpke and Dr. Marco Binder for their important guidance through my PhD project as members of my thesis advisory committee. Also, I would like to thank Prof. Ursula Klingmüller for being willing to share her lab expertise on the interferon field and for acting as examiner during my PhD defence.

I am grateful to all my collaboration partners. Prof. Ronald Robinson and Lynnsey Renn for providing me reagents and valuable advice how to set up the interferon stimulating gene screening. Prof. Thomas Höfer for giving me the opportunity to lead part of my project in the direction of modeling and for opening new scientific approaches for me. Soheil Rastgou Talemi for our great collaboration regarding the mathematical modelling part. I am really thankful for his patience to teach me basic principles of modelling and be always available to discuss my questions and worries. Many thanks go to Anja Rippert and Dorothee Albrecht for not only their vital contribution to my work but also for all their support to my daily lab life.

I am also very thankful to Prof. Jean Rommelaere, Dr. Christiane Dinsart. and Prof. Marianne Boes. I had the unique opportunity to met them through my master studies and since then I considered them mentors in research and scientific life. Thank you Jean, Christiane and Marianne for being always so willing to discuss all the challenges of my scientific life, for providing me your precious advice and for being so optimistic and supportive to me, anytime I knocked your door.

This work would not have been possible without the valuable help, long scientific discussions and daily unlimited support of all the members of Steeve Boulant Lab. Dr. Delia Bucher, Christian Kischnick, Marcus Mukenhirn thank you all very much for being always willing to listen to me and help solving my daily experimental problems and support me in my personal worries. Many thanks go also to all my master students, who were coming new to the lab and bringing fresh motivation to my project. I greatly appreciate their willingness to cope with my weird character and work hard. I want to particularly acknowledge the work of Stephanie Muenchau, who was my first master student, for her contribution to my paper and her daily support, always taking care for us having a cup of good coffee at the lab in the hard moments.

I do not have words how to thank Marta Fratini and Dr. Pranav Shah. We started as colleagues but we ended up as best friends. My life in Heidelberg would have been much more difficult without their support. I owe a great thank to Marta for putting up with my daily rants and freak outs, as well as for standing by me during the most difficult times throughout the past four years of my life. Pranav thank you for your countless patience, undivided support and for just always being so awesome to me. I would also like to thank my friends outside the lab Ioanna and Mikaella for their support in any kind of daily situation, asking about work and encouraging me being positive and motivated. Special thanks to my friends from school Evi, Manoli, Elena and Ioanna for feeling them always next to me no matter what happens and how far we are.

Δεν εχω λογια πως να σε ευχαριστησω Πανο, για την υπομονη και την αμεριστη υποστηριξη σου το τελευταιο και πιο απατητικο χρονο του διδακτορικου μου. Σε ευχαριστω που μου θυμησες ποια ειναι η δικη μου Ιθακη και ποιος ειναι ο πραγματικος πλουτος στη ζωη. Σε ευχαριστω που διπλα σου ζω την ομορφια της ζωης.

Most importantly I owe the greatest thank to my family for giving everything a family can give, support, love and care. Θελω να εκφρασω την ευγνωμοσυνη μου στους γονεις μου Μαρια και Μαρκο για την απεριοριστη αγαπη τους, τη συνεχη ενθαρρυνση και κατανοηση που εδειξαν καθ'ολη την πορεια των σπουδων μου. Επισης ενα μεγαλο ευχαριστω οφειλω σε ολους τους κοντινους μου συγγενεις (γιαγια Αννα και γιαγια Ποπη, Αννουλα και Γιαννη, Κωστουλα και Σωτηρη, Αντωνη και Δεσποινα, Μιχαλη και Δημητρη) για τη στήριξη και την ανοχή που έδειξαν στις προτεραιότητες που επέβαλε αυτή η προσπάθεια μου. Αναγνωριζω πως στερησα πολυ χρονο απο την οικογενεια μου τα ταλευταια χρονια και ευχομαι να μπορεσω να τον ανταποδωσω.

Abstract

Intestinal epithelial cells (IECs) lining the surface of our gastrointestinal tract tolerate the presence of the commensal microbiota, while maintaining responsiveness against enteric pathogens. How IECs regulate their innate immune response to maintain this finely tuned balance and establish an immune-homeostatic state in the gut remains unclear. Interferons (IFNs) are cytokines produced upon viral infection. While type I IFN receptors are ubiquitously expressed, type III IFN receptors are preferentially expressed on epithelial cells. This epithelium specificity strongly suggests exclusive functions at epithelial surfaces, but the relative roles of type I and type III IFNs in the establishment of an antiviral response in human IECs are not clearly defined.

Here, we utilized human mini-gut organoid cultures and human colon cell lines to delve into the antiviral properties of type I versus type III IFNs in the gut. We could show that although primary human IECs, produce transcript levels for both IFNs, they secrete only type III IFNs in the supernatant upon viral challenge. However, using genetic ablation of either type I or type III IFN receptors, we revealed that human IECs respond to both IFNs, by independently establishing an antiviral state, responsible for combating enteric viral infection. Importantly, we could identify differences in the establishment of each IFN antiviral activity. Contrary to type I IFN, the antiviral activity induced by type III IFN is strongly dependent on the mitogen-activated protein kinases signaling pathway, suggesting a pathway used by type III IFNs that non-redundantly contributes to the antiviral state. In addition, we showed that while type I IFN signaling is characterized by an acute strong induction of ISGs and confers fast antiviral protection, type III IFN mediated antiviral protection is characterized by a slow weak induction of ISGs. Combining data-driven mathematical modeling with experimental validation, we demonstrated that these kinetic differences are intrinsic to each signaling pathway and not due to different expression levels of the corresponding IFN receptors.

In conclusion, our results strongly suggest that type III IFN is specifically tailored to act on epithelial cells not only due to the restriction of its receptor but also by providing IECs with a distinct antiviral environment compared to type I IFN, which allows for efficient protection against pathogens without producing excessive inflammatory signals. We propose that this specific antiviral environment is key for mucosal surfaces, which are often challenged with the extracellular environment, to maintain gut homeostasis.

Zusammenfassung

Intestinale Epithelzellen, welche den gastointestinalen Trakt auskleiden, tolerieren die kommensale Darmflora während sie gleichzeitig gegen Darmpathogene reagieren. Es ist nicht klar, wie intestinale Epithelzellen ihre angeborene Immunabwehr regulieren, um im Darm das feinabgestimmte Gleichgewicht aufrecht zu erhalten und die Immunhomöostasis zu erreichen. Interferone sind Zytokine, welche bei viralen Infektionen produziert werden. Typ-I Interferonrezeptoren werden ubiquitär exprimiert, wohingegen Typ-III Interferonrezeptoren hauptsächlich auf Epithelzellen exprimiert werden. Diese Spezifität für Epithelien suggeriert eine Funktion ausschließlich in epithelialen Oberflächen, aber die jeweilige Rolle von Typ-I und Typ-III Interferonen bei der Etablierung einer antiviralen Immunantwort in humanen Epithelzellen ist nicht klar definiert.

Wir benutzten humane Miniatur-Darm Organoidkulturen und humane Dickdarmzelllinien, um die antiviralen Eigenschaften von Typ-I im Vergleich zu Typ-III Interferonen zu untersuchen. Wir konnten zeigen, dass bei viraler Infektion nur Typ-III Interferone von primären humanen Epithelzellen in den Zellkulturüberstand sekretiert werden, obwohl beide Interferone auf Transkriptebene produzieren werden. Jedoch konnten wir mit genetischer Entfernung von Typ-I oder Typ-III Interferonrezeptoren zeigen, dass intestinale Epithelzellen auf beide Interferone reagieren, indem diese unabhängig von einander einen antiviralen Zustand erzeugen, der für die Bekämpfung von viralen Darminfektionen verantwortlich ist. Wir konnten wichtige Unterschiede in der Herbeiführung der antiviralen Aktivität der einzelnen Interferone identifizieren. Im Unterschied zu Typ-I Interferonen ist die antivirale Aktivität, welche von Typ-III Interferonen herbeigerufen wird, stark abhängig vom „mitogen-activated protein kinases“-Signalweg, was darauf hindeutet, dass ein nicht redundanter Signalweg zum Typ-III interferoninduzierten antiviralen Zustand beiträgt. Außerdem war es uns möglich zu zeigen, dass die durch Typ-I Interferone ausgelöste Signaltransduktion zu eine charakteristischen starken und akuten Induktion von interferonstimulierten Genen führt und einen schnellen antivirale Schutz gewährleistet, im Gegensatz zum antiviralen Schutz, welcher durch Typ-III Interferone erzeugt wird, der sich durch eine langsame Induktion von interferonstimulierten Genen auszeichnet. Die Verknüpfung von datengetriebener mathematischer Modellierung mit experimenteller Validierung zeigte, dass diese kinetischen Unterschiede intrinsisch für den jeweiligen Signalweg sind und nicht durch unterschiedliche Expressionsniveaus der zugehörigen Interferonrezeptoren hervorgerufen wird.

Zusammenfassend betrachtet lassen unsere Daten darauf schließen, dass im Vergleich zu Typ-I Interferone, Typ-III Interferone spezifisch dafür produziert werden, auf Epithelzellen zu

wirken, nicht nur durch Beschränkung der Rezeptorexpression sondern auch durch das Bereitstellen einer eigenen antiviralen Umgebung für intestinale Epithelzellen, welche einen effizienten Schutz gegen Pathogene ohne übermäßige Entzündungsreaktion gewährleistet. Wir glauben, dass diese spezifische antivirale Umgebung sehr wichtig für die Aufrechterhaltung des Darmgleichgewichts durch die Oberflächen von Schleimhäuten ist, da diese der extrazellulären Umgebung ausgesetzt sind.

1 Introduction

1.1 Gastrointestinal tract: cellular composition and immune response

Mucosal tissue, strategically lining the surface of the respiratory, gastrointestinal and reproductive tract, constitutes the physical, chemical and immunological barrier that separates the inner milieu of multicellular complex organisms from their external environments. The gastrointestinal (GI) tract, being the largest of these mucosal surfaces, acts as the site of continuous contact with a diverse range of dietary antigens and the trillions of microorganisms living in the intestinal lumen[1,2]. Thus together with its overall function in digestion, absorption and excretion, the GI tract is adapted to prevent the entry of undesired foreign antigens and luminal pathogens, while enabling the colonization by commensal microorganisms that contribute to the digestion and significantly impact the development of intestinal mucosal immunity[3,4]

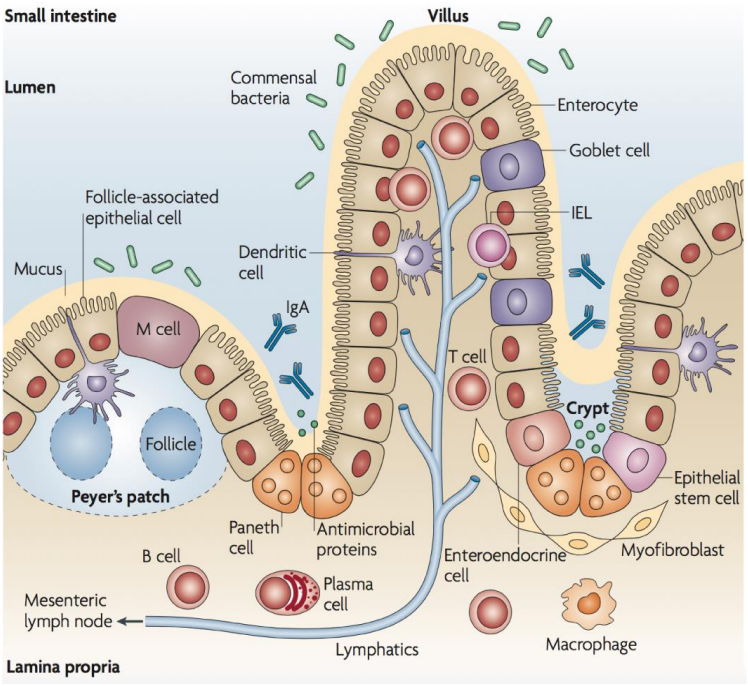

Figure 1. **Schematic of the human intestinal epithelium.** The surface of the epithelium is organized in finger-like protrusions known as villi and gland-like invaginations into the underlying connective tissue called crypts. A number of different highly specialized cell types (enterocytes, goblet cells, enteroendocrine cells, tuft cells, M cells and Paneth cells) create the continuous monolayer of the epithelium, which separates the lumen of the gut from the lamina propria, consisting mainly of myofibroblasts and immune cells. The epithelium is renewing every three days and the crypts harbor the stem cell niche Adapted from Abreu, (2010)[27].

1.1.1 Cellular components of the intestinal mucosal epithelium

To be able to function as a physical and immunological barrier with a primary role in digestion and absorption, the monolayer of the intestinal epithelium is composed of six differentiated cell types: the **enterocytes**, **goblet cells**, **enteroendocrine cells**, **tuft cells, Microfold cells** and **Paneth cells**

Enterocytes or enteroabsorptive cells are the most abundant cell population of the intestinal epithelium. They are covering approximately the 80% of the epithelium both along the proximal-distal axis and the crypt-villus axis and they present phenotypic differences regarding their position and their interaction with the other cell types[5,6]. Enterocytes are highly polarized with an apical brush border covered with microvilli, which protects against unwanted antigens, produces digestive enzymes and contributes to nutrient absorption[3,4]. Apart from their primary functions, they further contribute to the immune response of the epithelium by expressing a number of innate immune receptors[4,7]. In addition to this, they also support the adaptive immune system in the gut by promoting the transcytosis of the secretory IgA (SIgA) into the lumen[8]. **Goblet cells** are scattered through the intestinal epithelium with their percentage increasing from the small to the large intestine[9]. They function as secretory cells, and are responsible for the production of the major components of the mucus matrix such as the Mucin A family of proteins. This semisolid heavily glycosylated mucus layer covers the intestinal mucosal surface and serves as a protective barrier which prevents the direct contact of large particles and pathogenic microorganisms with the intestinal epithelial cells[10–12]. In addition, by acting as a trap also for commensal bacteria, Goblet cells regulate the localization of the intestinal microflora by generating the mucus matrix[6].

Enteroendocrine cells are a rare population of secretory cells residing along the crypt-villus axis of the epithelium[6]. In response to different stimulus such as dietary substances or harmful signals, they produce a diverse range of neuropeptides and hormones, which they secrete into the bloodstream, transfer to the enteric nervous system or diffuse over a short distance[13]. Thus, they contribute to regulating the digestive activity of the intestine and to mucosal protection. Another rare secretory cell subset of the intestinal epithelium are the **tuft cells**[14,15]. Tuft cells act as chemosensory cells, which produce and release endogenous opioids and inflammatory mediators such as prostanoids. Furthermore, they are believed to serve as the only source of interleukin-25 (IL-25) in the gut and to play a crucial role against parasitic infections and allergic responses[16].

Microfold cells (M cells) are specialized epithelial cells, which are located at specific positions of the intestinal epithelium. In particular, they reside in the follicle-associated epithelium (FAE), which covers the secondary mucosa-associated lymphoid tissue (MALT) of the gut such as the Peyer's Patches[6]. In addition to the FAE sites, cells refereed to as villous M cells can be found in the villi compartment. M cells' primary role is to transfer antigens from the intestinal lumen to intraepithelial antigen-presenting cells in the subepithelial lymphoid tissues[6]. Thus, they function as antigen-sampling cells responsible for

controlling the lumen content and are able to initiate an immune response in the presence of danger signals from pathogenic microoorganisms[17,18]. M cells are characterized by a unique morphology, which facilitates their antigen-sampling role. First of all, in contrast to the typical enterocytes, their apical side is covered with a short microvilli which enables close contact with microorganisms. Secondly, at their basal side, they are characterized by a pocket-like structure occupied by lymphocytes, macrophages or dendritic cells[6]. In addition, they present a unique glycosylation pattern by expressing the α-(1,2)-fucose and the glycoprotein 2 (GP2) on their surface, which facilitates bacteria binding and transcytosis[19].

Paneth cells are situated at the base of the crypts exclusively in the region of the small intestine. They are secretory cells that produce and release a diverse array of antimicrobial substances such as lysozymes, cathelicidins, defensins and C-type lectins[20,21]. In addition to this, they have an essential role in development, homeostasis and maintenance of the stem cell niche by providing a range of different growth factors to the Lgr5+ stem cells[22]. To be able to release high amounts of antimicrobial peptides and growth factors, Paneth cells are characterized by an extensive endoplasmic reticulum and Golgi system, which creates a lot of granules. Contrary to the other short-lived intestinal cell populations, Paneth cells are retained at the bottom of the crypts after their differentiation and live approximately six to eight weeks[14,22].

Intermingled with the Paneth cells, around ten to fifteen **pluripotent stem cells** are found at the very base of each crypt, which fuel the continuous self-renewal of the intestinal epithelium throughout life[23,24]. These Lgr5+ stem cells, known also as crypt base columnar (CBC) cells, are dividing approximately once per day, giving rise to one stem cell and one transient amplifying (TA) cell[9,25]. TA cells are rapidly proliferating, migrating upwards the crypt-villus axis and differentiate into one of the five specialized intestinal cell lineages: enterocytes, Goblet cells, enteroendocrinocytes, tuft cells and M cells[14]. The identity of each lineage is specified through a complex network of transcription factors, which are expressed in the presence of specific growth factors, cytokines, mitogenic stimuli and differentiation signals provided from the Paneth cells and the surrounding stroma cells.

1.1.2 Immune response at the intestinal epithelium

Numerous professional subepithelial **immune cells** such as T and B lymphocytes, macrophages, dendritic cells and intraepithelial lymphocytes (IELs) cohabit with the intestinal epithelium[4]. In particular, they are scattered through the lamina propria layer or they are collected in Peyer's Patches or other sites of the mucosa-associated lymphoid

tissue (MALT). From these sites squeezed between the epithelial cells, the immune cells extend protrusions (transepithelial dendrites) to sample the content of the intestinal lumen and to elicit an adaptive immune response upon the recognition of foreign antigens or components of pathogenic microorganisms.

However, multiple studies have demonstrated that the central mediator between the subepithelial immune cells and the luminal content is the intestinal epithelium. Being in a constant interplay with these professional immune cells, the intestinal epithelial cells (IECs) function as antigen presenting cells, which sample the external environment, decode the information and shift their gene expression profile to shape the epithelial host defense and to orchestrate the response of the adaptive immune branch[5,7]. Together with their primary role in the development of anti-pathogenic responses, IECs have the unique ability to direct a tolerogenic and immunoregulatory response by being in continuous interaction with symbiotic commensals. How IECs manage to tolerate the microbiota, while maintaining full responsiveness against enteric pathogens remains unclear. However, taking into account the importance of this finely tailored response in regulation of gut development, homeostasis, disease and inflammation, specific strategies of IECs have been proposed and discussed recently to explain how this subtly tuned balance is generated.

IECs express a diverse variety of pattern-recognition receptors (PRRs) such as Toll-like receptors (TLRs), RIG-I-like receptors (RLRs) and NOD-like receptor (NLRs), which recognize a wide range of pathogen-associated molecular patterns (PAMPs), associated with pathogenic bacteria, parasites and viruses as well as with the commensal flora, nutrient-derived stimuli and self antigens[4,26–28]. Upon infection, PRRs' stimulation initiates several signaling cascades to protect IECs against pathogens. Interestingly, in homeostatic conditions PRRs are also stimulated by several microbial stimuli present in the gut lumen but without causing a pro-inflammatory response. This constant homeostatic epithelial signaling has been proposed to be essential for the development of immune tolerance in IECs and for the maintenance of intestinal epithelial barrier integrity[26,29].

A second important feature of IECs that contributes to their altered responsiveness is their polarized organization. IECs are highly polarized cells with their apical side facing the lumen of the gut and their basolateral side attached to the lamina propria. Interestingly, taking into account that only the apical side of IECs is exposed to environmental stimuli and luminal microbes, it has been demonstrated that the localization of innate immune receptors in IECs is also influenced by the polarized nature of the cells[18,26,30,31].

Additionally, IECs posses the property of horizontal communication by lateral diffusion of

small molecules and signaling messengers or through gapjunctional intracellular pathways[4]. This form of cell-to-cell communication allows transferring of immune signals to neighboring cells and may also facilitate a well-orchestrated response on infection or tolerance to commensals[32–34].

Taken all together, homeostatic stimulation of innate immune receptors in combination with their functional compartmentalization and horizontal cell-to-cell communication are strategies that IECs have developed to tolerate the presence of the commensal microbiota while maintaining responsiveness against enteric pathogens.

1.2 Interferons

1.2.1 Interferons: Roles and classification

Over fifty years have passed since interferons (IFNs) have been discovered by Isaacs and Lindemann for their ability to ''interfere'' with influenza virus replication[35]. Since then it has been shown that animals can be protected against invading viruses and a diverse range of different pathogens via IFN-mediated innate immune responses[36]. When cells sense viral products, IFNs are produced and released, which in turn act in an autocrine or paracrine manner inducing the transcription of hundreds of antiviral molecules responsible for restriction of viral infection in target cells[37]. However, it is only the past decade that the complicated network of IFN family members, from their expression and signaling to their pleiotropic functions and therapeutic potential, has begun to be unraveled[38–40]. The IFN family of cytokines is divided into three types: I, II and III, based on common features in gene sequence, protein structure, expression pattern, receptor engagement and biological roles (Table 1).

Type I IFNs

Type I is the first group of IFNs discovered[35]. It is the largest and most thoroughly studied group within this cytokine family. In humans, type I IFNs consist of five subtypes: IFN-α, IFN-β, IFN-ε, IFN-κ, and IFN-ω[41–43] (Table 1). The human genome possesses 13 *IFN-α* genes (*IFN-α1-13)*, with *IFN-α1* and *IFN-α13* encoding for identical protein sequences[44]. Type I IFN genes are syntenic in a single locus on chromosome 9 and show sequence homology, which suggests that their origin may have been from a common ancestor gene and the subtypes arose from duplication and diversification events[45]. Additionally, in mammals, all type I IFN genes lack introns, apart from *IFN-κ* gene, which has an intron in the 3'-UTR[43,44].

Table 1: Members of the human interferon (IFN) family. Adapted from Takaoka and Yanai, (2006)[31].

Type	Subtype	Receptors	Gene locus	Amino acid residues	Molecular Weight (kDa)
I	IFN-α	IFNAR1/IFNAR2	9p21	165-166[a]	15-23
I	IFN-β	IFNAR1/IFNAR2	9p21	166[a]	15-23
I	IFN-ε	IFNAR1/IFNAR2	9p21	208	24.4
I	IFN-κ	IFNAR1/IFNAR2	9p21	180[a]	24.5
I	IFN-ω	IFNAR1/IFNAR2	9p21	172[a]	20-23
II	IFN-γ[b]	IFNGR1/IFNGR2	12q24.1	146[a]	34
III	IFN-λ1	IFNLR1/IL10Rb	19q1	200	20-33[c]
III	IFN-λ2	IFNLR1/IL10Rb	19q1	200	22
III	IFN-λ3	IFNLR1/IL10Rb	19q1	196	22
III	IFN-λ4	IFNLR1/IL10Rb	19q1	179	20

[a]: signal peptides are not included
[b]: acts as a homodimer
[c]: due to its glycosylation

Type I IFNs are pleiotropic cytokines, which exhibit a wide diversity of biological functions including antiviral, anti-proliferative and immunomodulatory activities in innate and adaptive immune responses. Since their pharmaceutical approval, type I IFNs, have also been used as potential anticancer agents and as treatment against several microbial infections[46]. Although type I IFNs are produced by almost all cell types, the different subtypes present some degree of cell type-specific expression. In particular, IFN-α is primarily expressed by leukocytes[47], with plasmacytoid dendritic cells (pDCs) to serve as the main source upon viral infection[48,49]. IFN-β is produced by most cell types, especially fibroblasts[50]. Similar to IFN-α, IFN-ω is mainly produced by leukocytes and shows similar biological functions[51], whereas IFN-κ expression is limited to keratinocytes and IFN-ε is mainly associated with the antiviral protection of the female reproductive tract[43,52]. Interestingly, apart from their limited structural similarity, all 17 subtypes signal through a common ubiquitously expressed heterodimeric receptor complex, composed of a single chain of IFN-α receptor 1 (IFNAR1) and IFN-α receptor 2 (IFNAR2)[41,53].

Type II IFNs

Contrary to type I IFNs, the type II IFN family consists of a sole member (IFN-γ), which signals as a homodimer and shows low sequence similarity with the other IFNs[54] (Table 1). IFN-γ is mainly expressed by immune cells and especially by macrophages, natural killer cells and activated T cells and although its production is not directly induced by viral infection, it shows response against viruses, as well as against intracellular bacteria and parasites[55]. In addition to this, while type I and type III IFNs are perceived as the main antiviral mediators, IFN-γ is frequently considered as an immunomodulatory cytokine. IFN-γ interacts with a tetrameric complex, including two subunits of IFN-γ receptor 1 (IFNGR1) and two subunits of IFN-γ receptor 2 (IFNGR2)[54]. IFNGR ternary complex presents a broad tissue expression pattern, giving the potential that all cell types can respond to IFN-γ[56].

Type III IFNs

More recently in 2003, the first members of type III IFN family, also termed as IFN-λs were discovered by two independent research groups. These novel cytokines, were initially characterized to exert antiviral activity similar to those of type I IFNs[38,39]. Initially, they were named interleukin-28 (IL-28) and IL-29 and grouped together with IL-10 family members based on their interaction with the IL-10 receptor subunit 2 (IL-10R2). However, subsequent studies have provided increasing evidence for their functional similarity with type I IFNs and for this they were considered as ‘’interferon-like cytokines’’[57,58].

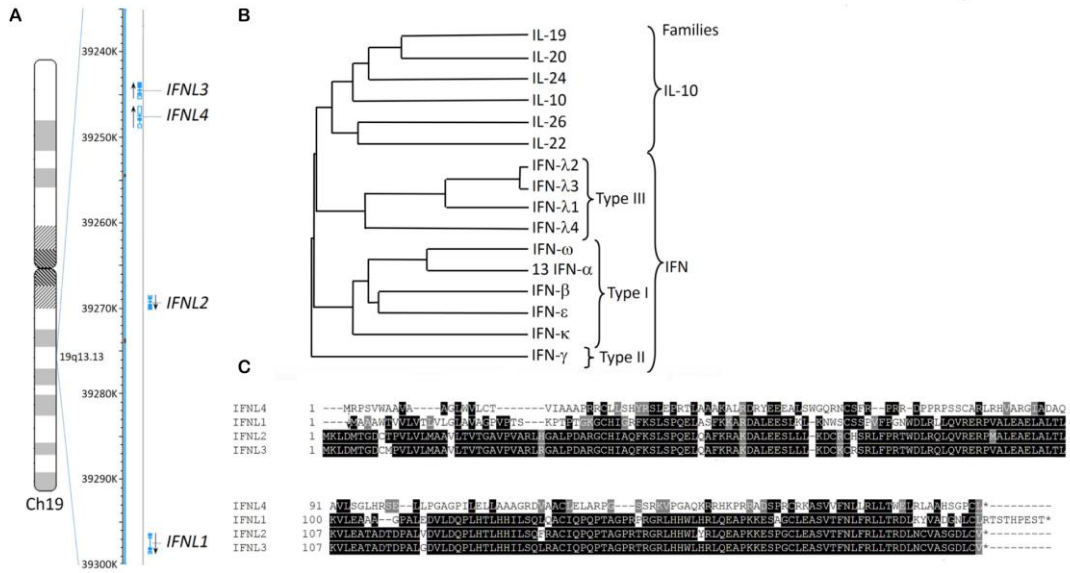

Figure 2. Human type III IFNs. (A) Schematic of the genomic organization of *IFNL* genes in human chromosome 19. (B) Phylogenetic tree of type I, II and III IFNs together with members of the IL-10

family of cytokines. (C) Protein sequence alignment of type III IFNs. Adapted from Kotenko and Durbin, (2017)[44].

In humans, the type III IFN family consists of four members: IFN-λ1 (IL-29), IFN-λ2 (IL-28A), IFN-λ3 (IL-28B) and IFN-λ4[44] (Table 1). All type III IFN genes are clustered on human chromosome 19 (Figure 2A). Whereas in mice, two functional orthologs exist encoding IFN-λ1 and IFN-λ2 and two pseudogenes *IFNL1-P1* and *IFNL1-P2,* clustered on chromosome 7[59]. All different subtypes of type III IFNs are closely related. For example IFN-λ1 shares a high degree of similarity (around 80%) in amino acid sequence with IFN-λ2 and IFN-λ3[39,60] (Figure 2B and 2C). Interestingly, IFN-λ2 and IFN-λ3 have almost indistinguishable amino acid sequences, 96% homology, which suggests that the evolution of type III IFNs has been subjected to positive selection via recent duplication events[39,60]. This might also reflect important and unique biological functions for type III IFNs, independently from the members of type I IFN family[61].

IFN-λ4 is the most recently described member of the family. It was identified in 2013 from genetic data in primary hepatocytes based on its 28% amino acid identity with the other type III IFNs[40]. This low similarity with the other type III IFN genes might suggest that IFN-λ4 has been introduced through a distinct duplication event[58]. The IFN-λ4 gene is located upstream of IFN-λ3 (Figure 2A) and is expressed only in a fraction of the human population, as in the most of individuals is out of frame and non-functional[40,62]. Due to a genetic polymorphism, in some individuals a 5'-proximal frameshift mutation is introduced which restores transcription of IFN-λ4 gene and the functional version of IFN-λ4 protein is produced, which shows antiviral potency similar to the other type III IFNs[63]. Notably, chronic hepatitis C virus (HCV) patients who express a functional IFN-λ4 version have been associated with poor spontaneous or IFN-α-induced clearance of HCV[64,65]. Thus it remains a paradox, how IFN-λ4 can block viral replication on one hand and on the other hand leads to HCV resistance to IFN-α treatment[65,66].

Contrary to their common functional characteristics, type III IFNs share limited homology with type I IFNs, such as 15-19% of similarity in their amino acid sequence with IFN-α[39,60]. However, type III IFNs have been shown to share homology also with members of the IL-10 family of cytokines, showing similarity of 11-13% in amino acid sequence with IL-10 and of 15-19% with IL-22[39,60] (Figure 2B). Despite this poor sequence conservation, type III IFNs have been shown to be closely associated in structure with the IL-10 superfamily cytokines[67–69], which is related also with the fact that both type III IFNs and the cytokines of the IL-10 family signal through a common receptor subunit (IL-10R2). In addition to this, it

has been shown that the complex structures of IFN-λ1/IFNLR1, IL-10/IL-10R1 and IL-22/IL-22LR1 present high similarity in their ligand-receptor docking topology[68–71].

Type III IFNs signal via a distinct heterodimeric receptor complex, composed of two chains: a unique alpha chain, the IFNLR1 (also known as IL-28Ra) and the IL-10Rb chain, which serves as a common receptor subunit for all the members of the IL-10 family (IL-10, IL-22 and IL-26)[41,72]. Whereas the IL-10Rb subunit is broadly distributed in various cell types, the expression of IFNLR1 chain is predominately restricted to epithelial cells[73–80]. In addition to this preferential expression of IFNLR1 in epithelial cells of the lung, skin, gastrointestinal tract, reproductive tract and liver, also some immune cell populations, such as specific subsets of conventional dendritic cells (cDCs), plasmacytoid dendritic cells (pDCs), human monocyte-derived macrophages and neutrophils have been demonstrated to express IFNLR1 and in turn, it has been shown that type III IFN stimulation can significantly affect their immune properties[74,81–89]. Of note, in recent years, further investigation of type III IFN responses in immune cells has resulted in some controversial results about which immune cells express IFNLR1 or respond to type III IFNs[90,91].

Therefore, the limited distribution of IFNLR1 and cellular responsiveness to type III IFNs might reflect unique properties of these cytokines for the epithelium of mucosal surfaces. This hypothesis is further supported by the fact that epithelial cells are able to generate high amounts of type III IFNs upon viral infection[74,79,80,92–100]. Although, it has been also shown that similarly to type I IFNs, a range of primary human cell types of the hematopoietic lineage can produce type III IFNs, with cDCs and pDCs to serve as the main source among them[83,85,101–103].

1.2.2 Induction of type I and type III IFN production

Apart from the central role of IFNs in controlling viral infections in all the different stages of viral lifecycle, there is an ever expanding set of functions discovered for type I and type III IFNs ranging from effects on cellular physiology such as regulation of cell survival, differentiation and proliferation, protein translation and metabolism to regulation of non-viral pathogenic infections and non-infectious diseases such as auto-immune and auto-inflammatory conditions and cancer[45,46,89,104–109]. Therefore, it is not surprising that the expression of type I and type III IFNs is the result of an intricate network of different signaling pathways, molecular elements and transcriptional factors tightly regulated and well-coordinated in all the different stages of IFN production. Additionally, the expression and action of many of these elements, responsible for IFN production, are themselves subjected

to both type I and III IFN control, leading to an even more complicated network of overlapping feed-forward and feedback loops[45,110].

Induction of type I and type III IFN production by PRRs

Upon invasion of viruses, type I and type III IFN production is mediated by PRRs located on the cell surface or the endosomes, which sense a broad range of PAMPs including viral ligands, such as nucleic acids[51,111] (Figure 3). On the endosomes, viral nucleic acids are sensed by the membrane-bound Toll-like receptors (TLRs), including TLR3, TLR7, TLR8 and TLR9[47,58,74,101,112,113]. Whereas, in the cytosol pathogen-derived RNA is recognized by the three members of the retinoic acid-inducible gene 1-(RIG-I)-like family of receptors (RLRs): the RIG-I, melanoma differentiation-associated protein 5 (MDA5), and laboratory of genetics and physiology 2 (LGP2)[47,114]. In addition, cytoplasmic DNA is recognized by the recently identified receptor cyclic GMP-AMP (cGAMP) synthase (cGAS), leading to IFN induction[47,115] (Figure 3). While the PRRs responsible for type I and type III IFN production predominantly overlap, there is one exception of the cytosolic DNA sensor Ku70, which has been demonstrated to cause induction of type III IFNs but not type I[116,117].

Toll-like receptors (TLRs)

TLRs are type I transmembrane proteins, acting as predominant PRRs that recognize a broad range of pathogenic ligands and DAMPs. Up to now, ten TLRs (TLR1-10) have been identified in human and mice and three more (TLR11-13) have been described only in mice[111,118]. Of the human TLRs, TLR3, TLR7, TLR8 and TLR9, act in endosomes, and are the most relevant to virus infection and IFN production, as they specialize in detecting viral genome or intermediates of virus replication (Figure 3). In particular, TLR3 binds to double stranded RNA and can recognize dsRNA viruses such as reoviruses[119,120]. TLR7 and TLR8 are functionally related and can bind to single-stranded RNA of viruses. TLR9 binds to unmethylated CpG DNA on bacteria genome and viral DNA[118]. TLR7, TLR8 and TLR9 are expressed in a cell-specific manner and are mainly produced by innate immune cells, with pDCs to serve as the main cell type related to virus recognition and IFN production downstream of these TLRs[50,111]. While TLR3 is present in a range of different cell types including epithelial cells, endothelial cells, fibroblasts and astrocytes[111]. Interestingly, apart from its endosomal localization, the presence of TLR3 has been reported at the basolateral cell membrane of ileal and colonic epithelium[27] and mainly at the apical surface of tracheal epithelium, leading to type III IFN production upon stimulation[94].

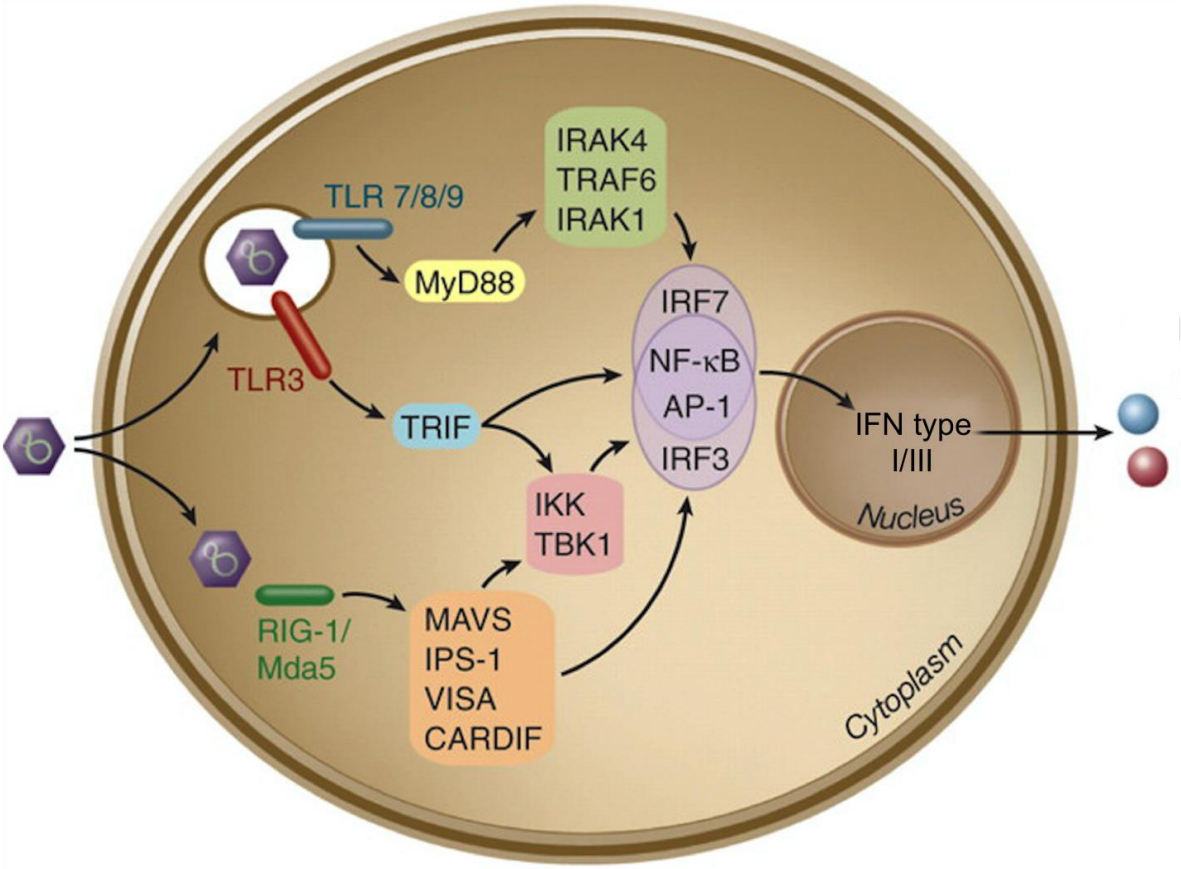

Figure 3. Induction of type I and type III IFN upon viral infection. Viral products are sensed by intracellular pattern recognition receptors (PRRs), localized on the endosomes such as TLR3, 7, 8, and 9 or in the cytoplasm like RLRs (RIG-1 or MDA5), which in turn mediate IFN production through a range of different signaling pathways involving the IRFs, the NF-kB and the MAPKs. Adapted from Garcia-Sastre and Biron, (2006)[356].

All TLRs share a common structure consisting of an ectodomain with multiple leucine-rich repeats, responsible for ligand binding, a transmembrane domain and a cytoplasmic Toll-interleukin (IL)-1 receptor (TIR) domain[111,118]. Ligand binding to TLR3, TLR7, TLR8 and TLR9 results in TLR dimerization and recruitment of TIR containing adaptor molecules such as the myeloid differentiation factor 88 (MyD88) and TIR-domain-containing adaptor-molecule 1 (TRIF)[57,111]. Downstream of MyD88 and TRIF, a number of other signaling elements are recruited leading to the activation of three distinct pathways involving the IkB kinases (IKK) complex, TANK-binding kinase 1 (TBK1)/IKKe complex and the MAPK pathway[121]. In turn the IKKs promote downstream activation and nuclear translocation of nuclear factor kB (NF-kB)[57,122], while TBK1 and IKKe phosphorylate and activate members of the interferon regulatory factor (IRF) family of transcriptional factors[123]. All together these pathways lead to the transcription of IFNs and other pro-inflammatory cytokines and chemokines.

RIG-I like receptors (RLRs)

RLRs belong to the DExD/H box RNA helicase family. They function as cytoplasmic helicases, present in all cell types, and are responsible for the recognition of RNA derived from viruses and in some cases bacteria[124] (Figure 3). The different RLRs present ligand-dependent specificity. RIG-1 typically signals the presence of short 5′-triphosphate uncapped double or single- stranded RNA[125,126]. MDA5 recognizes longer and branched double-stranded RNA molecules[125], while LGP2 serves as an auxiliary receptor in fine-tuning the innate immune response upon RNA sensing[127]. As far as the recognition of enteric viruses by RLRs is concerned, it has been shown that MRV is recognized by both RIG-I and MDA5[128], while other enteric viruses such as members of the picornavirus family, are recognized by MDA5[129].

In the absence of their ligands, RLRs are in an inactivated state. Upon binding of dsRNA or 5'ppp-RNA to the central cleft in their C-terminal domain (CTD), a conformational change is induced, which uncovers their N-terminal caspase activation and recruitment domain (CARD)[130]. In turn, through their CARD domain, RLRs associate with the CARD domain of the membrane bound mitochondrial antiviral-signaling protein (MAVS), also known as IPS-1, VISA and Cardif[131] and induce the aggregation of MAVS to a prion-like structure on the outer surface of mitochondrial membrane[132]. Following aggregation, MAVS promotes the recruitment of the kinases IKKs and TBK1, as well as members of the MAPKinase pathway, leading to the expression of type I and III IFNs and inflammatory cytokines via activation of the transcriptional factors NF-kB, IRFs and AP-1[133].

1.2.3 Transcriptional regulation of type I and III IFN gene expression: shared and distinct mechanisms

The general paradigm of type I and type III IFN gene activation, involves the recruitment of specific transcription factors including NF-kB, IRFs and AP-1, which are activated downstream of the PRRs (Figure 4). In particular, the promoter of *IFN-β* gene consists of four positive regulatory domains (PRDI-IV), localized in close proximity. PRDI and PRDIII, serve as the binding sites for IRF3 and IRF7, respectively, while the p50/RelA NF-kB complex interacts with PRDII and the ATF-2/c-Jun AP-1 complex is recruited in the PRDIV site of the *IFN-β* gene promoter[134]. Notably, it has been shown that upon viral infection, expression of the *IFN-β* gene requires the well orchestrated and cooperative binding of all these transcriptional factors in a complex known as the "enhanceosome"[134–136]. While IRF3 and IRF7 play a universal role in the induction of type I IFNs, the temporal sequence of their

engagement in the promoter of the IFN genes varies. Specifically, IRF3, being ubiquitously and constitutively expressed in cells, functions as the early activator upon viral infection, whereas IRF7 requires an IFN positive feedback loop for its expression and acts with delayed kinetics[45,110,137].

In contrast with IFN-β, the IFN-α gene expression requires the binding only of the members of the IRF transcription factor family[138] and is preferentially expressed by IRF7[139] (Figure 4). Except for IRF3 and IRF7, IRF1, IRF4, IRF5 and IRF8 have been described to be involved in the expression of the different IFN-α subtypes in a cell type-dependent manner[138]. This diversity of different IRF transcriptional factors may reflect a degree of gene specific regulation for the different type I IFN subtypes, as their promoters may present differential affinities for each IRF element[45,139].

The expression of type III IFN genes has been shown to be mediated by either the IRF or the NF-kB signaling pathway[114,140,141], without AP-1 being involved[114] (Figure 4). Again, contrary to type I IFNs, IRF3, IRF7 and NF-kB can act independently on type III IFN promoters, without the need of acting in concert for type III IFN synthesis[142,143]. However, there are also similarities in the regulation of type III and type I IFN genes. Specifically, it has been described that the early expression of *IFNL1* displays similar regulation as the *IFN-β* gene, induced by NF-kB, IRF3 and IRF7. While similarly to *IFN-α* gene, the *IFNL2* and *IFNL3* expression depends more on IRF7 and seems to be delayed[141,144]. Based on this, a positive feedback mechanism between type I and III IFN production has been described, with both IFN-λ1 and IFN-β being able to prime IFN-α, IFN-λ2 and IFN-λ3 gene expression through IRF7 upregulation upon viral infection[110,137,145].

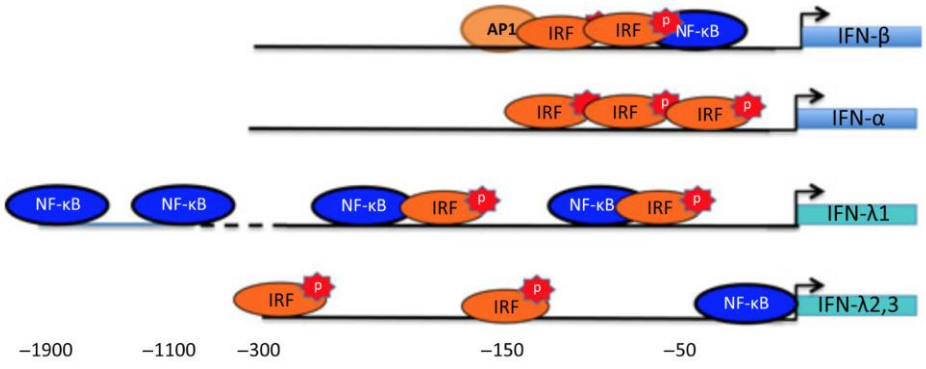

Figure 4. Promoter and enhancer regions involved in type I and type III IFN expression. A similar set of transcriptional factors regulates type I and type III IFN production with distinct mechanisms. *IFN-β* promoter activation requires coordinated binding of IRFs, NF-kB and AP1, while *IFN-α* transcription is mainly dependent on IRFs. *IFN-λ1* gene can be activated by either IRFs or NF-kB and *IFN-λ2,3* expression is largely IRF7 dependent Adapted from Durbin et al., (2013)[51].

1.3 Type I and type III IFN signaling and the effector mediators from the IFN receptor to the nucleus

Upon secretion, type I and type III IFNs act in an autocrine, paracrine, or systemic manner to induce different cellular responses, with their antiviral activity through the expression of antiviral genes to be the best characterized. IFN-induced assembly of the receptor ternary complex happens sequentially in a two-step binding event, which induces a conformational change in the intracellular part of the receptor subunits. The IFN receptor does not contain any catalytic activity. Upon IFN-induced receptor activation, members of the receptor-associated janus kinases (JAK) family, which are constitutively associated with the IFN receptor, are activated and in turn phosphorylate receptor tyrosine residues. This phosphorylation mediates the recruitment of signal transducer and activator of transcription (STAT) proteins, which are then phosphorylated by JAKs. STAT activation results in homo- or heterodimerization of STATs and the formation of the IFN-stimulated gene factor 3 (ISGF3) complex, consisting of STAT1, STAT2, and IRF9. Translocation of ISGF3 or dimers of STATS to the nucleus regulates the expression of ISGs (Figure 5).

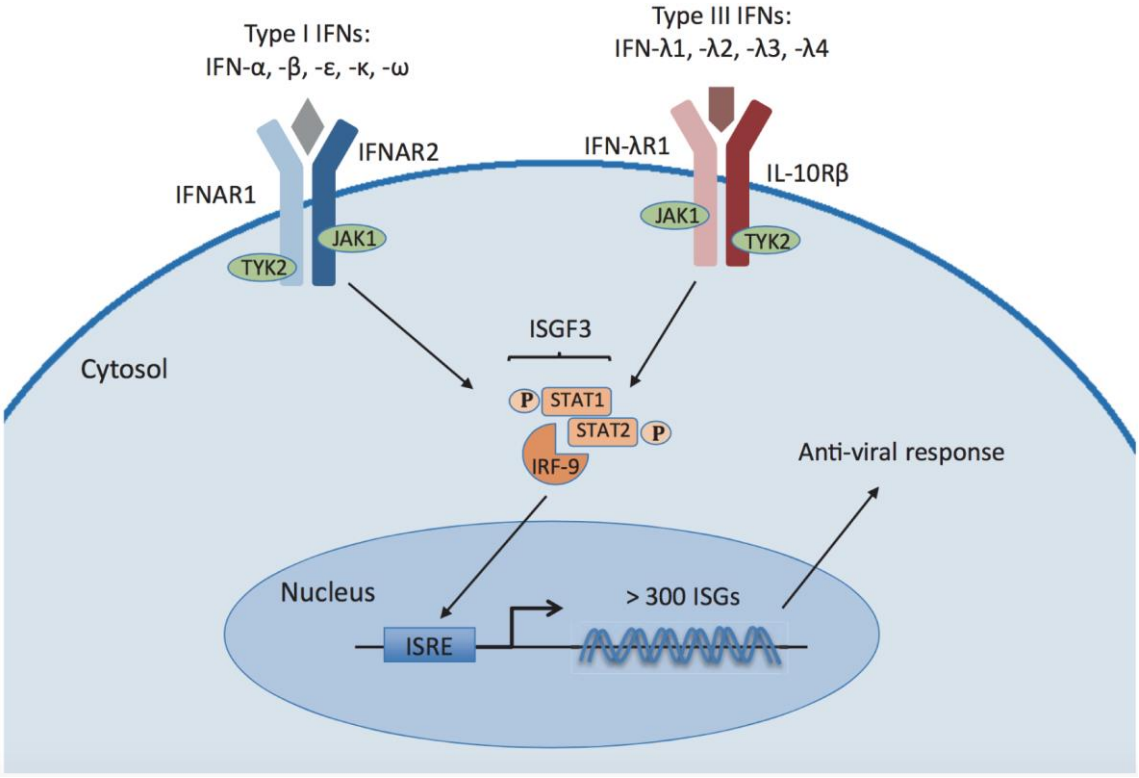

Figure 5. Classical type I and type III IFN signaling pathway. Type I and type III IFNs signal through distinct complexes of heterodimeric receptors, which lead to the activation of the same JAK/STAT signaling cascade. Downstream of receptor activation, phosphorylated STAT1/STAT2 together with IRF9 form the ISGF3 complex, which translocates into the nucleus and induces the upregulation of hundreds of interferon-stimulated genes (ISGs) Adapted from Galani et al., (2015)[60].

1.3.1.1 Type I and III IFN receptor system

All the IFN receptors belong to the class II helical cytokine receptors (hCRs) family, which includes the receptors also for tissue factor (TF), IL-10, IL-20 and IL-22, and are characterized by a type III fibronectin (FBN-III) domain in their extracellular region[72,146]. In the type I IFN receptor complex, IFNAR1 is considered the low affinity binding chain, while IFNAR2 serves as the high affinity one[147–151]. Remarkably, IFNAR1 is also required for the recognition of the different type I IFN subtypes[152,153]. It has been shown that the binding affinity to the IFNAR complex varies toward the different type I IFNs, correlating with the differences in the biological activities of type I IFN subtypes[150,154]. While all IFN-αs present similar low affinity for IFNAR1, IFN-β binds IFNAR1 more tightly[149,151]. This difference is in turn reflected in a stronger antiviral, anti-proliferative and transcriptional activity of IFN-β compared to IFN-α[154,155]. In addition to this, binding of the different type I IFN subtypes to their receptor might cause a different conformational assembly of the receptor ternary complex leading to differential activities[156]. Interestingly, it has also been reported that IFN-β is able to signal only by binding to the IFNAR1 subunit[52].

Although, two splice variants of IFNAR1 have been identified, further bioinformatic analysis confirmed the presence of only one variant, suggesting cell type specific expression of the former or an experimental artifact[157,158]. Unlike IFNAR1, IFNAR2 exists as three isoforms: IFNAR2c, IFNAR2b and the soluble form sIFNAR2a[152,153]. They are all generated from the same gene by alternative splicing and possible protease processing. Among them, IFNAR2c is the productive ‘’long’’ transmembrane form of IFNAR2, containing all the crucial signaling domains and thereby being responsible for the antiviral function of type I IFNs[147]. IFNAR2b is a short transmembrane form lacking the intracellular domain and suggested to serve as a decoy receptor blocking the IFN signaling[159]. sIFNAR2a is truncated before the transmembrane region and shown to circulate in the blood acting as either an agonist or antagonist. An alterative role suggested to be ascribed to sIFNAR2a is to mediate IFN biological effects by a mechanism known as ‘’trans-signaling’’, whereby sIFNAR2a can bind IFN-α or IFN-β and present them to IFNAR1, resulting in the induction of the IFN signal[160,161].

In type III IFN receptor complex, IFNLR1 (IL28RA) exists in three different isoforms generated from alternative splicing: IFNLR1v1, IFNLR1v2 and IFNLR1v3. IFNLR1v1 and IFNLR1v2 differ in their intracellular region, where IL28RAv3 is lacking a region of 29 amino acids. IFNLR1v3 is a truncated form predicted to serve as a non-functional soluble IFNLR1 form, as it is missing the transmembrane and the extracellular domains[39]. Expression of a non-functional splice variant has been reported in pDCs[162]. Unlike type I IFNs, which signal

through their own unique receptor complex, the second chain of the type III IFN receptor complex, IL10RB is engaged also in the signaling cascade of IL-10, IL-22 and IL-26. Interestingly, a functional crosstalk of type III IFNs with IL-22 and IL-10 has been shown. In particular, in the presence of IL-10, inhibition of the type III IFN activity has been reported, suggesting a competition of type III IFNs with IL-10 for the IL10RB receptor[163]. Conversely, in a recent study, enhancement of the signaling activity and the antiviral properties of type III IFNs was shown in the presence of IL-22[96].

In type III IFN receptor ternary complex, the IFNLR1 chain binds type III IFNs with high affinity, while IL10RB is the low affinity subunit. However, in comparison with type I IFNs, the binding affinity of type III IFNs for their receptor complex is much lower[67,68]. Even though all subtypes of type III IFN family bind to the same receptor complex, differences in their biological activities have been described. In particular, it has been shown that IFN-λ3 exhibits the highest potency among the different human type III IFNs, which is reflected in their signaling and biological activity[164,165].

1.3.1.2 Regulation of type I and III IFN receptor cell surface levels

Regulation of the IFN receptor cell surface levels by internalization and degradation, is considered to be the most specific and rapid step to limit IFN responses[166]. In a ligand dependent manner, the ternary IFNAR complex is internalized by clathrin-mediated endocytosis[167,168] (Figure 6). Several differences have been noted in the downregulation mechanisms of IFNAR1 and IFNAR2[153]. Remarkably, upon type I IFN stimulation, IFNAR1 is rapidly endocytosed and routed for lysosomal degradation, whereas after endocytosis, IFNAR2 can be recycled back to the cell surface or degraded[169,170].

Based on these studies, the mechanism of internalization and degradation of the ternary IFNAR complex is mainly determined by the endocytosis of IFNAR1 chain. In particular, a linear tyrosine based sequence in IFNAR1 serves as an endocytic motif, which is recognized by the AP2 endocytic complex. In basal levels, this motif is constitutively associated with TYK2 and remains masked from AP2[167,168]. Upon stimulation, phosphorylation of this motif decreases its binding with TYK2 and facilitates its exposure to AP2. This mechanism explains the importance of TYK2 for IFNAR1 cell surface stability[171,172]. In addition, several ubiquitination sites within the cytoplasmic region of IFNAR1 have been described to facilitate its degradation[167,173–175]. Notably, the cell surface levels of IFNAR2 seems not to be regulated through ubiquitination dependent degradation[176]. Unlike the various mechanisms proposed to regulate the IFNAR cell surface levels, there is no literature available

concerning the molecular mechanisms underpinning the IFNLR internalization and recycling.

1.3.1.3 Regulation of JAK activation

The next step in the regulatory network of IFN responses, targets the interaction of IFNAR and IFNLR with downstream signaling elements. This step includes the interactions of IFN receptor with the members of the JAK family. In particular, in the course of the canonical type I and type III IFN pathway TYK2 pre-associates with IFNAR1 and IL10RB, while JAK1 binds constitutively IFNAR2 and IL28RA. Interestingly, in two recent studies it was shown that JAK2 can be phosphorylated and activated downstream of the IFNLR and plays a specific role in the antiviral activity of type III IFNs[114,177].

Binding of the IFN, changes the proximity of the IFNAR1 and IFNAR2 and subsequently of the two kinases, leading to their activation via trans-phosphorylation at tyrosine residues Y1022 and Y1023 for JAK1 and Y1054 and Y1055 for TYK2[51]. Activated JAKs phosphorylate IFN receptor chains at multiple sites, creating docking sites for STAT1 and STAT2 via their SH2 domain. Within the intracellular region of IFNAR2 tyrosine phosphorylation at residues Y337 and Y512 have been shown to be crucial for STAT1 and STAT2 recruitment[178], while Y466 on IFNAR1 is also considered important for STAT2 activation[179]. Multiple other sites have been reported to play a role in IFNAR signaling in different human or mouse cell lines[51].

Although the IFNLR activation has not been investigated in such a detail, two tyrosine residues on IFNLR1 Y343 and Y517 have been shown to mediate STAT2 activation. Notably, the Y343 based motif of IFNLR1 resembles the sequence surrounding the Y466 of IFNAR1 and the C-terminal sequence including the Y517 of IFNLR1 shows some similarity with the C-terminal sequence containing the Y512 of IFNAR2[51,180]. Although these motifs reflect a degree of similarity in the STAT2 docking sites between IFNAR and IFNLR, the intracellular regions of IFNAR2 and IFNLR1 are dramatically different[145]. Interestingly, a recent study has reported striking differences also in the formation of the ligand-receptor complex between type I and III IFNs, suggesting the involvement of different signaling cascades activated downstream of IFNLR or IFNAR complex[181].

1.3.1.4 Negative regulation of JAK activation

As activation of IFN receptors and JAKs is mainly based on sequential phosphorylation events, a number of phosphatases have been shown to negatively modulate these components of IFN signaling cascade. In particular downstream of IFNAR, the protein-

tyrosine phosphatase 1B (PTPB1)[182] and T cell protein-tyrosine phosphatase (TCPTP)[183] have been shown to target TYK2, JAK2 and JAK1 for de-phosphorylation. The transmembrane PTPase CD45 has also been shown to serve as a JAK phosphatase in type I IFN dependent manner[184].

Apart from the reversal of JAKs' activation, another negative regulation in the receptor levels includes the blockade of the binding of IFNR with JAKs. The ubiquitin-specific protease USP18, despite its role in ISGylation of certain substrates, binds IFNAR2 and prevents the interaction with JAK1[185] (Figure 6). This association seems to be ligand dependent, as it inhibits specific signaling from IFN-α subtypes, which bind IFNAR2 with lower affinity in comparison with IFN-β[186–188]. USP18 dependent inhibition of IFN-α responses, can explain the shorter duration of IFN-α responses compared to IFN-β[165,189]. For type III IFNs, there is only one recent study showing a negative impact of USP18 on type III IFN induction of a subset of ISGs in the mouse system[190].

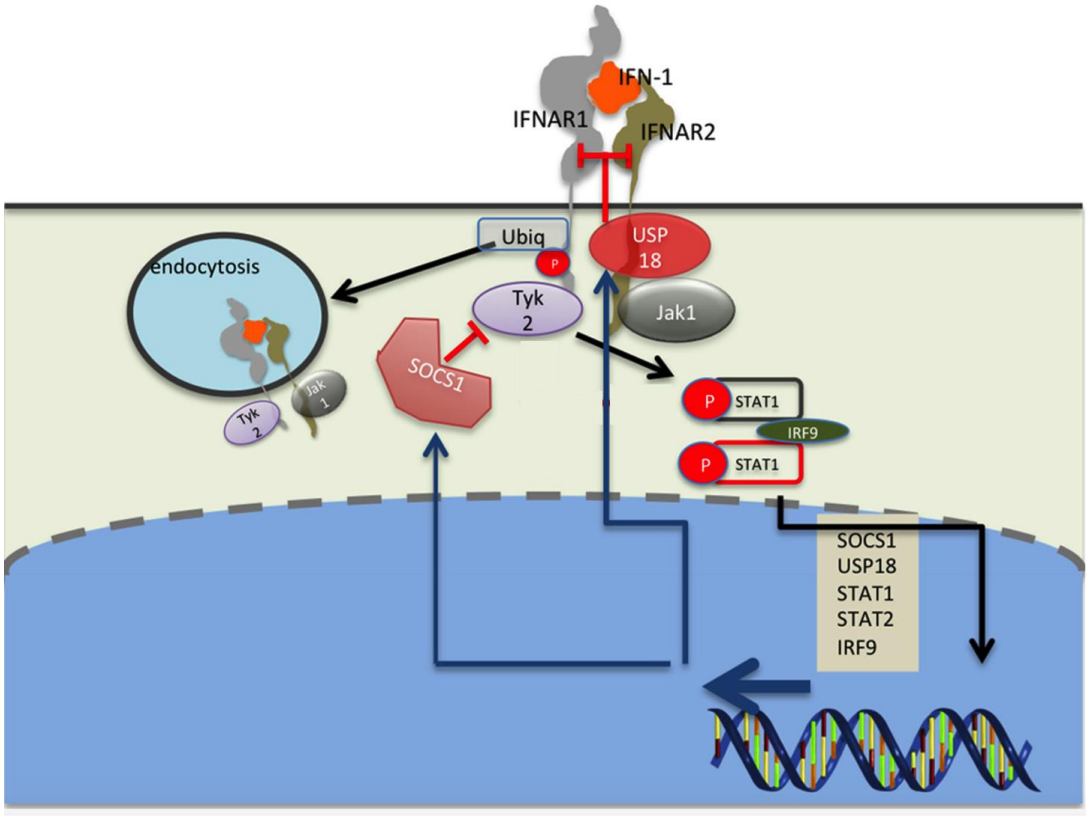

Figure 6. Negative regulation of type I IFN signaling at the receptor level. Upon IFN binding and activation of the JAK/STAT signaling cascade, the IFNAR complex is internalized by clathrin-mediated endocytosis, which is initiated by phosphorylation of IFNAR1 by Tyk2, leading to its ubiquitination. Another layer of IFNAR negative regulation is mediated by members of the SOCs family, which bind to TYK2, or by USP18, which interacts with IFNAR2 and suppresses IFNAR complex formation. These negative regulators are ISGs, which are expressed upon IFN signaling, promoting the negative feedback and ensuring IFNAR receptor inactivation. Adapted from Schreiber et al., (2017)[357].

In addition, members of the suppressor of cytokine signaling (SOCS) family such as SOCS1 and SOCS3 can interact with TYK2 and thereby negatively regulating the activation status of TYK2[191] (Figure 6). Among SOCS, SOCS1 is considered the more potent negative regulator. Recently, it has been shown that a SOCS1 dependent TYK2 destabilization, through ubiquitination, drives IFNAR1 downregulation[192,193]. Interestingly, it has also been described that type III IFNs up-regulate the expression levels of SOCS-1 and SOCS-3, suggesting a possible role of SOCS as negative regulators of type III IFNs signal transduction[194,195]. In addition, it should also be take into account that USP18 and SOCS are ISGs and might serve as a negative feedback loop in type I and type III IFN signaling cascades[153].

1.3.2 Regulation of type I vs type III IFN signaling from the receptor to the nucleus:

1.3.2.1 Regulation of STAT induction

In the canonical type I and type III IFN signaling pathway the next players downstream the IFN receptors and JAKs are STAT1, STAT2 and IRF9, which are regulated at the level of expression and activation. A major layer of control of these factors, which are themselves ISGs, relies on transcriptional regulation. For type I IFN it has been shown, that under homeostatic conditions low quantities of IFN-β are secreted and lead to physiological significant levels of STAT1, STAT2 and IRF9 through an autocrine loop[196]. Interestingly, it has been reported that commensal pathogens can serve as the trigger for this constitutive production of IFN by epithelial and immune cells[197,198]. The maintenance of this pool of STATs and IRF9 in uninfected cells has been shown to be important not only for priming cells for a fast response upon infection but also by regulating the hematopoietic stem cells, activation of immune cells, and for anti-tumor responses. Lack of this constitutive expression has also been reported in autoimmune and inflammatory syndromes[199].

Apart from basal levels of expression in homeostatic conditions, in the presence of a stimulus such as elevated levels of type I, II IFNs or other cytokines such as TNF-α and IL-6, high expression levels of STAT1 and IRF9 lead to prolonged ISG expression and sustained antiviral protection[200–202]. For type I IFN, together with STAT1 and STAT2, STAT3, STAT4, STAT5 and STAT6 have been shown to be induced in certain cell types and participate in the antiviral and anti-proliferative actions of IFNs[203–205]. Similar to type I IFNs, STATs 1-5 can be induced downstream of IFNLR[180,206,207]. However, given that STAT 3, 4, 5 activation by type III IFN has been observed only in few cultured cell lines, these results have to be

explored in a wider range of cells and tissues where the antiviral effects of type III IFN have been reported.

1.3.2.2 Regulation of STAT dimerization

The availability of the different STATs is the crucial determinant in the next step of STAT dependent regulation, which involves the activation of STATs and the formation of homo and heterodimeric STAT complexes. Apart from the STAT1:STAT2 heterodimer, which together with IRF9 forms the ISGF3 transcriptional complex in the canonical type I and III IFN cascade, a wide range of almost all the possible combinations of STATs, including STAT1:STAT1, STAT3:STAT3, STAT4:STAT4, STAT5:STAT5, STAT6:STAT6, STAT1:STAT2, STAT1:STAT3, STAT1:STAT4, STAT1:STAT5, STAT2:STAT3 STAT5:STAT6 have been reported in response to type I IFNs[203,208,209] (Figure 7). The ISGF3 transcriptional complex, binds a specific element in the promoter of ISGs denoted as IFN-stimulated response element (ISRE). However, the rest of the STAT homo and hetero dimers, upon their formation, translocate to the nucleus and show a binding affinity for another element in the promoter of ISGs known as IFN-γ activated site (GAS) element. Interestingly, in the promoter region of ISGs there are multiple STAT binding sites, which can contain only ISREs, only GAS elements or both. In this way, different subsets of ISGs can be activated by differential induction of STAT-containing complexes[203,208–210]. Taken all together, it has become clear that the multiplicity of STAT complexes reflects a degree of ISG specificity.

1.3.2.3 Alternative mechanisms of positive and negative regulation of STAT complexes

Positive regulation of STATs complexes

According to the classical signaling cascade of type I and type III IFNs, JAK dependent phosphorylation of STAT1 and STAT2 on tyrosines Y701 and Y609, respectively, drives their activation, dimerization and translocation to the nucleus. Nonetheless, a number of other modifications have been shown to positively regulate STATs action. For example, upon type I IFN stimulation, phosphorylation of STAT1 and STAT3 on serine S727 by cell specific kinases have been shown to enhance the transcriptional activity of STATs without being required for nuclear translocation[211,212]. Cyclin-dependent kinase 8[213,214], protein kinase C (PKC) family members like PKC-delta (PKC-δ) and PKC-epsilon (PKC-ε)[165,215] and

p38-MAPK pathway[216] have been documented to mediate phosphorylation of STAT1 on S727. In addition, IκB kinase epsilon (IKKε)-mediated serine phosphorylation of STAT1 at residue S708 has been positively related with ISGF3 formation and enhancement of transcriptional activity and antiviral response of type I IFN[123,217]. Interestingly, Bolen et al, have observed serine phosphorylation of STAT1 on residue S727 downstream of type III IFN signaling in hepatocytes[165].

Negative regulation of STATs complexes

In addition, a number of modulators have been demonstrated to negatively modify the functions of STATs and increase the complexity of IFNAR signaling. This is mainly accomplished by members of the protein tryrosine phosphatase family[218]. For instance, Src Homology phosphatase 2 (SHP-2) has been shown to be constitutively associated with IFNAR. Upon type I IFN stimulation, SHP-2 is activated and blocks JAK1, STAT1 and STAT2 phosphorylation[219,220]. In addition, SH2 domain-containing tyrosine phosphatase, SHPTP1, which is mainly expressed by hematopoietic cells, can also inhibit type I IFN induced JAK1 and STAT1 activation in macrophages[221]. Furthermore, nuclear STAT1 tyrosine phosphatases, such as TC45, a nuclear isoform of TCPTB, can target STAT1 and STAT3 phosphorylation downstream IFNAR[222]. Apart from phosphatase-dependent STAT deactivation, phosphorylation of STAT on residue S287 and T387 negatively regulates the transcriptional, antiviral and anti-proliferative actions of type I IFNs[223,224].

STAT1 is also negatively regulated by protein inhibitors of activated STAT (PIAS) family members. Recent studies have shown that PIAS1 and PIASy can bind STAT1 and block its transcriptional activity. In addition, STAT1 is also sumolylated by PIAS1[225,226], but the functional importance of this modification for IFNAR-induced gene activation needs to be further elucidated. Notably, acetylation and methylation sites on STATs have been reported and are proposed as sites for further important post-translational modifications in their regulated architecture[227,228].

1.3.2.4 Un-phosphorylated STAT complexes

In addition to the formation of the canonical ISGF3 complex, in certain milieu, the formation of alternative ISGF3 complexes containing unphosphorylates STATs have been reported. In addition, the ISGF3^{II} complex, including phosphorylated STAT1, unphosporylated STAT2 and IRF9, and the ISGF3-like complex formed by STAT2 and IRF9 have been shown to be assembled mainly upon type I and II IFN treatment[229–231].

1.3.2.5 JAK-STAT independent pathways triggered by type I and III IFNs

Apart from the above-mentioned canonical and non-canonical pathways involving the JAK-STAT axis, there is accumulating evidence that link the ISG transcription upon IFN treatment with a plethora of JAK-STAT independent cascades such as the Crk-like protein (CrkL)–Ras related protein 1 (RAP1) pathway[232–235] the mitogen-activated protein kinase (MAPK) pathway[209,236–238] and the phosphatidyl-inositol 3-kinase (PI3K)-signalling pathway[209] (Figure 7). We focus here on the role of members of the members of the MAP kinase family in type I and type III IFN-mediated signaling.

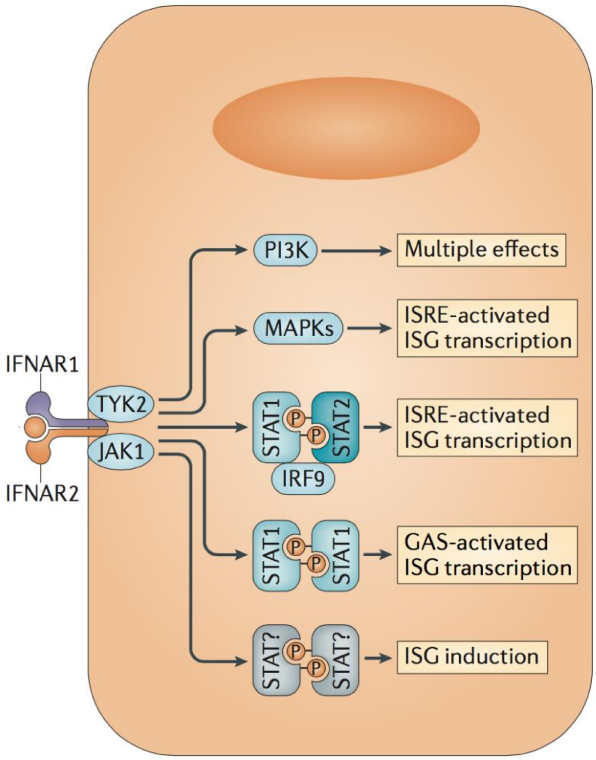

Figure 7. Alternative pathways activated downstream type I IFN receptor. Downstream the IFNAR complex, apart from the STAT1:STAT2 heterodimer, which together with IRF9 forms the ISGF3 complex, other STAT homo and heterodimers are formed or alternative pathways including the MAPKs and the PI3K are activated downstream IFNAR complex and lead to the upregulation of ISGs through the same or different promoter elements. Adapted from McNab et al., (2015)[358].

1.3.2.6 MAP Kinases in type I and type III IFN-mediated signaling

Type I IFN has been shown to signal through the MAP kinases pathway, including p38 mitogen-activated protein kinase (MAPK), the extracellular signal-regulated kinase (ERK) and the c-Jun N-terminal kinase (JNK) pathway in several IFN sensitive cell lines[209,236–238]. Among them, the p38 kinase is the best characterized and has been shown to be important for both the growth inhibitory and the antiviral functions of type I IFN in specific cell lines[236,239–242].

Although, p38 signaling pathway has been clearly shown to be activated downstream IFNAR, type I IFN dependent activation of ERK and JNK has not been investigated

thoroughly. Few studies have shown a cell specific activation of ERK and its involvement in IFN-α mediated antiviral activity against HCV and myxoma virus[243,244]. For JNK even more limited information is available. Li et al., have demonstrated JNK involvement in type I IFN antiviral responses by elimination of infected cells through apoptosis[245].

Similar to type I IFNs, activation of p38, ERK and JNK has been shown upon type III IFN treatment in a cell dependent manner[104,207,237]. However, in contrast to type I IFN, there is no conclusive information regarding the precise mode of action of these kinases in IFNLR signaling. Interestingly, although initially fibroblasts were considered as not sensitive to type III IFN treatment, Alase et al., showed that epidermal fibroblasts respond to type III IFN in a MAP Kinase dependent manner which leads to ISG induction and TGF-β induced collagen production. This recent study indicates a specific role of IFNLR-dependent MAP kinase activation in antiviral protection and repair processes of epidermal tissue[104].

1.3.3 Regulation of type I versus type III IFN signaling in the nucleus

The next step downstream, in the formation of the canonical ISGF3 complex or the activation of the above-described alternative signaling events takes place in the nucleus and drives the transcription of ISGs. Recent studies have described several regulatory mechanisms in the nucleus after type I IFN treatment, which can be mainly assessed in two layers: first, at the level of IFN-dependent chromatin remodeling at the target gene loci of ISGs and secondly, at the layer of interactions of STATs with other transcriptional factors, which are induced by the IFN pathway or by heterologous signaling cascades.

1.3.3.1 Epigenetic regulation of IFN responses

An emerging field in the regulation of IFN responses involves epigenetic modification. Epigenetic modifications are mediated by chromatin modulators such as histone acetyltransferases (HATs), which induce transcription by transforming chromatin into a more relaxed state or by histone deacetylases (HDACs), which inhibit gene induction by keeping chromatin into a highly organized condensed state. In addition, co-activators and co-repressors play an important role by facilitating interactions of specific transcriptional complexes (for instance, ISGF3 in the case of IFN responses) with the general transcriptional machinery and with chromatin modulators[246].

The focus on IFN-dependent epigenetic regulation is driven by recent studies, which show a high degree of nucleosome occupancy in the promoter region of ISGs, suggesting chromatin

remodeling as an indispensable step in the induction of ISG transcription upon IFN stimulation[247,248]. As type III IFN mediated chromatin remodeling has not yet been investigated we focus on type I dependent remodeling mediated through interactions of chromosomal modifiers with components of the ISGF3 complex. STAT2 is the most crucial mediator of these interactions, as STAT2 has an essential transactivation domain (TAD) that provides the fundamental transcriptional function of ISGF3 complex, while STAT1 and IRF9 are responsible for DNA sequence specificity[249].

1.3.3.2 Modifiers of ISG chromatin structure

The ATP-dependent nucleosome remodeling complexes SWI\SNF-A (BAF) and SWI\SNF-B (PBAF) are known chromatin modulators, which facilitate ISG promoter remodeling[247,250–252]. Upon type I IFN treatment, STAT2-dependent recruitment of BAF increases the accessibility of ISG promoter regions allowing expression of ISGs[253]. Furthermore, members of the HAT family such as binding protein p300[254], cAMP-responsive-element-binding protein (CREB)-binding protein (CBP)[255] and general control non-depressible 5 (GCN5) protein[256] have been shown to be recruited by direct interaction with STAT1 and STAT2 to the promoters of ISGs and facilitate their transcription. Unexpectedly, although HATs are considered positive modulators and HDACs negative regulators of general transcription, it has become clear that the histone-deacetylase activity (HDAC) is essential for type I IFN-dependent ISG transcription[257–259]. Although, these studies provide the basis for better understanding of HDAC mediated ISG regulation, HDACs have been also reported in co-repressor complexes to negatively target ISG transcription[260].

1.3.3.3 Co-activators and co-repressors of ISGs transcription

Apart from chromatin modifiers, interactions of the ISGF3 complex with co-activators such as minichromosome maintenance deficient 5 (MCM5) and minichromosome maintenance deficient 3 (MCM3)[261,262], N-Myc interactor (NMI)[263], glucocorticoid receptor-interacting protein 1 (GRIP1)[264], Vitamin D receptor-interacting protein complex component 150 (DRIP150)[265], the cyclin-dependent kinase 8 (CDK8) module of the Mediator co-activator complex[214] and the AAA+ ATP binding proteins RVB1 and RVB2[266] have been reported to enhance the transcriptional activation of ISGs upon IFN stimulation. On the other hand, for the fine-tuning of epigenetic regulation, involvement of co-repressors in the controlling of ISG activation has been observed with PIAS1, PIASy, TAF-1 and FOXO3 to serve as characteristic examples[267,268].

1.3.3.4 Cooperation with other transcriptional factors

Apart from epigenetic mechanisms, the control of IFN responses in the nucleus involves the coordinated activity of multiple other transcriptional factors, which cooperate with STATs[224,269,270]. Upon IFN stimulation, members of the interferon regulatory factor (IRF) family, such as IRF-1, are expressed and in turn induce the transcription of a subset of ISGs by recognizing specific DNA sequences (IRF-E site), which overlap with the ISRE sequence[138,271–273]. In this way, the cooperative action of IRFs and ISGF3 leads to an enhancement of ISG activation. In contrast, IRF-2 has been shown to operate as a suppressor of type I IFN responses, by competing with IRF-1 or IRF-9 for the same DNA binding sites[268,274,275]. Nonetheless, IRFs, by themselves can activate certain target genes independently of STATs[269]. Examples of genes activated by IRFs, without the help of STATs, upon type I IFN stimulation are MxA, GBP, MHC class I and B2M in immune cells[276]. In addition, upon IFN or virus stimulation IRF-7 expression amplifies various genes. Among them, IFN-α-mediated transcription serves as a positive feedback loop, which further enhances IFN responses[277,278]. Furthermore, independently of the ISGF3 action, upon virus infection, IRF-3 can directly bind the ISRE sequence and activate a subset of ISGs[279–282].

1.4 Functional significance of type I versus type III IFNs

After the discovery of type III IFNs, the last 15 years the research in the IFN field has predominantly focused on understanding whether the induction, the signaling and the function of these powerful cytokines are regulated differently than type I IFNs. Initially, despite the fact that type I and type III IFNs are structurally unrelated and engage different receptor complexes, it was largely accepted that the signaling pathways emanating from type I and type III IFN receptors exhibit remarkable similarity leading to the induction of common biological responses, especially antiviral protection, via the expression of nearly an identical pool of more than 300 interferon stimulated genes (ISGs).

However, a broad range of recent studies have shown not only overlapping but also distinct roles of type I and type III IFNs in viral infections. Thus, apart from the differences in the transcriptional regulation of type I versus type III IFN expression, which has been detailed above, crucial differences have begun to be unraveled regarding the cellular tropism of IFN production upon viral infection and expression of type I versus type III IFN receptor complexes

1.4.1 Type I versus type III IFN mediated antiviral responses at mucosal tissues

The antiviral activity of type I and type III IFNs has been shown *in vitro* and *in vivo* by exogenous administration of IFNs or with the use of IFN receptor deficient mice[38,39,73–77,79,80,99]. The type of infected tissue and the cellular tropism of the different viral pathogens are the two crucial factors, which could potentially give rise to specificity in type I versus type III IFN response. Type I IFN contributes to the antiviral response of many tissues including liver, kidney and spleen, while the type III IFN based defenses protect predominantly organs with mucosal surfaces[73–80].

Upon invading the mucosal lumen, a virus is able to infect the epithelial cells, the predominant cell type lining the mucosal surface, or the immune cells, residing in the sub-mucosa or the lymphoid associated mucosal tissues and from there spread to other tissues. Taking into account the predominant induction of type III IFNs by epithelial cells or the largely limited expression of type III IFN receptor complex on epithelial tissues[73–80,93,97,99,283], it becomes more and more apparent that type III IFNs are the preferential agents to combat viruses which infect epithelial cells of the respiratory tract, gastrointestinal tract, urogenital tract and the liver. While type I IFNs, produced mainly by immune cells, fibroblasts and endothelial cells of the epithelial sub-mucosa (lamina propria), contribute mainly to induce more systemic responses responsible for inhibiting viral dissemination beyond the mucosal barrier[78–80,96,97,99,283].

1.4.1.1 Type I versus type III IFNs in the gastrointestinal tract

Intestinal epithelial cells preferentially produce type III IFN rather than type I IFN and express high levels of IFNLR1[75,77,79,80,96–98]. Studies focusing on the mouse gastrointestinal tract have shown that type III IFNs may play a restricted role in gut epithelial cells irrespectively of type I IFNs. In particular, it has been demonstrated that mouse intestinal epithelial cells show a more compartmentalized response to IFNs in adult animals, with type III IFNs to act on epithelial cells, whereas type I IFNs have a significant effect on non-epithelial cells such as lamina propria cells, and only a minimal effect on intestinal epithelial cells[78–80,96,97,284] (Figure 8).

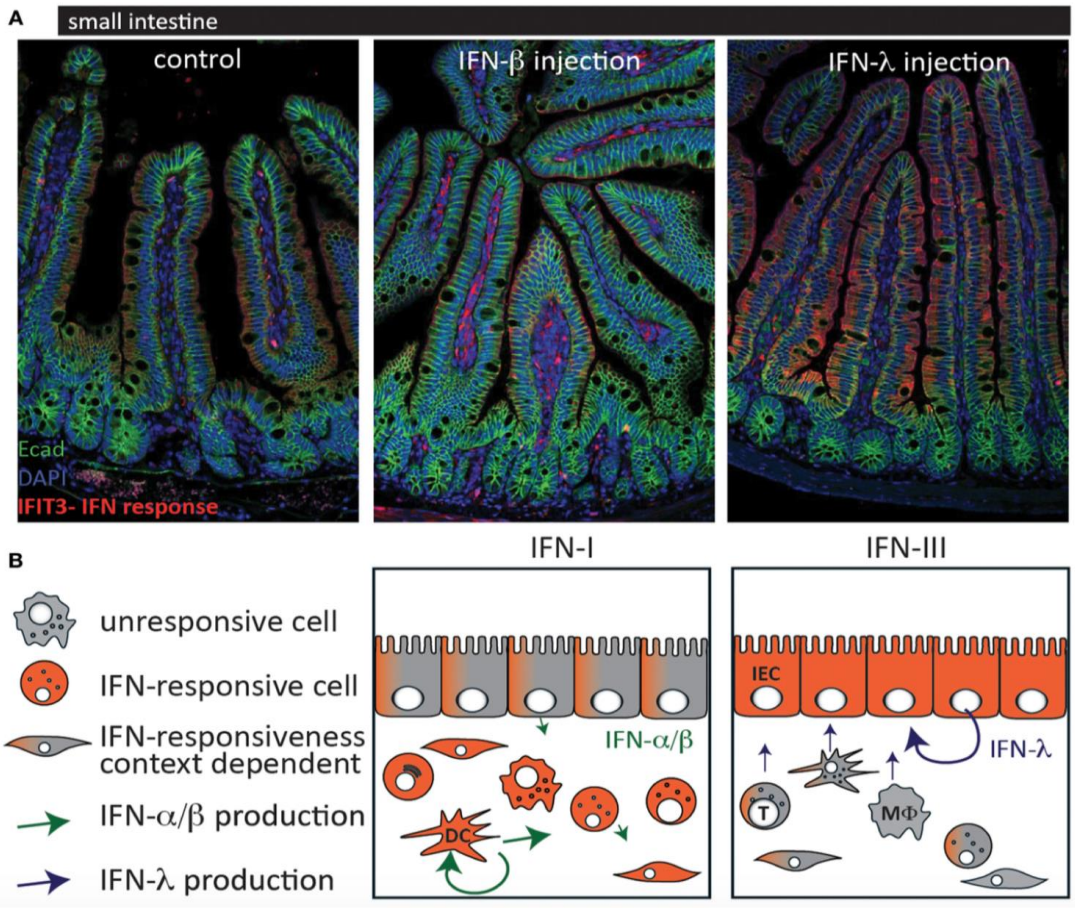

Figure 8. Epithelial specific responsiveness to type III IFNs in the mouse gastrointestinal tract. Mice were injected with type I or type IIII IFN and immunostaining of intestinal sections against the ISG IFIT3 was conducted. Upon type I IFN treatment, IFIT3 is mainly detected in the cells of the lamina propria, while type III IFN injection induces IFIT3 expression predominately on epithelial cells. (B) Schematic representation of the IFN induction and response in murine intestinal mucosa tissue upon viral challenge. IECs: intestinal epithelial cells, DC: Dendritic cells, T: T lymphocytes, MΦ: Macrophages. Adapted from Pott and Stockinger, (2017)[344].

This compartmentalization of type I versus type III IFN response in the mouse gut is also reflected in the restriction of enteric viruses with different cell tropism. For instance, rotavirus displays strong epithelial cell tropism and predominantly replicates in the epithelium of the small intestine[285]. Although both IFNs are induced following rotavirus infection in the gastrointestinal tract of adult mice, type III IFN based defense is predominantly responsible for the restriction of rotavirus replication in gut mucosal surface[79,96,97]. In line, rotavirus replication in mouse gut was inhibited only by parenteral administration of type III and not type I IFN[79]. However, in the case of reovirus, which replicates in both epithelial and non-epithelial cells, both type I and III IFNs are required in a non-redundant fashion for viral inhibition in the mouse gastrointestinal tract[80]. Specifically, type III IFN restricts replication of reovirus in epithelial cells[80,286], while type I IFN prevents systemic infection[80]. Recently, an

age-restricted dependence on IFNs in the mouse intestinal barrier has been shown with neonatal mice showing a response of epithelial cells to both IFNs, while adult mice are insensitive to type I IFNs[97]. In addition, it has been shown that reovirus infection induces mainly type III IFN production and lower levels of type I IFN in epithelial cells[80,114,286].

Similarly to reovirus, it has been shown that both IFNs act cooperatively for controlling norovirus infection, with type III IFNs inhibiting persistent shedding of virus in feces and type I IFN to prevent systemic spread[286–288]. In particular, using as a model, murine norovirus (MNoV), with acute and persistent strains, this differential sensitivity of type I and type III IFNs has been observed[108]. Acute MNoV, which exhibits cellular tropism to DCs, macrophages, B and T cells in the gut, reflects the importance of type I IFNs for elimination of viral infection[288,289]. Whereas, in the case of persistent MNoV strains type I IFN contributes to prevent systemic viral spread and type III IFNs are responsible for controlling viral load in the intestine[286–288,290]. Increased viral load has been shown in the gut and stool samples of IFNLR-/- mice and exogenous administration of type III IFNs inhibits persistent MNoV infection in intestinal tissue[286,287,290]. Tightening of the gastrointestinal epithelial barrier might be an explanation for the beneficial action of type III IFNs on reducing viral shedding. Interestingly, in the blood brain barrier, a similar action for type III IFNs has been described upon West Nile Virus infection, where type III IFN induction enhances the tight junction integrity of endothelial cells[44,105]. Notably, it has been reported that the protective effect of type III IFN system in norovirus infection is hampered by intestinal commensal bacteria, providing a possible explanation for why mice with functional type III IFN receptors are still susceptible to persistent norovirus infection[291]. Use of antibiotic treatment to deplete gut commensals, diminishes fecal shedding of norovirus in a type III IFN receptor dependent manner.

1.4.2 Differential pattern of type I versus type III IFN activity

Apart from the above described differences in the induction, response and antiviral protection under the prism of cellular and viral tropism mainly in mouse mucosal surfaces, type I and type III IFNs have also been shown to display significant subtle differences in their signal propagation in some recent *in vitro* studies utilizing different human cell lines. Interestingly, it has been shown that these differences are more quantitative than qualitative and related to the magnitude and the kinetics in type I versus type III IFN mediated cellular responses.

First of all, although type I and type III IFN antiviral response is less black and white and

there is a degree of redundancy between the two IFN systems, *in vitro* studies utilizing human lung epithelial cell lines and hepatocytes have demonstrated that type I IFNs confer a more potent antiviral protection[39,292–295]. In line with this, the magnitude of the gene expression promoted by type I IFNs has been described to be higher than the response triggered by type III IFNs, even though it has been reported that an overlapping pool of ISGs is induced with both IFN[39,93,97,165,189,237,292–294]. Moreover, *in vitro* work performed in hepatocytes revealed a differential kinetic pattern of ISGs induction between type I and type III IFN stimulation, with type I IFN promoting a significantly faster transcriptional response[165,189,293,294].

1.5 Objectives

Intestinal epithelial cells constitute the primary barrier that enteric viruses have to face. Viral infection of epithelial surfaces triggers the production of type I IFNs, which signal through the IFNAR complex to up regulate hundreds of ISGs, that inhibit viral replication and induce viral resistance to neighboring cells. Type III IFNs constitute a newer class of interferons that share low homology with type I IFNs. Type III IFNs are abundantly expressed at mucosal layers such as the respiratory and gastrointestinal tracts following viral infection and bind to cells using the IFNLR complex. Interestingly, while the type I IFN receptor is ubiquitously expressed, the type III IFN receptor is expressed mainly in epithelial cells.

Although type III IFNs signal through a unique receptor complex, they induce downstream signaling that appears remarkably similar to that of type I IFNs, driving the expression of a comparable set of ISGs. This has prompted speculation that type III IFNs are functionally redundant to type I IFNs. However, this model has been challenged more and more in recent studies which highlight that the cell type specific compartmentalization of IFNLR and the ligand availability provide type III IFNs a unique potential for targeting local infections at mucosal surfaces. However, up to now the epithelium specificity of type III IFNs has been supported mainly by *in vivo* studies focusing on murine epithelial surfaces, leaving unanswered questions about how and whether these two IFNs act differently in the human epithelium. Traditional experimental approaches utilizing human cell lines are limited to a comparative analysis of the response induced by type I versus type III IFN at the primary human intestinal epithelium. Here, we combined human IEC lines with human mini-gut organoids to study the relative role of type I and type III IFNs in protecting the human gut against viral infection.

In addition, differences in the antiviral activity conferred by both IFNs appear to be not only driven by the spatial restriction of their receptors but also by intrinsic subtle differences in signal propagation. As these differences in the kinetics and the magnitude of type I versus type III IFN mediated cellular responses could not be directly explained by their signaling cascade, an alternative explanation was proposed where type III IFN receptor is expressed at lower levels at the cell surface. Here, we combined mathematical modeling with experimental time-resolved data to elucidate whether the observed differences between type I and type III IFNs are intrinsic to each IFN specific signal transduction pathway.

Thus the presented work addresses the following, major objectives:

1. Characterize the functional differences in type I versus type III IFN mediated innate

immune responses in human intestinal epithelial cells

2. Determine the molecular mechanisms which are responsible for these differences

Taken together, by combining the most up to date *in vitro* culture conditions of primary non-transformed intestinal epithelial cells, with mathematical modeling and quantitative experimental data, this study aimed at providing molecular cues allowing us to determine how and why type III IFNs induce a distinct cellular response compared to type I IFNs in human epithelial cells and unravel how these differences in type I and type III IFNs function to maintain gut immuno-homeostasis (efficient protection against pathogens while limiting pro-inflammatory signals). Understanding these mechanisms could contribute to the development of new more efficient IFN therapies for combating viral infection without inducing excessive side effects.

2 Results

2.1 Type I and type III interferons display different dependency on mitogen-activated protein kinases to mount an antiviral state in the human gut

The text and figures of part 2.1 have been adapted from Pervolaraki et al. (2017)[100]. This corresponds to a co-first author published manuscript resulting directly from my PhD research project.

Intestinal epithelial cells (IECs) are constantly exposed to commensal flora and pathogen challenges. How IECs regulate their innate immune response to maintain gut homeostasis remains unclear. During viral infection of mucosal surfaces, IFNs are the predominant cytokines produced to combat viral replication and spread[36-40]. While type I IFN receptors are ubiquitously expressed, type III IFN receptors are mainly expressed on epithelial cells[73-80]. This epithelium specificity strongly suggests exclusive functions at epithelial surfaces, but the relative roles of type I and III IFNs in the establishment of an antiviral innate immune response in human IECs are not clearly defined. Here, we use human mini-gut organoids and human IEC lines in combination with genetic ablation of either type I or type III IFN receptors, to investigate the relative roles of type I and type III IFNs in protecting the human gut against viral infection. These studies will allow us to refine our understanding of the evolutionary benefit of possessing multiple antiviral IFNs.

2.1.1 Human Mini-Gut Organoids as a representative *ex vivo* model of human gastrointestinal epithelium

To unravel the antiviral activity of type I versus type III IFNs in human primary intestinal cells, we established human colon and intestinal mini-gut organoid cultures. Here we isolated intestinal crypts from human colon or small intestine resections. Human samples were derived from multiple donors undergoing biopsy or surgery and from different parts of the small intestine including duodenum, jejunum and ileum. After isolation, single crypts containing the stem cell niche were embedded into matrigel and cultured *ex vivo* in media supplemented with intestinal growth factors such as Wnt3a, Noggin, R-Spondin1 and epidermal growth factor (EGF). 24 hours post-isolation, open crypts started to re-seal resulting in 3-dimensional structures called mini-gut organoids. Over a course of approximately 3 to 5 days of culture, human colon and intestinal organoids present a characteristic cystic or multi-lobular morphology, respectively, with a single continuous

lumen surrounded by a monolayer of epithelial cells. At 7-10 days post-isolation the organoids grew significantly in size (Figure 9A).

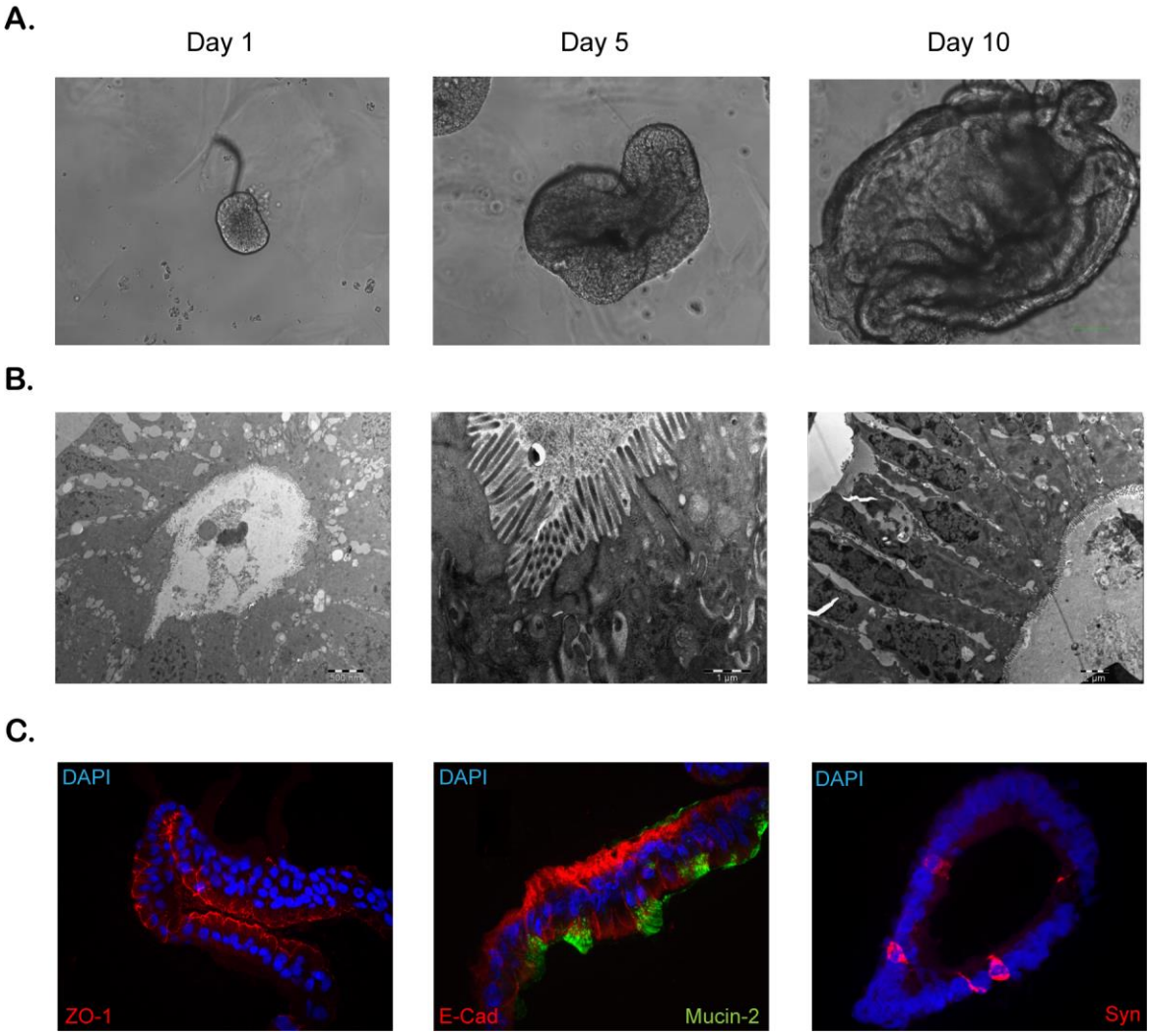

Figure 9. Characterization of differentiated human mini-gut organoids. (A) Human colon organoids were prepared according to methods. Representative images of human colon organoids grown over 10 days from intestinal crypts. (B) Electron microscopy pictures of organoids at day five post-differentiation. (C) Five days post-differentiation, organoids were fixed, cryosectioned and immunostained for tight junctions (ZO-1), adherent junctions E-cadherin (E-cad), Goblet cells (Mucin-2), and Enteroendocrine cells (synaptophysin, Syn). The data of panel (A) has been produced by Megan Stanifer, Heidelberg University. The data of panel (B) has been produced by Pranav Shah, Heidelberg University. Panels (A) and (C) were adapted from Pervolaraki et al., 2017.

After culture in differentiation medium, we noticed the typical organization of the human colon organoids with the presence of a clear and developed lumen, the brush boarder on the apical side of enterocytes and the tight junctions, which seal the paracellular space between the epithelial cells (Figure 9B). In addition, we were able to observe all the different cell types present in the human gastrointestinal epithelium based on the expression of specific

cellular markers by immunofluorescence. These included the adhesion junction protein E-cadherin (E-cad) for enterocytes, mucin (Mucin-2) for secreting Goblet cells, synaptophysin (Syn) for enteroendocrine cells (Figure 9C) and lysozyme for Paneth cells (data not shown). Furthermore, some physiological characteristics of organoids were demonstrated such as the polarized nature of the intestinal epithelium by the localization of E-cadherin at the basolateral side of cells and the detection of tight junctions at the apical side by staining of the zonula occludens-1 (ZO-1) protein (Figure 9C).

2.1.2 Preferential induction of type III IFN production in human mini-gut organoids upon viral infection

To evaluate the protective role of type I and/or type III IFNs in the human gut upon viral infection we utilized the mammalian reovirus (MRV). MRV is a well-known enteric virus model, which infects intestinal epithelial cells followed by induction of immune responses involving both type I and III IFNs[114,296]. In the rest of the thesis, the terms type I and type III IFNs refer to the use of IFN β1 and IFN λ1–3, respectively. Differentiated colon mini-gut organoids were removed from the matrigel in which they were embedded and inoculated with MRV with a low multiplicity of infection (MOI) of approximately 0.5. At 16 hours post-inoculation (hpi), organoids were harvested, embedded into optimal-cutting-temperature (OCT) freezing compound and frozen to make blocks for sectioning and staining. Immunofluorescence analysis using antibodies against the reovirus non-structural protein μNS was used to identify infected cells. By using confocal microscopy, μNS staining was evident in MRV-infected organoids but not in mock-infected samples (Figure 10A). Notably, MRV infection resulted in a change in the morphology of human mini-gut organoids creating fragmented pieces of the epithelial layer, compared to mock infected organoids, which maintained an intact structure (Figure 10A). This observation was not sample dependent as the same results were obtained after infection of multiple donors with MRV (Figures 11B and 12A). In addition to immunostaining, quantification of viral replication was assessed by quantitative real-time (qRT)-PCR. As shown in Figure 10B, MRV potently replicates over the course of infection. These results demonstrate that human mini-gut organoids are susceptible to MRV infection.

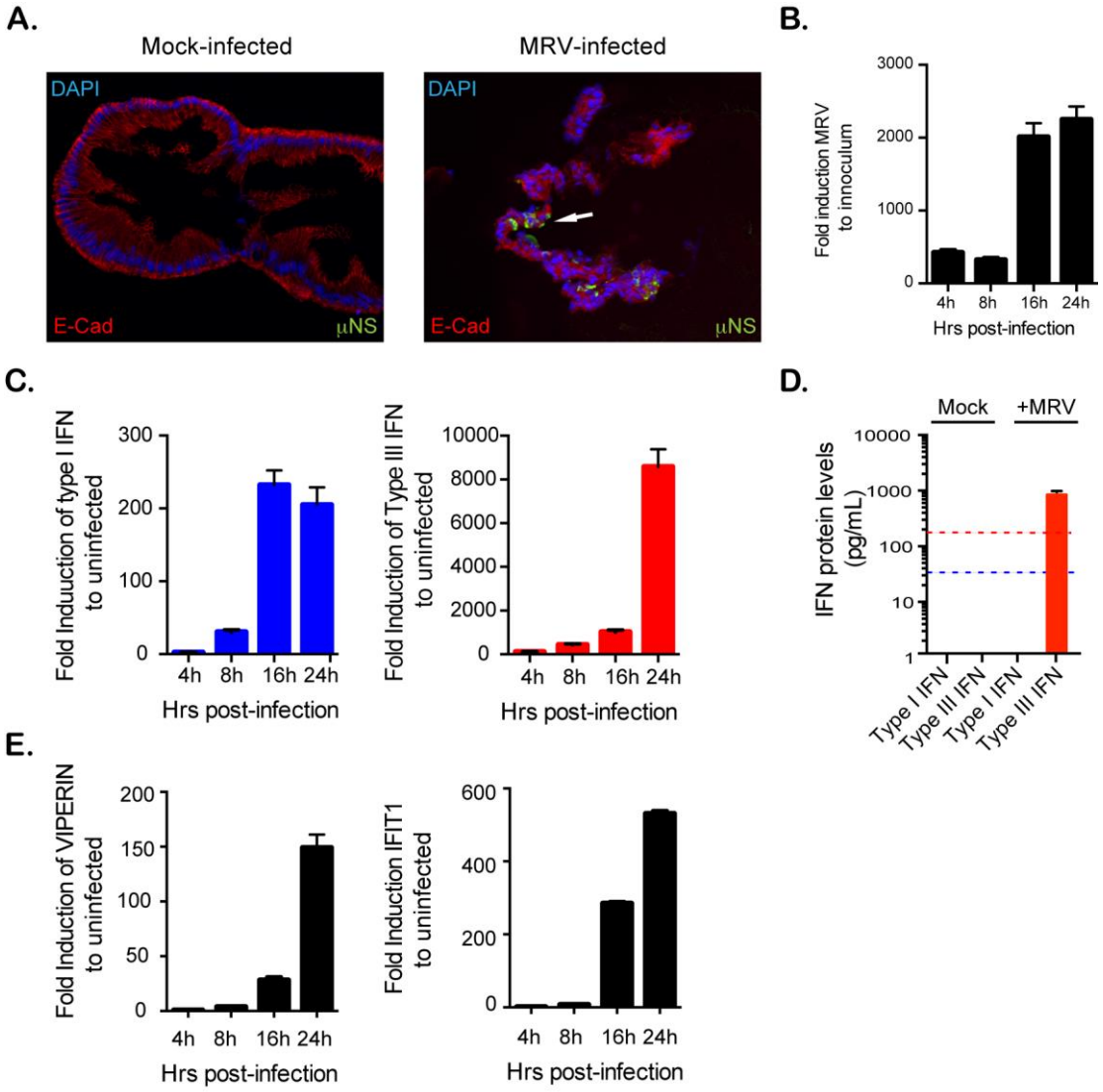

Figure 10. Infection of human mini-gut organoids with mammalian reovirus (MRV). Five days post-differentiation, organoids were mock or MRV infected (multiplicity of infection = 0.5). (A) 16 hpi, organoids were fixed, cryosectioned and immunostained. MRV-infected cells were detected using an antibody against the MRV non-structural protein µNS. Representative images are shown. White arrow indicates infected cells. (B-E) Quantitative real-time (qRT)-PCR and ELISA were used to detect (B) virus replication over a timecourse of 24 hours (C) time course of transcriptional upregulation of both type I interferons (IFNs) (β) and type III IFN (λ2/3) IFNs (D) 24 hpi the production and secretion of IFN proteins in the supernatant of infected organoids was determined by ELISA and (E) a time course of transcriptional upregulation of the IFN-stimulated genes Viperin and IFIT1. qRT-PCR data were normalized to TBP and HPRT1 (housekeeping genes) and are expressed relative to uninfected organoids at each time point. qRT-PCR data and ELISA data represent the mean values of three independent experiments. Error bars indicate the SD. The blue and red lines in (D) demarcate the limit of detection of our ELISA for type I and type III IFNs, respectively. The data of this figure has been produced jointly with Megan Stanifer, Heidelberg University and was adapted from Pervolaraki et al., 2017.

To assess the innate immune response generated by organoids upon viral infection, we monitored the upregulation of both type I (IFN-β) and type III (IFN-λ2–3) IFNs and the expression of ISGs over the course of MRV infection. Importantly, MRV infection triggered a

marked increase in type III IFN and to a lesser extent type I IFN expression as detected by interferon-specific qRT-PCR (Figure 10C). This was in line with the detection of only type III IFN in the supernatant of infected organoids (Figure 10D). The virus inhibitory protein, endoplasmic reticulum-associated, interferon-inducible (Viperin) and interferon-induced protein with tetratricopeptide repeats 1 (IFIT1) were used as two representative ISGs induced upon viral infection and were both shown to be upregulated after MRV infection (Figure 10E). These results closely demonstrate that human primary IECs respond to viral infection by up-regulating both type I and type III IFNs, but only type III IFN can be detected in the supernatant of infected cells.

2.1.3 Both type I and type III IFNs protect human mini-gut organoids against viral infection

From our previous experiment, we found that viral infection of human organoids induces the induction of both type I and type III IFNs at the transcriptional level. To address whether both types of IFN are in turn able to induce an antiviral response by promoting ISGs production, mini-gut organoids were exogenously treated with a wide range of IFN concentrations. Results revealed that both type I and III IFNs induce the upregulation of ISGs in a dose-dependent manner (Figure 11A). Interestingly, type I IFN appears to be more potent as it induces a higher expression of both the ISGs Viperin and IFIT1 compared to type III IFN (Figure 11A). These data were not dependent on specific ISGs, as similar results were obtained for multiple other ISGs including MXA, ISG15, ISG54 (data not shown). Of note, we also observed a continuous increase in ISG mRNA levels as the concentration of type I IFN increased, whereas ISG transcript levels quickly reached a plateau in type III IFN-treated cells.

To evaluate whether type I and/or type III IFN could protect primary human IECs from viral infection, mini-gut organoid cultures were stimulated with 8 ng/mL of type I IFN (IFN-β) (equivalent 2,000 RU/mL, see Materials and methods) or 300 ng/mL of type III IFN (IFN-λ1−3) prior to exposure to MRV. Organoids were harvested 16 hpi for analysis of viral infection/replication by immunostaining and immunoblotting against the reovirus non-structural protein μNS as well as by quantification of viral replication using qRT-PCR. Compared to mock-treated cells, pre-treatment of colon organoids with either IFN significantly reduced both the number of MRV-infected cells (Figure 11B) and the viral antigen levels within these organoids, as assessed by the quantification of the total fluorescence intensity of the μNS protein per organoid (Figure 11C) or by western blot

analysis (Figure 11D). Complementarily, viral replication was severely impaired when organoids were treated with either IFNs as assayed by qRT-PCR (Figure 11E).

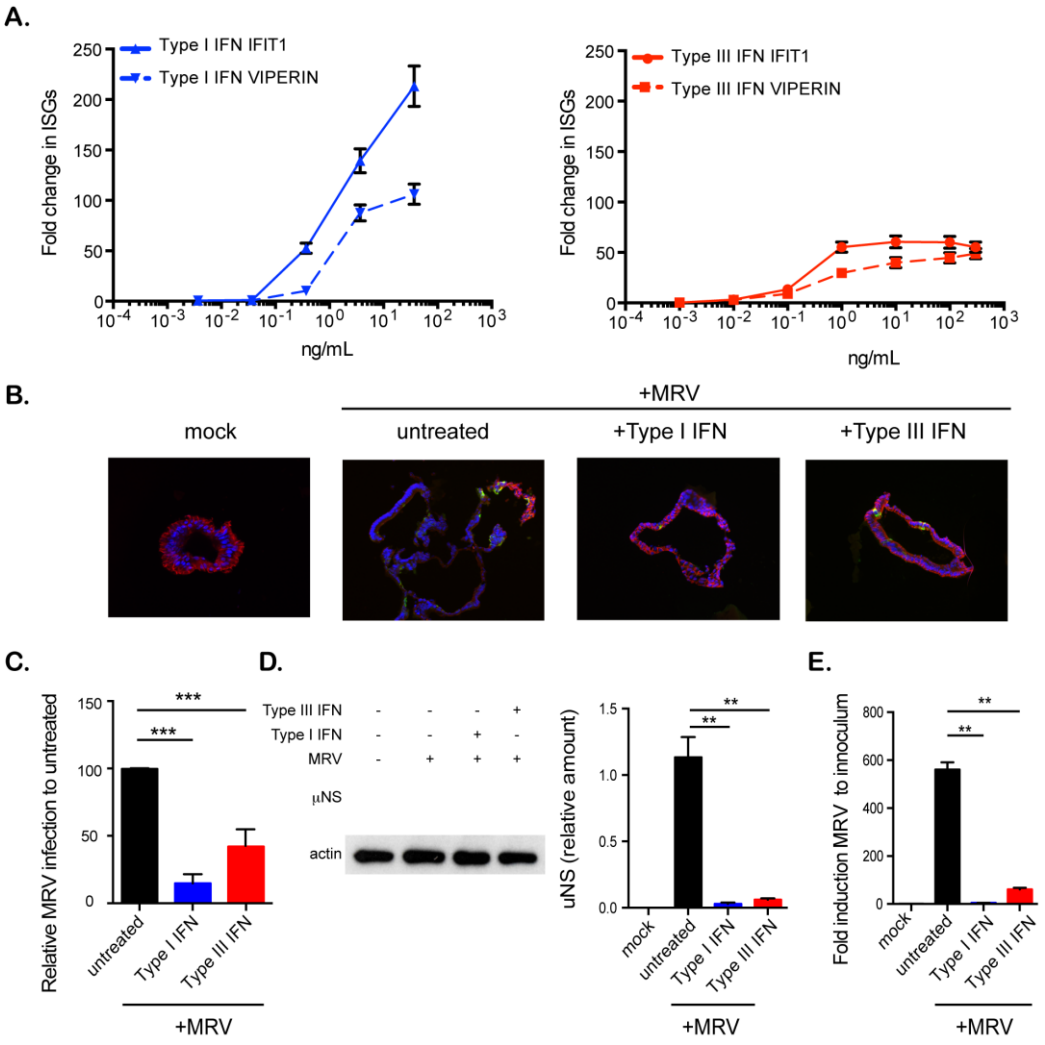

Figure 11. Both type I and type III IFNs confer human mini-gut organoids protection against viral infection. (A) Colon organoids were treated with increasing concentrations of type I IFN (β) and type III IFN (λ1–3). Six hours post-treatment, organoids were harvested and the transcriptional upregulation of the IFN-stimulated genes Viperin (Vip) and IFIT1 was measured using qRT-PCR. Data were normalized to TBP and HPRT1. (B–E) Colon organoids were treated with type I IFN (β) (2,000 RU/mL equivalent 8 ng/mL) or type III IFN (λ1−3) (300 ng/mL) for 2.5 hours prior to infection with MRV (multiplicity of infection = 0.5) (B) 16 hpi MRV-infected organoids were analyzed by μNS-specific immunofluorescence (green). The cells were stained against E-cadherin (red) and the nuclei were stained with DAPI (blue). Representative data from triplicate experiments are shown. (C) The fluorescence intensity of MRV μNS per organoid (panel B) was measured and expressed relative to untreated organoids (set as 100). (D) 16hpi MRV-infected organoids were analyzed for μNS production by Western blot. Actin was used as loading control. Production of μNS was quantified by densitometry. (E) The protective effect of type I or type III IFN was assayed by monitoring viral replication by qRT-PCR normalized to inoculum. Data represent the mean values of three independent experiments. Error bars indicate the SD. **P < 0.01, ***P < 0.001 (unpaired t-test). The data of this figure has been produced jointly with Megan Stanifer, Heidelberg University and was adapted from Pervolaraki et al., 2017.

To ensure that these findings were neither donor nor colon specific, colon organoids from different donors (colon D2–D3) and organoids derived from different parts of the small intestine such as the ileum or the jejunum were similarly treated with type I or type III IFNs prior to infection with MRV. Reduced viral infection characterized by the lower expression levels of the MRV μNS protein and the decreased MRV replication was detected in all the colon organoids generated from different donors (Figure 12A), as well as in the organoids derived from ileum (Figure 12B) and jejunum (Figure 12C). In addition, we confirmed that this inhibition was also true when using vesicular stomatitis virus (VSV), an unrelated model virus whose replication is also sensitive to both type I and type III IFNs[114,296] (Figure 12D). All together, these results demonstrate the antiviral protective role of both type I and type III IFNs in primary IECs derived from different parts of the human intestine including colon, ileum, and jejunum.

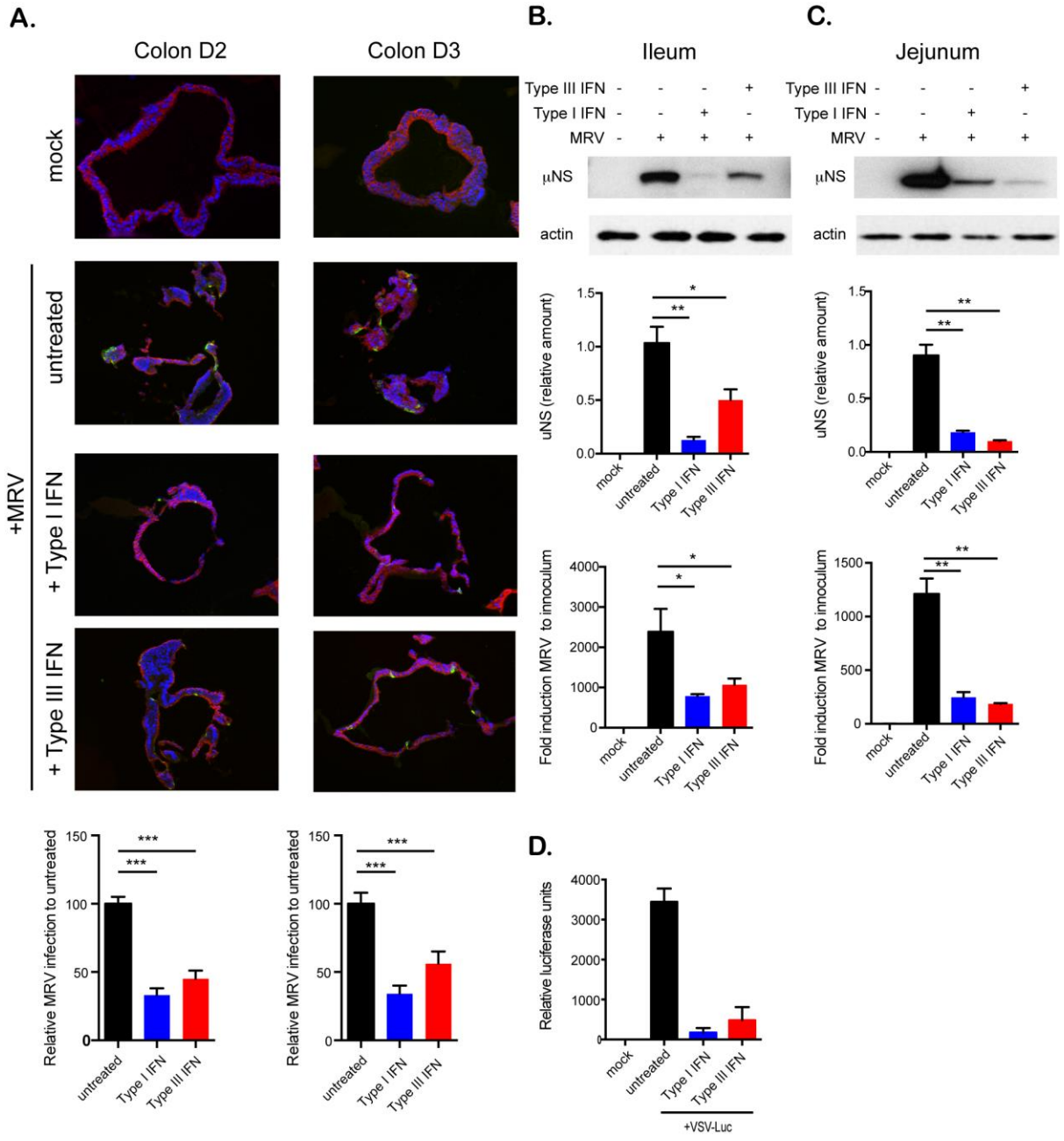

Figure 12. Type I and type III IFNs confer protection against MRV infection to all sections of the gut. Organoids from multiple colon donors and multiple intestinal sections were treated with type I IFN (β) (2,000 RU/mL equivalent 8 ng/mL) or type III IFN (λ1−3) (300 ng/mL) for 2.5 hours prior to infection with MRV (multiplicity of infection = 0.5). Infection was assessed 16 hpi. (A) MRV-infected colon organoids (donor 2 and 3) were analyzed by µNS-specific immunofluorescence (green). The cells were stained against E-cadherin (red) and the nuclei were stained with DAPI (blue). Representative image of triplicate experiments are shown. The fluorescence intensity of MRV µNS per organoid was measured and expressed relative to untreated organoids (set to 100). (B, C) MRV-infected organoids were analyzed for µNS production by Western blot. Actin was used as loading control. Production of µNS was quantified by densitometry. The protective effect of type I IFN (β) and III IFN (λ1−3) was assayed by monitoring the relative viral genome copies by quantitative real-time PCR normalized to inoculum. (B) Ileum. (C) Jejunum. (D) Colon organoids were treated with type I IFN (β) (2,000 RU/mL equivalent 8 ng/mL) or type III IFN (λ1−3) (300 ng/mL) for 2 hours prior to infection with VSV-expressing luciferase (multiplicity of infection = 1) Eight hpi VSV replication was assessed by measuring the luciferase activity. Data represent the mean values of three independent

experiments. Error bars indicate the SD. **P < 0.01, ***P < 0.001 (unpaired t-test). The data of this figure has been produced jointly with Megan Stanifer, Heidelberg University and was adapted from Pervolaraki et al., 2017.

2.1.4 Human IEC lines express type I and type III IFN upon MRV infection

Although the last years, human mini-gut organoids have been characterized as the best system to study *ex vivo* the properties of human primary intestinal epithelial cells, they are very difficult to genetically modify. Therefore, to better understand the functions and the mechanisms by which type I and type III IFNs confer hIECs an antiviral state, we used the human colon carcinoma-derived cell line T84. To test whether this cell line elicits a similar immune response as human mini-gut organoids, we infected T84 cells with MRV. 16 hpi, samples were harvested and the expression of 13 human type I and three type III IFNs were measured by qRT-PCR[103]. While T84 cells have low to non-detectable levels of IFNs under basal conditions, MRV infection induces the up-regulation of both type I (IFN-α and IFN-β) and type III IFNs (IFN-λ1, IFN-λ2 and IFN-λ3) (Figure 13A and 13B).

Notably, similar to human mini-gut organoids (Figure 10C), viral infection induces a higher transcriptional up-regulation of type III IFNs compared to type I IFN (Figure 13A and 13B). To address whether both IFNs were made at the protein level and secreted by infected T84 cells, we measure the amount of both IFNs in the supernatant of infected T84 cells using ELISA. Importantly, in agreement with the viral infection of mini-gut organoids (Figure 10D), only type III IFN was found in the supernatant (Figure 13C).

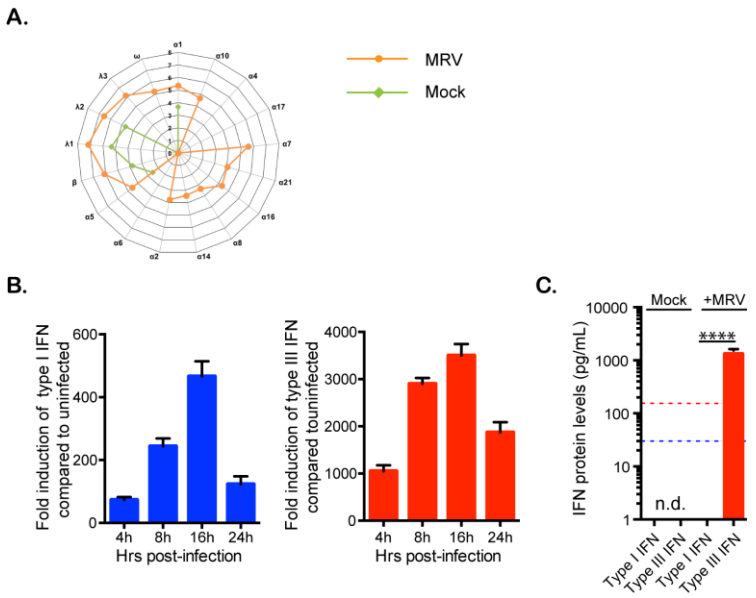

Figure 13. Expression pattern of IFN mRNA and protein in human intestinal epithelial cells upon viral infection. T84 cells were infected with MRV (multiplicity of infection = 1). (A) 16 hpi, cells

were harvested and the copy numbers of the expression of 13 human type I and three type III IFNs were determined by qRT-PCR analysis. The geometric means of the peak responses in mock and infected intestinal epithelial cells are shown in a log10 scale as copy numbers per µg RNA. (B) Relative quantification of type I IFN (β) and type III IFN (λ2/3) transcripts during the course of MRV infection of T84 cells. Data are normalized to TBP and HPRT1 and are expressed relative to uninfected cells at each time point. (C) Quantification of type I (IFNβ) and type III (IFN λ2/3) protein levels by ELISA in supernatants of uninfected or MRV-infected T84 cells. The blue and red dashed lines demarcate the limit of detection of our ELISA for type I and type III IFNs, respectively. n.d., not detectable. Data represent the mean values of three independent experiments. Error bars indicate the SD. ****P < 0.0001 (unpaired t-test). The data of panel (A) have been produced jointly with Lynnsey A. Renn, Food and Drug Administration, Silver Spring, MD, USA (B) has been produced jointly with Megan Stanifer, Heidelberg University. This figure was adapted from Pervolaraki et al., 2017.

To confirm whether T84 IECs respond to either type I and type III IFNs, we treated T84 IECs with type I or type III IFN and measured the expression levels of ISGs at different time points post-IFN treatment. Similar to human mini-gut organoids (Figure 11A), we found that type I IFN induces a higher expression of the ISGs Viperin and IFIT1 compared to type III IFN (Figure 14A). Transcriptome analysis of T84 cells

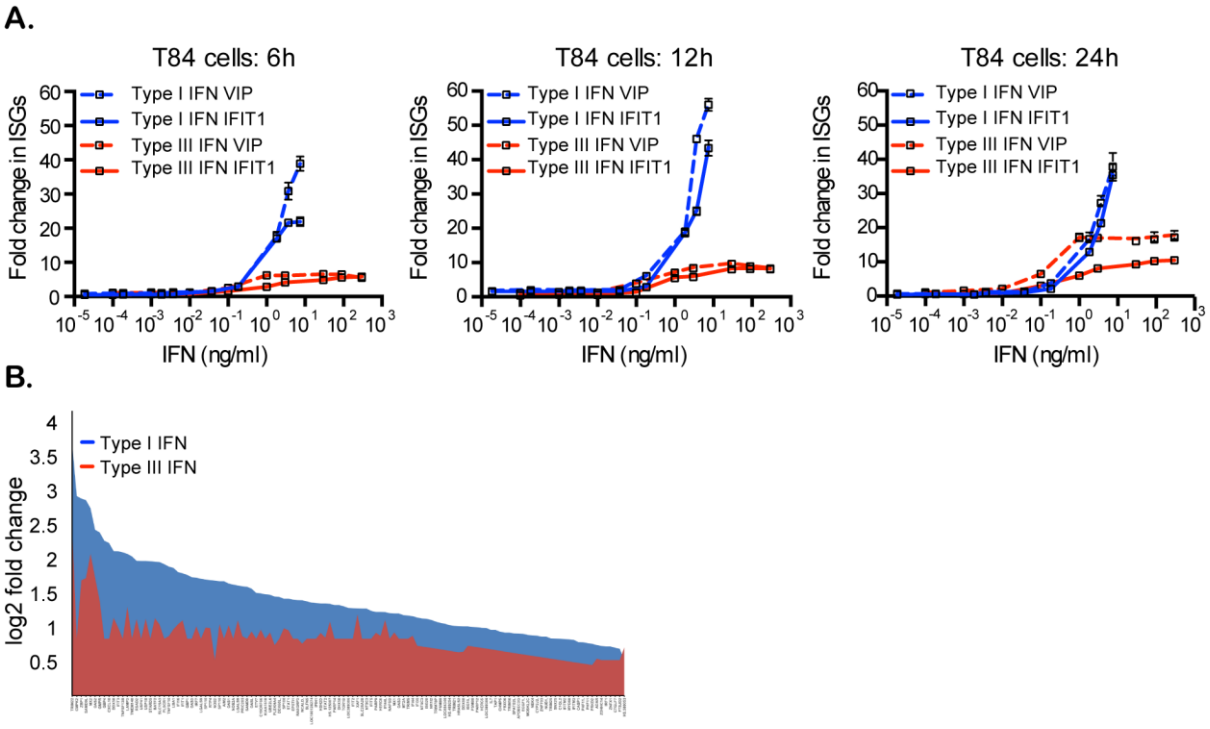

Figure 14. T84 cells respond to both type I and III IFNs by upregulating IFN-stimulated genes (ISGs). (A) T84 cells were stimulated with indicated concentrations of type I (β) or III IFN (λ1−3) for different times and the transcript levels of the ISGs Viperin (Vip) and IFIT1 were analyzed by qRT-PCR. Data are normalized to TBP and HPRT1 and are expressed relative to untreated cells at each time point. A representative experiment out of three independent experiments is shown. Mean values and SD are shown. (B) T84 cells were treated with type I IFN (β) (2,000 RU/mL equivalent 8 ng/mL) or type III IFN (λ1−3) (300 ng/mL) for 6 hours and identification of the IFN-induced ISGs was performed by transcript profiling using an Illumina microarray. The data of panel (B) has been produced jointly with Megan Stanifer, Heidelberg University. This figure was adapted from Pervolaraki et al., 2017.

treated with either type I or type III IFN revealed that type I IFN consistently induced higher expression level across all induced ISGs (Figure 14B).

To determine the antiviral potency of type I and type III IFNs in T84 cells, we pre-treated T84 cells with increasing concentrations of each IFN prior to infection with MRV. *De novo* production of viral proteins was monitored by immunoblotting against the MRV non-structural protein μNS. Figure 15A shows that both type I and type III IFNs limit viral infection in a dose-dependent manner. In addition, cells were fixed 16 hpi and the fraction of μNS-expressing cells was determined by immunofluorescence. These results demonstrate that either type I or type III IFN decrease both the number of MRV-infected cells and the level of viral antigen per cell (Figure 15B). To confirm that this observation was not virus-specific, T84 cells were treated with increasing concentrations of either type I or type III IFNs and subsequently infected with VSV-Luc as a reporter of viral replication. Assessment of viral infection by bioluminescence showed that similar to MRV, either type I or type III IFNs are capable of inhibiting VSV infection in human IECs in a dose-dependent manner (Figure 15C). In addition SKCO15, another colon cancer cell line, were used to exclude cell line-specific effects. Consistent with T84 cells, a dose-dependent protective effect of both IFNs was observed in SKCO15 cells (Figure 15D). All together these results show that either type I or type III IFNs confer human intestinal cell lines an antiviral state and that T84 cells phenocopy the antiviral response generated by primary human IECs.

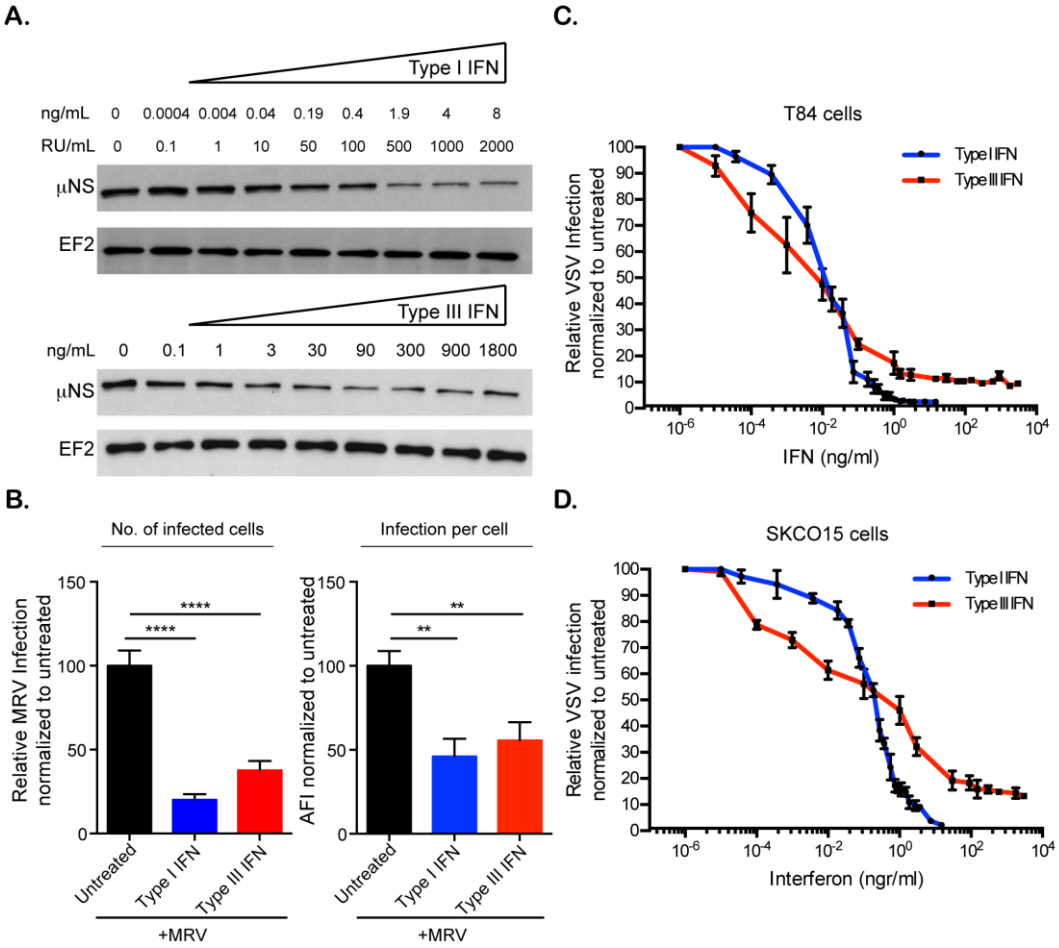

Figure 15. Both type I and type III IFNs mediate antiviral protection in human T84 cells. (A) T84 cells were pre-treated for 2.5 hours with the indicated concentrations of type I IFN (β) and type III IFN (λ1–3) IFNs and then subsequently infected with MRV [multiplicity of infection (MOI) = 1]. 16 hpi, the protective effect of type I or III IFN was assayed by immunoblotting for the viral non-structural protein μNS. EF-2 is used as a loading control. A representative immunoblot out of three independent experiments is shown. (B) T84 cells were treated with type I IFN (β) (2,000 RU/mL equivalent 8 ng/mL) or type III IFN (λ1−3) (300 ng/mL) for 2.5 hours prior to infection with MRV. 16 hpi MRV-infected cells were analyzed by μNS-specific immunofluorescence. (Left panel) The number of infected cells was quantified and is expressed relative to untreated cells (set to 100). (Right panel) MRV uNS staining intensity was measured to obtain the average fluorescent intensity per cell and is expressed relative to untreated cells (set to 100). Data represent the mean values of three independent experiments. (C) T84 cells and (D) SKCO15 cells were pre-treated with the indicated concentrations of type I or III IFNs for 2 hours prior to infection with vesicular stomatis virus (VSV) expressing Firefly luciferase VSV expressing luciferase (MOI = 1). Viral replication was assayed by measuring the luciferase activity 8 hpi. For each sample luciferase activity was measured in triplicates and is expressed as the percentage of the activity present in VSV-infected cells without IFN treatment (set to 100). The mean value obtained from three independent experiments is plotted. Error bars indicate the SD. **P < 0.005, ****P < 0.0001 (unpaired t-test). Panels (A-C) were adapted from Pervolaraki et al., 2017.

2.1.5 Type I & III IFN mediated antiviral responses independently protect human IECs

To understand whether type I and type III IFNs act in cooperation or independently in establishing the antiviral state of IECs, we generated T84 cell lines deficient for either the IFN alpha receptor 1 (IFNAR1) or the IFN lambda receptor 1 (IFNLR1) using CRISPR/Cas9 technology. In the rest of this part of my thesis, the IFNAR-/- and IFNLR-/- are used to describe the disruption of the IFNAR1 and IFNLR1 specific chains of type I and type III IFN receptor complexes, respectively.

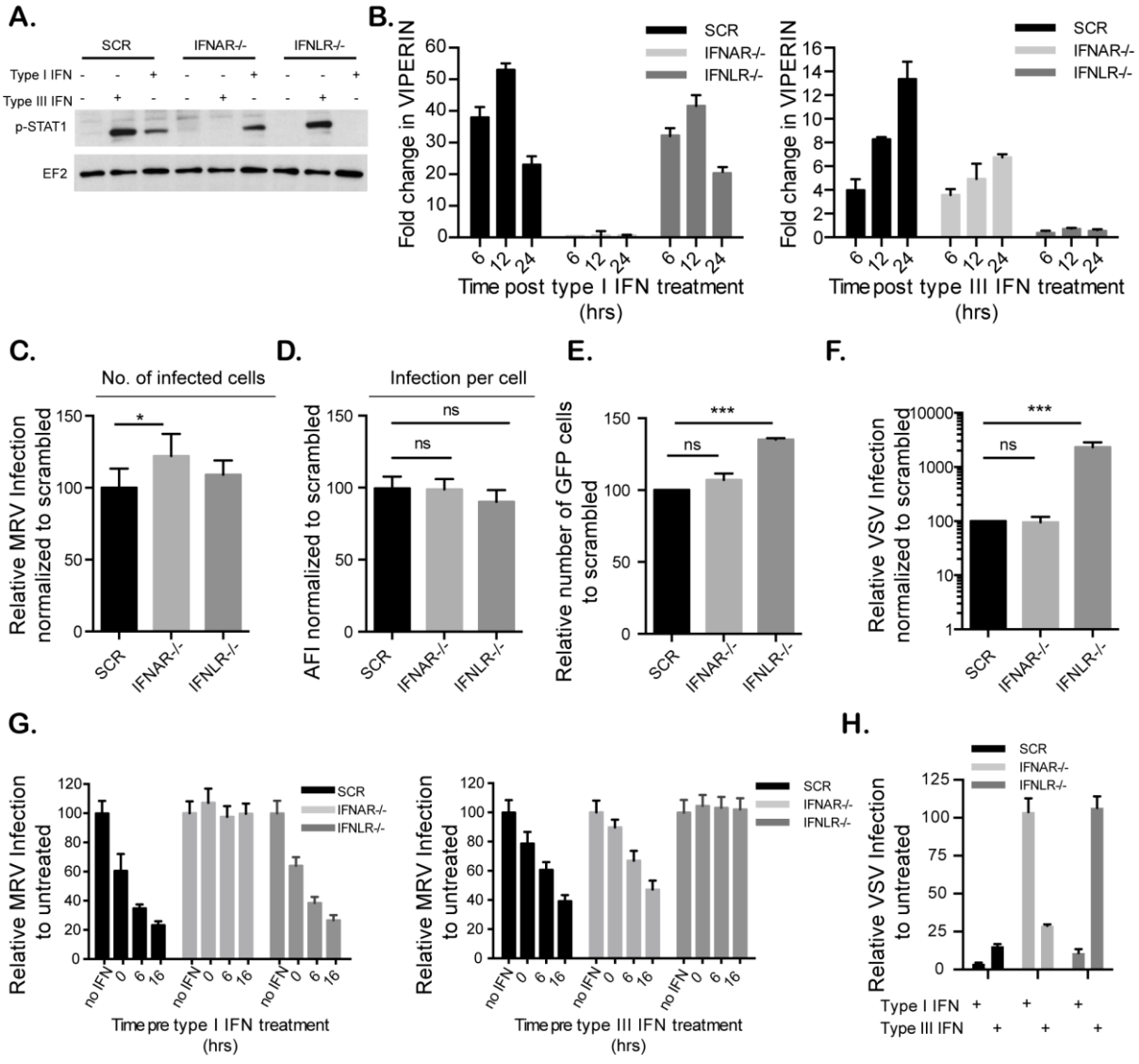

Figure 16. Type I and type III IFNs independently confer intestinal epithelial cells antiviral protection. T84 IFNAR1 and IFNLR1 knockout cell lines were generated using the CRISPR/Cas9 system. (A) T84 cell lines were treated with type I IFN (β) (2,000 RU/mL equivalent 8 ng/mL) or type III IFN (λ1−3) (300 ng/mL) for 1 hour and IFN signaling was measured by immunoblotting for pSTAT1 Y701. EF-2 is used as a loading control. A representative immunoblot out of three independent experiments is shown. (B) Same as (A), except that induction of IFN-stimulated genes was monitored

by relative qRT-PCR quantification of Viperin at indicated times post-IFN treatment. Data were normalized to TBP and HPRT1 and are expressed relative to untreated cells of each time point. (C,D) T84 cell lines were infected with MRV for 16 hours (multiplicity of infection (MOI) = 1) and MRV-infected cells were analyzed by μNS-specific immunofluorescence. (C) The number of infected cells is expressed relative to scramble control cells (set to 100). (D) MRV μNS staining intensity was measured to obtain the average fluorescence intensity per cell and expressed relative to scramble control cells (set to 100). (E) T84 cell lines were infected with VSV-GFP (MOI = 1) for 8 hours and the number of VSV-infected cells were analyzed by FACS. The percentage of infected cells is expressed relative to scramble control cells (set to 100). (F) Same as (E), except that T84 cell lines were infected with VSV expressing luciferase (VSV-Luc) (MOI = 1) and viral replication was assayed by measuring the luciferase activity. For each cell line luciferase activity was measured in triplicates and is expressed relative to scramble control cells (set to 100). (G) Same as (C), except that T84 cell lines were treated with type I IFN (β) (2,000 RU/mL equivalent 8 ng/mL) or type III IFN (λ1−3) (300 ng/mL) at indicated time points prior to infection with MRV. (H) Same as (F), except that T84 cell lines were treated with type I IFN (β) (2,000 RU/mL equivalent 8 ng/mL) or type III IFN (λ1−3) (300 ng/mL) for 2 hours prior to infection with VSV-Luc. Data (B–H) represent the mean values of three independent experiments. Error bars indicate the SD. *P < 0.05, ***P < 0.001, ns, not significant (unpaired t-test). The data of this figure was adapted from Pervolaraki et al., 2017.

Inactivation of these IFN receptors was confirmed by sequencing of the knockout (KO) cell lines, which revealed nucleotide deletions and changes of open reading frame in *IFNAR1* and *IFNLR1* genes (data not shown). As shown in Figure 16A and 16B, IFNAR−/− cells were no longer able to phosphorylate pSTAT1 and induce ISGs after type I IFN treatment, but remained fully responsive to type III IFN, indicating a selective disruption of the type I IFN signaling pathway. Conversely, IFNLR−/− cells were insensitive to type III IFN but responded to type I IFN (Figure 16A and 16B). To exclude cell clone specific effect, multiple clones of T84 cells KO for *IFNAR1* or *IFNLR1* gene were generated. As shown in Figure 17, our findings were consistent across multiple IFNAR−/− and IFNLR−/− cell clones (Figure 17A and 17B).

To assess whether deletion of *IFNAR1* or *IFNLR1* renders human IECs more susceptible to viral infection, cells lacking functional receptors for type I or type III IFN were infected by either MRV or VSV and compared to wild-type or scrambled guide RNA-exposed cells. Immunofluorescence analysis revealed that loss of IFNAR1 slightly increased the number of MRV-infected cells compared to control cells (Figure 16C), but did not affect the average fluorescent intensity of MRV antigen per infected cell (Figure 16D). Interestingly, IFNLR−/− cells appeared to be more susceptible to VSV infection. The number of VSV-infected cells and the amount of viral antigens in each cell were significantly increased in IFNLR−/− cells compared to control cells (Figure 16E and 16F). To further verify the protective role of type I and type III IFN against viral infection in human IECs, IFNAR−/− and IFNLR−/− cells were pre-treated with either type I or III IFNs and subsequently infected with MRV or VSV. Type I or type III IFN could efficiently inhibit infection by both MRV and VSV in control cells (Figure 16G and 16H). As expected, the protective effect of type I IFN against MRV (Figure 16G, left

panel) and VSV (Figure 16H) was no longer observed in IFNAR−/− cells, but was preserved in IFNLR−/− cells. Conversely, disruption of *IFNLR1* specifically abolished the protective effect of type III IFN, but not of type I IFN. Similar results were obtained with several KO clones (Figure 17C). All together these data demonstrate that in human T84 cells, either type I or type III IFNs are capable of independently mediating antiviral protection.

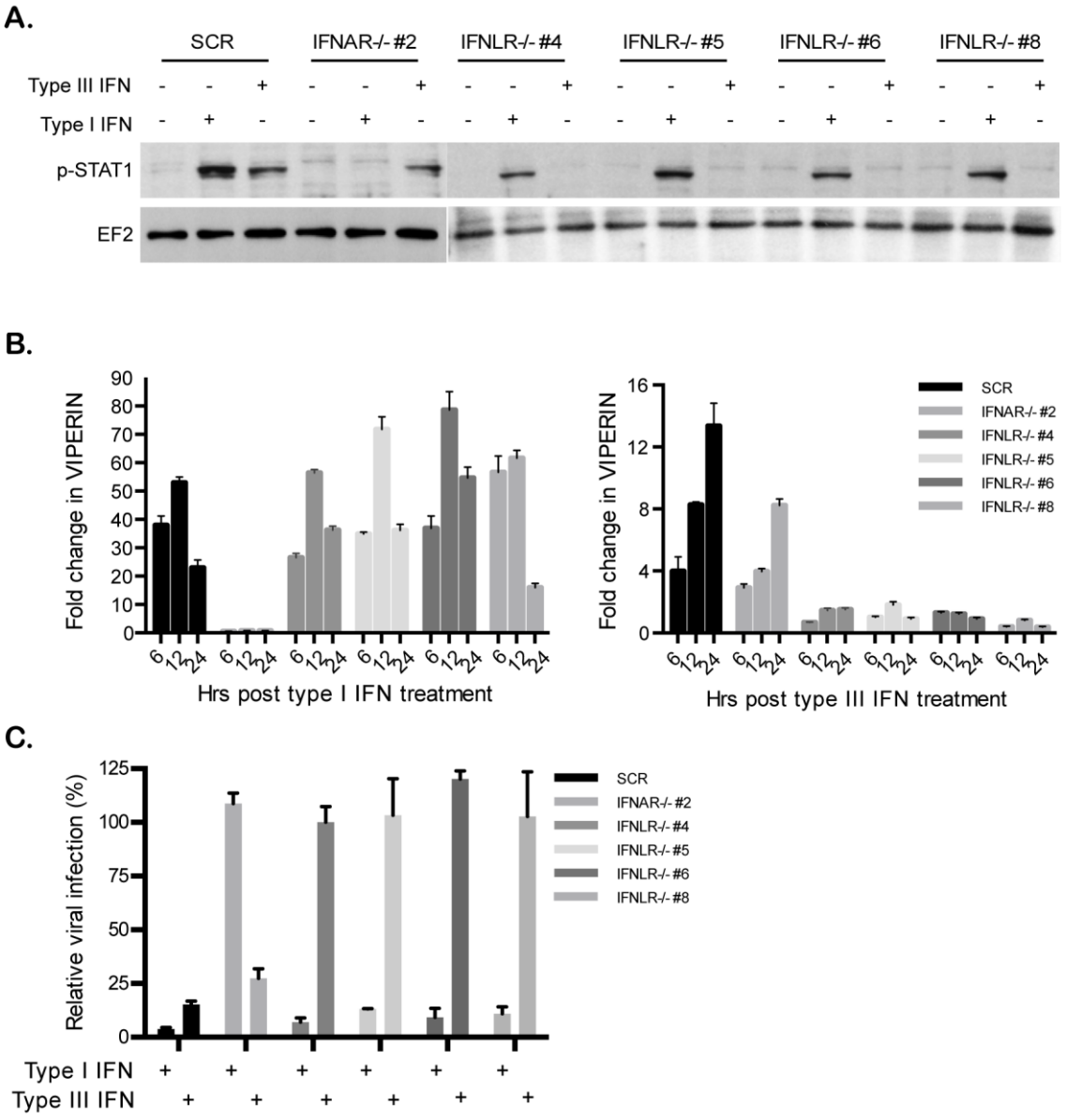

Figure 17. Characterization of different T84 IFNAR and IFNLR knockout (KO) cell clones generated using the CRISPR/Cas system. (A) IFNAR and IFNLR KO clones were treated with type I interferons (IFN) (β) (2,000 RU/mL equivalent 8 ng/mL) or type III IFN (λ1−3) (300 ng/mL) for 1 hour and IFN signaling was measured by immunoblotting for pSTAT1 Y701. EF-2 is used as a loading control. A representative immunoblot out of three independent experiments is shown. (B) Same as (A), except that IFN signaling was evaluated by monitoring induction of IFN-stimulated genes by relative quantification of Viperin at indicated times post-IFN treatment using qRT-PCR. Data are normalized to TBP and HPRT1 and are expressed relative to untreated control cells of each time point. A representative experiment, out of three independent experiments is shown. (C) T84 cell lines were treated with type I IFN (β) (2,000 RU/mL equivalent 8 ng/mL) or type III IFN (λ1−3) (300 ng/mL)

for 2 hours prior to infection with VSV-Luc (multiplicity of infection = 1) and viral replication was assayed by measuring the luciferase activity. Results are expressed relative to mock-IFN- treated control cells generated with a scrambled control gRNA (set to 100). The mean value obtained from two independent experiments is plotted. Error bars indicate the SD. The data of this figure was adapted from Pervolaraki et al., 2017.

2.1.6 Role of MAP Kinase signaling pathways in type III IFN based antiviral activity in human IECs

Type I and type III IFN signaling and antiviral activity are predominantly dependent on the JAK/STAT pathway, and inhibition of STAT1 phosphorylation blocks the production of ISGs and inhibits IFN-mediated antiviral protection[209,297–299]. In parallel, several MAPK signaling pathways, including the p38-mitogen activated protein kinase (p38-MAPK) pathway, the extracellular-signal regulated kinase (ERK) pathway and the c-Jun N-terminal kinases (JNK) pathway, have also been reported to be activated[207] and contribute to ISG up-regulation in type I or type III IFN-stimulated cells[104,237], but the role of the different MAPK pathways in the antiviral functions of type III IFNs remains unclear. We found that both type I or type III IFN treatment induced the phosphorylation of STAT1, STAT2, and STAT3 with similar kinetics in T84 cells (Figure 18). Type I or type III IFN treatment did not induce STAT5A, STAT5B, or STAT6 phosphorylation (data not shown).

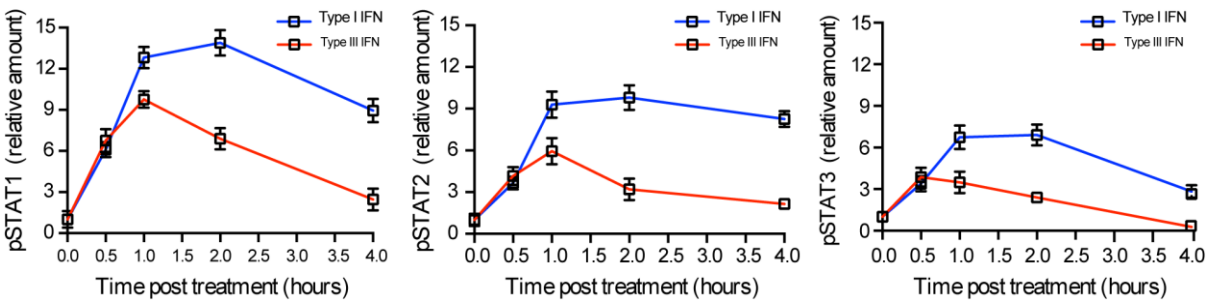

Figure 18. Type I and type III IFN mediated STAT1,2 and 3 phosphorylation. T84 cells were treated with 2000 RU/ml IFNβ or 300 ng/ml IFNλ for the indicated time points. The levels of phosphorylation of STAT1-6 was measured by Luminex technology. Only STAT1, 2 and 3 are shown as STAT5a, 5b and 6 were not activated upon type I or type III IFN treatment.

We next addressed whether type I and type III IFNs activate the different MAPKs. We found that both IFNs induce the phosphorylation of the MAPKs, p38, ERK, and JNK to the same extent and with similar kinetics (Figure 19A western blot analysis and quantification). To determine the role of the STAT and MAPK pathways in the antiviral activity of IFNs, we used specific pharmacological inhibitors in combination with IFN treatment. These inhibitors were shown to be non-toxic in cell viability assay (Figure 19B) and specific by Western blot analysis (Figure 20).

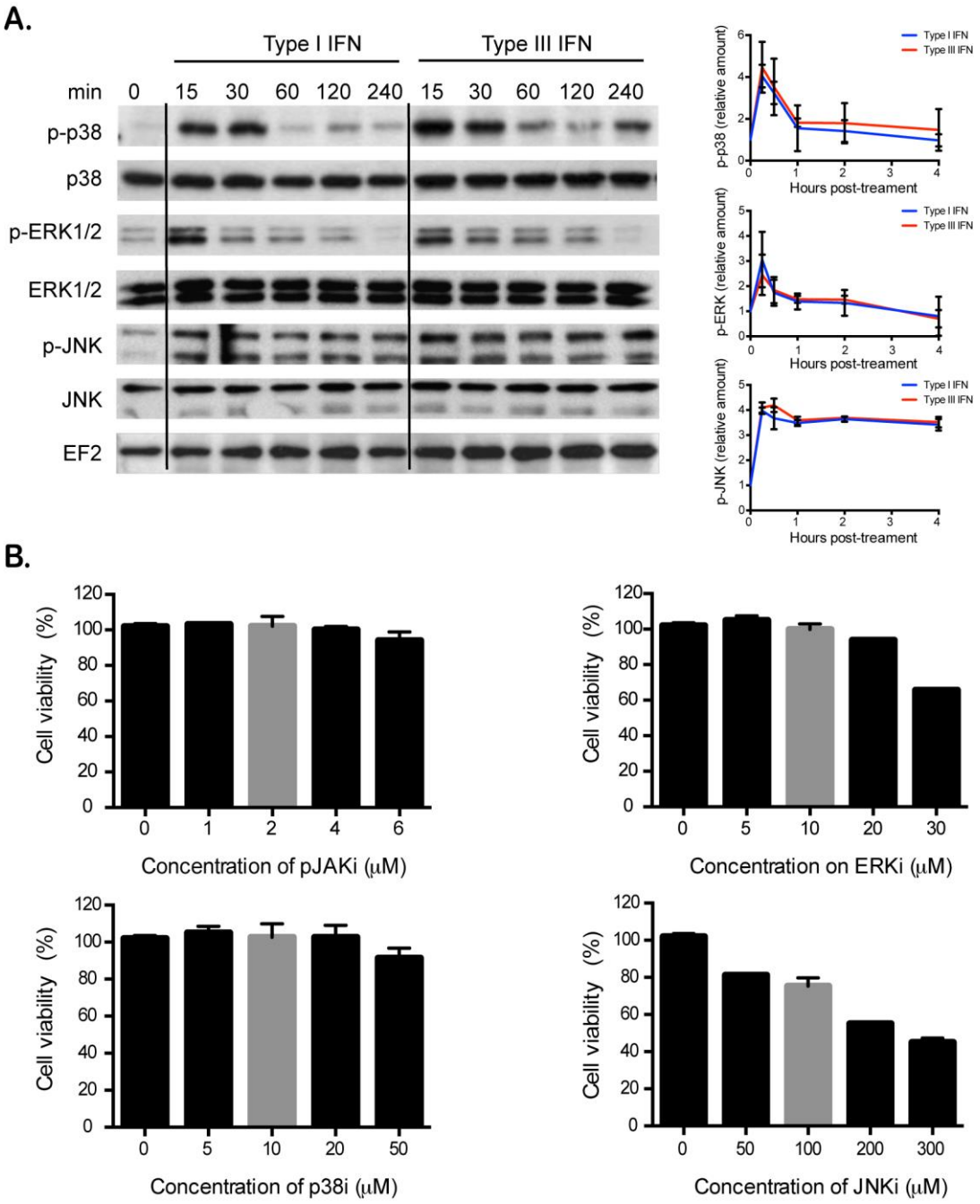

Figure 19. Role of MAP kinase pathway in type I and III IFN antiviral activity. (A) T84 cells were treated with type I IFN (β) (2,000 RU/ mL equivalent 8 ng/mL) or type III IFN (λ1−3) (300 ng/mL) for the indicated time points. The levels of phosphorylation of MAPkinases p38, ERK, and JNK were assessed by Western blot analysis. p38, ERK, JNK, and EF-2 were used as loading control. The phosphorylation of the MAP kinases was quantified and expressed relative to untreated cells (right panel). Data represent the mean values of three independent experiments. Quantification was performed by densitometry. (B) T84 cells were treated with increasing concentrations of JAK and MAP kinase inhibitors. 24 hours post-inhibitor treatment the cell viability was assessed by MTT assay. The mean value obtained from three independent experiments is shown. Error bars indicate the SD. The data of this figure was adapted from Pervolaraki et al., 2017.

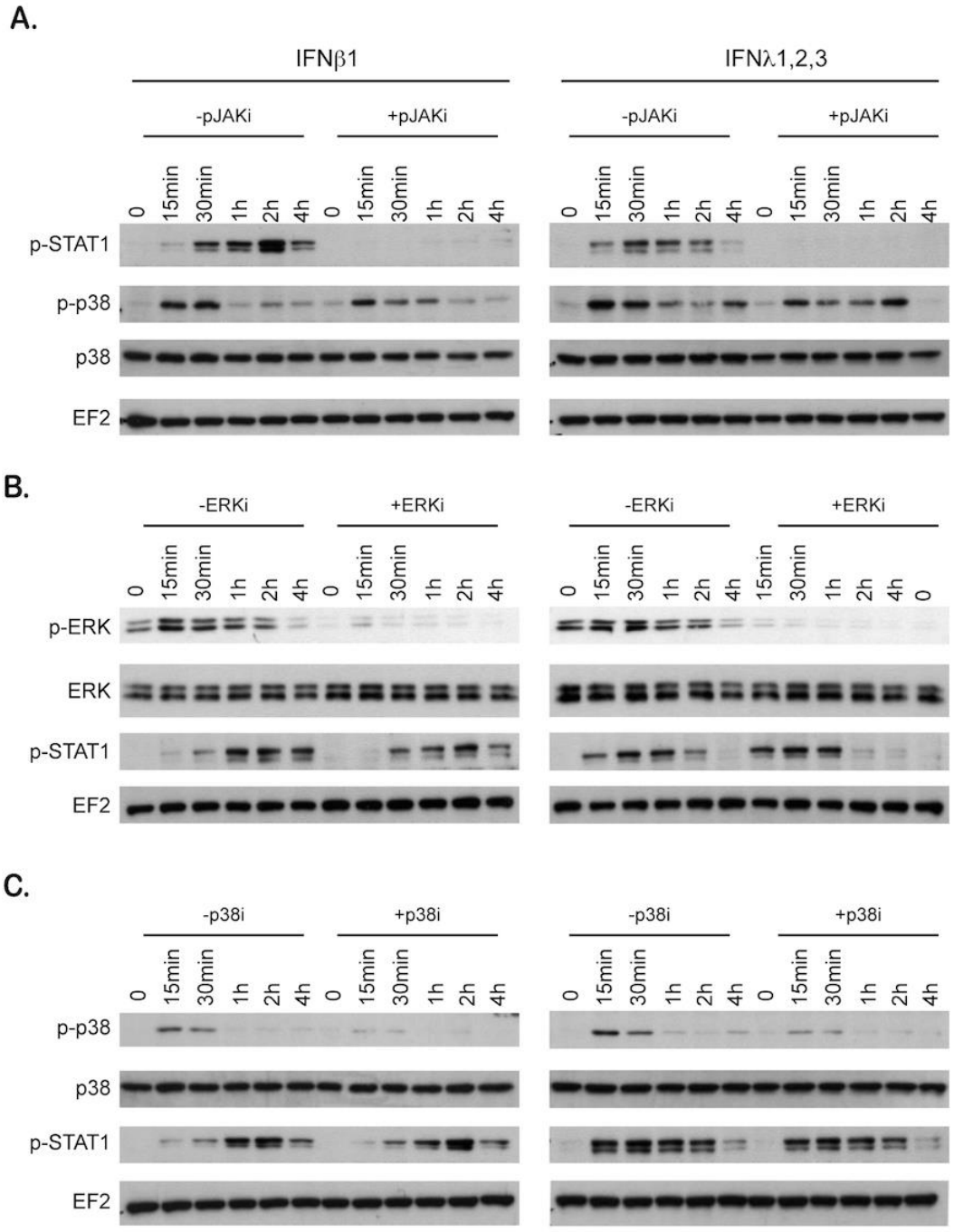

Figure 20. Specific inhibition of MAP kinases phosphorylation. T84 cells were pre-treated with JAK and MAPK inhibitors for 30 minutes prior to IFN treatment. Cells were harvested at different times post-treatment and the extent of JAK or MAPK inhibition was addressed by Western blot analysis. The specificity of each inhibitor was controlled by monitoring the phosphorylation status of JAK and all MAPKs. (A) 2 μM Pyridone 6 (pan-JAK inhibitor). (B) 10 μM U0126 (ERK inhibitor). (C) 10 μM SB202190 (p38 inhibitor). A representative plot out of from three independent experiments is shown. The data of this figure was adapted from Pervolaraki et al., 2017.

Inhibiting the JAK/STAT pathway with a pan-JAK inhibitor almost fully blocked phosphorylation of STAT1 (Figure 20A) and strongly impaired the antiviral activity of either

type I or III IFNs on both VSV and MRV (Figure 21A). Interestingly, inhibition of the MAPKs with specific inhibitors, had no effect on the phosphorylation kinetics of STAT1 (Figure 20B and 20C) but strongly affected the antiviral protection conferred by type III IFN only (Figure 21A). This specific inhibition is seen across a range of different concentrations used for the inhibitors (Figure 21B). Of note, a partial inhibition of the antiviral activity of type I IFN was observed at high concentration of JNK inhibitor (Figure 21B) but at this concentration cell viability was severely affected (Figure 19B). This type III IFN restricted dependence on MAPKs was independent of IFN concentration (Figure 21C), verifying that the non-dependence of type I IFN antiviral activity for MAPKs was not the result of differences in the IFN concentration used to stimulate the cells. Altogether, these results indicate the fundamental role of STAT-dependent signaling in conferring both type I and type III IFNs antiviral activity, and in addition demonstrate a unique role for MAPKs toward inducing the antiviral state induced by type III IFN but not type I IFN.

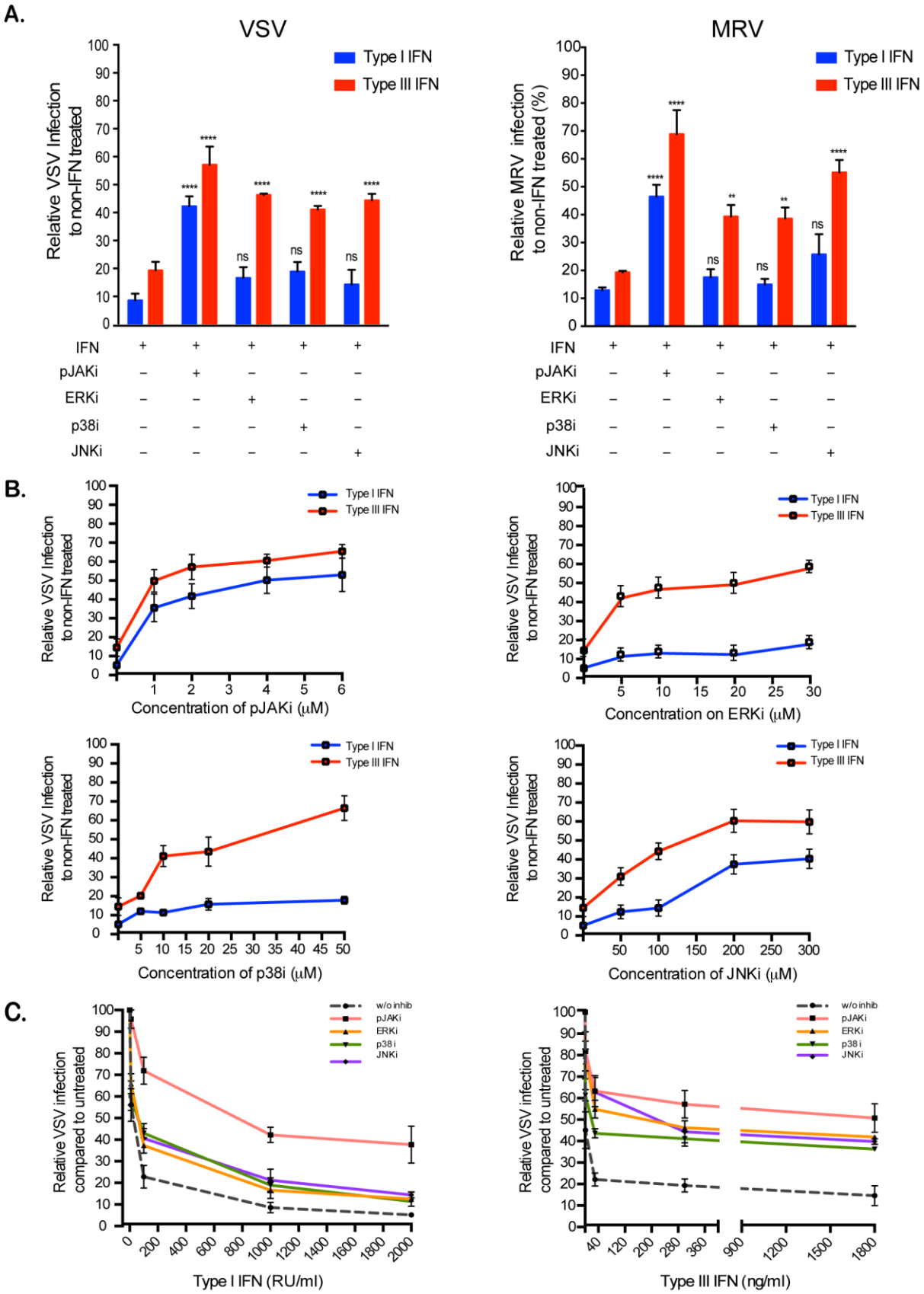

Figure 21. Type III IFNs require MAPKs for their antiviral response. (A) T84 cells were mock treated (black bar) or pre-incubated for 30 minutes with 2 μM Pyridone 6 (pan-JAK inhibitor), 10

μM U0126 (ERK inhibitor), 10 μM SB202190 (p38 inhibitor), or 100 μM SP600125 (JNK inhibitor). Subsequently, T84 cells were mock treated (black bar) or treated with type I IFN (β) (2,000 RU/mL equivalent 8 ng/mL) or type III IFN (λ1−3) (300 ng/mL) in the presence the inhibitor. 2 hours post-IFN treatment cells were infected with a MOI of 1 with VSV -Luc (left panel) or MRV (right panel). Viral replication was assayed by measuring the luciferase activity or by relative quantification of viral genome using qRT-PCR. Data were normalized to non-IFN-treated sample for each inhibitor (set to 100). (B) Same as (A), except T84 cells were pre-incubated with increasing concentrations of JAK or MAP kinase inhibitors prior to treatment with IFNs. (C) T84 cells were pre-incubated for 30 minutes with 2 μM Pyridone 6 (pan-JAK inhibitor), 10 μM U0126 (ERK inhibitor), 10 μM SB202190 (p38 inhibitor) and 100 μM SP600125 (JNK inhibitor). Then the indicative concentrations of type I or III IFN were added in parallel to the inhibitor. 2 hours post-IFN treatment cells were infected with VSV-Luc (MOI = 1) and viral replication was assayed by measuring the luciferase activity. Data were normalized to non-IFN-treated samples for each inhibitor. The mean value obtained from three independent experiments is shown. Error bars indicate the SD. ****P < 0.0001, **P < 0.005, ns, not significant (unpaired t-test). The data of this figure was adapted from Pervolaraki et al., 2017.

Although it has been shown in multiple cell lines that IFNs can induce the activation of MAPKs[104,207,237], the importance of these kinases in the IFN-mediated antiviral state has never been reported to our knowledge. This suggests that dependency on MAPKs might be cell type specific. To ensure that the antiviral activity of type III IFN in primary non-transformed human IECs depends on MAPKs, we used our mini-gut organoid culture system. Colon organoids were treated with pharmacological inhibitors of the JAK/STAT or MAPKs signaling pathways. Following pre-treatment with type I or type III IFNs, organoids were infected with VSV. 8 hpi, organoids were harvested and the impact of the pharmacological inhibitors on the antiviral activities of both IFNs was measured. As expected, inhibition of the JAK/STAT signaling pathway fully restores VSV infection to a level similar to infected organoids in the absence of IFNs (Figure 22). These results confirm that the JAK/STAT signaling pathway is key for both type I and type III IFN activity in primary human IECs. Importantly and similar to T84 cells, inhibition of either p38 or JNK signaling pathway partially impairs only the type III IFN antiviral activity in human mini-gut organoids (Figure 22). No significant effect of MAPK inhibition on type I IFN-mediated antiviral activity was observed. The effect of inhibiting ERK-dependent signaling on the antiviral activity of both IFNs was not determined (n.d.) since treatment of mini-gut organoids with ERK inhibitor induced disruption and death of the organoid culture (Figure 22 and data not shown). Altogether, these results corroborate that MAPK signaling pathways participate in the establishment of the antiviral state mediated by type III IFN in primary non-transformed human IECs.

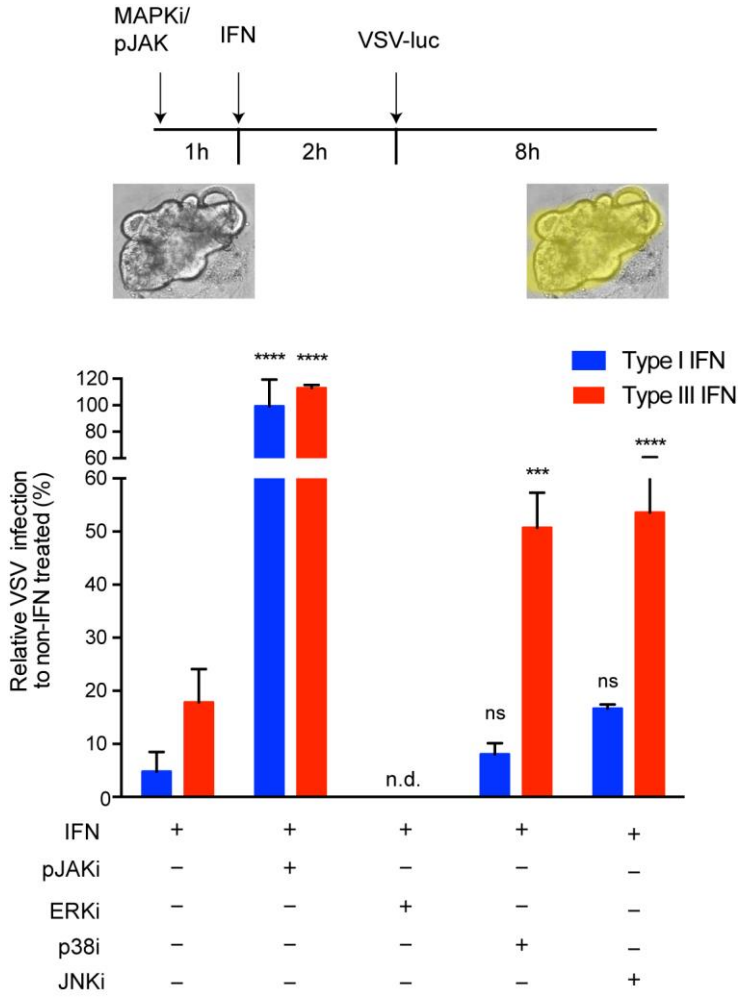

Figure 22. The antiviral activity of type III IFNs strongly dependent on MAPKs in primary human intestinal epithelial cells. Human colon organoids were mock treated (black bar) or pre-incubated with 2 μM Pyridone 6 (pan-JAK inhibitor), 10 μM U0126 (ERK inhibitor), 10 μM M SB202190 (p38 inhibitor) and 100 μM SP600125 (JNK inhibitor). One hour post-treatment, organoids were mock treated (black bar) or co-treated with type I IFN (β) (2,000 RU/mL equivalent 8 ng/mL) or type III IFN (λ1−3) (300 ng/mL) for 2 hours. Organoids were then infected with VSV-Luc (MOI = 1). 8 hpi, viral replication was assayed by measuring the luciferase activity. Data are normalized to non-IFN-treated sample for each inhibitor (set to 100). The mean value obtained from three independent experiments is plotted. Error bars indicate the SD. ****P < 0.0001, ***P < 0.001, ns, not significant (unpaired t-test), n.d. (not determined). The data of this figure was adapted from Pervolaraki et al., 2017.

2.2 Differential induction of interferon stimulated genes between type I and type III IFNS is independent of interferon receptor abundance

The text and figures of part 2.2 have been adapted from Pervolaraki et al. (2018), *under preparation*. This corresponds to a first author manuscript under preparation resulting directly from my PhD research project.

It is currently believed that type I and III IFNs have redundant functions. However, the preferential distribution of type III IFN receptor on epithelial cells[73-80] suggests functional differences at epithelial surfaces. In addition, apart from the spatial restriction of their receptors, quantitative differences in the cellular response of type I versus type III IFN suggest that type I and type III IFNs establish their antiviral program with distinct kinetics of response and magnitude of ISGs induction[39,165,189,237,292-295].

Comparative analysis of the profile of ISGs stimulation with type I and type III IFNs in human cells have so far been conducted only in hepatoma cells, lung epithelial cells and lymphocytes without including a direct correlation of the antiviral with the transcriptional activity of IFNs[165,189,237,293-295]. In addition, these studies by utilizing traditional experimental approaches focused on the signaling cascades downstream of IFN receptor and failed to explain the molecular mechanisms leading to this peculiar delayed and reduced induction of ISGs upon type III IFN treatment.

Thus in this part of the presented thesis we followed a systems biology approach and combined mathematical modeling with time-resolved experiment data and proposed an alternative explanation where type III IFN receptor is expressed at lower levels at the cell surface. This lower receptor expression level could provide a biochemical explanation for the observed differences in delayed kinetics and weaker amplitude of ISG expression compared to type I IFN. In addition by utilizing different human intestinal epithelial cells and primary human-mini gut oganoids with functional receptor overexpression approaches we investigated whether the observed differences between both IFNs are intrinsic to both specific signal transduction pathways and whether they are restricted to some cell types (e.g. hepatocytes) or represent a global signaling signature in all cells expressing both IFN receptors.

2.2.1 Type III IFN-mediated antiviral protection is delayed compared to type I IFN.

We have previously reported that both type I and III IFNs mediate antiviral protection in human IECs. To address whether type I and type III IFN have a different profile of antiviral activity in IECs, as reported in human lung cells[295], we compared the potency of both IFNs in our human T84 intestinal epithelial cell model. Cells were pre-treated with increasing concentrations of either type I or III IFNs for 2.5 hours and subsequently infected with VSV-Luc. Viral infection was assayed by bioluminescence and results showed that although both IFNs induced an antiviral state in a dose-dependent manner, type III IFNs were more efficient in protecting against viral infection at low concentrations, whereas type I IFN was more potent at higher concentrations (Figure 23A). The concentration of type I IFN necessary to provide 90% of relative antiviral protection (EC90) was significantly lower than the one for type III IFN (Figure 23B). Interestingly, at high concentrations, type I IFN could almost fully inhibit viral infection while type III IFN was only able to reduce infection to 90% (Figure 23A).

To determine whether type III IFN requires a prolonged treatment to achieve similar antiviral protection as observed with type I IFN, we performed a time course experiment in which cells were pre-treated for different times with either IFN prior infection with VSV-Luc at concentrations which elicited their maximum antiviral activity (Figure 23C). We found that approximately 1 h pre-treatment with type I IFN was sufficient to reduce VSV infection by 90% (10% remaining infection), while type III IFN required around 3.5 hours to achieve a 90% reduction of infectivity (Figure 23C and 23D). Interestingly, 16 hours of pretreatment was necessary for type III IFN to almost completely prevent VSV infection (Figure 23C). These results strongly suggest that both type I and type III IFN could have similar potency but that type III IFN requires more time to establish an antiviral state.

We next addressed how long after infection IFN treatment is still able to promote antiviral protection. T84 cells were infected with VSV-Luc and treated at different times post-infection with either type I or III IFNs. Interestingly, type I IFN could inhibit viral replication even when added several hours post-infection. In contrast, type III IFN appeared to require a much longer time to establish its antiviral activity, and was unable to efficiently protect cells after VSV infection has initiated (Figure 23E and 23F). Importantly, these kinetic differences were neither virus nor cell line specific as similar results were observed in T84 cells infected by MRV (data not shown) and in the SKCO15 colon carcinoma line (Figure 24). Taken together these results demonstrate that while both type I and III IFNs can promote similar antiviral

states into target cells, they do so with distinct kinetics. The cytokine-induced antiviral state is promoted faster by type I IFN compared to type III IFN.

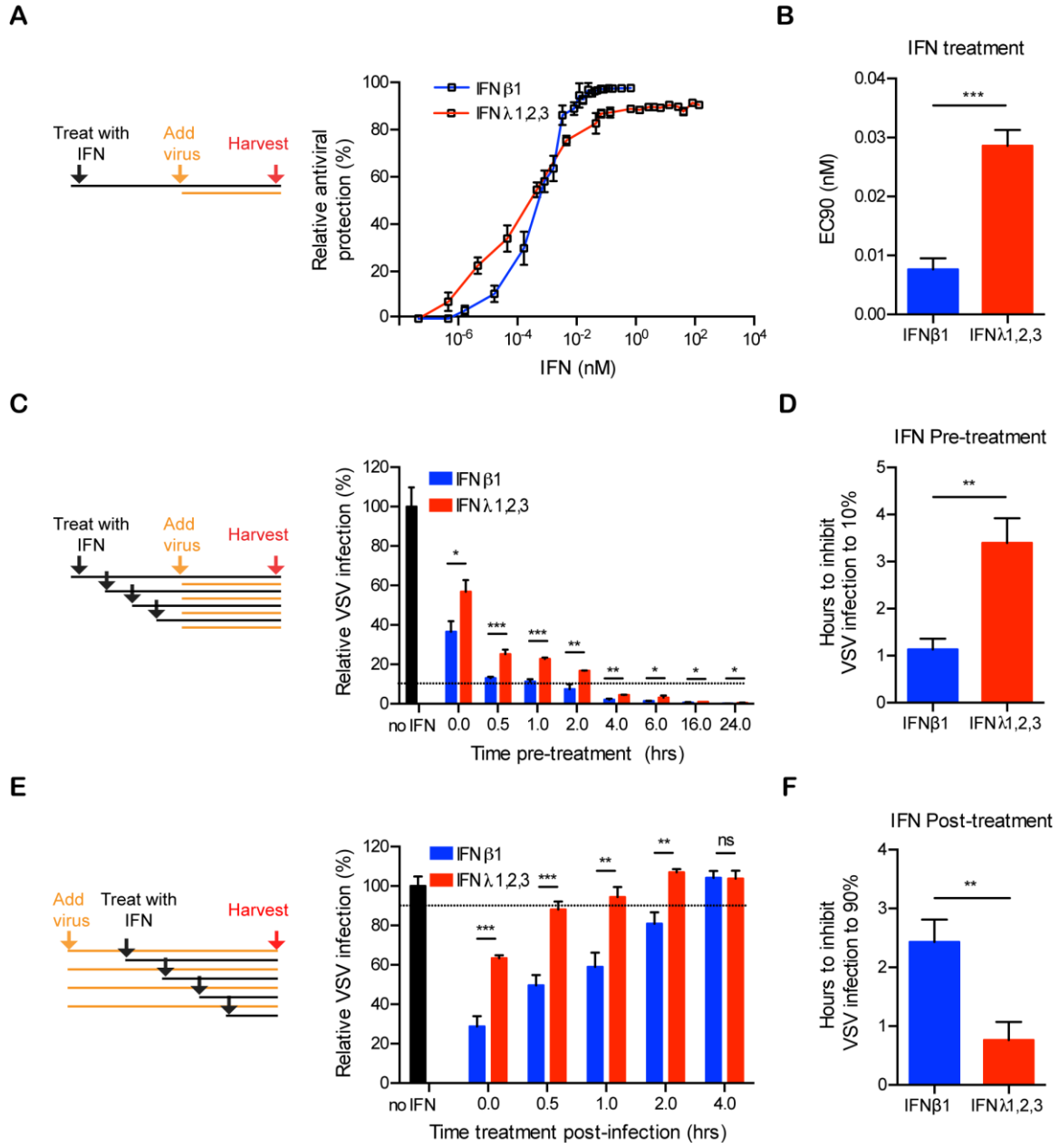

Figure 23. Kinetics of type I and type III IFN-mediated antiviral activities. (A-B) T84 cells were pre-treated with the indicated concentrations of type I IFN (β) or type III IFN (λ1−3) for 2.5 hours prior to infection with VSV-Luc using a MOI of 1. Viral replication was assayed by measuring the luciferase activity. (A) The relative antiviral protection is expressed as a percentage of total protection in VSV-infected cells or (B) as the EC90 corresponding to the concentration of type I IFN (β) or type III IFN (λ1−3) resulting in 90% inhibition (10% infection) of viral replication. (C-D) T84 cells were treated with type I IFN (β) (2,000 RU/mL equivalent 0.33 nM) or type III IFN (λ1−3) (100ng/mL each or total 300 ng/mL equivalent 13.7 nM) for indicated times prior to infection with VSV-Luc. Viral replication was assayed by measuring luciferase activity. (C) The relative VSV infection is expressed as the percentage of the luciferase activity present in VSV-infected cells without IFN treatment (set to 100). (D) Pre-incubation time of type I IFN (β) or type III IFN (λ1−3) required to inhibit VSV infection to 10% (90% inhibition). (E-F) Same as (C-D), except T84 cells were treated at the indicated times post-

infection with VSV-Luc. (F) Delayed-time post-infection for type I IFN (β) or type III IFN (λ1−3) to still inhibit VSV infection to 90% (10% inhibition). Data in (A–F) represent the mean values of three independent experiments. Error bars indicate the SD. *<P.05, **P < 0.01, ***P < 0.001, ****P < 0.0001, ns, not significant (unpaired t-test).

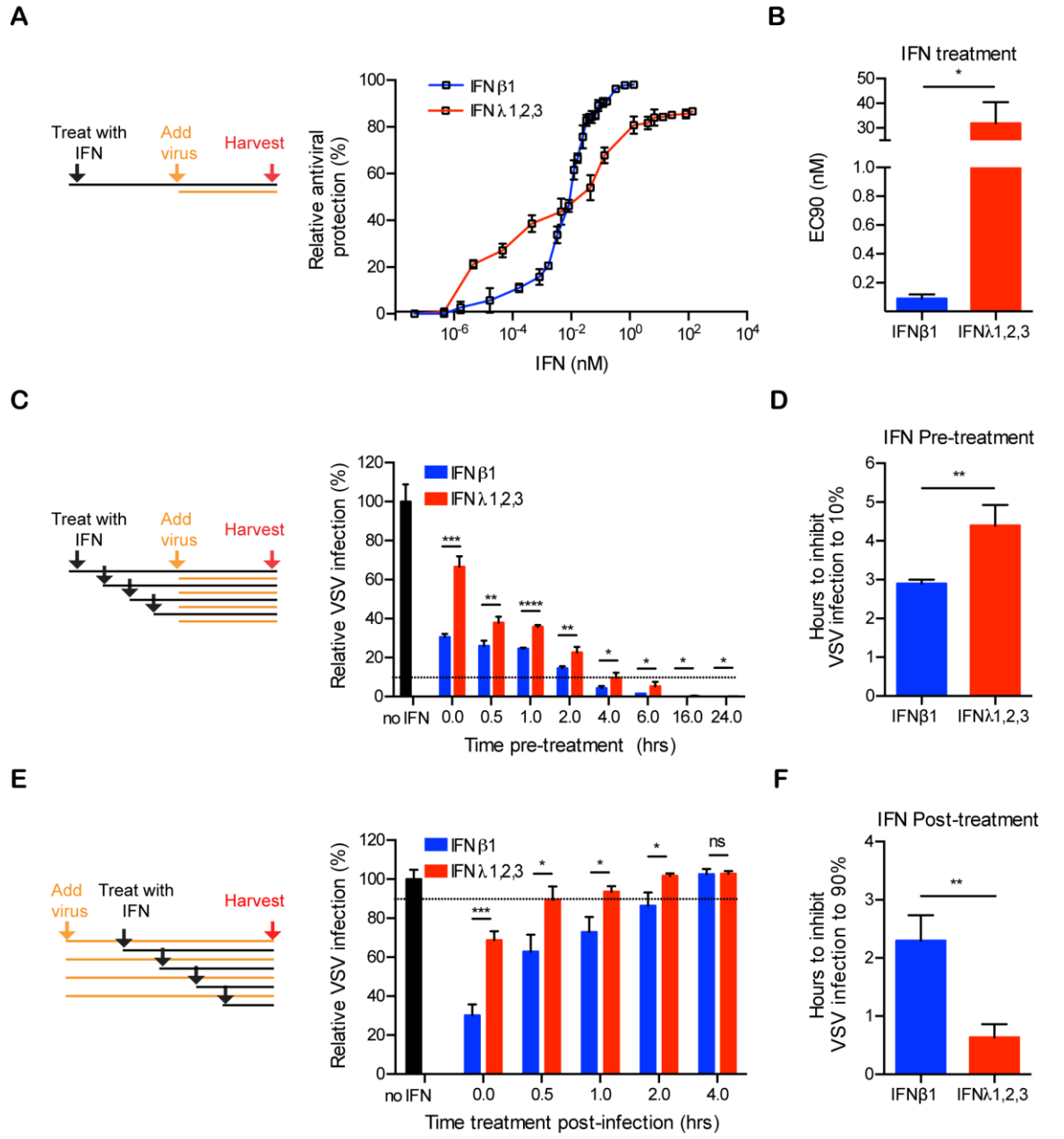

Figure 24. Kinetics of type I and type III IFN-mediated antiviral activities in SKCO15 cells. (A-B) SKCO15 cells were pre-treated with the indicated concentrations of type I IFN (β) or type III IFN (λ1−3) for 2.5 hours prior to infection with VSV-Luc using a MOI of 1. Viral replication was assayed by measuring the luciferase activity. (A) The relative antiviral protection is expressed as a percentage of total protection in VSV-infected cells or (B) as the EC90 corresponding to the concentration of type I IFN (β) or type III IFN (λ1−3) resulting in 90% inhibition (10% infection) of viral replication. (C-D) SKCO15 cells were treated with type I IFN (β) (2,000 RU/mL equivalent 0.33 nM) or type III IFN (λ1−3) (100ng/mL each or total 300 ng/mL equivalent 13.7 nM) for indicated times prior to infection with VSV-Luc. Viral replication was assayed by measuring luciferase activity. (C) The relative VSV infection is expressed as the percentage of the luciferase activity present in VSV-infected cells without IFN treatment (set to 100). (D) Pre-incubation time of type I IFN (β) or type III IFN (λ1−3) required to

inhibit VSV infection to 10% (90% inhibition). (E-F) Same as (C-D), except SKCO15 cells were treated at the indicated times post-infection with VSV-Luc. (F) Delayed-time post-infection for type I IFN (β) or type III IFN (λ1−3) to still inhibit VSV infection to 90% (10% inhibition). Data in (A–F) represent the mean values of three independent experiments. Error bars indicate the SD. *<P.05, **P < 0.01, ***P < 0.001, ****P < 0.0001, ns, not significant (unpaired t-test).

2.2.2 Type I and III IFNs induce different amplitudes and kinetics of ISG expression.

To understand how type I and type III IFNs promote an antiviral state in cells but with different kinetics, we analyzed the magnitude of ISG expression over time upon IFN treatment. T84 IECs were treated with increasing concentrations of either type I or type III IFN and the expression levels of two representative ISGs (IFIT1 and Viperin) were assayed at different times post-IFN treatment. Results revealed that type I IFN ultimately leads to a significantly higher induction of both IFIT1 and Viperin compared to type III IFN (Figure 25A and 25B). This difference in the magnitude of ISG stimulation was independent of both the duration of IFN treatment (Figure 25A and 25B) and the cell line used as similar results were obtained in the colon carcinoma derived SKCO15 and Caco2 cells and in non-transformed IECs using human mini-gut organoids (Figure 26A and 26B). To determine if this pattern of expression applies to other ISGs, we treated T84 cells with either type I or type III IFN over a 24-hour time course, and analyzed the mRNA levels of 132 different ISGs and transcription factors involved in IFN signaling (see complete list of genes and corresponding primers in S1 and S2 Table) (Figure 25C and 25D). Differential expression analysis revealed that both type I and type III IFNs induce almost the same set of ISGs and that most of the genes significantly induced by type III IFN were also induced by type I IFN (Figure 25C). However, similar to IFIT1 and Viperin (Figure 25A and 25B), we found that the magnitude of ISG expression was always greater for type I IFN compared to type III IFN (Figure 25D). To ensure that type III IFN induces globally a lower transcriptional response in primary non-transformed human IECs, the expression of the above set of 132 ISGs was analyzed in human mini-gut organoids upon stimulation with either type I or type III IFN over a 24-hour time course. Importantly, and similar to T84 cells, results revealed the weaker transcriptional activity of type III IFN compared to type I (Figure 26C and 26D).

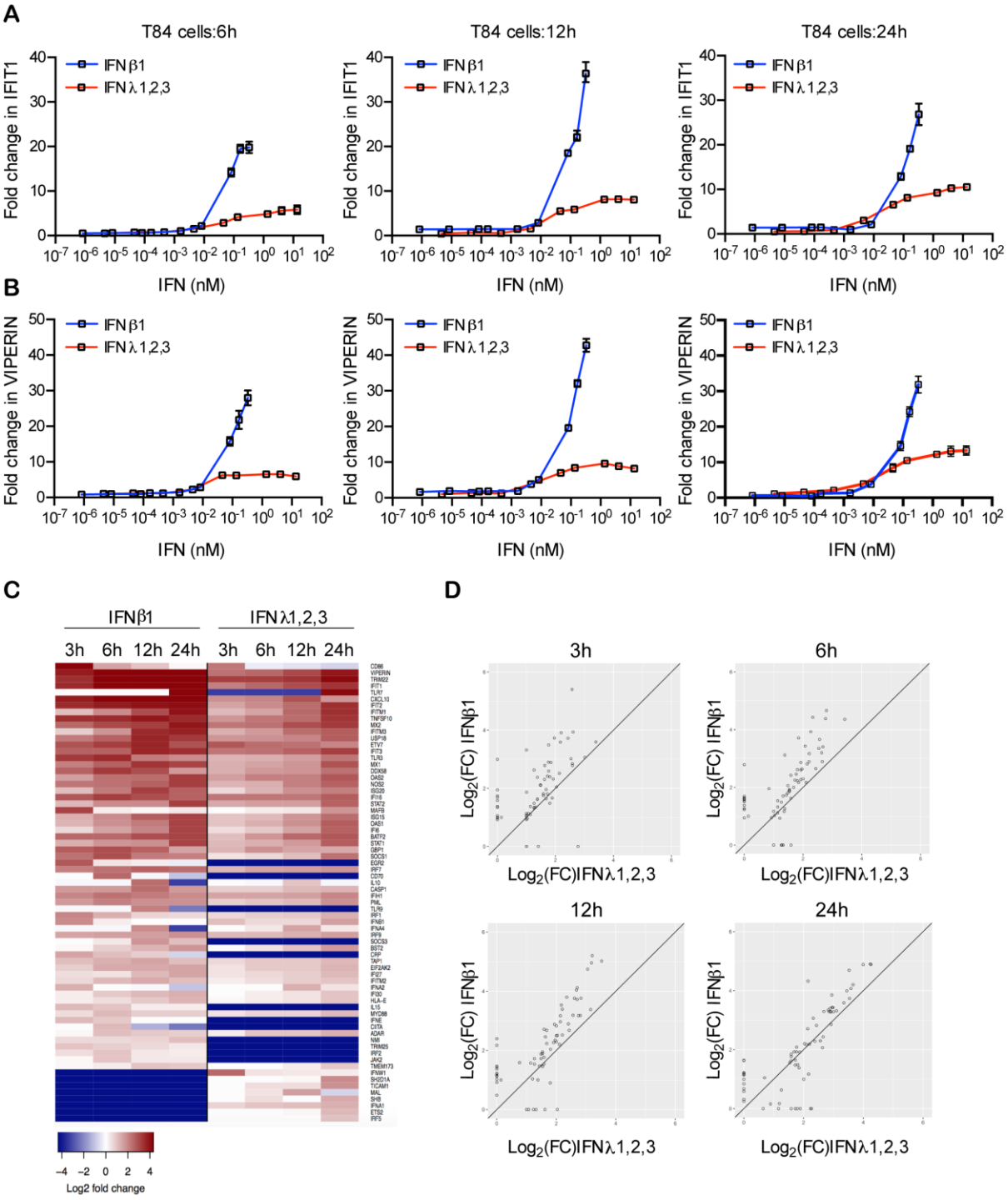

Figure 25. Type III IFNs have a lower transcriptional activity compared to type I IFNs. (A-B) T84 cells were stimulated with indicated concentrations of type I (β) or III IFN (λ1−3) for indicated times and the transcript levels of the ISGs IFIT1 and Viperin were analyzed by qRT-PCR. Data are normalized to TBP and HPRT1 and are expressed relative to untreated cells at each time point. A representative experiment with technical triplicates, out of three independent experiments is shown. Mean values and SD are shown. (C) T84 cells were treated with type I IFN (β) (2,000 RU/mL equivalent 0.33 nM) or type III IFN (λ1−3) (300 ng/mL equivalent 13.7 nM) for the indicated times and identification of the IFN-induced ISGs was performed by qRT-PCR. A total of 70 out of 132 ISGs tested were found to be significantly induced more than 2-fold compared with a baseline (mean of

untreated controls at the particular time points) for at least one time point by at least one IFN treatment. Data are normalized to TBP and HPRT1 and visualized in a heatmap using R after sorting the fold change of expression in response to type I IFN (β) in decreasing order. (D) Comparison of expression values (log2 (Fold Change)) for all genes induced at the indicated times with type I IFN (β) versus type III IFN (λ1−3). Solid line indicates equivalent expression.

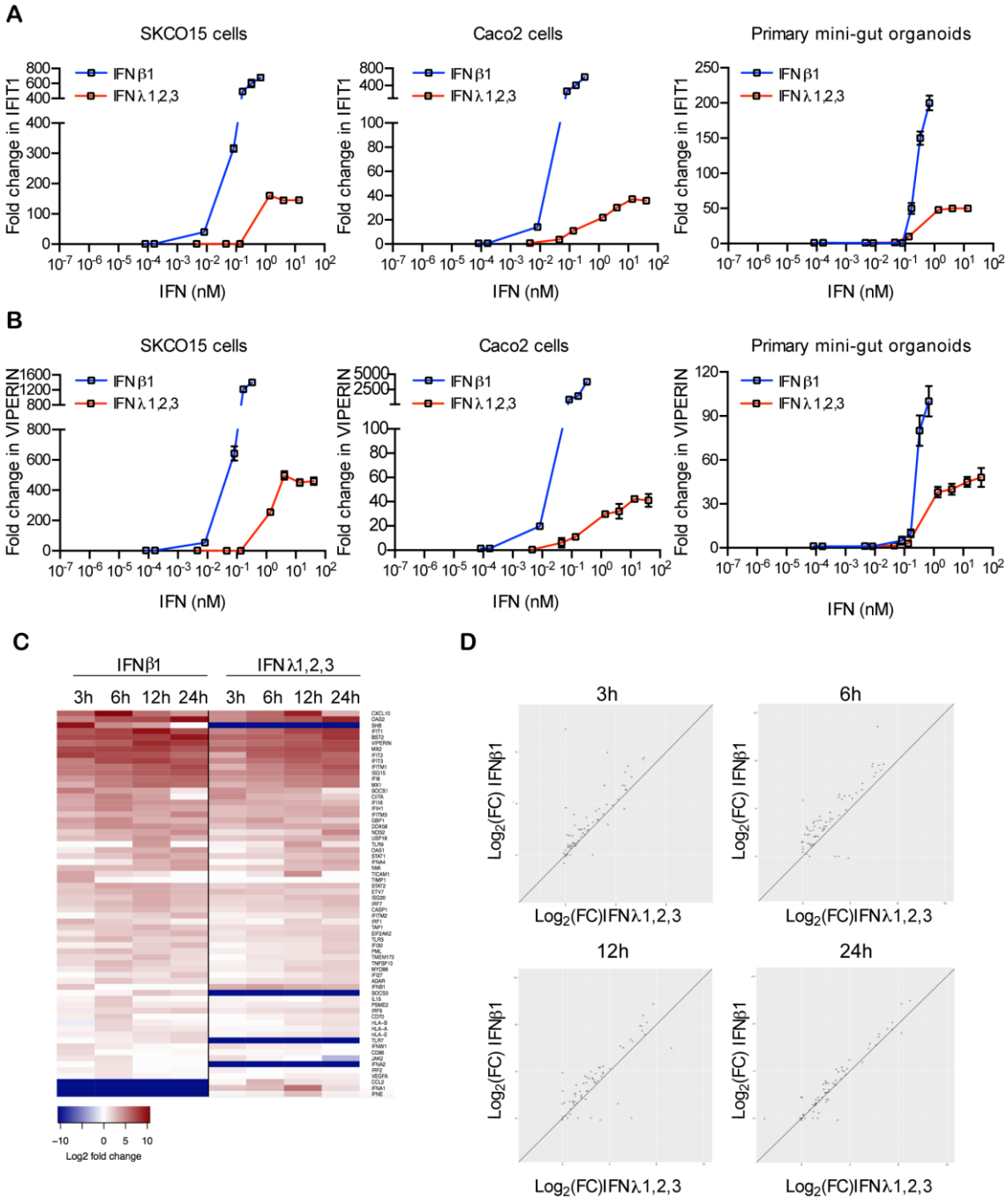

Figure 26. Type III IFNs have a lower transcriptional activity compared to type I IFNs in multiple intestinal epithelial cell lines. (A-B) SKCO15, Caco2 and primary IECs from human mini-gut organoids were stimulated with indicated concentrations of type I (β) or III IFN (λ1−3) for 6 hours and the transcript levels of the ISGs IFIT1 and VIPERIN were analyzed by qRT-PCR. Data are normalized to TBP and HPRT1 and are expressed relative to untreated cells. A representative experiment with

technical triplicates, out of three independent experiments is shown. Mean values and SD are shown. (C) Human mini-gut organoids were treated with type I IFN (β) (2,000 RU/mL equivalent 0.33 nM) or type III IFN (λ1−3) (300 ng/mL equivalent 13.7 nM) for the indicated times and identification of the IFN-induced ISGs was performed by qRT-PCR. A total of 65 out of 132 ISGs tested were found to be significantly induced more than 2-fold compared with a baseline (mean of untreated controls at the particular time points) for at least one time point by at least one IFN treatment. Data are normalized to TBP and HPRT1 and visualized in a heatmap using R after sorting the fold change of expression in response to type I IFN (β) in decreasing order. (D) Comparison of expression values (log2 (Fold Change)) for all genes induced at the indicated times with type I IFN (β) versus type III IFN (λ1−3). Solid line indicates equivalent expression.

To address whether there is any correlation between the different antiviral protection kinetics conferred by type I and III IFNs (Figure 23) and the kinetics of ISG expression, we analyzed the temporal expression of ISGs upon IFN treatment. Hierarchical clustering analysis of all ISGs up-regulated upon type I or type III IFN treatment defined four distinct expression profiles based on the time of their maximum induction (Figure 27A-C). Group 1 are ISGs whose expression peaks 3 hours post-IFN treatment. The expression of ISGs in group 2 and 3 peaks at 6 and 12 hours post-treatment, respectively. Group 4 corresponds to ISGs with a continuous increase in expression over time (Figure 27A and 27B). Under type I IFN treatment, ISGs were nearly equally distributed in all four expression groups (Figure 27A, 27C, and 27D). By contrast, although the same ISGs were induced by type III IFN, they almost all belong to the expression group 4, being expressed late after IFN treatment (Figure 27B-D). To exclude cell line specific effects, we analyzed the kinetic profiles of ISG expression in primary human intestinal epithelial cells. In line with our findings in T84 cells, by utilizing human mini-gut organoids, we could clearly demonstrate that type I and type III IFNs stimulate ISGs with very distinct kinetics in intestinal epithelial cells, with type III IFN inducing a more delayed transcriptional response (Figure 28A-D).

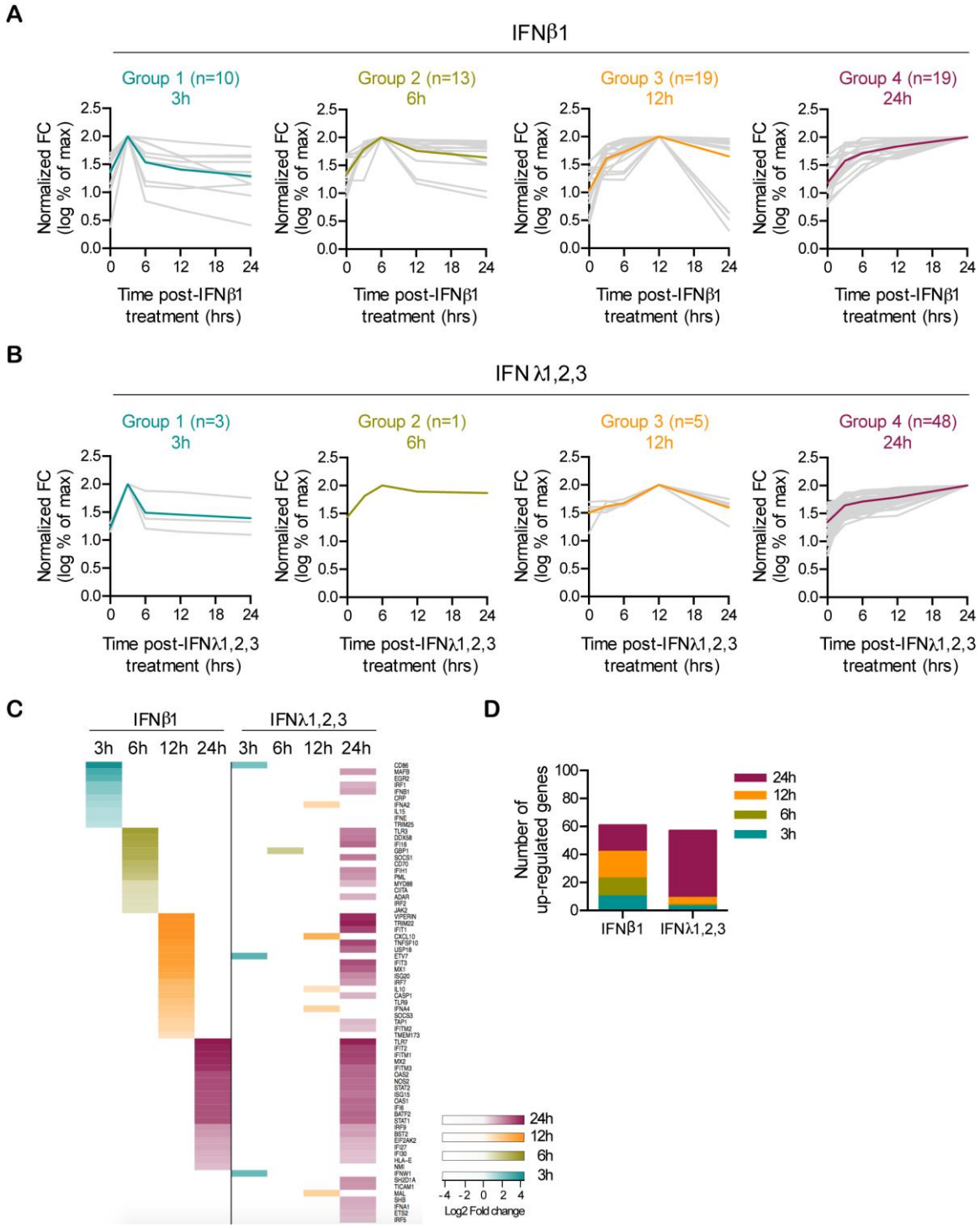

Figure 27. Type III IFNs present delayed transcriptional activity compared to type I IFNs in intestinal epithelial cells. (A-D) T84 cells were treated with type I IFN (β) (2,000 RU/mL equivalent 0.33 nM) or type III IFN (λ1−3) (300 ng/mL equivalent 13.7 nM) for 3, 6, 12 or 24 hours and the kinetic pattern of expression of the 70 significantly up-regulated ISGs were analyzed by qRT-PCR in triplicates. Data are normalized to TBP and HPRT1 and are expressed relative to untreated cells at each time point. Hierarchical clustering analysis of these genes produced four distinct temporal expression patterns (Groups 1-4) based on the time-point of the maximum induction in response to type I IFN (β) or type III IFN (λ1−3). Color codes have been used to visualize the induction peak per group. (A-B) Gray lines show the normalized kinetic expression of each gene for each group upon treatment with (A) type I IFN (β) or (B) type III IFN (λ1−3). The colored lines are the average of the

kinetic profiles for the genes of each group. (C) Gene expression heat map showing the genes clustered in their respective temporal expression patterns groups in response to type I IFN (β) or type III IFN (λ1−3). The genes per group are sorted in decreasing order on the basis of their fold change of expression in response to type I IFN (β) or type III IFN (λ1−3) and only showing the highest expressed values within the temporal groups omitting all other values for visualization. (D) Number of genes belonging to each group.

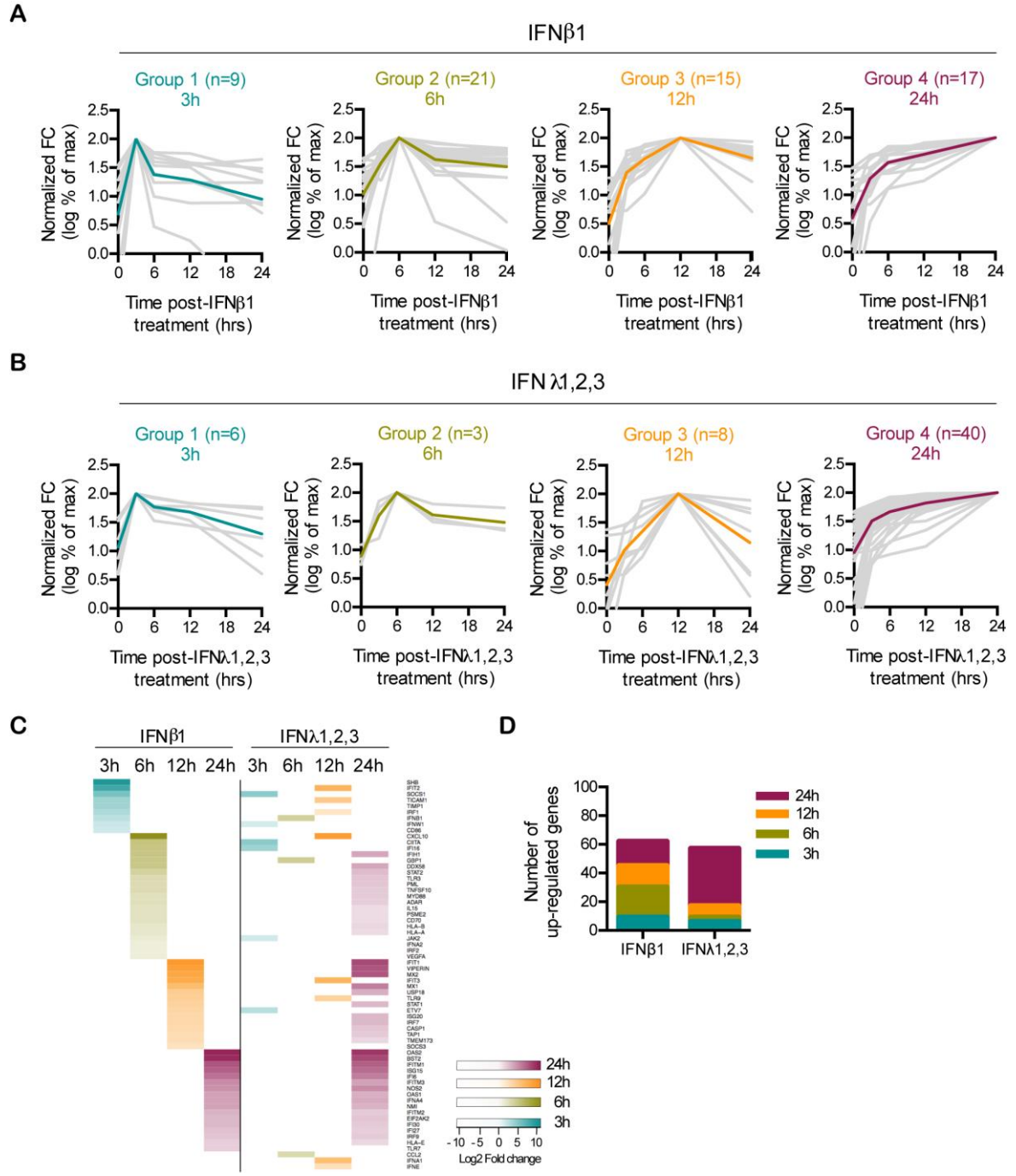

Figure 28. Type III IFNs present delayed transcriptional activity compared to type I IFNs in human mini-gut organoids. (A-D) Human mini-gut organoids were treated with type I IFN (β) (2,000 RU/mL equivalent 0.33 nM) or type III IFN (λ1−3) (300 ng/mL equivalent 13.7 nM) for 3, 6, 12 or 24 hours and the kinetic pattern of expression of the 65 significantly up-regulated ISGs were analyzed by qRT-PCR in triplicates. Data are normalized to TBP and HPRT1 and are expressed relative to untreated cells at each time point. Hierarchical clustering analysis of these genes produced four

distinct temporal expression patterns (Groups 1-4) based on the time-point of the maximum induction in response to type I IFN (β) or type III IFN (λ1−3). Color codes have been used to visualize the induction peak per group. (A-B) Gray lines show the normalized kinetic expression of each gene for each group upon treatment with (A) type I IFN (β) or (B) type III IFN (λ1−3). The colored lines are the average of the kinetic profiles for the genes of each group. (C) Gene expression heat map showing the genes clustered in their respective temporal expression patterns groups in response to type I IFN (β) or type III IFN (λ1−3). The genes per group are sorted in decreasing order on the basis of their fold change of expression in response to type I IFN (β) or type III IFN (λ1−3) and only showing the highest expressed values within the temporal groups omitting all other values for visualization. (D) Number of genes belonging to each group.

To control that the differences in ISG expression kinetics between type I and III IFNs are not only true at the transcriptional level but also at the protein level, we checked the protein expression of three ISGs (IRF1, IFIT1, MXA) over time post-IFN treatment. We found that the difference in the kinetics of ISG expression between both type I and type III IFNs is also present at the protein level (Figure 29A-C).

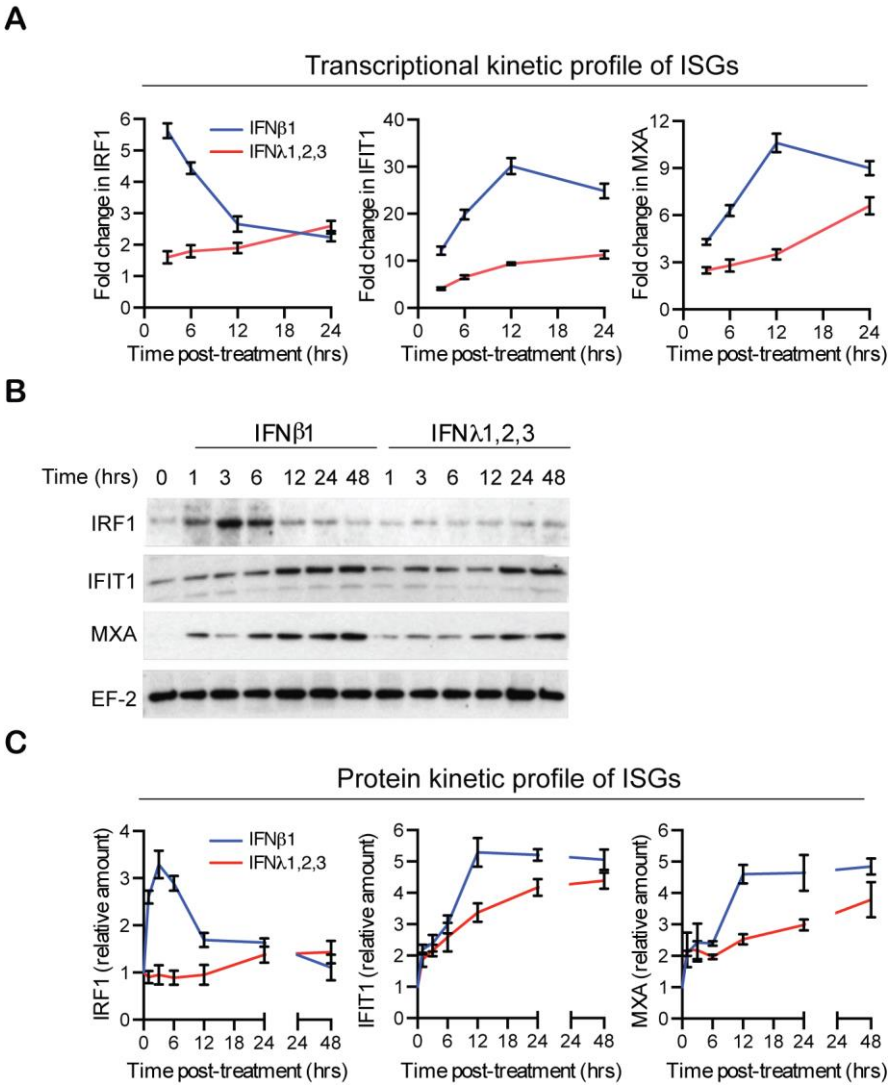

Figure 29. Temporal differences of ISG expression induced by type I and type III IFNs. (A-C) T84 cells were stimulated with type I IFN (β) (2,000 RU/mL equivalent 0.33 nM) or type III IFN (λ1−3) (300 ng/mL equivalent 13.7 nM) for the indicated times. (A) The transcript levels of the ISGs IRF1, IFIT1 and MXA were assessed by qRT-PCR. Data were normalized to HPRT1 and are expressed relative to untreated cells of each time point. The mean value obtained from three independent experiments is shown. Error bars indicate the SD. (B) The protein levels of the ISGs IRF1, IFIT1 and MXA are analyzed by Western blot. EF-2 was used as a loading control. A representative immunoblot is shown. (C) Quantification of ISGs levels from Western blot in (B). Quantification is expressed relative to untreated cells and normalized using EF-2 as loading control. Data represent the mean values of two independent experiments. Error bars indicate the SD.

We next wanted to control that our observed differences in the kinetics of ISGs expression induced by both cytokines were independent of IFN concentration. T84 cells were treated with increasing amounts of type I or type III IFNs and the transcriptional up-regulation of representative ISGs belonging to each of the expression profile groups (group 1-4, Figure 27) was measured over time. Consistent with our previous results, the temporal expression patterns of the representative ISGs were independent of the IFN concentration and the ISG expression kinetic signature was specific to each IFN (Figure 30A-D). Altogether, our results

strongly suggest that although both type I and type III IFNs induce a similar set of ISGs in hIECs, type III IFN induces globally a lower amplitude and a delayed ISG expression compared to type I IFN.

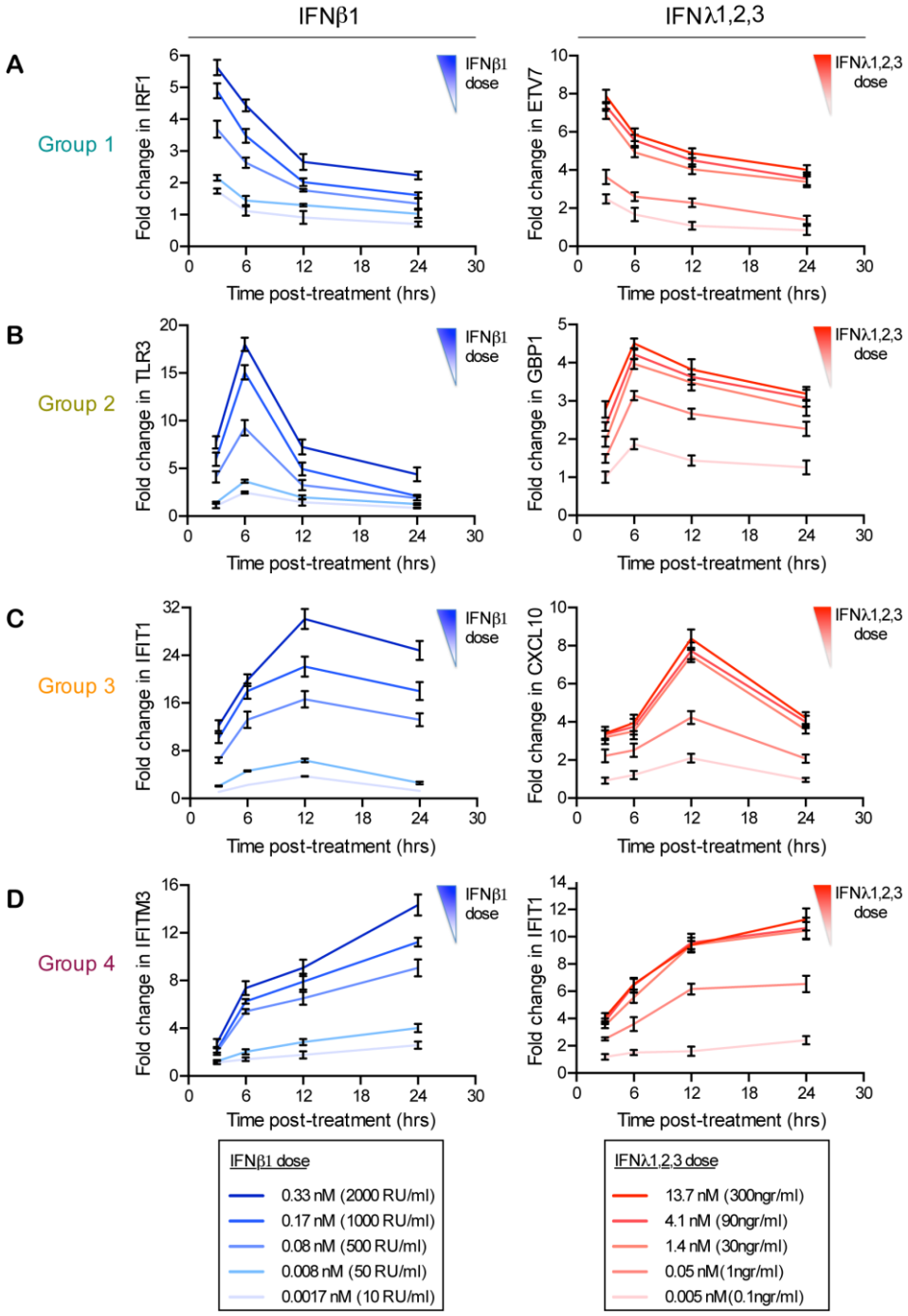

Figure 30. Validation of the unique kinetic patterns of ISG expression upon type I versus type III IFN treatment. (A-D) T84 cells were stimulated with increasing concentrations of type I IFN (β) or III IFN (λ1−3) for indicated times and the kinetic pattern of expression of one representative ISG from each temporal expression patterns groups 1-4 was analyzed by qRT-PCR, (left column) type I IFN (β), (right column) type III IFN (λ1−3) treated cells. Data are normalized to HPRT1 and are expressed relative to untreated cells at each time point. A representative experiment with technical triplicates, out of three independent experiments is shown. Mean values and SD are shown.

2.2.3 Mathematical modeling reveals that IFN receptor abundance modulates the magnitude of ISG response while its kinetic profile is largely preserved

Our data show remarkable differences in the magnitude and kinetics of ISGs induced by type I versus type III IFN (Figure 25-28), and in the subsequent induction of a differential antiviral state (Figure 23-24). To investigate the mechanisms underlying these differences, we developed a data-driven mathematical model of both IFNs. The model describes the dynamics of receptor activation and inactivation, STAT1/2 phosphorylation and STAT-dependent activation of ISG expression (Figure 31A). The model was implemented as a system of ordinary differential equations and fitted to the time-resolved data for the prototypical ISG, Viperin, measured with different doses of type I or type III IFNs (S1 Table). The model accounted for both the dose-response and the different Viperin expression kinetics triggered by type I or type III IFN, group 3 and group 4 expression kinetics respectively (Figure 31B-C). Using our mathematical model, we could predict that at low IFN concentrations, Viperin is induced almost equally by both IFNs whereas at higher concentrations, type I IFN induces a stronger transcriptional up-regulation of Viperin (Figure 31D). These predictions are in good agreement with our experimental data (Figure 31B, right panel).

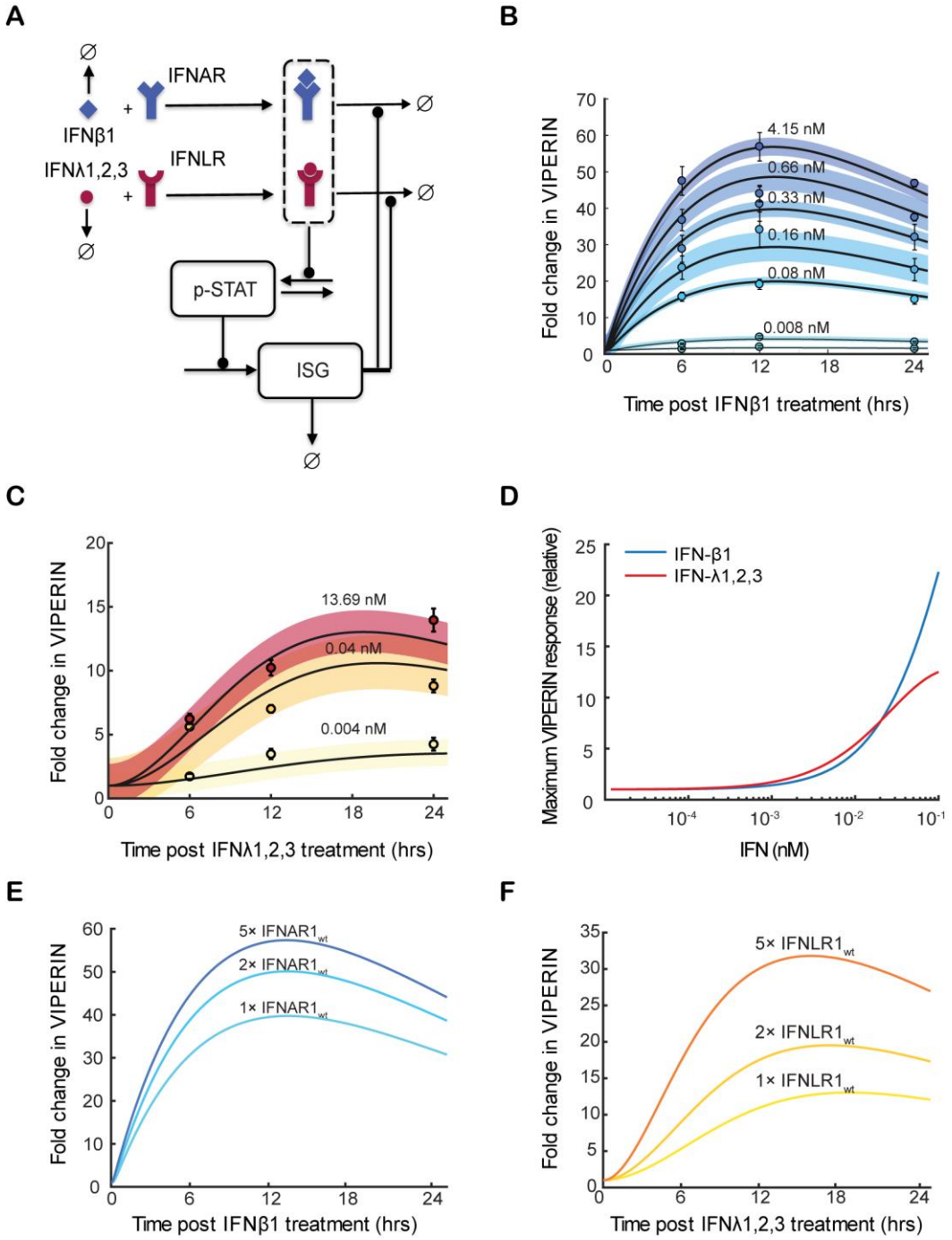

Figure 31. Mathematical modeling of type I and type III IFN responses. (A) Scheme of the mathematical model. The empty set sign "∅" represents sink. (B-C) The mathematical model reproduces the Viperin expression dynamics upon treatment with different concentrations of (B) type I IFN (β) and (C) type III IFN (λ1−3). In (B) and (C), the solid lines represent the best fits and the shaded areas are approximate 95% confidence intervals. (D) Simulation of the maximum Viperin induction upon treatment with equal concentrations of type I IFN (β) or type III IFN (λ1−3). (E-F) The mathematical model shows the effect of IFNAR1 and IFNLR1 overexpression up to 5-fold (5×IFNAR1wt and 5×IFNLR1wt) on Viperin activation upon treatment with representative concentrations of type I IFN (β) (2,000 RU/mL equivalent 0.33 nM) or type III IFN (λ1−3) (300 ng/mL equivalent 13.7 nM), respectively. Modeling has been performed by Soheil Rastgou Talemi, Heidelberg University and German Cancer Research Center (DKFZ).

Both type I and type III IFN receptor complexes mediate STAT-driven ISG expression but they do so at different rates. The components that are specific to each IFN pathway are the receptors[38,39] and therefore we assume that the activation and inactivation of type I and III IFN receptor complexes may be differentially regulated. The simulations of the parameterized model show transient activity of type I IFN receptor (IFNAR) complex and sustained activity of type III IFN receptor (IFNLR) complex (Figure 32). The model suggests that the sustained activity of IFNLR complex is mainly due to its longer half-life compared to IFNAR complex. This prediction is further supported by statistical analysis of the estimated model parameters, showing that the confidence bounds of the estimated inactivation rates of the two receptors do not overlap (S1 Figure). Altogether, our data-based mathematical model shows that the differential kinetics of the ISG responses to type I and type III IFNs could be explained by the different activation and inactivation kinetics of the respective receptors.

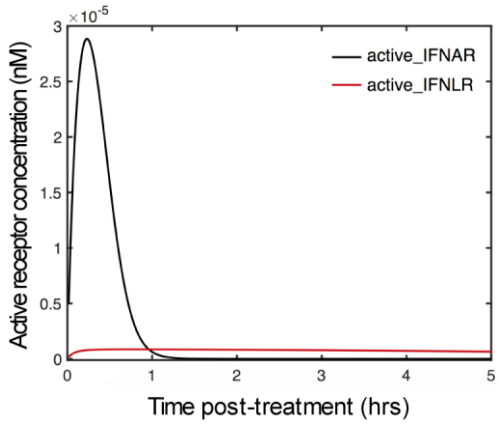

Figure 32. Comparative simulation of type I and type III IFN receptor complex activation. Cellular concentration of the activated type I or type III IFN receptor complex, upon treatment with 0.1 nM of IFNs, are simulated using the calibrated model. Modeling has been performed by Soheil Rastgou Talemi, Heidelberg University and German Cancer Research Center (DKFZ).

Additionally, according to our model the density of IFN receptors at the cell surface represents a critical determinant for the activity exhibited by the two IFNs. In particular, our model stimulation predicts that if we increase the receptor level, we increase the transcriptional potency of IFNs but the kinetic profiles of ISGs induction is largely preserved (Figure 31E-F). To experimentally validate the model predictions, IFNAR1 and IFNLR1 were overexpressed in T84 cells. Overexpression of the respective IFN receptor chain was confirmed by qRT-PCR (Figure 33A-C).

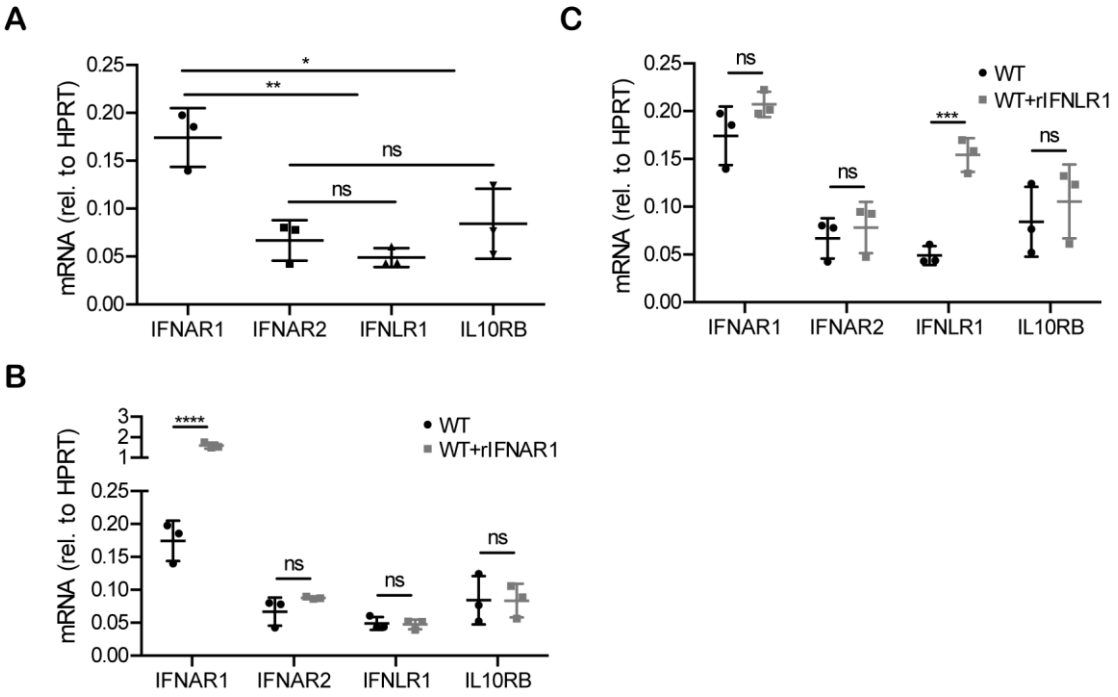

Figure 33. Expression levels of IFN receptors in T84 cells. (A) T84 wild-type cells, (B) T84 cells overexpressing rIFNAR1 (WT+rIFNAR1) and (C) T84 cells overexpressing rIFNLR1 (WT+rIFNLR1) were analyzed by qRT-PCR to quantify the transcript levels of IFNAR1, IFNAR2, IFNLR1 and IL10RB (IFNLR2). Data are normalized to HPRT1. The mean value obtained from three independent experiments is shown. Error bars indicate the SD. *<P.05, **P < 0.01, ***P < 0.001, ****P < 0.0001, ns, not significant (unpaired t-test).

To ensure the functionality of both IFN receptors, IFNAR1 or IFNLR1 were expressed in our previously characterized knockout T84 cell lines deficient for either the IFN alpha receptor 1 (IFNAR1-/-) or the IFN lambda receptor 1 (IFNLR1-/-)[100] (Figure 34A and 34F). Our results show that overexpression of IFNAR1 in our IFNAR1-/- T84 cells (IFNAR1-/-+rIFNAR1) restores their antiviral activity, their ability to phosphorylate STAT1 and their production of the ISGs IFIT1 and Viperin in the presence of type I IFN (Figure 34B-E). Similarly, although IFNLR1-/- cells were insensitive to type III IFN treatment, overexpression of IFNLR1 (IFNLR1-/-+rIFNLR1) restored their antiviral activity, pSTAT1 and ISG induction after addition of type III IFN (Figure 34G-J). These results demonstrate the functionality of both IFN receptors and validate our overexpression approach as a mean to increase IFNAR1 and IFNLR1 levels at the cell surface.

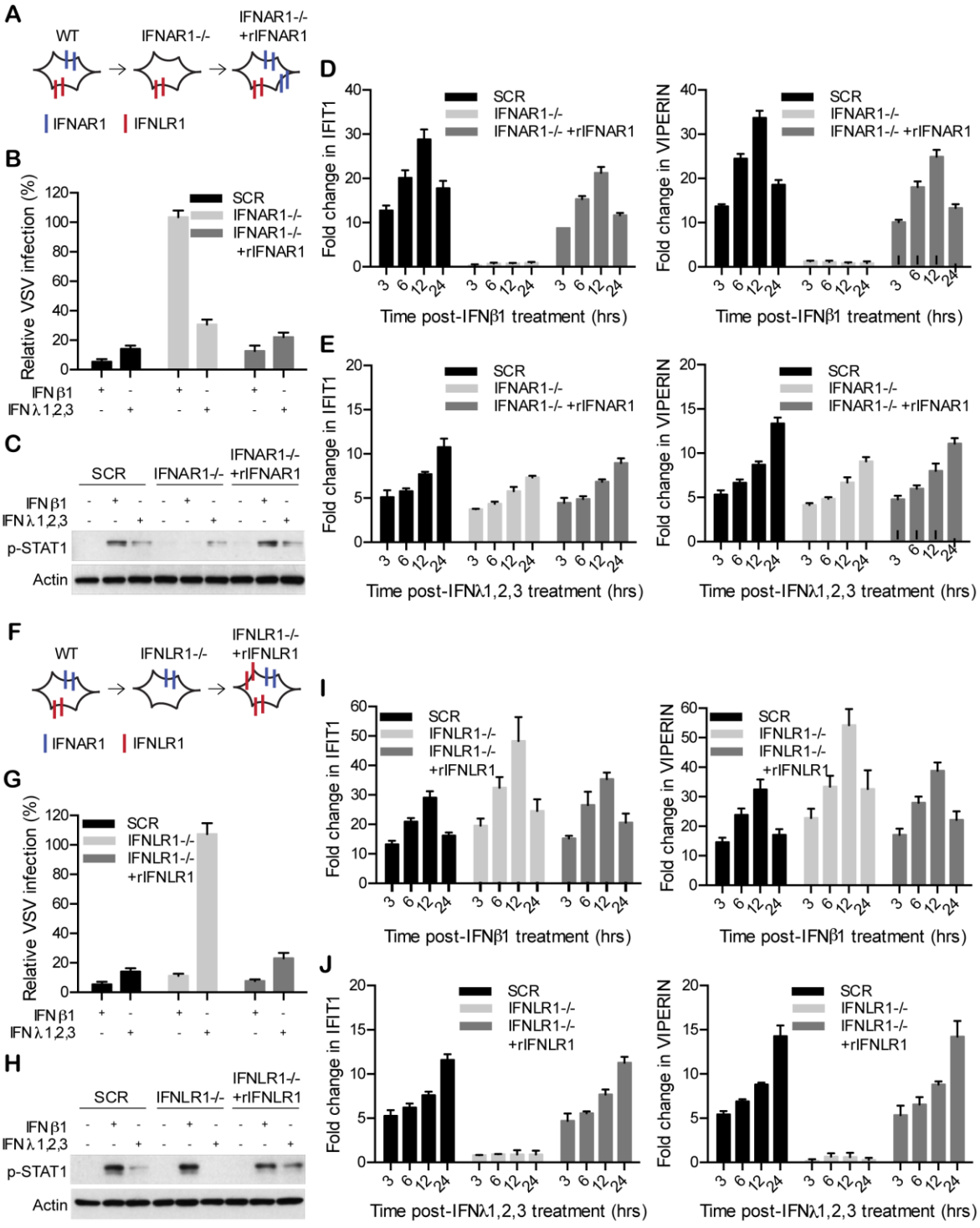

Figure 34. Type I and type III IFN receptors are functional when overexpressed into cells. (A-E) T84 IFNAR1-/- cells were rescued by stable expression of a cleavage resistant mutant of rIFNAR1 (see methods for details) (T84 IFNAR1-/- + rIFNAR1). (B-E) T84 IFNAR1-/-, T84 IFNAR1-/- + rIFNAR1 cells and control T84 cells scramble gRNA (SCR) were pre-treated with type I IFN (β) (2,000 RU/mL equivalent 0.33 nM) or type III IFN (λ1−3) (300 ng/mL equivalent 13.7 nM). (B) 2.5 h post-treatment, T84 cells were infected with VSV-Luc (MOI = 1). Viral replication was assayed by measuring the luciferase activity. For each sample luciferase activity was measured in triplicates and is expressed as the percentage of the luciferase signal in VSV-infected cells without IFN treatment

(set to 100) for each cell lines. (C) 1h post IFN treatment, IFN signaling was measured by immunoblotting for pSTAT1 Y701. Actin was used as a loading control. A representative immunoblot out of three independent experiments is shown. (D-E) same as (B), except that induction of IFN-stimulated genes was monitored by relative qRT-PCR quantification of IFIT1 and Viperin at the indicated times post-IFN treatment. (F-J) same as (A-E) except that T84 IFNLR1-/- were rescued by stable expression of a cleavage resistant mutant of rIFNLR1 (T84 IFNLR1-/- + rIFNLR1). Data were normalized to HPRT1 and are expressed relative to untreated cells of each time point. The mean value obtained from three independent experiments is shown. Error bars indicate the SD.

Wild-type T84 cells overexpressing type I IFN receptor (WT+rIFNAR1) were treated with increasing concentrations of type I IFN. Our results show elevated levels of STAT1 phosphorylation and ISG induction in response to stimulation with type I IFN compared to wild-type cells (Figure 35A-C). Importantly, the response of T84 cells overexpressing type I IFN receptor to type III IFN remained unchanged, indicating a selective enhancement of the type I IFN signaling pathway. Similarly, overexpression of type III IFN receptor (WT+rIFNLR1) shows a significant increase in phosphorylated STAT1 and ISG expression compared to wild-type cells upon type III IFN stimulation, while no difference was observed upon type I IFN treatment (Figure 35D-F). Altogether, our experimental data are consistent with the modeling predictions and confirm the crucial impact of surface receptor levels for regulating the magnitude of type I and III IFN response.

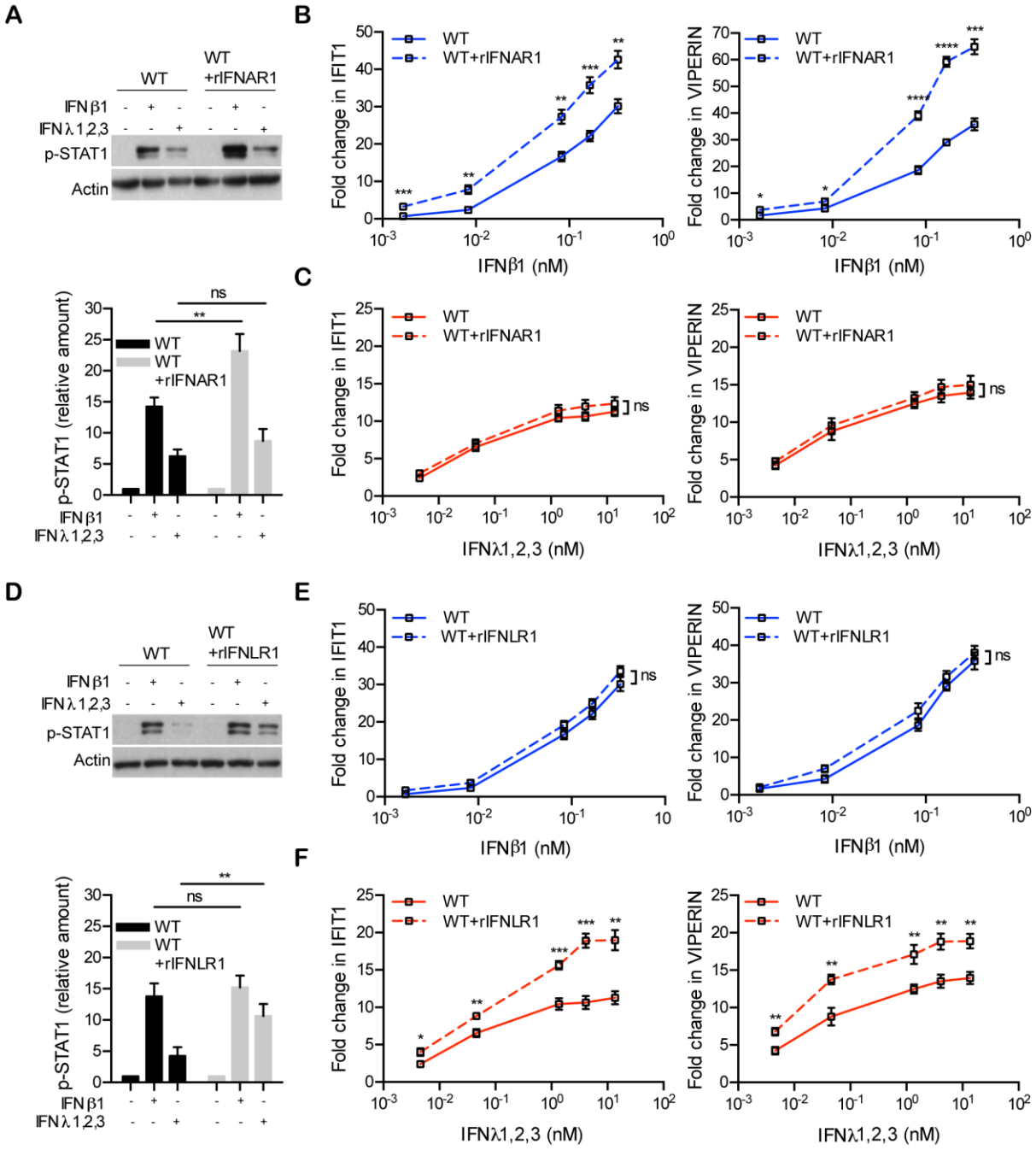

Figure 35. Overexpression of type I and type III IFN receptor increases the transcriptional activity of both cytokines. Wild-type T84 cells were transduced with rIFNAR1 or rIFNLR1 to create stable lines overexpressing either IFN receptors. (A) T84 wild-type cells (WT) and T84 cells overexpressing rIFNAR1 (WT+rIFNAR1) were treated with type I IFN (β) (2,000 RU/mL equivalent 0.33 nM) or type III IFN (λ1−3) (300 ng/mL equivalent 13.7 nM) for 1 hour and IFN signaling was measured by immunoblotting for pSTAT1 Y701. Actin was used as a loading control. A representative immunoblot out of three independent experiments is shown and the quantification of pSTAT1 levels. (B-C) T84 wild type cells (WT) and T84 cells overexpressing rIFNAR1 (WT+rIFNAR1) were treated with increasing concentrations of type I IFN (β) for 12 hours or type III IFN (λ1−3) for 24 hours and the transcript levels of the ISGs IFIT1 and VIPERIN were analyzed by qRT-PCR. Data are normalized to HPRT1 and are expressed relative to untreated cells at each time point. (D-F) Same as (A-C), except T84 cells overexpressing rIFNLR1 (WT+IFNLR1) were used. The mean value obtained from three independent experiments is shown. Error bars indicate the SD. *<P.05, **P < 0.01, ***P < 0.001, ****P < 0.0001, ns, not significant (unpaired t-test).

We next addressed whether this increase of ISG expression in cells overexpressing either the type I or type III IFN receptor was associated with an improved antiviral activity. Wild-type T84 cells overexpressing type I IFN receptor (WT+rIFNAR1) were treated with type I IFN at different time points prior to infection with VSV-Luc virus and their antiviral activity was compared to wild-type T84 cells. Our results showed that the potency and the kinetics of the antiviral activity of cells overexpressing type I IFN receptor does not present any significant change upon type I IFN treatment (Figure 36A-B). Similarly, there is no difference in the antiviral activity when cells overexpressing type I IFN receptor were treated with type I IFN at different time points post-infection (Figure 37A-B). The response of T84 cells overexpressing type I IFN receptor to type III IFN remained also unchanged (Figure 36C-D and 37C-D). However, overexpression of type III IFN receptor (WT+rIFNLR1) shows a modest but significant enhancement in type III IFN antiviral potency in the earlier time points of pre-treatment (between 30 minutes and 2 hours) compared to wild-type cells upon type III IFN stimulation (Figure 36G), while they responded similarly to wild-type cells upon type I IFN treatment (Figure 36E-F). Consistent with this, cells overexpressing type III IFN receptor are more protected than wild-type cells when type III IFN was added post-infection for the early time points (Figure 37G), while they responded similarly to wild-type cells upon type I IFN treatment (Figure 37E-F).

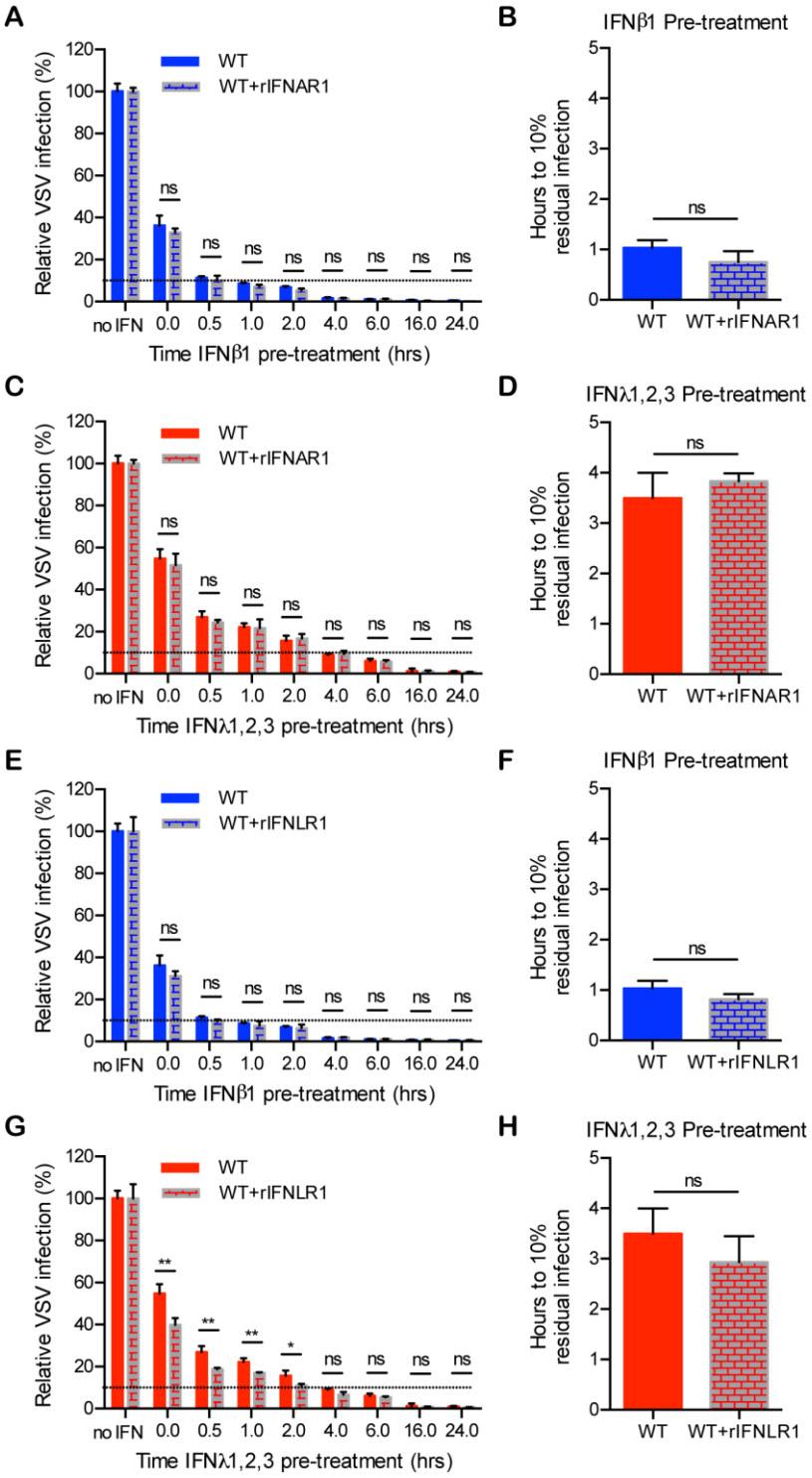

Figure 36. Establishment of an antiviral state in cells overexpressing the IFN receptors and treated with IFNs. Wild-type T84 cells were transduced with rIFNAR1 or rIFNLR1 to create stable lines overexpressing either receptor. (A-D) T84 wild-type cells (WT) and T84 cells overexpressing the IFNAR1 (WT+rIFNAR1) were treated with (A-B) type I IFN (β) (2,000 RU/mL equivalent 0.33 nM) or (C-D) type III IFN (λ1−3) (100ng/mL each =300 ng/mL equivalent 13.7 nM) at the indicated times prior to infection with VSV-Luc. Viral replication was assayed by measuring the luciferase activity. (A, C) The relative VSV infection is expressed as the percentage of the luciferase activity present in VSV-infected cells without IFN treatment (set to 100). (B, D) Pre-incubation time of type I IFN (β) or type III IFN (λ1−3) required to inhibit VSV infection to 10% (90% inhibition). (E-H) same as (A-D), but T84 wild-type cells (WT) and T84 cells overexpressing the IFNLR1 (WT+rIFNLR1) were treated with (E-F)

type I IFN (β) (2,000 RU/mL equivalent 0.33 nM) or (G-H) type III IFN (λ1−3) (100ng/mL each =300 ng/mL equivalent 13.7 nM) at the indicated times prior to infection with VSV-Luc. Data represent the mean values of three independent experiments. Error bars indicate the SD. *<P.05, **P < 0.01, ns, not significant (unpaired t-test).

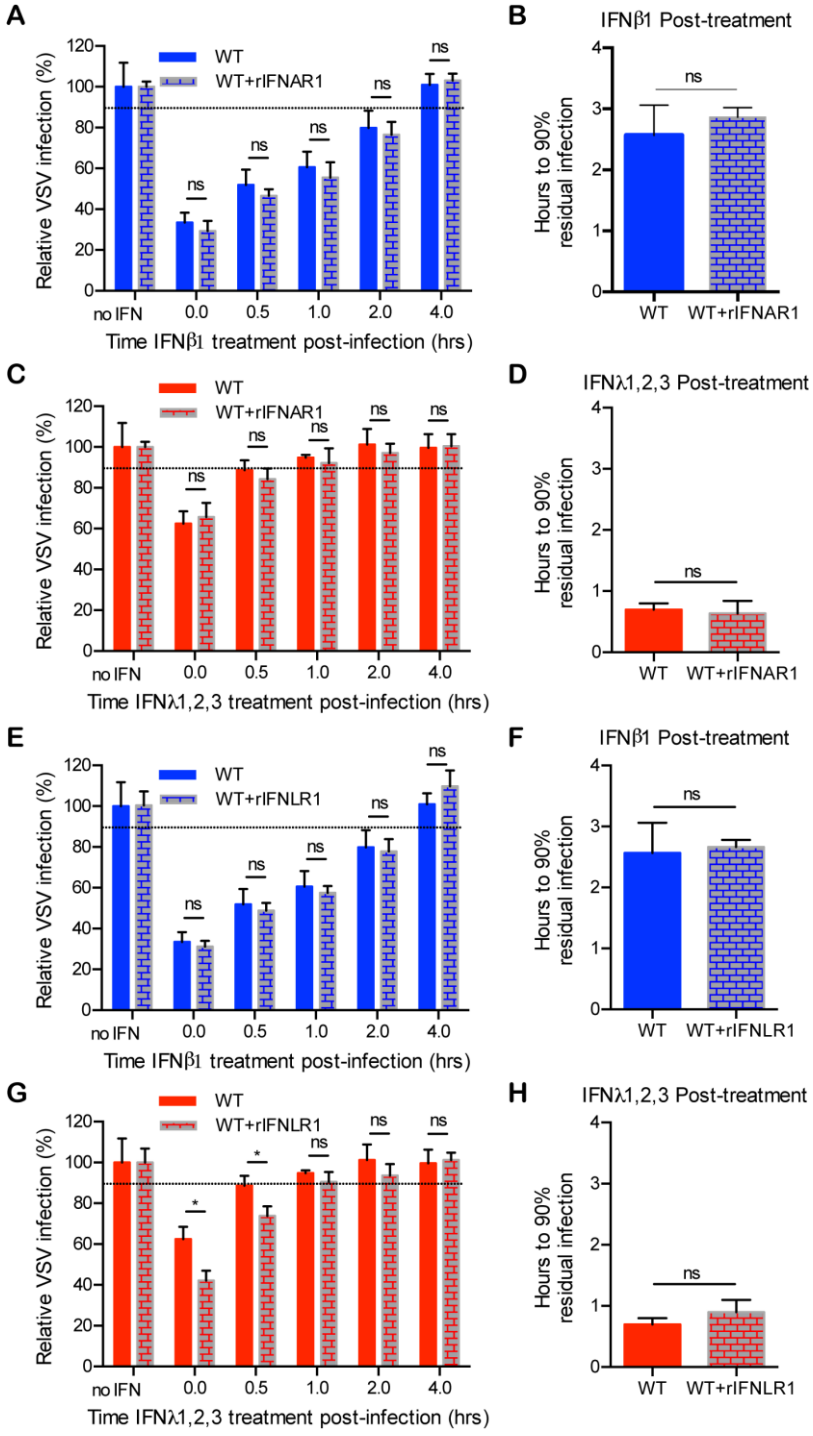

Figure 37. Establishment of an antiviral state in cells overexpressing the IFN receptors and treated with IFNs post-infection. Wild-type T84 cells were transduced with rIFNAR1 or rIFNLR1 to create stable lines overexpressing either receptor. (A-D) T84 wild-type cells (WT) and T84 cells overexpressing the IFNAR1 (WT+rIFNAR1) were treated with (A-B) type I IFN (β) (2,000 RU/mL equivalent 0.33 nM) or (C-D) type III IFN (λ1−3) (100ng/mL each =300 ng/mL equivalent 13.7 nM) at the indicated times post-infection with VSV-Luc. Viral replication was assayed by measuring the luciferase activity. (A, C) The relative VSV infection is expressed as the percentage of the luciferase

activity present in VSV-infected cells without IFN treatment (set to 100). (B, D) Delayed-time post-infection for type I IFN (β) or type III IFN (λ1−3) to still inhibit VSV infection to 90% (10% inhibition) is shown. (E-H) same as (A-D), but T84 wild-type cells (WT) and T84 cells overexpressing the IFNLR1 (WT+rIFNLR1) were treated with (E-F) type I IFN (β) (2,000 RU/mL equivalent 0.33 nM) or (G-H) type III IFN (λ1−3) (100ng/mL each =300 ng/mL equivalent 13.7 nM) at the indicated times post-infection with VSV-Luc. Data represent the mean values of three independent experiments. Error bars indicate the SD. *<P.05, ns, not significant (unpaired t-test).

Finally, to experimentally validate the limited impact of the IFN receptors abundance on the kinetic profile of ISG expression, as predicted by the model (Figure 31E-F), wild-type T84 cells overexpressing either of the IFN receptors were treated with increasing doses of type I or type III IFNs and the expression of ISGs was analyzed over time (Figure 38). The experimental data shows that the amplitude of IFIT1 and Viperin expression was dependent on both the dose of IFNs used to stimulate the cells and on the expression levels of the IFN receptors (Figure 38). Importantly, the kinetic profile of Viperin expression was similar between WT cells and cells overexpressing the IFNAR1 (WT+rIFNAR1), independent of the applied IFN type I dose (Figure 38A-B). Similarly, wild-type cells overexpressing the IFNLR1 (WT+rIFNLR1) showed no change in the kinetic profile of ISG induction upon type III IFN stimulation (Figure 38C-D). Moreover, we found that the model reproduced the kinetic dose-response data when the IFNAR1 and IFNLR1 expression levels were increased ~3 and ~1.6 fold, respectively, while all other parameters were held constant (Figure 39A). The relative magnitude of IFNAR1 versus IFNLR1 overexpression predicted by the model was confirmed by the transcriptional expression level of IFNAR1 versus IFNLR1 in overexpressing versus wild-type cells (Figures 39B and 34B-C).

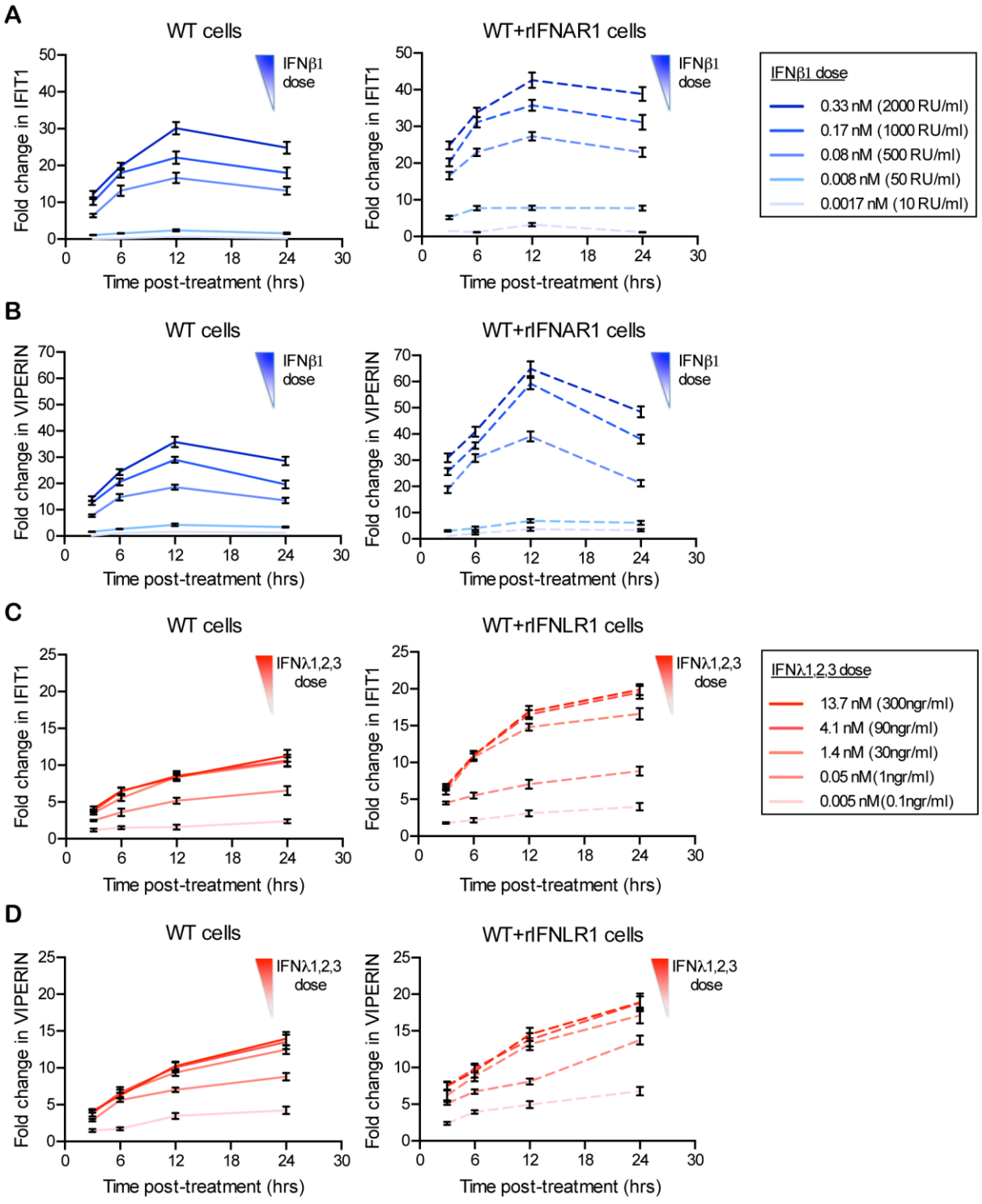

Figure 38. Expression kinetics of ISGs are independent of the IFN receptor levels. Wild-type T84 cells were transduced with rIFNAR1 or rIFNLR1 to create stable lines overexpressing either receptor. (A-B) T84 wild-type cells (WT) and T84 cells overexpressing the IFNAR1 (WT+rIFNAR1) were treated with increasing concentrations of type I IFN (β) for the indicated times and the expression kinetics of the ISGs IFIT1 (A) and VIPERIN (B) were analyzed by qRT-PCR. Data are normalized to HPRT1 and are expressed relative to untreated cells at each time point. (C-D) Same as (A-B), except T84 cells overexpressing the IFNLR1 (WT+IFNLR1) were used and treated with increasing concentrations of type III IFN (λ1−3). A representative experiment with technical triplicates, out of three independent experiments is shown. Mean values and SD are shown.

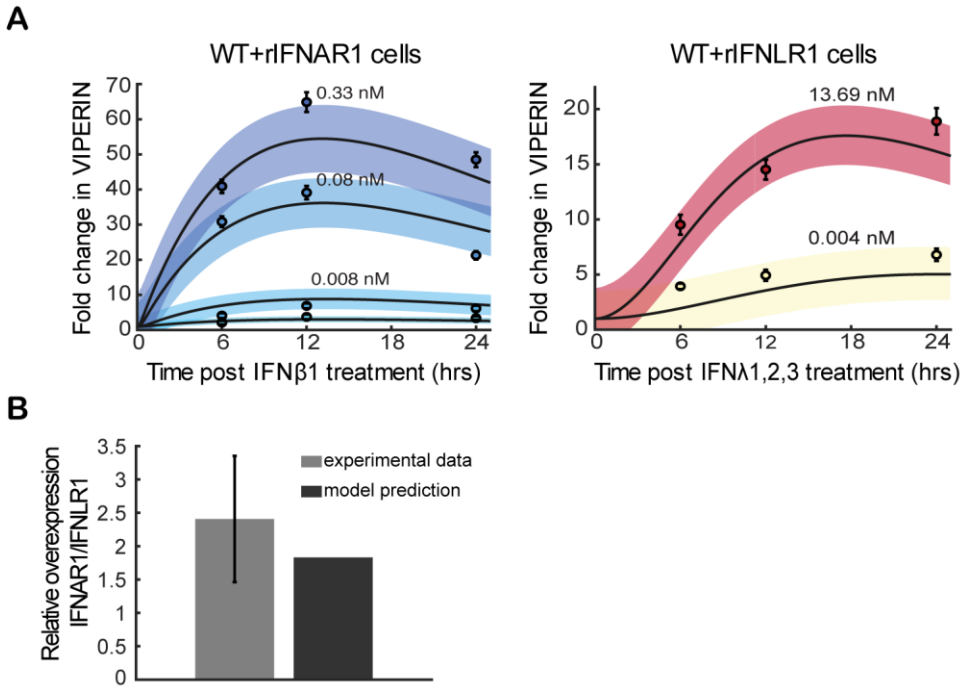

Figure 39. The mathematical model predicts the effect of IFNAR1 and IFNLR1 overexpression on ISGs activation. (A) The IFNAR1 and IFNLR1 levels were increased ~3 and ~1.6 fold, respectively, while all other parameters were held constant and the mathematical model predicts the Viperin activation upon treatment with different concentrations of type I IFN (β) and type III IFN (λ1−3). The solid lines are the best fits and the shaded areas are approximate 95% confidence intervals. (B) The mathematical model predicts the IFNAR1 versus IFNLR1 overexpression, measured experimentally by qRT-PCR. Modeling has been performed by Soheil Rastgou Talemi, Heidelberg University and German Cancer Research Center (DKFZ).

Altogether, our results demonstrate that type I and type III IFNs both induce an antiviral state in hIECs but with different kinetics. We could show that although both cytokines induce similar ISGs, type III IFN does it with slower kinetics and lower amplitude of individual ISG expression compared to type I IFN. Importantly, coupling mathematical modeling of both type I and type III IFN-mediated signaling and overexpression of functional IFN receptors approaches allowed us to demonstrate that these kinetic differences in type I and type III IFN ISG expression are not due to different expression levels of the respective IFN receptors but are intrinsic to type I and type III IFN signaling pathways.

3 Discussion

The text of the following paragraphs (3.1) and (3.3) has been adapted from Pervolaraki et al. (2017)[100]. This corresponds to a co-first author published manuscript resulting directly from my PhD research project.

3.1 Type I and type III IFNs display a different dependency on mitogen-activated protein kinases (MAPK) to mount an antiviral state in the human gut

In recent years, there has been a large interest in uncovering the specific roles of type III IFNs in epithelial cells including lung epithelium, gastrointestinal tract epithelium and in hepatocytes. In addition, taking into account that the majority of these studies have utilized *in vivo* mouse models, it is of great importance to evaluate the epitheliotropic nature of type III IFNs in the human host. In this work, by exploiting human mini-gut organoids, we performed a functional characterization of both type I and type III IFNs in a human primary intestinal cell context. We found that, upon viral infection, human IECs strongly upregulate both type I and type III IFNs at the transcriptional level. Although only type III IFN was found to be secreted by IECs, we demonstrated that either type I or type III IFNs induce the production of ISGs and that this production is associated with the establishment of an antiviral state that efficiently protects IECs from viral infection. Importantly, we revealed that type III IFN-mediated signaling allows for efficient protection against viral infection while limiting ISG production. We propose that this represents a mechanism to limit inflammation in the gut while remaining responsive to pathogens.

Additionally, genetic ablation of IFN signaling using CRISPR/ Cas9-mediated KO of IFN receptors further demonstrated that type I and III IFNs independently mediate an antiviral activity. Comparative analyses revealed that both IFNs induce the same set of ISGs and that both antiviral states depend on the JAK/STAT signaling pathway. Importantly, we discovered that the type III IFN-mediated, but not the type I IFN-mediated antiviral activity depends on MAPK signaling pathways. This work establishes that both type I and III IFNs provide potent antiviral protection in the human gut, and identifies, for the first time, fundamental differences in the mechanism by which these two IFN types establish the antiviral state in primary hIECs.

3.1.1 Both type I and type III IFNs establish an antiviral state in primary human IECs

In the past, a number of different human intestinal cell lines have been established to evaluate the response of the gastrointestinal tract epithelium to infection[120,207,300,301]. However, clonal expansion of a specific intestinal cell population does not reflect the complex multicellular composition of the GI tract and the transformed nature of the immortalized cell lines could potentially mask subtle but important differences in primary non-transformed cell responses. In addition, maintenance of human primary intestinal epithelial cells for *in vitro* culture has been restricted due to fast decline in cell viability[4,302]. For this, the implementation of organoid cultures has open new perspectives for functional analysis of the human intestinal responses and has gained substantial and increasing interest in the fields of cellular biology and medicine[303,304]. Even more interestingly, this system creates the unique opportunity to evaluate host responses from different individuals (different age, genetic background and disease state) and also from different parts of the GI tract. More recently, these organoids have been also used to study and describe infectious diseases and gave researches the chance to overcome the limitation of studying human pathogens *in vivo* (Foulke-Abel et al., 2014). Up to now, being the most cutting edge tool to investigate host-pathogen interactions in the GI tract, mini-gut organoids have been proven a precious model to study infection with different enteric bacteria and viruses such as *Salmonella* Typhimurium*, Helicobacter pylori,* norovirus, rotavirus and reovirus[100,305–308].

In the present study, we have exploited organoids not only to describe the response of hIECs upon pathogen challenges but even more importantly to perform a functional characterization of both type I and type III IFNs in the context of human primary non-transformed IECs. In contrast to data upon viral infection of the mouse GI tract, our results demonstrate that hIECs can mount an antiviral state in response to either type I or type III IFN treatment. Similar observations, have been made in human organoid cultures upon rotavirous infection in combination with exogenous stimulation with either type I or type III IFN[98].

Species specific differences in IFN system between mice and humans have been suggested as an explanation for the discrepancy between the *in vivo* murine studies in adult animals, where mouse intestinal epithelial cells respond mainly to type III IFN, while type I IFN act on endothelial and immune cells[75,77–80,96,97], and the *ex vivo* human intestinal organoid cultures[98,100]. However, this argument remains controversial as further experiments demonstrated that isolated murine IECs respond to both IFNs when they are cultured *ex vivo*, pointing out the subcellular localization of type I IFN receptor at the apical side of

polarized IECs as a possible explanation for the limitation in type I IFN response *in vivo* upon viral infection or parenteral administration of IFNs[79]. In line with these observations, recent studies have shown murine intestinal organoids to be fully responsive to both IFNs[309,310]. Down-regulation of type I IFN receptor level *in vivo*, triggered by immune or microbial factors, has been proposed as an explanation for this differential responsiveness[44,80]. However, the exact mechanism remains to be elucidated and although it is of great importance to unravel the subcellular localization of type I and type III IFN receptors and directly compare their cellular ratio at the protein level, these studies have been hindered for years by the lack of appropriate reagents such as specific antibodies against type I and type III IFN receptor.

Another potential explanation for the *in vivo* versus the *in vitro* responsiveness of IECs to IFN stimulation, might be the specific type I IFN subtypes utilized, which may present differential antiviral sensitivity[154,311]. In particular, IFN-α was utilized in the above-mentioned *in vivo* studies in the mouse GI tract[79,80], while murine and human organoids were exogenously treated with IFN-β[98,100,309,310]. Last but not least, another level of complexity has been added by a recent study describing age dependent responsiveness of murine IECs to type I IFN *in vivo*, where neonatal IECs respond and are protected by both IFNs, whereas adult IECs have a significantly limited responsiveness to type I IFN[97].

As far as the epithelium of other mucosal surfaces is concerned, *in vivo* and *in vitro* studies of mouse and human lung epithelial cells as well as human hepatoma cells are in accordance with our observations, where both type I and type III IFNs participate in the protection against viral infection. In particular, respiratory epithelial cells express both type I and III IFN receptors and respond to both IFNs, which explains the degree of redundancy shown between the two IFN systems in their activity against respiratory viruses[76,77,90,93,312]. Moreover, in concert with our data in human intestinal organoids, although mouse hepatocytes are less responsive to type III IFN, both IFNs contribute to the establishment of an antiviral state in human hepatoma cells and primary untransformed hepatocytes[165,189,293,294].

3.1.2 Type III IFN is predominantly produced in human IECs during viral infection

Our functional characterizations performed in both mini-gut organoids and colon carcinoma-derived cell lines revealed that although these cells transcriptionally upregulate both type I and III IFNs, they secrete very little to no type I IFN. A favored type III IFN response over type I IFN has been observed in other epithelial cells stimulated with various viruses and

pathogen-associated molecular patterns. Particularly, it was shown that although both IFNs can protect airway epithelial cells against viral infection, type III IFNs were preferentially made in response to respiratory viruses[74,92,93,99,313]. Similarly intestinal epithelial cells preferentially produce type III IFN rather than type I IFN in mouse GI tract[79,80,97,283]. However, in the above *in vivo* studies the induction of IFNs has been exclusively assessed at the transcript level. Interestingly, in agreement with our results, it has been described that upon stimulation of human intestinal organoids with the double strand RNA structural analog poly-inosinic:cytidylic acid (poly I:C), only type III IFN was secreted by the cells although both type I and III IFNs were upregulated at the transcriptional level[98]. Additionally, a preferential induction of type III IFNs has been reported upon HBV and HCV infection in hepatocytes[314,315]. Consequently, favoring type III IFN signaling appears to be a common strategy developed at epithelial surfaces (airway, hepatocytes, intestinal tract) to mount an antiviral response.

Despite the high importance of this ‘’pan-epithelial’’ preferential type III IFN induction, the molecular mechanisms that predispose type III IFN production by epithelial cells have not been unraveled, raising the possibility that it is regulated at differential levels from transcription to translation and secretion. At the transcriptional level, the production of both type I and type III IFNs has been shown to be triggered by similar stimuli and a set of overlapping and distinct transcriptional factors, mainly members of the IRF, the NF-kB and the MAP kinase pathway. Interestingly, while IFN-β induction requires simultaneous activation of all the transcriptional pathways[134–136], type III IFNs can be induced by either IRFs or NF-kB[142,316], which not only might explain the higher inducibility of type III IFNs in epithelial cells, but also may be beneficial in case of pathogen-mediated IRF or NF-kB inhibition[143].

Another difference in type I versus type III IFN production, is based on the differential contribution of peroxisomal MAVs, downstream the RIG-I-like receptors activation. Apart from mitochondrial-associated MAVs which induce the production of both type I and type III IFNs, it has been described that peroxisomal-bound MAVs induce only type III IFN expression in response to intracellular ligands without stimulating type I IFN production[114,296]. Moreover, while downstream of peroxisomal MAVs, type III IFN induction is mediated through IRF3, IRF7, NF-kB and IRF-1, type I IFN up-regulation has been shown to rely on a different combination of transcriptional factors downstream mitochondrial-bound MAVs including IRF3, IRF-7, NF-kB and AP-1[114,316,317]. Even more interestingly, it has been demonstrated that the abundance of cellular peroxisomes is directly associated with the differential induction of IFNs. In other words, an increase in the number of peroxisomes via polarization of epithelial cells has been reported to enhance type III IFN-mediated antiviral

responses[114] and has been proposed as an epithelial specific mechanism for explaining the favoring of type III IFN production in mucosal surfaces. However, taking into account that comparable contribution from both mitochondrial and peroxisomal MAVs in type III IFN induction has been shown in a recent study, further work is required to clarify the involvement of peroxisomal MAVs in the mechanism of type I versus type III IFN induction[318].

Recently, additional transcriptional factors related only to type III IFN production have been identified. For instance, a member of the Mediator complex Med23, has been shown to specifically interact with IRF7 and augment type III IFN up-regulation[319]. In addition, a specific binding of the transcriptional repressors ZEB1 and BLIMP1 in IFNL1 promoter has been described, which displaces IRF1 and specifically leads to down-regulation of type III IFN transcription in lung and intestinal epithelial cells[316,319].

Furthermore, yet unidentified tissue-specific transcriptional factors, present at epithelial tissues might be responsible for preferential production of type III IFN upon infection of barrier surfaces. In addition, it is notable that IFN genes behave also as ISGs and a functional interrelationship between the two IFN systems has been proposed, since type I IFN priming of hepatocytes and immune cells has been shown to enhance type III IFN production upon viral infection[112,320]. Priming of type I IFN induction by type III IFNs remains still controversial among different cell lines[44].

Downstream from the transcriptional regulation, the fact that, contrary to the intron-less type I IFN genes, type III IFN genes are composed of multiple exons and introns reflecting the possibility of post-transcriptional modification, which might differentially regulate type III IFN production[60]. In addition to this, it remains unclear whether translation or secretion of type I IFN is restricted in human IECs. To date, very little is known about the mechanisms that lead to type I and III IFN secretion. It has been shown that signaling downstream of mitochondrial-associated MAVS induces the secretion of type I IFN that can be inhibited by brefeldin A. On the contrary, the antiviral activity generated following activation of peroxisomal-associated MAVS was insensitive to brefeldin A[296]. It was later demonstrated that this brefeldin A-insensitive antiviral state was mediated by type III IFN, which was secreted following activation of peroxisomal MAVS[114]. These observations strongly suggest that type I and III IFNs are secreted from cells by two distinct mechanisms.

It is not known whether hIECS can protect themselves against viral infection by secreting and responding to their own IFNs. It was proposed that, during rotavirus infection, IFNs are produced by immune cells and not by epithelial cells[98]. Indeed, during rotavirus infection of hIECs, multiple strategies are developed by the virus to inhibit innate immune response

particularly the inhibition of both type I and III IFNs production[321]. Additionally, blocking IFN signaling in hIECs does not lead to an increased rotavirus replication[98]. Our data clearly show, for the first time, that when primary hIECs are infected with viruses that do not block IFN synthesis, hIECs produce and secrete at least type III IFN (maybe some type I IFN but under the detection limit of our ELISA assay) in order to protect themselves. Complementarily, KO of IFNLR renders hIECs more susceptible to viral infection (Figure 16).

3.1.3 Favored type III IFN response in human IECs

Although type III IFN stimulation of hIECs results in significantly less induction of ISGs compared to type I IFN (Figures 11 and 14), we found that type III IFN was only slightly less potent in protecting the cells against viral infection (Figures 11 and 15). This lower induction of ISGs is not cell type specific as recent publications addressing the role of these IFNs in human hepatocytes and Burkitt's lymphoma derived B (Raji) cells also reported that type III IFN induces less ISGs compared to type I IFN[165,189,237]. However, in these studies, the antiviral potency of both IFNs was not addressed side-by-side. As such, type III IFN could be considered a milder IFN favored at epithelial surfaces (at least intestinal epithelium) due to its ability to confer an antiviral state without inducing excessive amounts of ISGs, which might result in the induction of local pro-inflammatory signals.

3.1.4 MAP Kinase signaling pathways are required for type III but not type I IFN based antiviral protection in human IECs

Functional characterization of type III IFN in comparison to type I IFN suggests that both cytokines are functionally redundant by mainly activating the same signaling cascade, leading to the up-regulation of the same pool of ISGs[93,97,165,189,237,293,294]. However, the restriction of type III IFN receptor to epithelial cells and the preferential type III IFN production at mucosal surfaces suggest that type III IFN might have unique functions or provide specific advantages at epithelial surfaces. Several studies have tried to unravel functional differences both in human (hepatocytes)[165,189,293,294] and in murine model systems (lung and intestinal tract)[76,79,80,93,97]. In the liver, since the discovery of type III IFNs, extensive work has revealed that human hepatocytes can quickly become refractive to type I IFN, while maintaining their responsiveness to type III IFN[322]. Interestingly, two recent studies provide some new evidence for distinct roles of the type III IFN defense system also in the respiratory tract. First of all, Galani et al. have showed that upon influenza infection type III IFNs are the first IFNs produced to inhibit viral spread and if infection progresses, then type I IFNs come into play to reinforce viral inhibition by inducing pro-inflammatory responses[99]. In

addition, a preferential contribution of type III IFN system in the blockade of viral dissemination from the upper respiratory compartment to the lower (lungs) and in viral transmission among different animals has been described[323]

However, as far as the GI tract is concerned, up to date the main difference between both IFNs has been explained by the spatial restriction of type III IFN receptor at IECs. In this work, we demonstrate that type III IFN induces less ISGs compared to type I IFN. Most importantly, we unravel, for the first time, fundamental differences in the molecular mechanisms by which both IFNs mount the antiviral state in hIECs. We demonstrate that the antiviral activity of type III IFN partially depends on MAPKs, which is not the case for type I IFN.

Although, in recent years many studies have focused on defining the role of the MAP kinase pathway on the antiviral activity of type I IFNs, the results are controversial and their precise contribution is still under scrutiny. In particular, in human cell lines including hepatocytes, cervix epithelial cells and fibrosarcoma cells and in mouse embryonic cells a p38-dependent inhibition of virus replication upon HCV or EMCV infection in combination with IFN-α stimulation has been documented[239,241]. Similarly, p38-dependent IFN-β mediated blockade in influenza virus replication has been observed in human airway epithelial cells *in vitro* and in murine respiratory tract[242]. Nevertheless, it remains puzzling and needs to be further investigated not only the cell type specificity of the p38-dependent type I IFN antiviral activity, but also in which species (human or mouse) and cellular context this is true for the different subtypes of type I IFNs and the other members of the MAP Kinase family (ERK, JNK). In addition, taking into account that at least to our knowledge, the critical role of MAP kinase pathway on type III IFN antiviral activity has not been assessed in other studies, it is of great importance to be addressed in future reports whether the dependency of type III IFN for MAPKs is specific only for intestinal epithelial cells or for all epithelial surfaces.

Furthermore, in our experimental model of human IECs or human mini-gut organoids, despite the preferential contribution of MAP kinases on the antiviral outcome of type III IFNs, we observed a significant activation of MAPKs with both IFNs. This is in line with recent publications addressing the activation status of MAPKs in human lymphoma cells, fibroblasts, keratinocytes and intestinal epithelial cells, also reported that MAPKs are activated upon stimulation with type I or type III IFN[104,207,237]. However, based on the above limited reports on type III IFN, it is speculated that different members of the MAPK family (p38, ERK or JNK) might be activated downstream type I or type III IFN in a cell dependent manner. In addition, taking into account that IFNs are pleiotropic cytokines, the type I IFN mediated MAPK activation may contribute to other functions of type I IFN apart from their

antiviral activity. In line, a role of p38 on the growth inhibitory function of type I IFN has been reported[240].

Moreover, the molecular mechanisms, which couple the activation of MAPKs with the IFN receptor are still unclear. For type I IFNs, the small GTPase RAC1 has been reported to serve as a crucial mediator[324]. Upon type I IFN treatment, JAKs activate VAV, which acts as a guanine-nucleotide-exchange (GEF) factor for RAC1[325]. Taking into account that VAV is expressed only in hematopoietic cells, it remains to be determined whether other cell specific GEFs serve as RAC1 activators and whether other molecular elements lead to MAPK activation downstream of type I IFN receptor in epithelial cell lines. In addition, as the above studies have focused only on type I IFNs, comparative analysis of MAPK activation downstream type I and type III IFN receptors needs to be conducted.

In addition to the above open questions, the downstream targets of MAPKs, responsible for the antiviral activity of type III IFNs need to be identified. In our study, we demonstrated that the MAPK pathway acts independently of the JAK/STAT pathway upon type I or type III IFN stimulation. This is in agreement with publications showing that the MAPKs function in a STAT independent mechanism downstream type I IFN receptor[236,241,324,326,327]. However, an interaction between ERK2 and STAT1 upon type I IFN treatment has been reported in lymphocytes and it remains controversial, whether MAPKs can also induce STAT1 phosphorylation on Ser727[239,242]. Various downstream targets of p38 such as MAPK-activated protein kinase 2 (MAPKAPK2), MAPKAPK3, mitogen- and stress-activated kinase 1 (MSK1), MSK2 and MAPK-interacting protein kinase 1 (MNK1) have been shown to be activated and might play important role in type I IFN responses[328].

Contrary to previous publications, in our experiments, it was difficult to draw a clear conclusion on the influence of MAPK inhibition on IFIT1 and Viperin expression, as it seemed to be dependent on the dose of the IFN used. Previous studies demonstrated a regulatory effect of MAPKs on the transcriptional activity of both IFNs, by showing a significant decrease in the expression levels of ISGs[237]. However, a possible explanation for this discrepancy might be a cell type or ISG dependent effect. Even more interestingly, Alase et al, reported an inhibitory effect of p38 or ERK blockade on ISG expression only in protein level[104]. As such, it remains an important task for future work to dissect how signaling downstream of MAPKs participates in the antiviral activity of type III IFN only.

3.2 Differential induction of interferon stimulated genes between type I and type III IFNs is independent of interferon receptor abundance

The text of the following paragraph (3.2) has been adapted from Pervolaraki et al. (2018), *under preparation*. This corresponds to a first author manuscript under preparation resulting directly from my PhD research project.

In this work, we have for the first time, performed a parallel study of the role of type I and III IFN in human IECs and mini-gut organoids. Our results demonstrate that type I and III IFNs are unique in their magnitude and kinetics of ISG induction. Type I IFN signaling is characterized by a relatively strong expression of ISGs and confers to cells a fast antiviral protection. On the contrary, the slow acting type III IFN mediated antiviral protection is characterized by a weak induction of ISGs in a delayed manner compared to type I IFN. Our results are in line with previous studies which also demonstrated that type III IFN is less potent than its type I IFN counterpart[39,165,189,237,292–294,309]. Additionally, we have confirmed that the delayed ISG induction seen upon type III IFN treatment of hepatocytes[165,189,293,294] is not tissue specific but likely represents a global pattern of action of this cytokine in cells expressing the type III IFN receptor (i.e. human epithelial cells). In other words, the different kinetics of ISG expression induced by type I and type III IFNs are specific and intrinsic to each IFN signaling pathway.

3.2.1 Mathematical modeling characterizes key differences of ISG response to type I versus type III IFNs

In the current work, we have employed, a data-driven mathematical modeling approach to explain signal transduction kinetic differences downstream type I and type III IFN receptors. While type I IFN-mediated signaling has been previously modeled[329,330], type III IFN has not. Our model predicted that the receptor levels directly influence the magnitude of ISG expression however, the kinetics of ISG expression appear to be intrinsic to each IFN-signaling pathway and is largely preserved under receptor overexpression. This prediction was experimentally validated by studying the response of wild-type and IFN receptor overexpressing cells to different doses of IFN (Fig 38 and 39). We propose that these phenotypic differences reflect functional differences, which are important for mounting a well-tailored antiviral innate immune response at mucosal surfaces where type III IFN receptors are expressed.

We also compared the kinetic properties of the active IFNAR1 versus IFNLR1. Our model suggested less potency of the IFNLR1 compared to the IFNAR1 that was supported by the

well identified and bounded confidence bounds of the IFNLR1 efficacy factor (S1A Figure). The model also suggests that the IFNLR1 has longer half-life compared to the IFNAR1 which may explain its ability to induce a sustained ISG activation. By computing the confidence bounds of the IFNAR1 and IFNLR1 inactivation rate we show that this is a statistically significant prediction. Finally, the model predictions about the IFNAR1 and IFNLR1 become more credible when we show that our model is also able to explain the relative overexpression of the IFNAR1 versus IFNLR1 in the receptor-overexpression experiments (Figure 39). Altogether, this data-driven mathematical modeling and experimental validation approach provides strong evidence that the fundamental differences between IFNAR1 versus IFNLR1 mediated ISG expression cannot be explained only by changing the IFN receptor abundance. This suggests that the kinetic differences in the ISG induction are intrinsic to each IFN signaling pathway.

3.2.2 IFN receptor level affects the magnitude of ISG response

Both type I and III IFNs have unique and independent receptors which are structurally unrelated. These receptors are likely expressed at different levels on individual cells and their relative expression to each other might also be cell type specific[75,80]. To address whether the unique ISG and antiviral expression kinetics shown by each IFN were not due to differences in their expression levels, we overexpressed into cells functional type I (rIFNAR1) and type III IFN (rIFNLR1) receptors. Our results from IFNAR1 overexpressing cells (Figures 35 and 38) are in line with previous studies showing a direct relationship between the surface levels of type I IFN receptors and the magnitude of ISG induction[331,332]. Interestingly, we could demonstrate a similar relationship when overexpressing IFNLR1 (Figures 35 and 38), which was also associated with an increase of type III IFN antiviral potency (Figure 36G). These findings are in agreement with previous experiments which show that overexpression of IFNLR1 in cells which normally do not express this IFN receptor rescues both type III IFN-mediated signaling and IFN-mediated antiviral protection [39,237]. In line, a linear relationship between the endogenous transcript levels of type III IFN receptors and type III IFN-mediated responses in different cell lines has been illustrated[75,237,292,333,334]. Interestingly, there are two recent studies demonstrating that the endogenous type III IFN receptor levels can be elevated through blockade of histone deacetylases (HDACs) in a cell type specific manner or by induction of cell polarization in mouse IECs, promoting in turn the responsiveness of cells only to type III FNs[309,335]. Although, these are interesting observation and indicate the previously unrecognized importance of cellular epigenetic status in IFN receptor expression regulation, there are not in agreement with our results in human ICEs

and mini-gut organoids (data not shown) and further investigation is required to conclude whether these observations are species or cell specific.

Apart from the expression levels of IFN receptors, lower binding affinity towards their respective receptors could be an alternative explanation for the differential potencies of both type I and type III IFNs[145]. Multiple studies have tried to affect the binding affinity of type I IFNs with their receptors however; results suggest that wild-type I IFNs exert their antiviral activities already at maximum potency. Modifications leading to an increased affinity for their receptors do not lead to improvement of antiviral potency[151,181,332,336,337]. To address whether the weaker activity of type III IFN could be the result of its weaker affinity for its receptor, Mendoza et al, engineered a IFNλ3 variant with higher-affinity for the type III IFN receptor. They showed increased IFN signaling and antiviral activity in comparison with the wild-type IFNλ3. However, the engineered variant of IFNλ3 was still acting with weaker efficacy compared to type I IFNs[181]. This is similar to our results, where although we observed a significant increase of the amplitude of ISG expression and of the antiviral activity of type III IFNs in IFNLR1 overexpressing cells, the overall potency of type III IFN does not reach that of type I IFN.

3.2.3 Temporal differences between type I and type III IFN mediated responses are not influenced by the IFN receptor level

As far as the comparative analysis of type I versus type III mediated kinetic patterns of ISGs expression is concerned, our results indicate a model were inherent temporal differences exist between type I and type III IFNs signaling. Our IFN receptor overexpression approach in combination with mathematical modeling demonstrate that these differences are not the result of differential surface expression of the receptors but is the result of distinct signaling cascades from the receptors to the nucleus or within regulatory mechanisms of gene expressions.

While few studies have focused on the endocytosis and inactivation of IFNAR1, there is no information about how these processes occur for IFNLR1. It has been shown that the ternary IFNAR complex is internalized by clathrin-mediated endocytosis[167,168]. Additionally, IFNAR1 has been shown to serve as the critical player in the mechanism of internalization and degradation of the ternary IFNAR complex[167–170]. Our data-driven mathematical modeling approach suggests a longer half-life of the activated IFNLR1 compared to the IFNAR1 receptor (Figure 32). Therefore, further studies investigating trafficking of IFNLR1 will be important and may show that subtle changes in the time course of receptors internalization, recycling or degradation can have profound effect on kinetics of IFN activity.

Apart from receptor internalization and degradation, several molecular mechanisms leading to IFN receptor inactivation have been described, such as de-phosphorylation[182,183], or by negatively targeting the interaction of IFNAR1 with downstream signaling elements of the JAK/STAT signaling, for instance ubiquitin-specific protease USP18[185] and members of the suppressor of cytokine signaling protein (SOCS) family[191–193]. However limited information is available for negative regulators of IFNLR receptor complex[162,195,207]. Additionally, there is a lack of direct and temporal comparisons of these negative regulatory mechanisms in type I versus type III IFN signaling activity.

In the canonical type I and III IFN signaling pathway the next downstream players from the IFN receptors are the JAKs, STAT1, STAT2 and IRF9, which are all regulated on the level of expression and activation. Data not shown and previous studies could not explain the major differences in the kinetics of type I versus type III IFNs activity by focusing on the time course of phosphorylation of STAT1 and STAT2[189,293]. However, apart from the ISGF3 complex (STAT1:STAT2:IRF9), not only homodimers of STAT1 or STAT2 but also heterodimers of STAT1 or STAT2 with the other members of the STAT family (STAT3 , STAT4, STAT5 and STAT6), have been reported to participate in type I IFN signaling in a cell type dependent manner[203,208,328]. In addition, alternative modifications of STATs (*e.g.* phosphorylation on alternative residues, acetylation, methylation and sumoylation patterns or un-phosphorylated forms) have been proposed to contribute to the activity of type I IFNs[165,215,226–228,338] it might be possible that new modifiers of STAT activity may determine the kinetic pattern of action of type I versus type III IFNs. For instance, type I and type III IFN induced formation of the un-phosphorylated ISGF3 (U-ISGF3) complex, containing un-phosphorylated STAT1 and STAT2 together with IRF9, has been shown to mediate prolonged expression of a set of ISGs[339–341]. In addition, apart from the JAK/STAT axis, there is accumulating evidence which correlates ISG transcription upon IFN treatment with a plethora of JAK-STAT independent pathways, such as members of the CRK[208,209,235] and MAPKinase family[100,104,207,236,237], which might also temporally coordinate IFNs kinetic profile of action.

The next step in the classical type I and type III IFN signaling cascade takes place in the nucleus and involves the interaction of the ISGF3 complex with promoter elements of hundreds of ISGs, responsible for the IFN activity. Currently, an emerging field in the regulation of IFN responses focuses on epigenetic modifications. Importantly, by investigating the regulation of type I IFN response in the nucleus, recent studies have identified a number of different chromatin modifiers, which interact with the promoters of ISGs[247,250,252,257,259] together with the coordinated activity of multiple other transcriptional factors[224,269,270]. However, there is no information available for chromatin remodeling and

epigenetic modification downstream the type III IFN receptor signaling cascade in human epithelial cells. For this, further work in this area is necessary to understand the sequence of events shaping the type I IFN signaling cascade in the nucleus and compare it with type III IFNs qualitatively and quantitatively. Last but not least, apart from the differences in the signaling cascade of type I versus type III IFNs, an explanation for their differential kinetics of action might stem from the physiology of the different cell types. For example, in a recent study Bhushal et al. reported that polarization of mouse intestinal epithelial cells eliminates the kinetic differences between type I and type III IFNs, by accelerating type III IFN responses[309,310].

3.2.4 Functional advantages for the differential pattern of ISG induction between type I and type III IFNs

Several studies describing the transcriptional activities of both type I and type III IFNs have reported that very similar sets of ISGs are produced upon both type I and type III IFN stimulation[93,97,165,189,237,293,294], while only few ISGs appear to be predominantly expressed upon type III IFN treatment in murine IECs[310]. Here, we confirmed that almost the same ISGs are induced with both IFNs, but there are significant quantitative differences in the amplitude and the kinetic pattern of the establishment of the transcriptional activity of type I versus type III IFN. We believe that there are several functional advantages for adopting a lower and slower activity, like the profile of action of type III IFN, in the antiviral protection of epithelial tissues. The differences in the temporal expression of ISGs could create unique antiviral environments for each IFN. Many ISGs function as pro-inflammatory factors[342–344]. By stimulating ISGs production in high magnitude, an excessive amount of antiviral and pro-inflammatory signals could be produced which on the one hand will eliminate efficiently viral spreading but on the other hand may cause local exacerbated inflammation and irreversible tissue damage, leading to chronic inflammation in mucosal surfaces.

In addition, the expression of different functional groups of ISGs at early and at late time points (Figures 27 and 28) might allow cells to create two distinct phases within the antiviral response. At early time points, minimum levels of ISGs may act to protect the host against viral infection. Antiviral ISGs will be responsible for fighting the pathogens and pro-inflammatory ISGs will stimulate members of the adaptive immune system to assist the antiviral protection. Our results show that very low levels of ISG transcriptional up-regulation is sufficient to fight pathogens in human IECs and show that type III IFN confers similar or even better protection against viruses at low concentration compared to type I IFN (Figure 23A and data not shown). However, the produced ISGs at later time points, may be involved in anti-inflammatory processes, such as resolving of inflammation and tissue healing and

repair[104,107]. To exert this anti-inflammatory role, ISGs may need to be produced in higher levels, as they might act more paracrine and spread through the tissue to balance again the tissue homeostasis after the viral attack.

Apart from the well-known pro-inflammatory aspects and the systemic side effects related to type I IFNs[342,345,346], a new unique role for type III IFN in shaping the immune responses has recently been emerging[109,343]. Significant immune-modulatory properties for type III IFN have been already demonstrated in mucosal surfaces (e.g. skin, lung, GI tract and liver) and involve not only the production and secretion of anti-inflammatory factors, which in turn act directly on the epithelium but also, as an indirect phenomenon, the establishment and promotion of an intercommunication between epithelial cells and tissue specific immune cells[86,87,107,342,347]. This is clearly illustrated by the characteristic example of neutrophils in the lung and the intestinal tissue[89,99]. These recent studies have paved the way for the discovery of the unique involvement of type III IFNs in the resolution phase of inflammation and maintenance of the barrier functions of mucosal tissues[89,99,104,107,348]. This is of great importance for the complex environment at mucosal sites, where a wide range of different highly specialized cell types (e.g. epithelial cells, goblet cells, neuroendocrinocytes, stem cells, tissue specific immune cells and cells of lamina propria) co-exist together with a variety of micro-organisms (commensal bacteria, viruses, fungi and pathogenic microorganisms) in a fine-tuned balance.

In conclusion, we propose that type III IFN-mediated signaling is not only set to act predominantly at epithelium surfaces due to the restriction of its receptor but also is specifically tailored to mount a distinct immune state compared to other IFNs which is critical for mucosal surfaces that face the challenge.

3.3 General conclusions and perspectives

It is currently believed that type I and III IFNs have redundant functions. However, the preferential distribution of type III IFN receptor on epithelial cells suggests functional differences at epithelial surfaces. Here, we utilized human mini-gut organoid cultures to delve into the antiviral properties of type I versus type III IFNs in the human gut. We reported that although primary human IECs produce transcript levels for both IFNs, they secrete only type III IFNs upon viral infection. However human IECs respond to both IFNs, by independently establishing a differential antiviral state. First of all, contrary to type I IFN, the antiviral activity induced by type III IFNs is strongly dependent on the MAPK signaling pathway. In addition, we showed that while type I IFN signaling is characterized by an acute strong induction of ISGs and confers fast antiviral protection, type III IFN mediated antiviral protection is based on a slow weak induction of ISGs. Combining data-driven mathematical modeling with experimental validation, we demonstrated that these kinetic differences are intrinsic to each signaling pathway and not due to different expression levels of the corresponding IFN receptors.

Considering our results that only type III IFN is secreted by hIECs and based on the distinct antiviral environment that type III IFN creates, it is tempting to propose that IECs have evolved to favor type III IFN over type I, as it allows for efficient protection against pathogens while limiting production of ISGs. From the perspective of an epithelium, which is always exposed to the extracellular environment and commensal challenges, this might represent a “smart strategy” to regulate the immune response in order to achieve the balance between responsiveness to pathogens versus tolerance of commensals. Restricting signaling to type III IFNs allows for spatial segregation of the response ,as type III IFN signaling is restricted mostly to epithelial cells[75,77–80,97], thereby limiting systematic inflammation.

In perspective, from our findings in epithelial cells of the gastrointestinal tract, we can speculate that the first response to pathogen threats will be generated by hIECs. This response will be mediated by type III IFNs, characterized by a moderate and delayed peak of transcriptional activity, leading to limiting ISGs and pro-inflammatory cytokine production. This first wave response of type III IFN produced by IECs, alone might be enough to clear enteric virus infection[80,99,287]. A second wave response might be generated through recruitment of immune cells at the site of epithelium infection, which in turn will produce various cytokines including type I IFN. This IFN will then mediate a fast and strong induction of ISGs and pro-inflammatory signals to powerfully combat pathogen at the infected mucosa and also will provide systemic protection. This uniquely tailored response would be fundamental for the maintenance of human gut homeostasis.

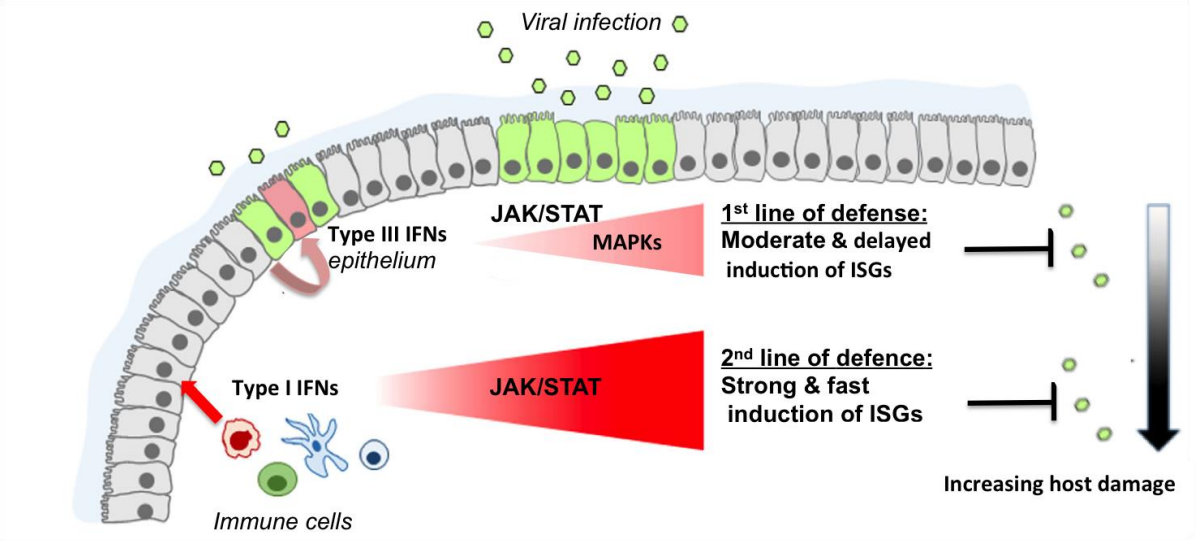

Figure 40. Fine tuning of type I versus type III IFN response in epithelial cells of the gastrointestinal tract. Upon infection of the intestinal epithelial cells, type III IFNs are produced by human IECs and induce a moderate and delayed induction of ISGs, responsible for eliminating viral replication without causing excessive production of pro-inflammatory cytokines. This first line of type III IFN dependent defense is mediated through the JAK/STAT and the MAPkinases signaling cascade. A second line of antiviral protection is generated by type I IFNs, induced mainly by immune cells. In turn type I IFNs act on epithelial cells generating a fast and strong ISG response, responsible for eliminating viral replication but also for causing immunopathology. Adapted from Andreakos et al (2017)[343].

4 Materials and methods

4.1 Materials

4.1.1 General chemicals, media, enzymes and reagents

Chemicals and reagents not listed below are described at the methods part (4.2) together with the methods for which they were used.

Table 2: List of chemicals, media, enzymes and reagents

Name	Manufacturer
30% Acrylamide/Bis-acrylamide solution (37.5:1)	Carl Roth
Agarose Standard	Carl Roth
Albumin Standard	Thermo Scientific
Ammonium Persulfate (APS)	Carl Roth
Ampicillin (100 mg/mL)	Carl Roth
Antibiotic-Antimycotic (Anti-Anti)	Gibco™/Invitrogen
Avidin-HRP 1000x	BioLegend
A-83-01	Tocris
β-Mercaptoethanol	Sigma-Aldrich
Bovine Serum Albumin	New England Biolabs™
BsmbI	New England Biolabs™
Bromophenol Blue	AppliChem
B-27	Invitrogen
Collagen (from rat tail)	Sigma-Aldrich
Complete protease inhibitor cocktail EDTA-free	Roche
DAPI	Sigma
DC Protein Assay Kit I	Bio-Rad
dNTP set (100 mM)	Thermo Fisher Scientific
Dulbecco's Modified Eagle Medium (DMEM)	Gibco™/Invitrogen
Dulbecco's Modified Eagle Medium: Nutrient Mixture F-12 (DMEM/F-12) (1:1) (1X)	Gibco™/Invitrogen
DMSO (Dimethyl Sulfoxide), anhydrous	Life Technologies

Enhanced chemiluminescence (ECL) film (Amersham Hyperfilm ECL)	GE Healthcare
Enhanced chemiluminescence (ECL) Western Blotting reagents	GE Healthcare
Ethylenediaminetetraacetic acid (EDTA)	Sigma-Aldrich
Ethanol	Thermo Fisher Scientific
Ethidium bromide solution (10 mg/mL)	Carl Roth
Fetal Bovine Serum (FBS) Superior	Biochrom AG
Gateway BP-Clonase Enzyme Mix II	Thermo Fisher Scientific
Gateway LR-Clonase Enzyme Mix II	Thermo Fisher Scientific
Gel Loading Dye, purple, 6x	New England Biolabs™
GlutaMax	Gibco™/Invitrogen
HEPES	Invitrogen
Human IL-6 ELISA MAX™ Standard Sets	BioLegend
Human recombinant R-spondin	Produced in HEK293 cells
Human recombinant IFN-beta1a (IFNβ)	Biomol
Human recombinant IFNλ1 (IL-29)	Peprotech
Human recombinant IFNλ2 (IL28A)	Peprotech
Human recombinant IFNλ3 (IL-28B)	Cell signaling
Iscove's Modified Dulbecco's Medium (IMDM)	Gibco™/Invitrogen
Isopropanol	Carl Roth
Kanamycin (50 mg/mL)	Carl Roth
LB agar and medium powder	Carl Roth
[Leu15]-Gastrin I	Sigma-Aldrich
Matrigen	BD-bioscience
Methanol	Sigma-Aldrich
Mouse recombinat Epidermal Growth Factor (EGF)	Invitrogen
Mouse recombinat Noggin	Peprotech
NEBuffer 3.1	New England Biolabs™
Nicotinamide	Sigma-Aldrich
Nitrocellulose membrane (Amersham Hybond ECL)	GE Healthcare

Non-Essential Amino Acids (NEAA)	Gibco
Non-fat dried milk powder	AppliChem
N-acetyl-cysteine	Sigma-Aldrich
N-2	Invitrogen
PenStrep (Penicillin Streptomycin)	Gibco™/Invitrogen
Phosphate buffered saline (PBS)	Sigma-Aldrich
PhosphoSTOP phospatase inhibitor coctail	Roche
Phusion HF buffer (5x)	Thermo Fisher Scientific
Phusion hot start II DNA polymerase	Thermo Fisher Scientific
Proteinase K	Thermo Fisher Scientific
Precision Plus Protein Dual Colour	Bio-rad
ProLong Gold Antifade Mountain with DAPI	Molecular Probes
2-Propanol	Sigma
Puromycin (10 mg/ml)	Sigma
Pyridone-6 (pJAKi)	Calbiochem
Quick-Load 1 kb DNA ladder	New England Biolabs™
SB202190 (p38i)	Tocris
SOC Outgrowth medium	New England Biolabs™
Sodium chloride	Carl Roth
Sodium dodecyl sulfate (SDS)	Carl Roth
SP600125 (JNKi)	Tocris
SsoAdvanced Universal SYBR Green	Bio-Rad
TEMED	Carl Roth
TMB High Sensitivity Substrate Solution	BioLegend
Trypsin – EDTA 0,25% and 0,05%	Gibco by Life Technologies,
T4 DNA Ligase Reaction Buffer, 10x	New England Biolabs™
Tris base	Sigma-Aldrich
TritonX-100	Sigma-Aldrich
Tween 20	MP Biomedical
U0126 (ERKi)	Cell Signaling

Western Bright Chemiluminescent Substrate Sirius	Biozym
Wnt3A	Produced in L929 cells
Y27632	Sigma-Aldrich
β-mercapoethanol	Sigma-Aldrich

4.1.2 4.1.2 Media and buffers

Table 3: List of media and buffers

Name	Composition
Advanced Dulbecco's Modified Eagle Medium: Nutrient Mixture F-12 (DMEM/F-12)(1:1) for organoid media	Advanced DMEM/Ham's F-12 10 mM HEPES 1 x GlutaMAX 1% (v/v) PenStrep
Blocking solution (western blot) I	Nonfat dried milk powder 5% (w/v) 1 x TBS-T
Blocking solution (western blot) II	BSA 5% (w/v) 1 x TBS-T
Blotting buffer (western blot)	25 mM Tris base, 190 mM Glycine
Culture medium for HEK293T human embryonic kidney cells cells	IMDM, 1°% (v/v) FBS 1% (v/v) 100 U/mL PenStrep
Culture medium for T84 coloncarcinoma cells	DMEM/F-12 10% (v/v) FBS 1% (v/v) PenStrep
Basal Culture medium for human intestinal & colon organoids	Advanced DMEM/F-12 50% (v/v) Wnt3a conditioned media 20% (v/v) R-Spondin conditioned media 1 x B-27 1 x N-2 500 nM A-83-1

	50 ngr/ml EGF 10 nM Gastrin 2 mM GlutaMAX 10 mM HEPES 1 mM N-acetyl-cystein 10 mM Nicotinamide 100 ngr/ml Noggin 1 x PenStrep 10 µM Sb202190
ELISA coating buffer	8.4 g $NaHCO_3$ 3.56 g Na_2CO_3 in 1L H_2O
ELISA reagent diluent/block	1% BSA 1x PBS
ELISA stop solution	2N (1M) H_2SO_4
ELISA wash buffer	0,05% Tween 20 1x PBS
Laemmli buffer (4x)	200 mM Tris base (pH 6.8) 8% (w/v) SDS 40% (v/v) glycerol 4% (v/v) β-mercapoethanol 0.08% (v/v) bromphenol blue
LB agar (pH 7.0)	10 g LB agar powder 150 mL H_2O
LB medium (pH 7.0)	12,5 g LB medium powder 500 mL H_2O
Phosphate buffered saline (PBS) 10x	137 mM NaCl 2,7 mM KCl 10 mM Na_2HPO_4 2 mM KH_2PO_4 in H_2O

RIPA	150 mM sodium chloride 1% (v/v) Triton X-100 0.5% (w/v) sodium deoxycholate 0.1% (w/v) SDS 50 mM Tris base (pH 8.0) Complete protease inhibitor PhosphoSTOP phospatase inhibitor
SDS-Tris-Glycine buffer (1x)	25 mM Tris base 200 mM Glycine 0.1% (w/v) SDS
SDS-PAGE seperation gel buffer (4x)	1.5 M Tris base (pH 8.8) 0.4% (w/v) SDS
SDS-PAGE seperation gel (12%)	3.6 ml 30% Acrylamide/Bis-acrylamide solution 3.15 ml millipore H_2O 2.25 ml running gel buffer 75 ul APS (10% w/v) 15 ul TEMED
SDS-PAGE stacking gel buffer (4x)	0.5 M tris base (pH 8.8) 0.4% (w/v) SDS
SDS-PAGE stacking gel (5%)	0.5 ml 30% Acrylamide/Bis-acrylamide solution 1.75 ml millipore H_2O 0.75 ml seperation gel buffer 25 ul APS (10% w/v) 5 ul TEMED
SOC medium	2.66% (w/v) SOB-medium powder 20 mM D-(+)-Glucose
TBE buffer (0.5%)	50 mM Tris-base 50 mM Boric-acid 1 mM EDTA-Na_2
TBS	50 mM Tri-HCL, pH 7.5

	150 mM NaCL
TBS-T	50 mM Tri-HCL, pH 7.5 150 mM NaCL 0.1% Tween
Transfer buffer	20 mM Tris-base 160 mM Glycine 20% methanol
Tris-borate EDTA (TBE) running buffer 5x (agarose gel electrophoresis)	60,5 g Tris base 31 g H_3BO_3 3,7 g EDTA in H_2O

4.1.3 Antibodies

Table 4: List of primary antibodies

Antibody	Source	Species	Application
Anti-β actin	Sigma (#A5441)	monoclonal mouse	WB: 1:5,000
Anti-E-cadherin	BD (#610181)	monoclonal mouse	IF: 1:100
Anti-EF2	Santa Cruz (# sc-13004)	polyclonal goat	WB: 1:3,000
Anti-ERK	Cell signaling (#4695)	polyclonal rabbit	WB: 1:1,000
Anti-IFIT1	Abnova (#H00003434-DO1)	polyclonal rabbit	WB: 1:1,000
Anti-IRF1	Cell signaling (#8478)	polyclonal rabbit	WB: 1:1,000
Anti-Mucin-2	Santa Cruz (#sc-15334)	polyclonal rabbit	IF: 1:100
Anti-MxA	Georg Kochs-Freiburg, Germany	monoclonal mouse	WB: 1:1,000
Anti-p38	Cell signaling (#8690)	polyclonal rabbit	WB: 1:1,000
Anti-phospho p38	Cell signaling (#4511)	polyclonal rabbit	WB: 1:1,000
Anti-phospho ERK1/2	Cell signaling (#4370)	polyclonal rabbit	WB: 1:1,000
Anti-phospho-SAPK/JNK	Cell signaling (#4668)	polyclonal rabbit	WB: 1:1,000
Anti-phospho-STAT1	BD (#612233)	monoclonal mouse	WB: 1:1,000
Anti-SAPK/JNK	Cell signaling (#9258)	polyclonal rabbit	WB: 1:1,000
Anti-STAT1	BD (#610115)	monoclonal mouse	WB: 1:1,000

Anti-Syn	Santa Cruz (#sc-17750)	monoclonal mouse	IF: 1:100
Anti-ZOI	Invitrogen (#339100)	monoclonal mouse	IF: 1:100
Anti-μNS	GenScript, USA	monoclonal mouse	WB, IF: 1:1,000

Table 5: List of secondary antibodies

Antibody	Source	Species	Application
anti-mouse IgG Alexa Fluor 568	Invitrogen (A-11004)	polyclonal goat	IF: 1:1,000
anti-mouse IgG Alexa Fluor 647	Invitrogen (A-21235)	polyclonal goat	IF: 1:1,000
anti-rabbit IgG Alexa Fluor 568	Invitrogen (A-11011)	polyclonal goat	IF: 1:1,000
anti-rabbit IgG Alexa Fluor 647	Invitrogen (A-21244)	polyclonal goat	IF: 1:1,000
ECL anti-goat IgG HRP	Jackson (#705-035-147)	polyclonal donkey	WB: 1:5,000
ECL anti-mouse IgG HRP	GE-Healthcare (NA931)	polyclonal sheep	WB: 1:5,000
ECL anti-rabbit IgG HRP	GE-Healthcare (NA934)	polyclonal donkey	WB: 1:5,000

4.1.4 Primer

Table 6: List of primer sequences used for qRT-PCR analysi

	Gene Symbol	Forward primer (5'-3')	Reverse primer (5'-3')
#1	ARID3A	CCACGGCGACTGGACTTA	GCTGAACAAGTCATCCAGGAAT
#2	BLZF1	CATTAACAAATCACAAGTTGGCAAA	TGCAGAATTCAACTGTTGATGG
#3	CBFB	GCGAGTGTGAGATTAAGT	AGAGACAGATTGGTTCCT
#4	CEBPD	ACTTACCACCACTAAACTGC	TGTACCTTAGCTGCATCAAC
#5	CREB3L3	TTTAGCTGCTGGAAAGATGG	TCCACGTGTCTCAGGATG
#6	CSDA	TTCTCGCCACCAAAGTCCTTG	TTCTTCTTGATGGCAGTCTGATGT
#7	CXCL10	TGAAATTATTCCTGCAAGCCAA	GACATCTCTTCTCACCCTTCTTT
#8	DRAP1	ACATCCCACCTGAAGCAG	ATCCATGTGGTTGTCTTCC
#9	EGR1	CAGCACCTTCAACCCTCAG	AGCGGCCAGTATAGGTGATG
#10	EGR2	GCTGACACGGCACATCC	ACAGTAGTCACAGGCGAAGG
#11	ELF1	TGTCATGCTGCAGTCACAAA	ACTGCGAGGAGAAAAGGTCA
#12	ELK4	CTGGTGCCAAGACCTCTAGC	TCGGCTGGATTCTCAGTCTT
#13	ETS2	TCTGCCTCAATAAGCCAACC	TAAACTCCCATCCGTCTCCA
#14	ETV6	AAGCCCATCAACCTCTCTCA	CCATCGGATGAAGTTTTCGT
#15	ETV7	AAGAACCGGGTGAACATGAC	TTGTCCTGGACCATCTTTCC
#16	EWSR1	TAGGATATGGACAGAGTAAC	GTAGAGGAATAGCTGGTAG
#17	FUBP1	ACGCTTTCAAAGATGCACTG	TTTTTGTCCCCCATAACCAT
#18	GBP1	CTATGAGGAACCGAG	CACGTTCCACTTCAATCTCC
#19	HDAC2	AGCATCAGGATTCTGTTACGTTAATGA	CAACACCATCACCATGATGAATATCT
#20	HIF1A	GCTATTTGCGTGTGAGGAAAC	CACCATCATCTGTGAGAACCA
#21	HPRT1	CCTGGCGTCGTGATTAGTGAT	AGACGTTCAGTCCTGTCCATAA
#22	IFIT1	AAAAGCCCACATTTGAGGTG	GAAATTCCTGAAACCGACCA
#23	IFITM3	GATGTGGATCACGGTGGAC	AGATGCTCAAGGAGGAGCAC
#24	IFNAR1	CACTGACTGTATATTGTGTGAAAGCCA GAG	CATCTATACTGGAAGAAGGTTTAAGTGATG
#25	IFNAR2	ATTTCCGGTCCATCTTATCAT	ACTGAACAACGTTGTGTTCC
#26	IFN-β	GCCGCATTGACCATCTAT	GTCTCATTCCAGCCAGTG
#27	IFN-λ2/3	GCCACATAGCCCAGTTCAAG	TGGGAGAGGATATGGTGCAG

#28	IL10RB	TTGCTGTGGTGCGTTTACAAG	CTTTCAGGTGCTGTGGAAGAGA
#29	IFNLR1	ACCTATTTTGTGGCCTATCAGAGC	CGGCTCCACTTCAAAAAGGTAAT
#30	IRF1	CCAAGAGGAAGTCATGTG	TAGCCTGGAACTGTGTAG
#31	IRF4	ATCACAGCTCACGTAGAA	ATAGAGGAATGGCGGATA
#32	IRF8	GGCATTCTCGGAGGAGTAGA	GTTACAGCATCCAGGCCATC
#33	JUN	GAGGACCGGAGACAAGTG	CCTTCTTCTCTTGCGTGG
#34	JUNB	CATACACAGCTACGGGATAC	TTTGAGACTCCGGTAGGG
#35	MAFB	GACGCAGCTCATTCAGCAG	CCGGAGTTGGCGAGTTTCT
#36	MAFF	GATTGAGAGATACAGAGCCG	CTAGCTTTGAATCCTGGGAG
#37	MAX	AACCGAGGTTTCAATCTGC	GGGATGCCTTCTCTCCTTG
#38	MYC	GATTCTCTGCTCTCCTCGAC	CTTGTTCCTCCTCAGAGTC
#39	MXA	GAGCTGTTCTCCTGCACCTC	CTCCCACTCCCTGAAATCTG
#40	NFIL3	AATGCAGACCGTCAAAAAGG	AGCAGCTCCTCACCTGTTGT
#41	NFE2	AGCTGCAGGGTCTGAATG	CAGAATCTGGGTGGATTGAG
#42	NPAS2	AGGAGCTGGCTCTGGAAGAC	CCGAGGTTCCAGGCTTGAG
#43	RASD1	CAAGACCGGGGAGAATACCTG	GCGAGAATGTCCAAATACTCACC
#44	REO (µ2)	GTGTACACCACGACGGACAG	TCAACCCCACTCATGACAAA
#45	RELA	TATCAGTCAGCGCATCCAGACCAA	AGAGTTTCGGTTCACTCGGCAGAT
#46	SMAD3	AGCAATATTCCAGAGACC	GCAGGTCCAAGTTATTATG
#47	SMAD4	TTACCATCATAACAGCACTA	CAAGCTCATTGTGAACAG
#48	SOCS3	GCGAGGATCCTGGTGACA	CCAGGATGGTTCCCTTCAG
#49	SREBF1	ACTTCTGGAGGCATCGCAAGCA	AGGTTCCAGAGGAGGCTACAAG
#50	TBP	TGCACAGGAGCCAAGAGTGAA	CACATCACAGCTCCCCACCA
#51	TCF7L2	CATATGGTCCCACCACATCA	CACTCTGGGACGATTCCTGT
#52	TEAD4	ATGATCATCACCTGCTCCAC	GTCCATTCTCATAGCGAGCA
#53	TLR3	TTGTCTTCTGCACGAACCTGCGC	AACGCAAGGATTTTATT
#54	TRIM21	TGGAGACCTTTAGGGGGTTT	TGAGCGGAAACTGAAAGTGA
#55	TRIM22	GGATGCCAGCACGCTCATCTCAG	TTCAGCATCACGTCCACCCAGTAGT
#56	TRIM25	AACATCTCTCAAGGCCAAGGT	AGATGCCTACCCCACAGAAGT
#57	USP18	ATGTGAGCCAGGCACGAT	TCCCGACGTGGAACTCAG
#58	VIPERIN	GAGAGCCATTTCTTCAAGACC	CTATAATCCCTACACCACCTCC
#59	ZFP36L2	CTTGATAGTTAGCCCTCAGC	CCAAGTAACCAGTATGGACC

Table 7: List of primers used in predesigned 384 well assay qRT-PCR

	Gene Symbol	RefSeq Accession No		Gene Symbol	RefSeq Accession No
#1	ADAR	NC_000001.10, NG_011844.1, NT_004487.19	#45	IL15	NC_000004.11, NT_016354.19
#2	B2M	NC_000015.9, NG_012920.1, NT_010194.17	#46	IL6	NC_000007.13, NG_011640.1, NT_007819.17
#3	BAG3	NC_000010.10, NG_016125.1, NT_030059.13	#47	IRF1	NC_000005.9, NG_011450.1, NT_034772.6
#4	BST2	NC_000019.9, NT_011295.11	#48	IRF2	NC_000004.11, NT_016354.19
#5	CASP1	NC_000011.9, NT_033899.8	#49	IRF3	NC_000019.9, NT_011109.16
#6	CAV1	NC_000007.13, NT_007933.15, NG_012051.1	#50	IRF5	NC_000007.13, NT_007933.15, NG_012306.1
#7	CCL2	NC_000017.10, NG_012123.1, NT_010799.15	#51	IRF7	NC_000011.9, NT_009237.18
#8	CCL5	NC_000017.10, NG_015990.1, NT_010799.15	#52	IRF9	NC_000014.8, NT_026437.12
#9	CD70	NC_000019.9, NT_011255.14	#53	ISG15	NC_000001.10, NT_004350.19
#10	CD80	NC_000003.11, NT_005612.16	#54	ISG20	NC_000015.9, NT_010274.17
#11	CD86	NC_000003.11, NT_005612.16	#55	JAK1	NC_000001.10, NG_023402.1, NT_032977.9
#12	CDKN1B	NC_000012.11, NG_016341.1, NT_009714.17	#56	JAK2	NC_000009.11, NG_009904.1, NT_008413.18
#13	CIITA	NC_000016.9, NG_009628.1, NT_010393.16	#57	MAL	NC_000002.11, NT_022171.15
#14	CRP	NC_000001.10, NG_013007.1, NT_004487.19	#58	MET	NC_000007.13, NT_007933.15, NG_008996.1
#15	CXCL10	NC_000004.11, NT_016354.19	#59	MNDA	NC_000001.10, NT_004487.19
#16	DDX58	NC_000009.11, NT_008413.18	#60	MX1	NC_000021.8, NG_027788.1, NT_011512.11
#17	EIF2AK2	NC_000002.11, NT_022184.15	#61	MX2	NC_000021.8, NT_011512.11
#18	GBP1	NC_000001.10, NT_032977.9	#62	MYD88	NC_000003.11, NG_023225.1, NT_022517.18, NG_016964.1
#19	GUSB	NC_000007.13, NG_016197.1, NT_007933.15	#63	NMI	NC_000002.11, NT_005403.17
#20	HLA-A	NC_000006.11, NT_007592.15, NT_113891.2, NT_167244.1	#64	NOS2	NC_000017.10, NG_011470.1, NT_010799.15
#21	HLA-B	NC_000006.11, NG_002397.2, NG_023187.1, NT_007592.15, NT_113891.2,	#65	OAS1	NC_000012.11, NT_009775.17, NG_011530.1
		NT_167246.1, NT_167247.1, NT_167248.1, NT_167249.1	#66	OAS2	NC_000012.11, NT_009775.17
#22	HLA-E	NC_000006.11, NT_007592.15, NT_113891.2, NT_167245.1, NT_167246.1,	#67	PML	NC_000015.9, NT_010194.17
		NT_167247.1, NT_167248.1, NT_167249.1	#68	PRKCZ	NC_000001.10, NT_004350.19
#23	HLA-G	NC_000006.11, NT_007592.15, NT_113891.2, NT_167245.1, NT_167246.1,	#69	PSME2	NC_000014.8, NT_026437.12
		NT_167247.1, NT_167248.1, NT_167249.1	#70	RPLP0	NC_000012.11, NT_009775.17
#24	HPRT1	NC_000023.10, NG_012329.1, NT_011786.16	#71	SH2D1A	NC_000023.10, NT_011786.16, NG_007464.1

#25	IFI16	NC_000001.10, NT_004487.19	#72	SHB	NC_000009.11, NT_008413.18
#26	IFI27	NC_000014.8, NT_026437.12	#73	SOCS1	NC_000016.9, NT_010393.16
#27	IFI30	NC_000019.9, NT_011295.11	#74	STAT1	NC_000002.11, NG_008294.1, NT_005403.17
#28	IFI6	NC_000001.10, NT_004610.19	#75	STAT2	NC_000012.11, NT_029419.12
#29	IFIH1	NC_000002.11, NG_011495.1, NT_005403.17	#76	STAT3	NC_000017.10, NT_010783.15, NG_007370.1
#30	IFIT1	NC_000010.10, NT_030059.13	#77	TAP1	NC_000006.11, NG_011759.1, NG_028165.1, NT_007592.15, NT_113891.2, NT_167244.1,
#31	IFIT2	NC_000010.10, NT_030059.13			NT_167245.1, NT_167246.1, NT_167247.1, NT_167248.1, NT_167249.1
#32	IFIT3	NC_000010.10, NT_030059.13	#78	TBP1	NC_000006.11, NT_025741.15, NG_008165.1
#33	IFITM1	NC_000011.9, NT_009237.18	#79	TICAM1	NC_000019.9, NT_011255.14
#34	IFITM2	NC_000011.9, NT_009237.18	#80	TIMP1	NC_000023.10, NG_008437.1, NG_012533.1, NT_079573.4
#35	IFITM3	NC_000011.9, NT_009237.18	#81	TLR3	NC_000004.11, NG_007278.1, NT_016354.19
#36	IFNA1	NC_000009.11, NT_008413.18	#82	TLR7	NC_000023.10, NG_012569.1, NT_167197.1
#37	IFNA2	NC_000009.11, NT_008413.18	#83	TLR8	NC_000023.10, NG_012882.1, NT_167197.1
#38	IFNA4	NC_000009.11, NT_008413.18	#84	TLR9	NC_000003.11, NT_022517.18
#39	IFNAR1	NC_000021.8, NT_011512.11	#85	TMEM173	NC_000005.9, NT_029289.11
#40	IFNAR2	NC_000021.8, NG_012089.1, NT_011512.11, NG_016003.1	#86	TNFSF10	NC_000003.11, NT_005612.16
#41	IFNB1	NC_000009.11, NT_008413.18	#87	TRAF3	NC_000014.8, NT_026437.12, NG_027973.1
#42	IFNE	NC_000009.11, NT_008413.18	#88	TYK2	NC_000019.9, NG_007872.1, NT_011295.11
#43	IFNW1	NC_000009.11, NT_008413.18	#89	VEGFA	NC_000006.11, NG_008732.1, NT_007592.15
#44	IL10	NC_000001.10, NG_012088.1, NT_167186.1			

4.2 Methods

The text of part 4.2 has been adapted from Pervolaraki et al. (2017)[100] and from Pervolaraki et al. (2018), *under preparation.*

4.2.1 Cell culture, viruses and viral infection

4.2.1.1 Culture of human cell lines

T84 human colon adenocarcinoma cells (ATCC CCL-248) were maintained in a 1:1 nutrient mixture of Dulbecco's modified Eagle's medium (DMEM) and F-12 supplemented with 10% fetal bovine serum (FBS) and 1% (100 U/ml) penicillin and 1% (100 µg/mL) streptomycin. SKCO15 human colon adenocarcinoma cells were a kind gift from Prof. Asma Nusrat, Department of Pathology, University of Michigan and maintained in DMEM with 10% FBS, 1% penicillin/streptomycin, 15 mM HEPES and 1% Non-Essential Amino Acids (NEAA). Caco2 human colon adenocarcinoma cells (ATCC HTB 37) were maintained in DMEM with 10% fetal bovine serum and 1% penicillin/streptomycin. T84, SKCO15 and Caco2 cells were cultured in collagen coated T25 flasks and split in 1:2 ratio every 3-4 days by treatment with 0.25% Trypsin/EDTA. HEK293T human embryonic kidney cells (ATCC) were cultured in T75 cell culture flasks using Iscove's modified Dulbecco's medium (IMDM) supplemented with 10% FBS and 1% penicillin/streptomycin. All mammalian cells were cultured at 37^{o}C and 5% $CO_{2.}$

4.2.1.2 Culture of human colon and intestinal mini-gut organoids

Human colon and intestinal tissue was received from colon resections from the University Hospital Heidelberg, Germany and human ileum and jejunum were purchased from Baylor University, USA. The resected tissue was washed several times with ice-cold PBS containing 1 x Antibiotic-Antimycotic (Anti-Anti) and stem cells containing crypts were isolated following 2 mM EDTA dissociation of tissue sample for 1 hour at 4°C, with rocking. Crypts were spun and washed in ice-cold PBS. Fractions enriched in crypts were resuspended in Matrigel and maintained in Advanced DMEM/F-12, supplemented with penicillin/streptomycin, HEPES, Wnt3A, B-27, N-2, GlutaMax, EGF, R-Spondin, Noggin, Gastrin, N-acetyl-cysteine, nicotinamide and A-83-01 (basal organoid medium). 24 hours post-isolation, the open crypts were resealed and round organoid structures were apparent. Medium was changed every 2-3 days and for the first two days post isolation, the Rho–associated coiled-coil containing protein kinase (ROCK) inhibitor Y-27632 (10 µM) was

added to the basal organoid culture medium. Organoids were split every 7-10 days by passaging the Matrigel containing organoids through a 27½ gauge needle several times. Differentiation media is the same as above except without Wnt3A, nicotinamide and 50% reduced levels of R-Spondin and Noggin[24,349,350].

Ethics Statement

Human gut tissue was received from colon and small intestine resection from the University Hospital Heidelberg, Germany. All subjects gave written informed consent in accordance with the Declaration of Helsinki. All samples were received and maintained in an anonymized manner. The protocol was approved by the "Ethic commission of University Hospital Heidelberg" under the approved study protocol S-443/2017. Human ileum and jejunum were purchased from Baylor University, USA and transferred by signed MTA.

4.2.1.3 Viruses and viral infection

VSV-Luc was a kind gift from Sean Whelan (Harvard Medical School) and was produced as previously described[351]. An MOI of 1 was used to infect T84 cells and organoids. Titers were determined as previously described[352]. Reovirus MRV strains Type 3 clone 9 derived from stocks originally obtained from Bernard N. Fields were grown and purified by standard protocols[120]. For T84 cell MRV infections, MRV was purified on CsCl-gradient and stocks were titred by fluorescence foci forming assay (expressed in FFU) in T84 cells. Titers were calculated by determining the 50% tissue culture infective dose and expressed in FFU/mL. T84 cells were infected as previously described[120]. The MOI was determined as the ratio of infected cells (determined by fluorescence foci forming assay)/total number of cells. An MOI of 1 was used in T84 based experiments resulting in about 50–60% of infected as determined by fluorescence assay. For mini-gut organoids MRV infection, organoids were removed from Matrigel by adding cold-PBS for 5 min, liquefied Matrigel and organoids were separated by centrifugation (400xg 5 min), the total number of cells per organoid samples was measured using an haematocytometer. Organoids were resuspended in culture medium containing or not MRV. When using an MOI of 1 (as determined in T84 cells) to infect mini-gut organoids, very few infected cells were detected per organoid. This discrepancy between T84 and organoid infectivity might be due to the 3-dimensional nature of the organoids and to residual Matrigel that might absorb and neutralize MRV. As such MRV stocks were titred directly in organoids by serial dilution infection and subsequent immunostaining. The MOI was calculated by the ratio of the number of infected/total number of cells/organoid. An MOI of 0.5 was used to infect organoids.

4.2.2 Cloning and generation of stable cells lines

4.2.2.1 Cloning and generation of IFN receptor KO cell lines

Knockouts of IFNAR1 and IFNLR1 in T84 cells were achieved by using the CRISPR/Cas9 system. Three different single-guide RNAs (sgRNAs) per gene were used to target the coding region of IFNAR1 and IFNLR1 and inserted into the lentiviral vector lentiCRISPR v2 (Addgene #52961) also encoding the Cas9 nuclease. The following sgRNAs were used: IFNAR1 (#1) 5′ GCGGCTGCGGACAACACCCA 3′, (#2) 5′ GACCCTAGT- GCTCGTCGCCG 3′, (#3) 5′CTAGGGTCGTCGCGCCCAGG3′,IFNLR1(#1) 5′ACTGGATCTGAAGTATGAGG3′, (#2) 5′CC TGGTGCTCACCCAGACGG3′ (#3) 5′ TGAGGTGGCATTCTG GAAGG 3′. Lentiviruses were produced and T84 cells were transduced two times using 1:2 diluted stocks of lentiviral particles encoding sgRNA #1, 2 or 3. Data at Figure 16 were obtained by using a cell clone treated with the sgRNA #2 for IFNAR1 and IFNLR1 and analogous results were obtained with cell clones generated with the other sgRNAs (Figure 17). 36 hours post-transduction, transduced cells were selected for using puromycin for 2-3 weeks and then used for experiments. To establish IFNAR1 and IFNLR1 KO cells, clonal selection was performed via single-cell dilution in a 96-well plate. KOs were confirmed by sequencing and functional tests.

4.2.2.2 Cloning and generation of IFN receptor overexpressing cell lines

For back-compensation of the IFN receptor KO cell lines and for generation of wild-type T84 cells overexpressing the IFNAR1 and IFNLR1, plasmids containing the cDNA of IFNAR1 and IFNLR1 were obtained from a gateway compatible ORF bank (pENTRY221-IFNAR1) and from GE Healthcare (pCR_XL_TOPO_IFNLR1, #MHS6278-213246004), respectively. Caspase-cleavage resistant IFNAR1 and IFNLR1 were generated using the Quick Change II XL site directed mutagenesis kit (Agilent Technologies, Germany), following manufacturer's instructions. Point mutations were controlled by plasmid sequencing. The expression vectors were generated by inserting the respective constructs into the lentiviral vector pDest GW35 by using the Gateway cloning technology (Life Technologies, Germany) according to manufacturer's instructions. Lentiviruses were produced and T84 cells were transduced two times using concentrated stocks of lentiviral particles encoding the cleavage resistant IFNAR1 and IFNLR1. 36 hours post-transduction, transduced cells were selected for using blasticidin.

4.2.2.3 Production and use of lentiviral vectors

Hek293T cells with a low passage number were cultured in 10 cm dishes until 80-90% confluence. After reaching the appropriate confluence, medium was changed and the cells were transfected with a transfection mixture of 4 µg pMDG.2, 4 µg psPAX2 and 8 µg of the expression vector containing the construct of interest using polyethylenimine (PEI). The Transfection mixture was added dropwise to cells and culture medium was exchanged the next day. After three days, virus containing supernatant was harvested, centrifuged at 4,000xg for 10 minutes and filtered (Millex-HA, 0.45µm, Millipore, SLHA033SS). Purified virus was concentrated by ultracentrifugation at 134,000 rcf in an SW40 Ti rotor (Beckman-Counter) at 4^{o}C for 2 hours and stored at -80 °C.

For transduction of T84 cells with lentivirus, 300,000 cells per well were seeded in a 6-well plate and 20-40 µl of the concentrated lentivirus stock was added in 3 ml of cell culture medium together with 10 µg/ml polybrene. After two days, cells were transduced for second time with the same mixture of lentivirus stock and polybrene and two days later, the medium was replaces with selection medium containing the appropriate antibiotic (10 µgr/ml puromycin or blasticidin). Cells were cultured in selection medium for 2-3 weeks, before being used for experiments.

4.2.3 Cell biology techniques and protein biochemistry

4.2.3.1 Protein extraction

At time of harvest, media was removed, cells or mini-gut organoids were rinsed one time with 1 x cold PBS and lysed with 1 x RIPA buffer. Cells were incubated at 4^{o}C for 20 minutes. Afterwards, lysates were collected and centrifuged at 12,000xg for 20 minutes at 4^{o}C. Supernatant was transferred to a new tube and protein concentration was determined using the DC Protein Assay Kit I (Biorad), according to the manufacture's instructions. Absorption was measured at a wavelength of 750 nm using the Biorad iMark microplate reader and protein concentration was calculated by using the BSA standard curve.

4.2.3.2 Western blot (WB)

Lysates of equal protein amounts (6-12 µg, depending on the experiment) were supplemented with Laemmli buffer, boiled at 95^{o}C for 10 minutes, spun down at 12,000xg for 1 minute and separated by Sodium dodecyl sulfate polyacrylamide gel electrophoresis (SDS-PAGE). Proteins were separated according to their electrophoretic mobility in 8-12%

SDS-PAGE gels at 100V. For immunoblotting, proteins were transferred to a nitrocellulose blotting membrane with 0.45 µm pore size (GE Healthcare) by wet-blotting at 100V for 1.5 hour in pre-cooled transfer buffer by using the Bio-Rad Tank blot system. After blotting, membranes were blocked for 1-2 hours shaking at room temperature in TBS containing 0.1% Tween 20 (TBS-T) with 5% milk or 5% BSA, when the phospho antibodies were used. Primary antibodies were diluted in blocking buffer and incubated overnight at 4°C. Membranes were washed 4 x in TBS-T for 15 minutes at RT. Secondary antibodies were diluted in blocking buffer and incubated at RT for 1 hour with rocking. Membranes were washed 4 x in TBS-T for 15 minutes at RT. For protein visualization, HRP detection reagent (ECL Western Blotting Detection Reagents or Western Bright Chemiluminescent Substrate Sirius) was mixed 1:1 and incubated at RT for 3-5 minutes. Membranes were exposed to high performance chemiluminescence films (GE healthcare) and developed. Quantitative immunoblot analysis was performed using Fiji.

4.2.3.3 Indirect Immunofluorescence (IF) assay

T84 cells were seeded in a 24-well plate were fixed in 2% paraformaldehyde for 20 minutes at RT, washed with PBS and permeabilized using 0.5% Triton X-100 for 15 minutes. After blocking with 3% BSA in PBS for 1 hour at RT, cells were incubated with primary antibodies in 3% BSA for 1 hour at RT. After washing with PBS, cells were stained with secondary antibodies in 3% BSA for 45 minutes at RT. To stain human mini-guts, organoids were embedded in optimal cutting temperature (OCT) compound (Tissue-Tek) and cryosectioned using the Leica CM1950 (Leica) cyrostat. 10 µm cryosections were fixed in 80% ethanol for 10 minutes at RT, followed by a 2 minute incubation in ice-cold acetone. After blocking in 5% goat serum in PBS containing 1% Triton for 1 hour at RT, sections were incubated with primary antibodies in blocking solution for 2 hours at RT or overnight at 4°C. After washing in PBS, sections were stained with secondary antibodies in 1% BSA in PBS containing 0.5% Triton for 2 hours at RT. Nuclear DNA was stained with ProLong Gold DAPI. Slides were imaged by epifluorescence using a Nikon Eclipse Ti-S (Nikon) microscope or by confocal tile scans on a Zeiss LSM 780 (Zeiss) microscope. Image processing was performed using the Fiji software. For infection experiments, the percentage of infected cells was determined by counting at least 600–1,000 cells detected in 10 fields of view for each condition.

4.2.3.4 VSV luciferase assay

Luciferase activity was measured as read out for VSV-Luc replication. T84 cells were seeded in a white F-bottom 96-well plate (Greiner bio-one) 1 day prior experiment. Cells or

organoids were pre-treated prior to infection or treated post-infection as indicated with increasing concentrations of type I or type III IFNs. VSV-Luc was added to the wells and the infection was allowed to proceed for 8 hours. At the end of the infection, media was removed, cells and organoids were washed 1 x with PBS and lysed with luciferase cell Lysis Buffer (Promega) at RT for 20 minutes. A 1:1 dilution of Steady Glo (Promega) and Lysis Buffer were added to the cells and organoids and incubated at RT for 15 minutes. Luminescence was measured using an Omega microplate Luminometer reader (BMG-Labtech).

4.2.3.5 Enzyme-Linked Immunosorbent Assay (ELISA)

Supernatant from cells and organoids was collected at the indicative time points and centrifuged at 12,000xg at RT to remove cellular debris. IFNβ contained in the supernatant was quantified by using the human IFN-beta ELISA kit (PBL-Interferon Source) according to manufacturer's instructions. IFN-λ 2/3 was analyzed by using the VeriKine-DIYTM human IFN-λ 2/3 (IL-28A/28B) ELISA kit (Pestka Biomedical Laboratories) and all volumes were adjusted to fit to a half-area assay plate. Briefly, the plate was incubated over night with the capture antibody (2 µg/ml anti-IFNλ in reagent diluent at 4°C) and blocked at room temperature for 1 hour with vertical shaking at 200 rpm. 50 µl of cytokine standards and samples were loaded on the plate and incubated at RT for 2 hours with vertical shaking at 200 rpm. The biotinylated detection antibody was diluted to 100 ng/ml in reagent diluent and incubated at RT for 2 hours with shaking at 200 rpm. After incubation with Avidin-HRP (diluted 1:1000, BioLegend) was performed for 20 minutes. Between each step, three washes with ELISA washing buffer were performed. Lastly, 50 µl of mixed A and B (1:1) TMD substrate solutions (BioLegend) were added to each well, the plate was incubated in the dark until the standard curve was clearly visible in blue and the reaction was stopped by adding 20 µl of 2 N Sulfuric acid (H2SO4). The final absorbance was measured at 450 nm on a Bio-Rad iMark microplate reader.

4.2.4 mRNA analysis

4.2.4.1 RNA purification and cDNA-synthesis

Purification of total RNA from cells or mini-gut organoids was performed using the NucleoSpin RNA extraction kit (Macherey-Nagel) as per manufacturer's instructions. In summary, cell lysates were passed through a DNA elimination column and the flow through was mixed with 70% ethanol, added to a RNeasy spin column, allowing RNA binding to the

membrane. Columns were washed with two buffers of decreasing salt concentration and RNA samples were eluted in 40-60 µl nuclease free water and stored at -80^{o}C for further analysis. RNA concentration was determined by measuring the absorbance at 260 nm with the NanoDrop Lite spectrophotometer (Thermo Scientific). For cDNA generation, 50-200 ng of total RNA was reverse transcribed using the iScriptTM cDNA Synthesis kit (BioRad) according to the manufacture's instructions using the following reaction:

Table 8: Components of cDNA synthesis reaction

Component	Volume (µl)
iScript reaction buffer	4
Reverse transcriptase	1
RNA template	15

Components were mixed together and reverse transcription was performed according to the following program using the thermal cycler (Biorad):

Table 9: Thermal cycler program for cDNA synthesis

Step	Temperature (°C)	Time (min)
Priming	25	5
Reverse transcription	42	30
Reverse transcription termination/Termination	85	5

4.2.4.2 Quantitative real time polymerase chain reaction (qRT-PCR)

Following cDNA-synthesis, the resulting cDNA was diluted 1:1 with nuclease free water before proceeding to the quantitative real time polymerase chain reaction (qRT-PCR). qRT-PCR was performed in 96-well format using Sso Advanced Universal SYBR Green Supermix (Bio-Rad) with the following reaction per well:

Table 10: Components of the qRT-PCR reaction

Component	Volume (µl)
SsoAdvanced Universal SYBR Green Supermix	7,5
Primer reverse (2 µM)	1,9
Primer forward (2 µM)	1,9
Millipore H_2O	1,7
cDNA (1:2 diluted)	2

The reaction was performed using the Bio-Rad CFX96 Real-Time PCR Detection System with the following settings:

Table 11: Program for qRT-PCR

Step	Temperature (°C)	Time	Number of cycles
Activation	95	30”	
Melting	95	5”	40
Primer annealing and Elongation	60	30”	40
Plateread			
Melting curve generation	65	5”	
		+0,5°C/cycle to 95°C	

The obtained data were then analyzed with the Bio-Rad CFX Manager 3.0 using HPRT1 and/or TBP as housekeeping genes to normalize mRNA expression. The data obtained by qRT-PCT were calculated as relative expression levels (ΔΔCq) normalized to input mock sample of initial time point.

4.2.4.3 Gene expression analysis of interferon stimulating genes

T84 cells and mini-gut organoids were treated with 2000 RU/ml of type I IFN (β) or 100 ng/ml of each type III IFN (λ□□□). Total RNA was isolated at 3, 6, 12 and 24 hours post-treatment as described above. For the gene expression analysis of interferon stimulated genes (ISGs), qRT-PCR was performed using the predesigned 384-well assay of type I IFN response for use with SYBR Green assaying the expression of 87 ISGs (Biorad # 10034592). The expression of 45 additional ISGs and transcriptional factors was analyzed by qRT-PCR with primer sets obtained as previously described[353]. The complete gene list monitored in this study and the primers used to amplify each gene are available in Table 5 and 6. Differential expression analysis of each treatment was performed by comparing the baseline expression of genes in an untreated control at each time point. Only genes which were either induced or reduced more than 2-fold in any of the samples were considered to be significantly regulated. These genes were either analyzed using scatterplots or visualized by a heatmap after sorting the fold change of expression in response to type I IFN (β) in decreasing order. All fold change values above 20 and below 0.05 were replaced with 20 and 0.05 respectively to center the heatmap around 0 (white) and to avoid errors in logarithmic calculations. When visualizing the expression peaks, only the highest value is shown per time point for each gene. All analyses were performed using R version 3.3.0 and 3.3.3 including the packages gplots and ggplot2.

4.2.4.4 Microarray

Total RNA was purified as described above from T84 cells treated with 2,000 RU/mL of type I IFN (β) or 100 ng/mL of each type III IFN (λ1−3) for 6 hours. Microarray data were processed using the software package R. Differentially expressed probe sets were determined by comparing the triplicate stimulated samples with the three unstimulated samples. Significance was defined by a minimum absolute of 2-fold change in expression and a q-value (false discovery rate) <0.05.

4.2.5 Mathematical modeling

Mathematical modeling has been performed by Soheil Rastgou Talemi, Heidelberg University and German Cancer Research Center (DKFZ).

4.2.5.1 Model simulation and parameter estimation

The mathematical model was implemented in terms of ordinary differential equations (ODEs)

in MATLAB 2016b (S1 Table). The numerical simulations were conducted using the CVODES, a module from SUNDIALS numerical simulation package, in the MATLB environment. The model was initially set to a steady state condition and most of the initial conditions were set (S2 Table). Only, the IFNLR efficacy factor was estimated using time-resolved ISG expression data that we measured with different doses of type I IFN (β) or III IFN (λ1−3). All of the ISG expression data for the IFNAR1 and IFNLR1 overexpression experiments were reproduced only by fitting new initial values of IFNAR1 and IFNLR1 (S3 Table).

Parameter estimation was conducted by minimizing the weighted nonlinear least squares,

$$\mathrm{wSSR} = \sum_{i=1}^{N}\left(\frac{1}{Average\left(y_{observed\_i}\right)}\right)\sum_{j=1}^{M}\left(y_{simulation\_i,j} - y_{observed\_i,j}\right)^2,$$

of model simulations versus data points, j = 1, … , M, of different experiments, i = 1, … , N. The inverse of the average of every time-resolved experimental data was used as a weighting factor for fitting the corresponding data.

4.2.5.2 Profile-likelihood analysis

To assess the uncertainty in the estimated parameter values, we used the profile-likelihood method[354]. In this method, the parameter confidence bounds are calculated based on their contribution to the likelihoods, or in another word, the objective function (wSSR). This computational approach is conducted in a stepwise manner. In every step, the respective parameter is fixed at a new value distant from the optimum estimated one. Then, the new maximum likelihood is calculated ($\mathrm{wSSR}_{\min}(\theta)$). Using this approach, we can calculate the profile of the maximum likelihoods over different values of the considered parameter. Then a threshold, Δ_α,

$$\Delta\chi^2 = \mathrm{wSSR}_{\min}(\theta) - \mathrm{wSSR}_{\min}\left(\theta_{optimum}\right),$$

$$\{\theta|\Delta\chi^2 < \Delta_\alpha\},$$

is used to define the confidence bounds for the respective parameter. The threshold, Δ_α, is the α quantile of the chi-squared distribution.

4.2.5.3 Approximate 95% confidence bands calculation

To investigate the effect of the parameter uncertainty on model predictions we calculated approximate 95% confidence bands, as explained in Seber and Wild[355].

$$\text{Approx } 95\% \text{ confidence bands} = y_{simulated} \pm t_{inv}{}^{\alpha}_{N-P} \cdot \sqrt{MSE} \cdot (1 + S \cdot (S \cdot S)^{-1} \cdot S)^{\frac{1}{2}}$$

where "$t_{inv}{}^{\alpha}_{N-P}$" is the α quantile of student's t distribution, "N" is the number of data points and "P" is the number of estimated model parameters, "MSE" is the mean standard error and "S" is the sensitivity matrix of the respective simulated observable.

5 References

1. Ley, R. E., Peterson, D. A. & Gordon, J. I. Ecological and evolutionary forces shaping microbial diversity in the human intestine. *Cell* **124,** 837–848 (2006).

2. O'Hara, A. M. & Shanahan, F. The gut flora as a forgotten organ. *EMBO Rep.* **7,** 688–693 (2006).

3. David A. Hill, D. A. Intestinal Bacteria and Regulation of Immune Cell Homeostasis. *Annu Rev Immunol.* **28,** 623–667 (2010).

4. Pott, J. & Hornef, M. Innate immune signalling at the intestinal epithelium in homeostasis and disease. *EMBO Rep.* **13,** 684–698 (2012).

5. Turner, J. R. Intestinal mucosal barrier function in health and disease. *Nat. Rev. Immunol.* **9,** 799–809 (2009).

6. Goto Y, K. H. Epithelial barrier: an interface for the cross-communication between gutflora and immune system. *Immunol. Rev.* **245,** 147–63 (2012).

7. Peterson, L. W. & Artis, D. Intestinal epithelial cells: regulators of barrier function and immune homeostasis. *Nat. Rev. Immunol.* **14,** 141–53 (2014).

8. Mantis, N. J., Rol, N. & Corthésy, B. Secretory IgA's complex roles in immunity and mucosal homeostasis in the gut. *Mucosal Immunol.* **4,** 603–611 (2011).

9. van der Flier, L. G. & Clevers, H. Stem Cells, Self-Renewal, and Differentiation in the Intestinal Epithelium. *Annu. Rev. Physiol.* **71,** 241–260 (2009).

10. Van der Sluis, M. *et al.* Muc2-Deficient Mice Spontaneously Develop Colitis, Indicating That MUC2 Is Critical for Colonic Protection. *Gastroenterology* **131,** 117–129 (2006).

11. Kim, Y. S. & Ho, S. B. Intestinal goblet cells and mucins in health and disease: Recent insights and progress. *Curr. Gastroenterol. Rep.* **12,** 319–330 (2010).

12. Johansson, M. E. V., Larsson, J. M. H. & Hansson, G. C. The two mucus layers of colon are organized by the MUC2 mucin, whereas the outer layer is a legislator of host-microbial interactions. *Proc. Natl. Acad. Sci.* **108,** 4659–4665 (2011).

13. Schonhoff, S. E., Giel-Moloney, M. & Leiter, A. B. Minireview: Development and differentiation of gut endocrine cells. *Endocrinology* **145,** 2639–2644 (2004).

14. Clevers, H. & Batlle, E. SnapShot: The intestinal crypt. *Cell* **152,** 1198–1198.e2 (2013).

15. Gerbe, F. & Jay, P. Intestinal tuft cells: Epithelial sentinels linking luminal cues to the immune system. *Mucosal Immunol.* **9,** 1353–1359 (2016).

16. Grencis, R. K. & Worthington, J. J. Tuft Cells: A New Flavor in Innate Epithelial Immunity. *Trends Parasitol.* **32,** 583–585 (2016).

17. Jang, M. H. *et al.* Intestinal villous M cells: An antigen entry site in the mucosal epithelium. *Proc. Natl. Acad. Sci.* **101,** 6110–6115 (2004).

18. Chabot, S., Wagner, J. S., Farrant, S. & Neutra, M. R. TLRs Regulate the Gatekeeping Functions of the Intestinal Follicle-Associated Epithelium. *J. Immunol.*

176, 4275–4283 (2006).

19. Hase, K. *et al.* Uptake through glycoprotein 2 of FimH + bacteria by M cells initiates mucosal immune response. *Nature* **462,** 226–230 (2009).

20. Ayabe, T. *et al.* Secretion of microbicidal alpha-defensins by intestinal Paneth cells in response to bacteria. *Nat. Immunol.* **1,** 113–8 (2000).

21. Mukherjee, S., Vaishnava, S. & Hooper, L. V. Multi-layered regulation of intestinal antimicrobial defense. *Cell. Mol. Life Sci.* **65,** 3019–3027 (2008).

22. Sato, T. *et al.* Paneth cells constitute the niche for Lgr5 stem cells in intestinal crypts. *Nature* **469,** 415–418 (2011).

23. Barker, N. *et al.* Identification of stem cells in small intestine and colon by marker gene Lgr5. *Nature* **449,** 1003–1007 (2007).

24. Sato, T. *et al.* Single Lgr5 stem cells build crypt-villus structures in vitro without a mesenchymal niche. *Nature* **459,** 262–265 (2009).

25. Beumer, J. & Clevers, H. Regulation and plasticity of intestinal stem cells during homeostasis and regeneration. *Development* **143,** 3639–3649 (2016).

26. Lee, J. *et al.* Maintenance of colonic homeostasis by distinctive apical TLR9 signalling in intestinal epithelial cells. *Nat. Cell Biol.* **8,** 1327–1336 (2006).

27. Abreu, M. T. Toll-like receptor signalling in the intestinal epithelium: How bacterial recognition shapes intestinal function. *Nat. Rev. Immunol.* **10,** 131–143 (2010).

28. Pott, J. *et al.* Age-dependent TLR3 expression of the intestinal epithelium contributes to rotavirus susceptibility. *PLoS Pathog.* **8,** (2012).

29. Steinbrecher, K. A., Harmel-Laws, E., Sitcheran, R. & Baldwin, A. S. Loss of Epithelial RelA Results in Deregulated Intestinal Proliferative/Apoptotic Homeostasis and Susceptibility to Inflammation. *J. Immunol.* **180,** 2588–2599 (2008).

30. Gewirtz, A. T., Navas, T. A., Lyons, S., Godowski, P. J. & Madara, J. L. Cutting Edge: Bacterial Flagellin Activates Basolaterally Expressed TLR5 to Induce Epithelial Proinflammatory Gene Expression. *J. Immunol.* **167,** 1882–1885 (2001).

31. Takaoka A. and Yanai H, IFN signaling network in innate dfence. Cell Microbiol. 6, 907–22 (2006).

32. Ey, B., Eyking, A., Gerken, G., Podolsky, D. K. & Cario, E. TLR2 mediates gap junctional intercellular communication through connexin-43 in intestinal epithelial barrier injury. *J. Biol. Chem.* **284,** 22332–22343 (2009).

33. Dolowschiak, T. *et al.* Potentiation of epithelial innate host responses by intercellular communication. *PLoS Pathog.* **6,** (2010).

34. Kasper, C. A. *et al.* Cell-cell propagation of NF-κB transcription factor and MAP kinase activation amplifies innate immunity against bacterial infection. *Immunity* **33,** 804–816 (2010).

35. ISAACS, A. & LINDENMANN, J. Virus interference. I. The interferon. *Proc. R. Soc. London. Ser. B, Biol. Sci.* **147,** 258–267 (1957).

36. Levin, D. *et al.* Multifaceted activities of type I interferon are revealed by a receptor

antagonist. *Sci. Signal.* **7,** ra50 (2014).

37. Schneider, W. M., Chevillotte, M. D. & Rice, C. M. Interferon-stimulated genes: a complex web of host defenses. *Annu. Rev. Immunol.* **32,** 513–45 (2014).

38. Kotenko, S. V *et al.* IFN-lambdas mediate antiviral protection through a distinct class II cytokine receptor complex. *Nat. Immunol.* **4,** 69–77 (2003).

39. Sheppard, P. *et al.* IL-28, IL-29 and their class II cytokine receptor IL-28R. *Nat. Immunol.* **4,** 63–68 (2003).

40. Prokunina-Olsson, L. *et al.* A variant upstream of IFNL3 (IL28B) creating a new interferon gene IFNL4 is associated with impaired clearance of hepatitis C virus. *Nat. Genet.* **45,** 164–171 (2013).

41. Pestka, S. *et al.* Interleukin-10 and related cytokines and receptors *Annu. Rev. Immunol.* **22,** 929–979 (2004).

42. Langer, J. A., Cutrone, E. C. & Kotenko, S. The Class II cytokine receptor (CRF2) family: Overview and patterns of receptor-ligand interactions. *Cytokine Growth Factor Rev.* **15,** 33–48 (2004).

43. LaFleur, D. W. *et al.* Interferon-κ, a Novel Type I Interferon Expressed in Human Keratinocytes. *J. Biol. Chem.* **276,** 39765–39771 (2001).

44. Kotenko, S. V. & Durbin, J. E. Contribution of type III interferons to antiviral immunity: Location, location, location. *J. Biol. Chem.* **292,** 7295–7303 (2017).

45. Levy, D. E., Marié, I. J. & Durbin, J. E. Induction and function of type i and III interferon in response to viral infection. *Curr. Opin. Virol.* **1,** 476–486 (2011).

46. Pestka, S. The interferons: 50 Years after their discovery, there is much more to learn. *J. Biol. Chem.* **282,** 20047–20051 (2007).

47. Hoffmann, H. H., Schneider, W. M. & Rice, C. M. Interferons and viruses: An evolutionary arms race of molecular interactions. *Trends Immunol.* **36,** 124–138 (2015).

48. Siegal, F. P. The Nature of the Principal Type 1 Interferon-Producing Cells in Human Blood. *Science (80-.).* **284,** 1835–1837 (1999).

49. Liu, Y.-J. IPC: Professional Type 1 Interferon-Producing Cells and Plasmacytoid Dendritic Cell Precursors. *Annu. Rev. Immunol.* **23,** 275–306 (2005).

50. Swiecki, M. & Colonna, M. Type i interferons: Diversity of sources, production pathways and effects on immune responses. *Curr. Opin. Virol.* **1,** 463–475 (2011).

51. Durbin, R. K., Kotenko, S. V. & Durbin, J. E. Interferon induction and function at the mucosal surface. *Immunol. Rev.* **255,** 25–39 (2013).

52. De Weerd, N. A. *et al.* Structural basis of a unique interferon-β signaling axis mediated via the receptor IFNAR1. *Nat. Immunol.* **14,** 901–907 (2013).

53. Gibbert, K., Schlaak, J. F., Yang, D. & Dittmer, U. IFN-α subtypes: Distinct biological activities in anti-viral therapy. *Br. J. Pharmacol.* **168,** 1048–1058 (2013).

54. Bach, E. A., Aguet, M. & Schreiber, R. D. The IFNγ receptor:A Paradigm for Cytokine Receptor Signaling. *Annu. Rev. Immunol.* **15,** 563–591 (1997).

55. Schroder, K., Hertzog, P. J., Ravasi, T. & Hume, D. A. Interferon- y : an overview of signals , mechanisms and functions. *J. Leukoc. Biol.* **75,** 163–189 (2004).

56. Valente, G., Ozmen, L., Novelli, F. & Geuna, M. Distribution of interferon-γ receptor in human tissues. *Eur. J. Immunol* 2403–2412 (1992).

57. Nan, Y., Nan, G. & Zhang, Y. J. Interferon induction by RNA viruses and antagonism by viral pathogens. *Viruses* **6,** 4999–5027 (2014).

58. Hemann, E. A., Gale, M. & Savan, R. Interferon lambda genetics and biology in regulation of viral control. *Front. Immunol.* **8,** (2017).

59. Lasfar, A. *et al.* Characterization of the mouse IFN-λ ligand-receptor system: IFN-λs exhibit antitumor activity against B16 melanoma. *Cancer Res.* **66,** 4468–4477 (2006).

60. Galani, I. E., Koltsida, O. & Andreakos, E. Crossroads Between Innate and Adaptive Immunity V. **850,** 1–15 (2015).

61. Ingle, H., Peterson, S. & Baldridge, M. Distinct Effects of Type I and III Interferons on Enteric Viruses. *Viruses* **10,** 46 (2018).

62. Amanzada, A., Kopp, W., Spengler, U., Ramadori, G. & Mihm, S. Interferon-λ4 (IFNL4) transcript expression in human liver tissue samples. *PLoS One* **8,** (2013).

63. Hamming, O. J. *et al.* Interferon lambda 4 signals via the IFNλ receptor to regulate antiviral activity against HCV and coronaviruses. *EMBO J.* **32,** 3055–3065 (2013).

64. Terczyńska-Dyla, E. *et al.* Reduced IFNλ4 activity is associated with improved HCV clearance and reduced expression of interferon-stimulated genes. *Nat. Commun.* **5,** (2014).

65. Fan, W. *et al.* IFN-λ4 desensitizes the response to IFN-α treatment in chronic hepatitis c through long-term induction of USP18. *J. Gen. Virol.* **97,** 2210–2220 (2016).

66. Obajemu, A. A. *et al.* IFN-λ4 Attenuates Antiviral Responses by Enhancing Negative Regulation of IFN Signaling. *J. Immunol.* ji1700807 (2017). doi:10.4049/jimmunol.1700807

67. Gad, H. H. *et al.* Interferon-lambda is functionally an interferon but structurally related to the interleukin-10 family. *J. Biol. Chem.* **284,** 20869–20875 (2009).

68. Miknis, Z. J. *et al.* Crystal Structure of Human Interferon-γ1 in Complex with Its High-Affinity Receptor Interferon-γR1. *J. Mol. Biol.* **404,** 650–664 (2010).

69. Zdanov, A. Structural analysis of cytokines comprising the IL-10 family. *Cytokine Growth Factor Rev.* **21,** 325–330 (2010).

70. Josephson, K., Logsdon, N. J. & Walter, M. R. Crystal structure of the IL-10/IL-10R1 complex reveals a shared receptor binding site. *Immunity* **15,** 35–46 (2001).

71. Jones, B. C., Logsdon, N. J. & Walter, M. R. Crystallization and preliminary X-ray diffraction analysis of human IL-22 bound to the extracellular IL-22R1 chain. *Acta Crystallogr. Sect. F Struct. Biol. Cryst. Commun.* **64,** 266–269 (2008).

72. Pestka, S., Krause, C. D. & Walter, M. R. Interferons, interferon-like cytokines, and their receptors. *Immunol. Rev.* **202,** *8-32*(2004).

73. Ank, N. *et al.* Lambda Interferon (IFN- λ), a Type III IFN , Is Induced by Viruses and

IFNs and Displays Potent Antiviral Activity against Select Virus Infections In Vivo. *J. Virol.* **80,** 4501–4509 (2006).

74. Ank, N. *et al.* An Important Role for Type III Interferon (IFN- /IL-28) in TLR-Induced Antiviral Activity. *J. Immunol.* **180,** 2474–2485 (2008).

75. Sommereyns, C., Paul, S., Staeheli, P. & Michiels, T. IFN-lambda (IFN-λ) is expressed in a tissue-dependent fashion and primarily acts on epithelial cells in vivo. *PLoS Pathog.* **4,** 1–12 (2008).

76. Mordstein, M. *et al.* Interferon-λ contributes to innate immunity of mice against influenza A virus but not against hepatotropic viruses. *PLoS Pathog.* **4,** 1–7 (2008).

77. Mordstein, M. *et al.* Lambda interferon renders epithelial cells of the respiratory and gastrointestinal tracts resistant to viral infections. *J. Virol.* **84,** 5670–5677 (2010).

78. Pulverer, J. E. *et al.* Temporal and Spatial Resolution of Type I and III Interferon Responses In Vivo. *J. Virol.* **84,** 8626–8638 (2010).

79. Pott, J. *et al.* IFN-lambda determines the intestinal epithelial antiviral host defense. *Proc. Natl. Acad. Sci. U. S. A.* **108,** 7944–7949 (2011).

80. Mahlakõiv, T., Hernandez, P., Gronke, K., Diefenbach, A. & Staeheli, P. Leukocyte-Derived IFN-α/β and Epithelial IFN-λ Constitute a Compartmentalized Mucosal Defense System that Restricts Enteric Virus Infections. *PLoS Pathog.* **11,** 1–19 (2015).

81. Mennechet, F. J. D., Uzé, G. & Uze, G. proliferation of FOXP3-expressing suppressor T cells Interferon- □ – treated dendritic cells specifically induce proliferation of FOXP3-expressing suppressor T cells. *Blood* **107,** 4417–4423 (2009).

82. Jordan, W. J. *et al.* Human interferon lambda-1 (IFN-lambda1/IL-29) modulates the Th1/Th2 response. *Genes Immun.* **8,** 254–261 (2007).

83. Lauterbach, H. *et al.* Mouse CD8α $^{+}$ DCs and human BDCA3 $^{+}$ DCs are major producers of IFN-λ in response to poly IC. *J. Exp. Med.* **207,** 2703–2717 (2010).

84. Liu, B. S., Janssen, H. L. & Boonstra, A. IL-29 and IFNalpha differ in their ability to modulate IL-12 production by TLR-activated human macrophages and exhibit differential regulation of the IFNgamma receptor expression. *Blood* **117,** 2385–2395 (2011).

85. Yin, Z. *et al.* Type III IFNs Are Produced by and Stimulate Human Plasmacytoid Dendritic Cells. *J. Immunol.* **189,** 2735–2745 (2012).

86. Dolganiuc, A. *et al.* Type III Interferons, IL-28 and IL-29, Are Increased in Chronic HCV Infection and Induce Myeloid Dendritic Cell-Mediated FoxP3+ Regulatory T Cells. *PLoS One* **7,** 1–10 (2012).

87. Blazek, K. *et al.* IFN-λ resolves inflammation via suppression of neutrophil infiltration and IL-1β production. *J. Exp. Med.* **212,** 845–853 (2015).

88. Kelly, A. *et al.* Immune Cell Profiling of IFN-λ Response Shows pDCs Express Highest Level of IFN-λR1 and Are Directly Responsive via the JAK-STAT Pathway. *J. Interf. Cytokine Res.* **36,** 671–680 (2016).

89. Broggi, A., Tan, Y., Granucci, F. & Zanoni, I. IFN-λ suppresses intestinal inflammation by non-translational regulation of neutrophil function. *Nat. Immunol.* **18,** 1084–1093

(2017).

90. Wack, A., Terczyńska-Dyla, E. & Hartmann, R. Guarding the frontiers: The biology of type III interferons. *Nat. Immunol.* **16,** 802–809 (2015).

91. Hermant, P. & Michiels, T. Interferon-λ in the context of viral infections: Production, response and therapeutic implications. *J. Innate Immun.* **6,** 563–574 (2014).

92. Jewell, N. a *et al.* Interferon-{lambda} is the predominant interferon induced by influenza A virus infection in vivo. *J Virol* **84,** 11515–11522 (2010).

93. Crotta, S. *et al.* Type I and Type III Interferons Drive Redundant Amplification Loops to Induce a Transcriptional Signature in Influenza-Infected Airway Epithelia. *PLoS Pathog.* **9,** (2013).

94. Ioannidis, I., Ye, F., McNally, B., Willette, M. & Flano, E. Toll-Like Receptor Expression and Induction of Type I and Type III Interferons in Primary Airway Epithelial Cells. *J. Virol.* **87,** 3261–3270 (2013).

95. Baños-Lara, M. D. R. *et al.* Impact and regulation of lambda interferon response in human metapneumovirus infection. *J. Virol.* **89,** 730–42 (2015).

96. Hernández, P. P. *et al.* Interferon-λ and interleukin 22 act synergistically for the induction of interferon-stimulated genes and control of rotavirus infection. *Nat. Immunol.* **16,** (2015).

97. Lin, J. Da *et al.* Distinct Roles of Type I and Type III Interferons in Intestinal Immunity to Homologous and Heterologous Rotavirus Infections. *PLoS Pathog.* **12,** 1–29 (2016).

98. Saxena, K. *et al.* A paradox of transcriptional and functional innate interferon responses of human intestinal enteroids to enteric virus infection. *Proc. Natl. Acad. Sci.* 201615422 (2017).

99. Galani, I. E. *et al.* Interferon-λ Mediates Non-redundant Front-Line Antiviral Protection against Influenza Virus Infection without Compromising Host Fitness. *Immunity* **46,** 875–890.e6 (2017).

100. Pervolaraki, K. *et al.* Type I and type III interferons display different dependency on mitogen-activated protein kinases to mount an antiviral state in the human gut. *Front. Immunol.* **8,** 1–16 (2017).

101. Coccia, E. M. *et al.* Viral infection and Toll-like receptor agonists induce a differential expression of type I and λ interferons in human plasmacytoid and monocyte-derived dendritic cells. *Eur. J. Immunol.* **34,** 796–805 (2004).

102. Megjugorac, N. J., Gallagher, G. E. & Gallagher, G. Modulation of human plasmacytoid DC function by IFN-lambda1 (IL-29). *J. Leukoc. Biol.* **86,** 1359–1363 (2009).

103. Hillyer, P. *et al.* Expression profiles of human interferon-alpha and interferon-lambda subtypes are ligand- and cell-dependent. *Immunol. Cell Biol.* **90,** 774–783 (2012).

104. Alase, A. a *et al.* IFNλ Stimulates MxA Production in Human Dermal Fibroblasts via a MAPK-Dependent STAT1-Independent Mechanism. *J. Invest. Dermatol.* 1–29 (2015). doi:10.1038/jid.2015.317

105. Lazear, H. M., Nice, T. J. & Diamond, M. S. Interferon-λ: Immune Functions at Barrier

Surfaces and Beyond. *Immunity* **43,** 15–28 (2015).

106. Lasfar, A., Gogas, H., Zloza, A., Kaufman, H. L. & Kirkwood, J. M. IFN-λ cancer immunotherapy: New kid on the block. *Immunotherapy* **8,** 877–888 (2016).

107. Chiriac, M. T. *et al.* Activation of Epithelial Signal Transducer and Activator of Transcription 1 by Interleukin 28 Controls Mucosal Healing in Mice With Colitis and Is Increased in Mucosa of Patients With Inflammatory Bowel Disease. *Gastroenterology* **153,** 123–138.e8 (2017).

108. Lee, S. & Baldridge, M. T. Interferon-lambda: A potent regulator of intestinal viral infections. *Front. Immunol.* **8,** (2017).

109. Zanoni, I., Granucci, F. & Broggi, A. Interferon (IFN)-λ takes the helm: Immunomodulatory roles of type III IFNs. *Front. Immunol.* **8,** 1–8 (2017).

110. Marie, I. Differential viral induction of distinct interferon-alpha genes by positive feedback through interferon regulatory factor-7. *EMBO J.* **17,** 6660–6669 (1998).

111. Kawai, T. & Akira, S. The role of pattern-recognition receptors in innate immunity: Update on toll-like receptors. *Nat. Immunol.* **11,** 373–384 (2010).

112. Siren, J., Pirhonen, J., Julkunen, I. & Matikainen, S. IFN-alpha regulates TLR-dependent gene expression of IFN-alpha, IFN-beta, IL-28, and IL-29. *J. Immunol.* **174,** 1932–1937 (2005).

113. Iwasaki, A. A Virological View of Innate Immune Recognition. *Annu. Rev. Microbiol.* **66,** 177–196 (2012).

114. Odendall, C. *et al.* Diverse intracellular pathogens activate type III interferon expression from peroxisomes. *Nat. Immunol.* **15,** 717–726 (2014).

115. Sun, L., Wu, J., Du, F., Chen, X. & Chen, Z. J. Cyclic GMP-AMP Synthase Is an. *Science (80-.).* **339,** 786–791 (2013).

116. Zhang, X. *et al.* Cutting Edge: Ku70 Is a Novel Cytosolic DNA Sensor That Induces Type III Rather Than Type I IFN. *J. Immunol.* **186,** 4541–4545 (2011).

117. Sui, H. *et al.* STING is an essential mediator of the Ku70-mediated production of IFN-l 1 in response to exogenous *DNA.Sci. Signal.* **5054,** (2017).

118. Blasius, A. L. & Beutler, B. Intracellular Toll-like Receptors. *Immunity* **32,** 305–315 (2010).

119. Alexopoulou, L., Czopik Holt, A., Medzhitov, R. & Flavell, R. A. Recognition of double-stranded RNA and activation of NF-kappa B by Toll-like receptor 3. *Nature* **413,** 732–738 (2001).

120. Stanifer, M. L. *et al.* Reovirus intermediate subviral particles constitute a strategy to infect intestinal epithelial cells by exploiting TGF-beta dependent pro-survival signaling. *Cell. Microbiol.* **18,** 1831–1845 (2016).

121. Bartonand, G. M. & Kagan, J. C. A cell biological view of Toll-like receptor function: regulation through compartmentalization. *Nat Rev Immunol* **9,** 535–542 (2014).

122. Moynagh, P. N. TLR signalling and activation of IRFs: Revisiting old friends from the NF-κB pathway. *Trends Immunol.* **26,** 469–476 (2005).

123. Sharma, S. *et al.* Triggering the interferon antiviral response through an IKK-related pathway. *Science (80-.).* **300,** 1148–1151 (2003).

124. Schlee, M. Master sensors of pathogenic RNA - RIG-I like receptors. *Immunobiology* **218,** 1322–1335 (2013).

125. Kato, H. *et al.* Length-dependent recognition of double-stranded ribonucleic acids by retinoic acid–inducible gene-I and melanoma differentiation–associated gene 5. *J. Exp. Med.* **205,** 1601–1610 (2008).

126. Schlee, M. & Hartmann, G. The chase for the RIG-I ligandrecent advances. *Mol. Ther.* **18,** 1254–1262 (2010).

127. Satoh, T. *et al.* LGP2 is a positive regulator of RIG-I- and MDA5-mediated antiviral responses. *Proc. Natl. Acad. Sci.* **107,** 1512–1517 (2010).

128. Loo, Y.-M. *et al.* Distinct RIG-I and MDA5 Signaling by RNA Viruses in Innate Immunity. *J. Virol.* **82,** 335–345 (2008).

129. Triantafilou, K. *et al.* Visualisation of direct interaction of MDA5 and the dsRNA replicative intermediate form of positive strand RNA viruses. *J. Cell Sci.* **125,** 4761–4769 (2012).

130. Takahasi, K. *et al.* Nonself RNA-Sensing Mechanism of RIG-I Helicase and Activation of Antiviral Immune Responses. *Mol. Cell* **29,** 428–440 (2008).

131. Seth, R. B., Sun, L., Ea, C. K. & Chen, Z. J. Identification and characterization of MAVS, a mitochondrial antiviral signaling protein that activates NF-κB and IRF3. *Cell* **122,** 669–682 (2005).

132. Hou, F. *et al.* MAVS forms functional prion-like aggregates to activate and propagate antiviral innate immune response. *Cell* **146,** 448–461 (2011).

133. McWhirter, S. M., TenOever, B. R. & Maniatis, T. Connecting mitochondria and innate immunity. *Cell* **122,** 645–647 (2005).

134. Thanos, D. & Maniatis, T. Virus induction of human IFNβ gene expression requires the assembly of an enhanceosome. *Cell* **83,** 1091–1100 (1995).

135. Sato, M. *et al.* Distinct and essential roles of transcription factors IRF-3 and IRF-7 in response to viruses for IFN-α/β gene induction. *Immunity* **13,** 539–548 (2000).

136. Panne, D. The enhanceosome. *Curr. Opin. Struct. Biol.* **18,** 236–242 (2008).

137. Sato, M. *et al.* Positive feedback regulation of type I IFN genes by the IFN-inducible transcription factor IRF-7. *FEBS Lett.* **441,** 106–110 (1998).

138. Tamura, T., Yanai, H., Savitsky, D. & Taniguchi, T. The IRF Family Transcription Factors in Immunity and Oncogenesis. *Annu. Rev. Immunol.* **26,** 535–584 (2008).

139. Génin, P., Vaccaro, A. & Civas, A. The role of differential expression of human interferon-A genes in antiviral immunity. *Cytokine Growth Factor Rev.* **20,** 283–295 (2009).

140. Osterlund, P. I., Pietila, T. E., Veckman, V., Kotenko, S. V. & Julkunen, I. IFN Regulatory Factor Family Members Differentially Regulate the Expression of Type III IFN (IFN-) Genes. *J. Immunol.* **179,** 3434–3442 (2007).

141. Onoguchi, K. *et al.* Viral infections activate types I and III interferon genes through a common mechanism. *J. Biol. Chem.* **282,** 7576–7581 (2007).

142. Thomson, S. J. P. *et al.* The role of transposable elements in the regulation of IFN-lambda1 gene expression. *Proc. Natl. Acad. Sci. U. S. A.* **106,** 11564–9 (2009).

143. Odendall, C. & Kagan, J. C. The unique regulation and functions of type III interferons in antiviral immunity. *Curr. Opin. Virol.* **12,** 47–52 (2015).

144. Osterlund, P. I., Pietilä, T. E., Veckman, V., Kotenko, S. V & Julkunen, I. IFN regulatory factor family members differentially regulate the expression of type III IFN (IFN-lambda) genes. *J. Immunol.* **179,** 3434–3442 (2007).

145. Kotenko, S. V. IFN-lambdas. *Curr. Opin. Immunol.* **23,** 583–590 (2011).

146. Bazan, J. F. Structural design and molecular evolution of a cytokine receptor superfamily. *Proc. Natl. Acad. Sci. USA* **87,** 6934–6938 (1990).

147. Cohen, B., Novick, D. & Barak, S. Ligand-Induced Association of the Type I Interferon Receptor Components. *Mol Cell Biol.* **15,** 4208–4214 (1995).

148. Piehler, J. & Schreiber, G. Mutational and structural analysis of the binding interface between type I interferons and their receptor ifnar2. *J. Mol. Biol.* **294,** 223–237 (1999).

149. Lamken, P., Lata, S., Gavutis, M., Piehler, J. & Wolfgang, J. Ligand-induced Assembling of the Type I Interferon Receptor on Supported Lipid Bilayers. *J. Mol. Biol.* 303–318 (2004).

150. Jaks, E., Gavutis, M., Uzé, G., Martal, J. & Piehler, J. Differential Receptor Subunit Affinities of Type I Interferons Govern Differential Signal Activation. *J. Mol. Biol.* **366,** 525–539 (2007).

151. Lavoie, T. B. *et al.* Binding and activity of all human alpha interferon subtypes. *Cytokine* **56,** 282–289 (2011).

152. Weerd, N. A. De, Samarajiwa, S. A. & Hertzog, P. J. Type I Interferon Receptors : biochemistry and biological function. *J Biol. Che*. **282,** 20053–20057 (2007).

153. Weerd, N. A. De & Nguyen, T. The interferons and their receptors — distribution and regulation. *Immunol. Cell Biol.* **90,** 483–491 (2012).

154. Jaitin, D. A. *et al.* Inquiring into the Differential Action of Interferons (IFNs): an IFN- a2 Mutant with Enhanced Affinity to IFNAR1 Is Functionally Similar to IFN- . *Mol. Cell. Biol.* **26,** 1888–1897 (2006).

155. Piehler, J., Thomas, C., Christopher Garcia, K. & Schreiber, G. Structural and dynamic determinants of type I interferon receptor assembly and their functional interpretation. *Immunol. Rev.* **250,** 317–334 (2012).

156. Thomas, C. *et al.* Structural linkage between ligand discrimination and receptor activation by Type i interferons. *Cell* **146,** 621–632 (2011).

157. Abramovich, C., Ratovitski, E., Lundgrenb, E. & Revela, M. Identification of mRNAs encoding two different soluble forms of the human interferon a-receptor. *FEBS Lett.* **338,** 295–300 (1994).

158. Cook, J. R., Cleary, C. M., Mariano, T. M., Izotova, L. & Pestka, S. Differential Responsiveness of a Splice Variant of the Human Type I Interferon Receptor to

Interferons *J Biol. Che*. **271,** 13448–13453 (1996).

159. Gazziola, C. *et al.* The relative endogenous expression levels of the IFNAR2 isoforms influence the cytostatic and pro-apoptotic effect of IFNalpha on pleomorphic sarcoma cells. *Int. J. Oncol.* **26,** 129–140 (2005).

160. Samarajiwa, S. A. *et al.* Soluble IFN Receptor Potentiates In Vivo Type I IFN Signaling and Exacerbates TLR4-Mediated Septic Shock. *J. Immunol.* **192,** 4425-35 (2017).

161. Hardy, M. P. *et al.* The soluble murine type I interferon receptor Ifnar-2 is present in serum , is independently regulated , and has both agonistic and antagonistic properties. Blood. **97,** 473–483 (2017).

162. Zhang, S., Kodys, K., Li, K. U. I. & Szabo, G. Interferon- ⎵ in Response to Hepatitis C Virus Infection LIVER. 414–425 (2013).

163. Jordan, W. J. *et al.* Modulation of the human cytokine response by interferon lambda-1 (IFN-λ1/IL-29). *Genes Immun.* **8,** 13–20 (2007).

164. Dellgren, C., Gad, H. H., Hamming, O. J., Melchjorsen, J. & Hartmann, R. Human interferon-λ3 is a potent member of the type III interferon family. *Genes Immun.* **10,** 125–131 (2009).

165. Bolen, C. R., Ding, S., Robek, M. D. & Kleinstein, S. H. Dynamic expression profiling of type I and type III interferon-stimulated hepatocytes reveals a stable hierarchy of gene expression. *Hepatology* **59,** 1262–1272 (2014).

166. Fuchs, S. Y. Hope and Fear for Interferon : The Receptor-Centric Outlook on the Future of Interferon Therapy. *J. Interferon Cytokine Res.* **33,** (2013).

167. Suresh Kumar, K. G. *et al.* Site-specific ubiquitination exposes a linear motif to promote interferon-α receptor endocytosis. *J. Cell Biol.* **179,** 935–950 (2007).

168. Papers, J. B. C. *et al.* Basal Ubiquitin-independent Internalization of Interferon alpha Receptor Is Prevented by Tyk2-mediated Masking of a Linear Endocytic Motif . *J. Biol. Chem.* **283,** 18566–18572 (2008).

169. Kumar, K. G. S. *et al.* SCF HOS ubiquitin ligase mediates the ligand-induced down-regulation of the interferon- a receptor. *EMBO J.* **22,** (2003).

170. Marijanovic, Z., Ragimbeau, J., Kumar, K. G. S., Fuchs, S. Y. & Pellegrini, S. TYK2 activity promotes ligand-induced IFNAR1 proteolysis. *Biochem. J.* **397,** 31–38 (2006).

171. Colamoniciso, O. R., Uyttendaelen, H., Domanskis, P., Ymn, H. & Krolewskio, J. J. an Interferon-a-activated Tyrosine Kinase , Is Physically Associated with an Interferon-a Receptor *. 3518–3522 (1994).

172. Ragimbeau, J. *et al.* The tyrosine kinase Tyk2 controls IFNAR1 cell surface expression. *EMBO J.* **22,** 537–547 (2003).

173. Kumar, K. G. S., Krolewski, J. J. & Fuchs, S. Y. Phosphorylation and Specific Ubiquitin Acceptor Sites Are Required for Ubiquitination and Degradation of the IFNAR1 Subunit of Type I Interferon Receptor *J. Biol. Chem*. **279,** 46614–46620 (2004).

174. Bhattacharya, S. *et al.* Ligand-independent Degradation of the IFNAR1 Chain of Type I Interferon Receptor *. **285,** 2318–2325 (2010).

175. Zheng, H., Qian, J., Baker, D. P. & Fuchs, S. Y. Tyrosine Phosphorylation of Protein Kinase D2 Mediates Ligand-inducible Elimination of the Type 1 Interferon. *J. Biol. Chem.* **286,** 35733–35741 (2011).

176. Marijanovic, Z., Ragimbeau, J., van der Heyden, J., Uze, G. & Pellegrini, S. Comparable potency of IFNalpha2 and IFNbeta on immediate JAK/STAT activation but differential down-regulation of IFNAR2. *Biochem. J.* **407,** 141–151 (2007).

177. Lee, S., Kim, W. & Moon, S. Role of the p38 MAPK signaling pathway in mediating interleukin-28A-induced migration of UMUC-3 cells. *Int. J. Mol. Med.* 945–952 (2012).

178. Wagner, T. C. *et al.* Interferon Signaling Is Dependent on Specific Tyrosines Located within the Intracellular Domain of IFNAR2c. *J. Biol. Chem.* **277,** 1493–1499 (2002).

179. Yan, H. *et al.* Phosphorylated interferon-a receptor 1 subunit (IFNaR1) acts as a docking site for the latent form of the 113 kDa STAT2 protein. *EMBO J.* **15,** 1064–1074 (1996).

180. Dumoutier, L. *et al.* Role of the Interleukin (IL) -28 Receptor Tyrosine Residues for Antiviral and Antiproliferative Activity of IL-29 / Interferon-lambda 1. *J. Biol. Chem.* **279,** 32269–32274 (2004).

181. Mendoza, J. L. *et al.* The IFN- l -IFN- l R1-IL-10R b Complex Reveals Structural Features Underlying Type III IFN Functional Plasticity Article The IFN- l -IFN- l R1-IL-10R b Complex Reveals Structural Features Underlying. *Immunity* **46,** 379–392 (2017).

182. Myers, M. P., Andersen, J. N., Cheng, A. & Tremblay, M. L. TYK2 and JAK2 are Substrates of Protein Tyrosine Phosphatase 1B. *J. Biol. Chem.* **276,** 47771-4 (2001).

183. Simoncic, P. D., Lee-loy, A., Barber, D. L., Tremblay, M. L. & Mcglade, C. J. The T Cell Protein Tyrosine Phosphatase Is a Negative Regulator of Janus Family Kinases 1 and 3. *Curr. Biol.* **12,** 446–453 (2002).

184. Irie-Sasaki, J. *et al.* CD45 is a JAK phosphatase and negatively regulates cytokine receptor signalling. *Nature* **409,** 349–354 (2001).

185. Malakhova, O. A. *et al.* UBP43 is a novel regulator of interferon signaling independent of its ISG15 isopeptidase activity. *EMBO* **25,** 2358–2367 (2006).

186. François-Newton, V. *et al.* USP18-based negative feedback control is induced by type I and type III interferons and specifically inactivates interferon α response. *PLoS One* **6,** (2011).

187. Makowska, Z., Duong, F. H. T., Trincucci, G., Tough, D. F. & Heim, M. H. Interferon- b and Interferon- lambda Signaling Is Not Affected by Interferon-Induced Refractoriness to Interferon- a InVivo. *Hepatology* **53,**1154–1163 (2011).

188. Basters, A., Geurink, P. P., Oualid, F. El, Ketscher, L. & Casutt, M. S. Molecular characterization of ubiquitin-specific protease 18 reveals substrate specificity for interferon-stimulated gene 15. *FEBS J.* **281,** 1918–1928 (2014).

189. Jilg, N. *et al.* Kinetic differences in the induction of interferon stimulated genes by interferon-α and interleukin 28B are altered by infection with hepatitis C virus. *Hepatology* **59,** 1250–1261 (2014).

190. Burkart, C. *et al.* Usp18 deficient mammary epithelial cells create an antitumour environment driven by hypersensitivity to IFN-λ and elevated secretion of Cxcl10.

EMBO Mol. Med. **5,** 1035–1050 (2013).

191. Song, M. M. & Shuai, K. The Suppressor of Cytokine Signaling (SOCS) 1 and SOCS3 but Not SOCS2 Proteins Inhibit Interferon-mediated Antiviral and Antiproliferative Activities *J. Biol. Chem.* **273,** 35056–35062 (1998).

192. Fenner, J. E. *et al.* Suppressor of cytokine signaling 1 regulates the immune response to infection by a unique inhibition of type I interferon activity. *Nat. Immunol.* **7,** 33–39 (2006).

193. Piganis, R. A. R. *et al.* Suppressor of Cytokine Signaling (SOCS) 1 Inhibits Type I Interferon (IFN) Signaling via the Interferon ␣ Receptor (IFNAR1) -associated Tyrosine Kinase Tyk2 *. **286,** 33811–33818 (2011).

194. Brand, S. *et al.* SOCS-1 inhibits expression of the antiviral proteins 2′,5′-OAS and MxA induced by the novel interferon-λs IL-28A and IL-29. *Biochem. Biophys. Res. Commun.* **331,** 543–548 (2005).

195. Liu, B., Chen, S., Guan, Y. & Chen, L. Type III Interferon Induces Distinct SOCS1 Expression Pattern that Contributes to Delayed but Prolonged Activation of Jak/STAT Signaling Pathway: Implications for Treatment Non-Response in HCV Patients. *PLoS One* **10,** e0133800 (2015).

196. Gough, D. J. *et al.* Functional Crosstalk between Type I and II Interferon through the Regulated Expression of STAT1. *Plos Biol* **8,** (2010).

197. Abt, M. C. *et al.* Article Commensal Bacteria Calibrate the Activation Threshold of Innate Antiviral Immunity. Immunity **37,** 158-70 (2012).

198. Kawashima, T. *et al.* Article Double-Stranded RNA of Intestinal Commensal but Not Pathogenic Bacteria Triggers Production of Protective Interferon- b. *Immunity* **38,** 1187–1197 (2013).

199. Gough, D. J., Messina, N. L., Clarke, C. J. P., Johnstone, R. W. & Levy, D. E. Review Constitutive Type I Interferon Modulates Homeostatic Balance through Tonic Signaling. *Immunity* **36,** 166–174 (2012).

200. Levy, D. E., Lew, D. J., Decker, T., Kessler, D. S. & Darnell, J. E. Synergistic interaction between interferon-a and interferon-y through induced synthesis of one subunit of the transcription factor ISGF3. *EMBO* **9,** (1990).

201. Tassiulas, I. *et al.* Amplification of IFN- a -induced STAT1 activation and inflammatory function by Syk and ITAM-containing adaptors. *Nat Immunol* **5,** 1181–1189 (2004).

202. Fink, K. *et al.* IFN β / TNF α synergism induces a non-canonical STAT2 / IRF9-dependent pathway triggering a novel DUOX2 NADPH Oxidase-mediated airway antiviral response. *Nat. Publ. Gr.* **23,** 673–690 (2013).

203. Darnell JE Jr, Kerr, M. & Stark, G. R. Jak-STAT Pathways and Transcriptional Activation in Response to IFNs and Other Extracellular Signaling Proteins. *Science* **264,** (1994).

204. Stoiber, D., Meinke, A., Barahmand-pour, F., Wo, S. & Decker, T. Activation of Different Stat5 Isoforms Contributes to Cell-Type- Restricted Signaling in Response to Interferons. *Mol Cell Biol.* **16,** 6937–6944 (1996).

205. Farrar, J. D., Smith, J. D., Murphy, T. L. & Murphy, K. M. Recruitment of Stat4 to the Human Interferon-alpha/beta receptor requires activated Stat2 *. *J. Biol. Chem.* **275,**

2693–2697 (2000).

206. Kotenko, S. V. The family of IL-10-related cytokines and their receptors: Related, but to what extent? *Cytokine Growth Factor Rev.* **13,** 223–240 (2002).

207. Brand, S. *et al.* IL-28A and IL-29 mediate antiproliferative and antiviral signals in intestinal epithelial cells and murine CMV infection increases colonic IL-28A expression. *Am. J. Physiol. Gastrointest. Liver Physiol.* **289,** G960–G968 (2005).

208. Platanias, L. C. & Fish, E. N. Signaling pathways activated by interferons. *Exp. Hematol.* **27,** 1583–1592 (1999).

209. Platanias, L. C. Mechanisms of type-I- and type-II-interferon-mediated signalling. *Nat. Rev. Immunol.* **5,** 375–386 (2005).

210. Darnell JE. Jr. STATs and Gene Regulation. *Science* **277,** 1630-5 (1997).

211. Wen, Z. & Darnell, J. E. Mapping of Stat3 serine phosphorylation to a single residue (727) and evidence that serine phosphorylation has no influence on DNA binding of Stat1 and Stat3. *Nucleic Acids Res.* **25,** 2062–2067 (1997).

212. Wen, Z., Zhong, Z. & Darnell, J. E. Maximal Activation of Transcription by Statl and Stat3 Requires Both Tyrosine and Serine Phosphorylation. **82,** 241–250 (1995).

213. Staab, J., Herrmann-lingen, C. & Meyer, T. CDK8 as the STAT1 serine 727 kinase? JAKSTAT. 8–11 (2013).

214. Mikulic, I. *et al.* Article CDK8 Kinase Phosphorylates Transcription Factor STAT1 to Selectively Regulate the Interferon Response. *Immunity* **38,** 250-262 (2012).

215. Uddin, S. *et al.* Protein Kinase C-delta (PKC-delta) Is Activated by Type I Interferons and Mediates Phosphorylation of Stat1 on Serine 727 *J. Biol. Chem.* **277,** 14408–14416 (2002).

216. Ramsauer, K. *et al.* p38 MAPK enhances STAT1-dependent transcription independently of Ser-727 phosphorylation. *Proc Natl Acad. Sci USA* **99,** 12859–12864 (2002).

217. Ng, S. *et al.* I κ B kinase ε (IKK ε) regulates the balance between type I and type II interferon responses. *Proc Natl Acad. Sci USA* **108,** 1–6 (2011).

218. Xu, D. *et al.* Article Promyelocytic Leukemia Zinc Finger Protein Regulates Interferon-Mediated Innate Immunity. *Immunity* **30,** 802–816 (2008).

219. You, M. I. N., Yu, D. & Feng, G. Shp-2 Tyrosine Phosphatase Functions as a Negative Regulator of the Interferon-Stimulated Jak / STAT Pathway. *Mol. Cell Biol.* **19,** 2416–2424 (1999).

220. Wu, T. R. *et al.* SHP-2 Is a Dual-specificity Phosphatase Involved in Stat1 Dephosphorylation at Both Tyrosine and Serine Residues in Nuclei *J Biol. Chem.* **277,** 47572–47580 (2002).

221. David, M., Chen, H. E., Goelz, S., Larner, A. C. & Neel, B. G. Differential Regulation of the Alpha / Beta Interferon-Stimulated Jak / Stat Pathway by the SH2 Domain-Containing Tyrosine Phosphatase SHPTP1. *Mol. Cell Biol.* **15,** 7050–7058 (1995).

222. Hoeve, J. *et al.* Identification of a Nuclear Stat1 Protein Tyrosine Phosphatase. *Mol. Cell Biol.* **22,** 5662–5668 (2002).

223. Steen, H. C. *et al.* Identification of STAT2 Serine 287 as a Novel Regulatory Phosphorylation Site in Type I Interferon-induced Cellular. *J Biol. Chem.***288,** 747–758 (2013).

224. Wang, Y. *et al.* Negative regulation of type I IFN signaling by phosphorylation of STAT 2 on T 387. *EMBO J.* **36,** 202–212 (2017).

225. Ungureanu, D. *et al.* PIAS proteins promote SUMO-1 conjugation to STAT1. *Blood* **102,** 3311–3314 (2017).

226. Song, L., Bhattacharya, S., Yunus, A. A., Lima, C. D. & Schindler, C. Stat1 and SUMO modification. **108,** 3237–3245 (2017).

227. Yang, J. *et al.* Reversible methylation of promoter-bound STAT3 by histone-modifying enzymes. *Proc Natl Acad. Sci USA* **107,** 21499-504 (2010).

228. Wieczorek, M., Ginter, T., Brand, P., Heinzel, T. & Kra, O. H. Cytokine & Growth Factor Reviews Acetylation modulates the STAT signaling code. **23,** 293–305 (2012).

229. Perry, S. T., Buck, M. D., Lada, S. M., Schindler, C. & Shresta, S. STAT2 Mediates Innate Immunity to Dengue Virus in the Absence of STAT1 via the Type I Interferon Receptor. *Plos Pathog.* **7,** (2011).

230. Brierley, M. M., Marchington, K. L., Jurisica, I. & Fish, E. N. Identification of GAS-dependent interferon-sensitive target genes whose transcription is STAT2-dependent but ISGF3 independent manner. *FEBS J.* **273,** 1569–1581 (2006).

231. Fink, K. & Grandvaux, N. STAT2 and IRF9. *Jak-Stat* 1–8 (2013).

232. Fish, E. N. *et al.* Activation of a CrkL-Stat5 Signaling Complex by Type I Interferons *J Biol. Chem*. 571–574 (1999).

233. Platanias, L. C. *et al.* CrkL and CrkII participate in the generation of the growth inhibitory effects of interferons on primary hematopoietic progenitors. *Exp Hematol.* **27,** 1315–1321 (1999).

234. Grumbach. *et al.* Engagement of the CrkL adaptor in interferon a signalling in BCR-ABL expressing cells. *Br. J. Haematol* **112, 327-36** (2001).

235. Lekmine, F. *et al.* The CrkL Adapter Protein Is Required for Type I Interferon-Dependent Gene Transcription and Activation of the Small G-Protein Rap1. *Biochem. Biophys. Res. Commun.* **750,** 744–750 (2002).

236. Uddin, S. *et al.* Activation of the p38 Mitogen-activated Protein Kinase by Type I Interferons *J Biol. Chem*. **274,** 30127–30131 (1999).

237. Zhou, Z. *et al.* Type III interferon (IFN) induces a type I IFN-like response in a restricted subset of cells through signaling pathways involving both the Jak-STAT pathway and the mitogen-activated protein kinases. *J. Virol.* **81,** 7749–7758 (2007).

238. Zhao, L.-J., Hua, X., He, S.-F., Ren, H. & Qi, Z.-T. Interferon alpha regulates MAPK and STAT1 pathways in human hepatoma cells. *Virol. J.* **8,** 157 (2011).

239. Goh, K. C., Haque, S. J. & Williams, B. R. G. p38 MAP kinase is required for STAT1 serine phosphorylation and transcriptional activation induced by interferons. *EMBO J.* **18,** 5601–5608 (1999).

240. Mayer, I. A. *et al.* The p38 MAPK Pathway Mediates the Growth Inhibitory Effects of

Interferon- ␣ in BCR-ABL-expressing Cells *J Biol. Chem*. **276,** 28570–28577 (2001).

241. Ishida, H. *et al.* Involvement of p38 signaling pathway in interferon-alpha-mediated antiviral activity toward hepatitis C virus. *Biochem. Biophys. Res. Commun.* **321,** 722–7 (2004).

242. Börgeling, Y. *et al.* Inhibition of p38 mitogen-activated protein kinase impairs influenza virus-induced primary and secondary host gene responses and protects mice from lethal H5N1 infection. *J. Biol. Chem.* **289,** 13–27 (2014).

243. Wang, F. *et al.* Disruption of Erk-dependent type I interferon induction breaks the myxoma virus species barrier. *Nat. Immunol.* **5,** 1266–1274 (2004).

244. Zhao, L., Wang, W., Wang, W., Ren, H. & Qi, Z. Cytokine Involvement of ERK pathway in interferon alpha-mediated antiviral activity against hepatitis C virus. *Cytokine* **72,** 17–24 (2015).

245. Li, G., Xiang, Y., Sabapathy, K. & Silverman, R. H. An Apoptotic Signaling Pathway in the Interferon Antiviral Response Mediated by RNase L and c-Jun NH 2 -terminal Kinase *. **279,** 1123–1131 (2004).

246. Bell, O., Tiwari, V. K., Thomä, N. H. & Schübeler, D. Determinants and dynamics of genome accessibility. *Nat. Publ. Gr.* **12,** 554–564 (2011).

247. Liu, H., Kang, H., Liu, R., Chen, X. & Zhao, K. Maximal Induction of a Subset of Interferon Target Genes Requires the Chromatin-Remodeling Activity of the BAF Complex. Mol. Cell Biol. **22,** 6471–6479 (2002).

248. Bhatt, D. M. *et al.* Transcript Dynamics of Proinflammatory Genes Revealed by Sequence Analysis of Subcellular RNA Fractions. *Cell.* **150,** 279–290 (2012). doi:10.1016/j.cell.2012.05.043

249. Bluyssen, H. A. R. & Levy, D. E. Stat2 Is a Transcriptional Activator That Requires Sequence- specific Contacts Provided by Stat1 and p48 for Stable Interaction with DNA *J. Biol. Chem.*. **272,** 4600–4605 (1997).

250. Cui, K. *et al.* The Chromatin-Remodeling BAF Complex Mediates Cellular Antiviral Activities by Promoter Priming. *Mol. Cell. Biol.* **24,** 4476–4486 (2004).

251. Ni, Z. *et al.* Apical role for BRG1 in cytokine-induced promoter assembly. *Proc Natl. Acad. Sci. USA* **102,** 14611–14616 (2005).

252. Yan, Z. *et al.* PBAF chromatin-remodeling complex requires a novel specificity subunit , BAF200 , to regulate expression of selective interferon-responsive genes. *Genes Dev.* 1662–1667 (2005).

253. Huang, M. *et al.* selectively activates a subset of interferon- α -inducible genes. **4,** (2003).

254. Bhattacharya, S. *et al.* Cooperation of Stat2 and p300/CBP in signalling induced by interferon-alpha. *Nature* **383,** 344–347 (1996).

255. Zhang, J. J. *et al.* Two contact regions between Stat1 and CBP/p300 in interferon gamma signaling. *Proc. Natl. Acad. Sci. U. S. A.* **93,** 15092–15096 (1996).

256. Paulson, M., Press, C., Smith, E., Tanese, N. & Levy, D. E. IFN-Stimulated transcription through a TBP-free acetyltransferase complex escapes viral shutoff. *Nat Cell. Biol.* **4,** (2003).

257. Nusinzon, I. & Horvath, C. M. Interferon-stimulated transcription and innate antiviral immunity require deacetylase activity and histone deacetylase 1. *Proc Natl. Acad. Sci. USA* **100,** 14742-7 (2003).

258. Chang, H. *et al.* Induction of interferon-stimulated gene expression and antiviral responses require protein deacetylase activity. *Proc Natl. Acad. Sci. USA* **101,** 9578-83 (2004).

259. Sakamoto, S., Potla, R. & Larner, A. C. Histone Deacetylase Activity Is Required to Recruit RNA Polymerase II to the Promoters of Selected Interferon-stimulated Early Response Genes *J. Biol. Chem.* **279,** 40362–40367 (2004).

260. Icardi, L. *et al.* The Sin3a repressor complex is a master regulator of STAT transcriptional activity. *Proc Natl. Acad. Sci. USA* **109,** 1–6 (2012).

261. Zhang, J. J. *et al.* Ser727-dependent recruitment of MCM5 by Stat1 α in IFN- γ -induced transcriptional activation. *EMBO J.* **17,** 6963–6971 (1998).

262. Dafonseca, C. J., Shu, F. & Zhang, J. J. Identification of two residues in MCM5 critical for the assembly of MCM complexes and Stat1- mediated transcription activation in response to IFN- gamma. *Proc Natl. Acad. Sci. USA* **98,** 3034-3039 (2001).

263. Zhu, M., John, S., Berg, M. & Leonard, W. J. Functional Association of Nmi with Stat5 and Stat1 in IL-2- and IFN gamma -Mediated Signaling. *Cell* **96,** 121–130 (1999).

264. Flammer, J. R. *et al.* The Type I Interferon Signaling Pathway Is a Target for Glucocorticoid Inhibition *Mol. Cell Biol.* **30,** 4564–4574 (2010).

265. Lau, J. F., Nusinzon, I., Burakov, D., Freedman, L. P. & Horvath, C. M. Role of Metazoan Mediator Proteins in Interferon-Responsive Transcription. *Mol. Cell Biol.* **23,** 620–628 (2003).

266. Gnatovskiy, L., Mita, P. & Levy, E. The Human RVB Complex Is Required for Efficient Transcription of Type I Interferon-Stimulated Genes. *Mol. Cell Biol.* **33,** 3817–3825 (2013).

267. Tahk, S. *et al.* Control of specificity and magnitude of NF- k B and STAT1-mediated gene activation through PIASy and PIAS1 cooperation. *Proc Natl. Acad. Sci. USA* **104,** 11643–11648 (2007).

268. Porritt, R. A. & Hertzog, P. J. Dynamic control of type I IFN signalling by an integrated network of negative regulators. *Trends Immunol.* **36,** 150–160 (2015).

269. Boxel-dezaire, A. H. H. Van, Rani, M. R. S. & Stark, G. R. Complex Modulation of Cell Type-Specific Signaling in Response to Type I Interferons. *Immunity.* **25,** 361–372 (2006). doi:10.1016/j.immuni.2006.08.014

270. Ivashkiv, L. B. & Donlin, L. T. Regulation of type I interferon responses. *Nat. Rev. Immunol.* **14,** 36–49 (2014).

271. Chatterjee-Kishore, M., Wright, K. L., Ting, J. P. & Stark, G. R. How Stat1 mediates constitutive gene expression: a complex of unphosphorylated Stat1 and IRF1 supports transcription of the LMP2 gene. *EMBO J.* **19,** 4111–22 (2000).

272. Taniguchi, T., Ogasawara, K., Takaoka, A. & Tanaka, N. IRF family of transcriptional factors as regulators of host defense. *Ann. Rev. Immunol.* **19,** 623-55

273. Xu, L. *et al.* IFN regulatory factor 1 restricts hepatitis E virus replication by activating STAT1 to induce antiviral IFN-stimulated genes. *FASEB J.* **30,** 3352–3367 (2017).

274. Harada, H., Takahashi, E., Itoh, S. & Harada, K. Structure and Regulation of the Human Interferon Regulatory Factor 1 (IRF-1) and IRF-2 Genes : Implications for a Gene Network in the Interferon System. *Mol. Cell Biol.* **14,** 1500–1509 (1994).

275. Hida, S. *et al.* CD8 + T Cell – Mediated Skin Disease in Mice Lacking IRF-2 , the Transcriptional Attenuator of Interferon- alpha/beta Signaling. *Immunity.* **13,** 643–655 (2000).

276. Kanno, Y., Levi, B.-Z., Tamura, T. & Ozato, K. Immune cell-specific amplification of interferon signaling by the IRF-4/8-PU.1 complex. *J. Interferon Cytokine Res.* **25,** 770–779 (2005).

277. Levy, D. E., Marié, I., Smith, E., Prakash, A. & Al, L. E. T. Enhancement and Diversification of IFN Induction by IRF-7-Mediated Positive Feedback. *J. Interferon Cytokines Res* .**93,** 87–93 (2002).

278. Honda, K., Takaoka, A. & Taniguchi, T. Type I Inteferon Gene Induction by the Interferon Regulatory Factor Family of Transcription Factors. *Immunity* **25,** 349–360 (2006).

279. Grandvaux, N. *et al.* Transcriptional Profiling of Interferon Regulatory Factor 3 Target Genes : Direct Involvement in the Regulation of Interferon-Stimulated Genes. *J.Virol.* **76,** 5532–5539 (2002).

280. Collins, S. E., Noyce, R. S. & Mossman, K. L. Innate Cellular Response to Virus Particle Entry Requires IRF3 but Not Virus Replication. *J.Virol.* **78,** 1706–1717 (2004).

281. Hiscott, J. Triggering the Innate Antiviral Response through IRF-3. *J. biol. Chem.* **282,** 15325–15329 (2007).

282. Andersen, J., VanScoy, S., Cheng, T.-F., Gomez, D. & Reich, N. C. IRF-3-dependent and augmented target genes during viral infection. *Genes Immun.* **9,** 168–175 (2008).

283. Sen, A. *et al.* Innate immune response to homologous rotavirus infection in the small intestinal villous epithelium at single-cell resolution. *Proc. Natl. Acad. Sci. U. S. A.* **109,** 20667–72 (2012).

284. Angel, J., Franco, M. A., Greenberg, H. B. & Bass, D. Lack of a role for type I and type II interferons in the resolution of rotavirus-induced diarrhea and infection in mice. *J Interf. Cytokine Res* **19,** 655–659 (1999).

285. López, S. & Arias, C. F. Multistep entry of rotavirus into cells: A Versaillesque dance. *Trends Microbiol.* **12,** 271–278 (2004).

286. Baldridge, M. T. *et al.* Expression of *Ifnlr1* on Intestinal Epithelial Cells Is Critical to the Antiviral Effects of Interferon Lambda against Norovirus and Reovirus. *J. Virol.* **91,** e02079-16 (2017).

287. Nice, T. J. *et al.* Interferon-λ cures persistent murine norovirus infection in the absence of adaptive immunity. *Science (80-.).* **347,** 269–273 (2015).

288. Nice, T. J. *et al.* Type I Interferon Receptor Deficiency in Dendritic Cells Facilitates Systemic Murine Norovirus Persistence Despite Enhanced Adaptive Immunity. *PLoS Pathog.* **12,** 1–19 (2016).

289. Grau, K. R. *et al.* The major targets of acute norovirus infection are immune cells in the gut-associated lymphoid tissue. *Nat. Microbiol.* **2,** (2017).

290. Lee, S. *et al.* Norovirus Cell Tropism Is Determined by Combinatorial Action of a Viral Non-structural Protein and Host Cytokine. *Cell Host Microbe* **22,** 449–459.e4 (2017).

291. Baldridge, M. T. *et al.* Commensal microbes and interferon- l determine persistence of enteric murine norovirus infection. *Science.* 347, 266-9

292. Meager, A., Visvalingam, K., Dilger, P., Bryan, D. & Wadhwa, M. Biological activity of interleukins-28 and -29: Comparison with type I interferons. *Cytokine* **31,** 109–118 (2005).

293. Marcello, T. *et al.* Interferons alpha and lambda Inhibit Hepatitis C Virus Replication With Distinct Signal Transduction and Gene Regulation Kinetics. *Gastroenterology* **131,** 1887–1898 (2006).

294. Kohli, A. *et al.* Distinct and overlapping genomic profiles and antiviral effects of Interferon-lambda and -alpha on HCV-infected and noninfected hepatoma cells. *J. Viral Hepat.* **19,** 843–853 (2012).

295. Voigt, E. a. & Yin, J. Kinetic Differences and Synergistic Antiviral Effects Between Type I and Type III Interferon Signaling Indicate Pathway Independence. *J. Interf. Cytokine Res.* **0,** 150504080007003 (2015).

296. Dixit, E. *et al.* Peroxisomes Are Signaling Platforms for Antiviral Innate Immunity. *Cell* **141,** 668–681 (2010).

297. Goody, R. J., Beckham, J. D., Rubtsova, K. & Tyler, K. L. JAK-STAT signaling pathways are activated in the brain following reovirus infection. *J. Neurovirol.* **13,** 373–383 (2007).

298. Zhang, L., Jilg, N., Shao, R., Lin, W. & Fusco, D. IL28B inhibits hepatitis C virus replication through the JAK–STAT pathway. *J. Hepatol.* **55,** 289–298 (2011).

299. Liu, M. Q. *et al.* IFN-??3 inhibits HIV infection of macrophages through the JAK-STAT pathway. *PLoS One* **7,** 1–9 (2012).

300. Blank, C. A., Anderson, D. A., Beard, M. & Lemon, S. M. Infection of Polarized Cultures of Human Intestinal Epithelial Cells with Hepatitis A Virus : Vectorial Release of Progeny Virions through Apical Cellular Membranes.*J.Virol* **74,** 6476–6484 (2000).

301. Stanifer, M. L., Kischnick, C., Rippert, A., Albrecht, D. & Boulant, S. Reovirus inhibits interferon production by sequestering IRF3 into viral factories. *Sci. Rep.* **7,** 1–14 (2017).

302. Kozuka, K. *et al.* Developmenta and characterization of a human and mouse intestinal epithelial cell monolayer platform *Stem Cell Reports* **9,** 1976–1990 (2017).

303. Clevers, H. Review The Intestinal Crypt , A Prototype Stem Cell Compartment. *Cell* **154,** 274–284 (2013).

304. Clevers, H. Modeling Development and Disease with Organoids. *Cell* **165,** 1586–1597 (2016).

305. Finkbeiner, S. R. *et al.* Stem cell-derived human intestinal organoids as an infection model for rotaviruses. *MBio* **3,** 1–6 (2012).

306. Bartfeld, S. et al., In vitro expansion of human gastric epithelial stem cells and their responses to bacterial infection. *Gastroenterology.* **148,** 126–136 (2016).

307. Saxena, K. *et al.* Human Intestinal Enteroids: a New Model To Study Human Rotavirus Infection, Host Restriction, and Pathophysiology. *J. Virol.* **90,** 43–56 (2016).

308. Ettayebi, K. *et al.* Replication of human noroviruses in stem cell – derived human enteroids - SUPP. *Science (80-.).* **5211,** (2016).

309. Bhushal, S., Wolfsmüller, M., Selvakumar, T. A. & Kemper, L. Cell Polarization and Epigenetic Status Shape the Heterogeneous Response to Type III Interferons in Intestinal Epithelial Cells. *Front Immunol.* **8,** 671 (2017).

310. Selvakumar, T. A. *et al.* Identification of a predominantly interferon-λ-induced transcriptional profile in murine intestinal epithelial cells. *Front. Immunol.* **8,** (2017).

311. Ng, C. T., Mendoza, J. L., Garcia, K. C. & Oldstone, M. B. A. Minireview Alpha and Beta Type 1 Interferon Signaling : Passage for Diverse Biologic Outcomes. *Cell* **164,** 349–352 (2016).

312. Mahlakõiv, T. *et al.* Combined action of type I and type III interferon restricts initial replication of severe acute respiratory syndrome coronavirus in the lung but fails to inhibit systemic virus spread. *J. Gen. Virol.* **93,** 2601–2605 (2012).

313. Contoli, M. *et al.* Role of deficient type III interferon-lambda production in asthma exacerbations. *Nat. Med.* **12,** 1023–1026 (2006).

314. Sato, S. *et al.* The RNA Sensor RIG-I Dually Functions as an Innate Sensor and Direct Antiviral Factor for Hepatitis B Virus Article The RNA Sensor RIG-I Dually Functions as an Innate Sensor and Direct Antiviral Factor for Hepatitis B Virus. *Immunity* **42,** 123–132 (2015).

315. Thomas, E. *et al.* HCV infection induces a unique hepatic innate immune response associated with robust production of type III interferons. *Gastroenterology* **142,** 978–988 (2012).

316. Siegel, R., Eskdale, J. & Gallagher, G. Regulation of IFN- 1 Promoter Activity (IFN- 1/IL-29) in Human Airway Epithelial Cells. *J. Immunol.* **187,** 5636–5644 (2011).

317. Ueki, I. F. *et al.* Respiratory virus – induced EGFR activation suppresses IRF1-dependent interferon and antiviral defense in airway epithelium. J. Exp. Med.**210,** 1929–1936 (2013).

318. Binder, S. *et al.* Activation of type I and III IFN response by mitochondria and peroxisomal MAVS and inhibition by hepatitis C virus *Plos Pathog.* **11,** (2015).

319. Griffiths, S. J. *et al.* A Systematic Analysis of Host Factors Reveals a Med23-Interferon- l Regulatory Axis against Herpes Simplex Virus Type 1 Replication. *Plos Pathog.* **9,** (2013).

320. Veckman, V. & Sire, J. Gene Expression and Antiviral Activity of Alpha / Beta Interferons and Interleukin-29 in Virus-Infected Human Myeloid Dendritic Cells. *Society* **79,** 9608–9617 (2005).

321. Arnold, M. M., Sen, A., Greenberg, H. B. & Patton, J. T. The Battle between Rotavirus and Its Host for Control of the Interferon Signaling Pathway. *Plos Pathog.* **9,** 1–8 (2013).

322. Friborg, J. *et al.* Impairment of type I but not type III IFN signaling by hepatitis C virus infection influences antiviral responses in primary human hepatocytes. *PLoS One* **10,** 1–20 (2015).

323. Klinkhammer, J. *et al.* IFN-λ prevents influenza virus spread from the upper airways to the lungs and limits virus transmission. *Elife* **7,** e33354 (2018).

324. Uddin, S. *et al.* The Rac1 / p38 Mitogen-activated Protein Kinase Pathway Is Required for Interferon ␣ -dependent Transcriptional Activation but Not Serine Phosphorylation of Stat Proteins *. **275,** 27634–27640 (2000).

325. Uddin, S., Sweet, M., Colamonici, O. R., Krolewski, J. J. & Platanias, L. C. The vav proto-oncogene product (p95 mw) interacts with the Tyk-2 protein tyrosine kinase. *FEBS Lett.* **403,** 31–34 (1997).

326. Li, Y. *et al.* Role of p38 ␣ Map Kinase in Type I Interferon Signaling *J. Biol. Chem.* **279,** 970–979 (2004).

327. Li, Y. *et al.* Activation of Mitogen-activated Protein Kinase Kinase (MKK) 3 and MKK6 by Type I Interferons *J. Biol. Chem.*. **280,** 10001–10010 (2005).

328. Platanias, L. C. Mechanisms of type I and type II Interferon mediated signalling. *Nat Rev. Immunol. 5,* 375-86 (2005)

329. Rand, U. *et al.* Multi-layered stochasticity and paracrine signal propagation shape the type-I interferon response. *Mol. Syst. Biol.* **8,** 1–13 (2012).

330. Maiwald, T. *et al.* Combining theoretical analysis and experimental data generation reveals IRF9 as a crucial factor for accelerating interferon-α induced early antiviral signalling. *FEBS J.* **277,** 4741–4754 (2010).

331. Moraga, I., Harari, D., Schreiber, G., Uze, G. & Pellegrini, S. Receptor Density Is Key to the Alpha2/Beta Interferon Differential Activities. *Mol. Cell. Biol.* **29,** 4778–4787 (2009).

332. Levin, D., Harari, D. & Schreiber, G. Stochastic Receptor Expression Determines Cell Fate upon Interferon Treatment. *Mol. Cell. Biol.* **31,** 3252–3266 (2011).

333. Witte, K. *et al.* Despite IFN- receptor expression, blood immune cells, but not keratinocytes or melanocytes, have an impaired response to type III interferons: Implications for therapeutic applications of these cytokines. *Genes Immun.* **10,** 702–714 (2009).

334. Duong, F. H. T. *et al.* IFN-λ receptor 1 expression is induced in chronic hepatitis C and correlates with the IFN-λ3 genotype and with nonresponsiveness to IFN-α therapies. *J. Exp. Med.* **211,** 857–68 (2014).

335. Ding, S., Khoury-Hanold, W., Iwasaki, A. & Robek, M. D. Epigenetic Reprogramming of the Type III Interferon Response Potentiates Antiviral Activity and Suppresses Tumor Growth. *PLoS Biol.* **12,** (2014).

336. Kalie, E., Jaitin, D. A., Abramovich, R. & Schreiber, G. An interferon ??2 mutant optimized by phage display for IFNAR1 binding confers specifically enhanced antitumor activities. *J. Biol. Chem.* **282,** 11602–11611 (2007).

337. Kalie, E., Jaitin, D. A., Podoplelova, Y., Piehler, J. & Schreiber, G. The stability of the ternary interferon-receptor complex rather than the affinity to the individual subunits dictates differential biological activities. *J. Biol. Chem.* **283,** 32925–32936 (2008).

338. Antonio, S. A Linear Signal Transduction Pathway Involving Phosphatidylinositol 3-Kinase , Protein Kinase C ⑀ , and MAPK in Mesangial Cells Regulates Interferon-gamma -induced. *J. Biol. Chem.* **279,** 27399–27409 (2004).

339. Cheon, H. & Stark, G. R. Unphosphorylated STAT1 prolongs the expression of interferon-induced immune regulatory genes. *Proc. Natl. Acad. Sci. U. S. A.* **106,** 9373–9378 (2009).

340. Cheon, H. *et al.* IRF9 mediate resistance to viruses and DNA damage. *EMBO J.* **32,** 2751–2763 (2013).

341. Sung, P. S. *et al.* Roles of unphosphorylated ISGF3 in HCV infection and interferon responsiveness. *Proc. Natl. Acad. Sci. U. S. A.* **112,** 10443–10448 (2015).

342. Davidson, S. *et al.* IFN k is a potent anti-influenza therapeutic without the inflammatory side effects of IFN a treatment. *EMBO Mol. Med.* **8,** 1–14 (2016).

343. Andreakos, E., Salagianni, M., Galani, I. E. & Koltsida, O. Interferon-λs: Front-line guardians of immunity and homeostasis in the respiratory tract. *Front. Immunol.* **8,** 1–7 (2017).

344. Pott, J. & Stockinger, S. Type I and III interferon in the gut: Tight balance between host protection and immunopathology. *Front. Immunol.* **8,** 1–15 (2017).

345. Giordano, G. *et al.* Type I interferon signaling contributes to chronic inflammation in a murine model of silicosis. *Toxicol. Sci.* **116,** 682–692 (2010).

346. Goritzka, M. *et al.* Alpha / Beta Interferon Receptor Signaling Amplifies Early Proinflammatory Cytokine Production in the Lung during Respiratory Syncytial Virus Infection. *J. Virol.* **88,** 6128–6136 (2014).

347. Chrysanthopoulou, A., Kambas, K., Stakos, D., Mitroulis, I. & Mitsios, A. Interferon lambda1 / IL-29 and inorganic polyphosphate are novel regulators of neutrophil-driven thromboin fl ammation. *J. Pathol.* **243,** 111–122 (2017).

348. Odendall, C., Voak, A. A. & Jonathan, C. Type III IFNs Are Commonly Induced by Bacteria-Sensing TLRs and Reinforce Epithelial Barriers during Infection. *J. Immunol.* **199**, 3270-79 (2017).

349. Epithelium, B. *et al.* Long-term Expansion of Epithelial Organoids From Human Colon, Adenoma, Adenocarcinoma, and Barrett's Epithelium. *YGAST* **141,** 1762–1772 (2011).

350. Date, S. & Sato, T. Mini-Gut Organoids : Reconstitution of the Stem Cell Niche. *Annu Rev. Cell. Dev. Biol.* **31,** 269–292 (2015).

351. Cureton, D. K., Massol, R. H., Saffarian, S., Kirchhausen, T. L. & Sean, P. J. Vesicular Stomatitis Virus Enters Cells through Vesicles Incompletely Coated with Clathrin That Depend upon Actin for Internalization. *Plos Pathog.* **5,** (2009).

352. Stanifer, M. L., Cureton, D. K. & Whelan, S. P. J. A Recombinant Vesicular Stomatitis Virus Bearing a Lethal Mutation in the Glycoprotein Gene Uncovers a Second Site Suppressor That Restores Fusion *J. Virol.* **85,** 8105–8115 (2011).

353. Novatt, H. *et al.* Distinct Patterns of Expression of Transcription Factors in Response to Interferonbeta and Interferonlambda1. *J. Interferon Cytokine Res.* **36,** 589–598 (2016).

354. Raue, A. *et al.* Structural and practical identifiability analysis of partially observed dynamical models by exploiting the profile likelihood. *Bioinformatics* **25,** 1923–1929 (2009).

355. Seber, G. A. F. & Wild, C. J. *Nonlinear Regression*. *John Wiley & Sons* (2003).

356. Garcia-Sastre A. and Biron CA. Type I interferons and the virus-host relationship:a l lesson in détente. *Science* **312,** 879–82 (2006).

357. Schreiber G. Molecular basis for differntial type I IFN signaling. *J. Bio. Chem* **292,** 7285–7294 (2017).

358. McNab F. et al., Type I interferons in infectious diseases. *Nat. Rev. Immunol.* **2,** 87–103 (2015).

6 Appendix

6.1 List of abbreviations

AP-1	activator protein-1
BSA	bovine serum albumin
CARD	caspase activation and recruitment domain
cDC	conventional dendritic cells
CRISPR	clustered regularly interspaced short palindromic repeats
E-cad	E-cadherin
EGF	epidermal growth factor
ERK	extracellular signal-regulated kinase
FAE	follicle-associated epithelium
FBS	fetal bovin serum
GAS	IFN-γ activated site
GEF	guanine nucleotide exchange factor
HAT	histone acetyltransferase
HCV	hepatitis C virus
HDAC	histone deacetylase
HPRT	hypoxanthine-guanine phosphoribosyltransferase
IEC	intestinal epithelial cells
IEL	intraepithelial lymphocyte
IF	immunofluorecence
IFIT1	interferon-induced protein with tetratricopeptide repeats 1
IFN	interferon
IFNR	interferon recetor
IL	interleukin
IRF	interferon regulatory factor
ISG	interferon-stimulated gene
ISGF3	interferon-stimulated gene factor 3
ISRE	interferon-stimulated response element
JAK	Janus kinase
JNK	c-Jun N-terminal kinase
LB	Lysogeny broth
LGP2	laboratory of genetics and physiology 2

MALT	mucosa-associated lymphoid tissue
MAPK	mitogen-activated protein kinase
MAVS	mitochondrial antiviral-signaling protein
MDA5	melanoma differentiation-associated protein 5
MNoV	murine norovirus
MOI	multiplicity of infection
MRV	mammalian reovirus
MXA	mx dynamin like GTPase 1
MyD88	myeloid differentiation factor 88
ng	nanogram
NFKB	nuclear factor kappa-light-chain-enhancer of activated B cells
NLR	nucleotide-binding oligomerization domain-like receptors
nM	nanomolar
OCT	optimal-cutting-temperature
PAMP	pathogen-associated molecular pattern
PBS	phosphate buffer saline
pDC	plasmacytoid dendritic cell
PEI	polyethylenimine
PFA	paraformaldehyde
PIAS	protein inhibitors of activated STAT
PI3K	phosphatidyl-inositol 3-kinase
poly I:C	poly-inosinic:cytidylic acid
PRR	pattern-recognition receptor
PTP1B	protein-tyrosine phosphatase 1B
P38-MAPK	p38-mitogen activated protein kinase
qRT-PCR	quantitative real-time Polymerase chain reactions
RCF	relative centrifuge force
RIG-1	retinoic acid-inducible gene 1
RLR	retinoic acid-inducible gene-I-like receptor
RNA	ribonucleic acid
Rpm	round per minutes
RT	room temperature
RU	reactive units
SDS-PAGE	sodium dodecyl sulfate polyacrylamide gel electrophoresis
SHP-2	Src Homology phosphatase 2

SOC	suppressor of cytokine signaling
STAT	signal transducer and activator of transcription
Syn	synaptophysin
TAD	transactivation domain
TBP	TATA-binding protein
TBS	Tris buffer saline
TBK1	TANK-binding kinase 1
TCPTP	T cell protein-tyrosine phosphatase
TLR	toll-like receptor
TRIF	toll/interleukin 1-domain-containing adaptor-molecule 1
TYK2	tyrosine kinase 2
USP18	ubiquitin-specific protease
VIPERIN	virus inhibitory protein, endoplasmic reticulum associated, interferon-inducible
VSV	vesicular stomatitis virus
WB	Western blot
WT	wild type
ZO-1	zonula occludens-1
µNS	reovirus non-structural protein

6.2 Supplementary figure

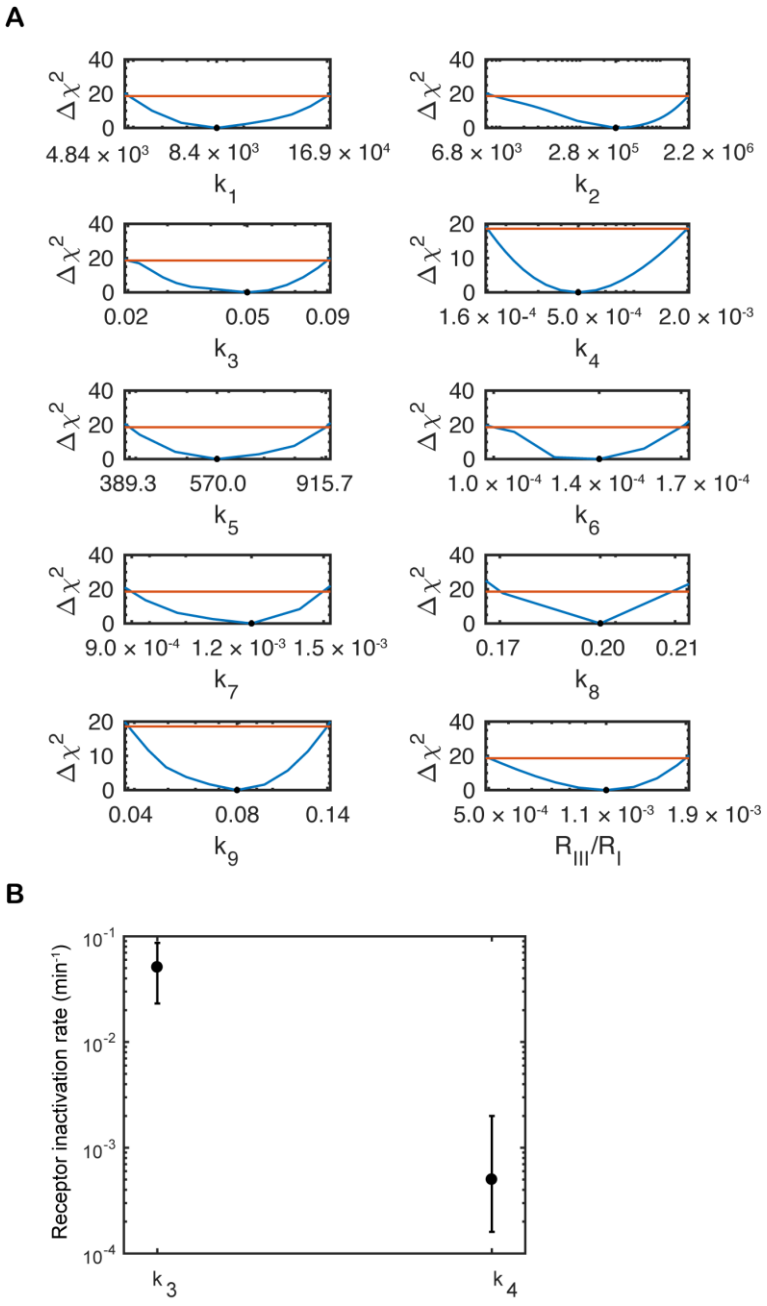

Figure S1. Profile likelihoods of model parameters. The uncertainty of the estimated model parameters is calculated using profile likelihood method. (A) The solid blue line is the change in the weighted sum of squared residuals ($\Delta\chi^2$), the filled circle indicates optimum parameter value and the solid red line indicates the 95% threshold calculated using χ^2 distribution. (B) The 95% confidence bounds of type I or type III IFN receptor complex inactivation rate constants are calculated using profile likelihood method. Our calculations show that the type III IFN receptor complex inactivation rate constant (k4) is significantly less than the corresponding value of type I IFN receptor complex (k3). Modeling has been performed by Soheil Rastgou Talemi, Heidelberg University and German Cancer Research Center (DKFZ)

6.3 Supplementary tables

The supplementary tables S1-S3 have been produced by Soheil Rastgou Talemi, Heidelberg University and German Cancer Research Center (DKFZ).

S1 Table. Mathematical formulation of the model.

ODEs model biological system dynamics	Explanation
$\frac{d[R_I]}{dt} = -Area \cdot k_1 \cdot IFN_\beta \cdot R_I$	IFNAR dynamics
$\frac{d[R_I^*]}{dt} = Area \cdot k_1 \cdot IFN_\beta \cdot R_I - k_3 \cdot R_I^* \cdot ISG$	Activated IFNAR dynamics
$\frac{d[R_{III}]}{dt} = -Area \cdot k_2 \cdot IFN_\lambda \cdot R_{III}$	IFNLR dynamics
$\frac{d[R_{III}^*]}{dt} = Area \cdot k_2 \cdot IFN_\lambda \cdot R_{III} - k_4 \cdot R_{III}^* \cdot ISG$	Activated IFNLR dynamics
$\frac{d[pST]}{dt} = k_5 \cdot (R_I^* + R_{III}^*) \cdot (1 - pST) - k_6 \cdot pST$	Activated STAT1/2 dynamics
$\frac{d[ISG]}{dt} = k_7 + k_8 \cdot pST - k_7 \cdot ISG$	ISG activation dynamics (Viperin)
$\frac{d[IFN_\beta]}{dt} = -k_9 \cdot IFN_\beta$	IFN-β dynamics
$\frac{d[IFN_\lambda]}{dt} = -k_9 \cdot IFN_\lambda$	IFN-λ dynamics

S2 Table. State variables and initial values.

State variable	Initial value	Explanation
IFN-β	8.30×10^{-7}-0.33 nM	Interferon beta
IFN-λ	4.56×10^{-6}-13.70 nM	Interferon lambda
R_I	8.3×10^{-4} nM	Cellular IFNAR concentration[1]
R_I^*	0 nM	Activated IFNAR concentration
R_{III}	EF_{IFNLR} · $R_{I\text{-}0}$ nM	Cellular IFNLR concentration [2]
R_{III}^*	0 nM	Activated IFNLR
pST	0 $\#_{pST}$	Activated/Phospho STAT1/2 (relative value between 0-1)
ISG	1 $\#_{ISG}$	Interferon stimulated Gene (relative value)

1-The initial value is calculated assuming 10^3 IFNAR molecule per cell.

2-The initial IFNLR value is calculated relative to the initial IFNAR level using the estimated IFNLR efficacy factor (EFIFNLR).

S3 Table. Estimated parameter values.

Estimated parameters	Estimated value	Parameter bounds	Dimension	Respective reaction
k_1	8.45×10^{3}	4.84×10^{3} 1.69×10^{4}	$(cm^2 \cdot min \cdot nM)^{-1}$	IFNAR activation
k_2	2.79×10^{5}	6.89×10^{3} 2.24×10^{6}	$(cm^2 \cdot min \cdot nM)^{-1}$	IFNLR activation
k_3	0.051	0.023 0.087	min^{-1}	IFNAR inactivation
k_4	4.9×10^{-4}	1.58×10^{-4} 2.0×10^{-3}	min^{-1}	IFNLR inactivation
k_5	569.98	389.30 915.72	$(min \cdot nM)^{-1}$	STAT1/2 activation
k_6	1.4×10^{-3}	1.0×10^{-3} 1.7×10^{-3}	min^{-1}	STAT1/2 inactivation
k_7	1.2×10^{-3}	8.55×10^{-4} 1.5×10^{-3}	min^{-1}	Basal ISG activation
k_8	0.20	0.17 0.22	$\#_{ISG} \cdot (\#_{pST} \cdot min)^{-1}$	STAT mediated ISG activation
k_9	0.08	0.04 0.14	min^{-1}	IFN inactivation
EF_{IFNLR}	1.1×10^{-3}	5.26×10^{-4} 1.9×10^{-3}	#	IFNLR efficacy factor (relative value)
OE_{IFNAR}	3.05	-	#	IFNAR over-expression factor
OE_{IFNLR}	1.67	-	#	IFNLR over-expression factor